U/PB ZIRCON GEOCHRONOLOGY, PETROLOGY, AND STRUCTURAL GEOLOGY OF THE CRYSTALLINE ROCKS OF THE SOUTHERNMOST SIERRA NEVADA AND TEHACHAPI MOUNTAINS, KERN COUNTY, CALIFORNIA

Thesis by

David Bruce Sams

In Partial Fulfillment of the Requirements

for the Degree of

Doctor of Philosophy

California Institute of Technology

Pasadena, California

1986

(Submitted October 7, 1985)

ACKNOWLEDGMENTS

I would first like to thank my thesis advisor Dr. Jason B. Saleeby for his generous support throughout this investigation. This support has taken many forms: technical discussions, editing of manuscripts, guidance and encouragement, as well as financial and laboratory support.

Dr. Leon T. Silver provided many of the laboratory facilities required for this study. He was also vitally interested in all aspects of my work. I would like to thank him and the rest of my thesis committee, Drs. Arden L. Albee, Clarence R. Allen, and Hugh P. Taylor, Jr., for their critical review and discussions of this material.

I would like to thank Donald C. Ross for his support in laying the groundwork for this investigation, posing many of the problems in the southernmost Sierra Nevada, and for his subsequent encouragement and discussions. I also appreciate his assistance and that of the U.S.G.S. in Menlo Park in providing $\delta^{18}O$ and Rb/Sr isotopic analyses of my geochronology samples, and that of Ivan Barnes and R.W. Kistler at the U.S.G.S. for doing the oxygen and strontium analyses. R.W. Kistler was also helpful in many discussions about the geochemistry of the area. John Sharry was very helpful in providing much of the original geological groundwork in the gneiss complex of the Tehachapi Mountains, in initiating the investigative pursuit of high-grade crystalline rocks in the southern Sierras, and in many subsequent discussions.

I would like to thank A. Howard and M. Murrell for their assistance in the fission track radiation studies, and J. Mayne for her drafting expertise. C.C. Allen critically read this manuscript.

This investigation would not have been possible without the assistance of the many private landowners on whose property field work was carried out. Special

thanks to the people at the Tejon Ranch Company, in particular to Duncan Patty, and to Jack Hunt, John Ortega, and the many ranch hands I met in the field. Additional thanks to the people at Stallion Springs, Bear Valley Springs, Keene Ranch, and Loop Ranch, and in the White Oak and Caliente areas.

Financial support for this investigation was obtained from the National Science Foundation and the Geological Society of America. Part of the field and thin section expenses were covered by GSA Penrose Research Grants numbers 2906-81, 3054-82, and 3214-83. Salary support and laboratory expenses for geochronological work were supported by NSF grants numbers EAR80-18811 and EAR82-18460 to J.B. Saleeby, in whose laboratory the work was carried out.

Finally, and most of all, I extend wholehearted thanks to my wife Amy Dianne, whose assistance and encouragement carried me through my studies. In addition, she was a capable field assistant on many occasions, and assisted in the collection of a number of geochronology samples, once to the extent of packing out some 25-30 kg of sample.

ABSTRACT

Field mapping, petrography, U/Pb zircon geochronology, and Rb/Sr geochemistry on the crystalline rocks of the southernmost Sierra Nevada and Tehachapi Mountains north of the Garlock fault have 1) generated a structural, geochemical, and geochronological framework; 2) demonstrated a continuation of Sierran plutonic and metasedimentary rocks into the Tehachapi Mountains; 3) indicated that the region, in particular the gneiss complex of the Tehachapi Mountains, represents the deepest exposed levels of the Sierra Nevada batholith; 4) placed constraints on possible mixing models between upper mantle and metasedimentary components to generate the observed geochemical signatures of the rocks; and 5) resolved a major mid-Cretaceous deformation event.

The main crystalline rocks of the study area are the rocks of the Bear Valley Springs intrusive suite and the gneiss complex of the Tehachapi Mountains. The Bear Valley Springs suite is a mid-Cretaceous tonalite batholith complex with coeval gabbroic intrusives. The gneiss complex of the Tehachapi Mountains consists dominantly of early-Cretaceous orthogneiss, with subordinate paragneiss and local domains having granulite affinities. The orthogneisses are dominantly tonalitic in composition, with significant layers and domains of granodioritic to granitic and lesser dioritic to gabbroic gneiss. Quartz-rich metasedimentary rocks and marble constitute the main framework assemblage into which the plutonic rocks were emplaced. Field relations demonstrate assimilation of metasedimentary material into the orthogneisses and magma mixing between mafic, tonalitic, and anatectic granitic material derived from the metasediments.

Crystalline rocks of the region, with the exception of metasedimentary framework rocks, fall into a narrow age range of 90-120 Ma, and exhibit three main age suites. Most samples have zircon populations with systematics indica-

tive of igneous crystallization, with signs of zircon inheritance or entrainment in the vicinity of metamorphic septa. Strongly discordant samples are relatively rare, and include the granodiorite of Claraville (concordia intercepts of 90/1900 Ma), the paragneiss of Comanche Point (108/1450), and a quartzite in the Kings sequence metasedimentary framework rocks (1700 Ma upper intercept).

The rocks in the first age suite (gneiss complex of the Tehachapi Mountains and augen gneiss of Tweedy Creek) exhibit a greater degree of deformation, especially under moderate to high grade conditions. Major deformational fabrics are expressed as gneissic banding, mylonitization, recrystallization, boudinaging, and transposition of internal contacts. Internally and externally concordant zircon systematics of the orthogneisses in this suite indicate igneous crystallization between 110-120 Ma. Discordant zircon systematics suggest entrainment of minor amounts of mid-Proterozoic zircon and/or open system lead loss in response to the 100 Ma magmatic culmination (Bear Valley Springs event).

The second suite, 100±2 Ma Bear Valley Springs intrusive suite (tonalite of Mount Adelaide, tonalite of Bear Valley Springs, hypersthene tonalite of Bison Peak, and metagabbro of Tunis Creek) contains igneous rocks which locally cross-cut the older suite. These rocks have a late-stage deformational fabric shown primarily in the tonalites as pervasive foliation and faint gneissic banding. The zircon systematics of this suite are internally and externally concordant, indicating igneous crystallization ages, with only local evidence of entrainment of mid-Proterozoic zircon. The deformation of the suite was synplutonic, with later phases within the suite lacking significant deformational fabrics. The major deformational fabrics exhibited in the Tehachapi and Bear Valley Springs suites may be the result of the intrusion of the tonalite batholith into the lower crust, and/or the result of intra-arc shearing that was preferentially concentrated in various intrusive bodies.

The third suite, late deformational intrusive rocks, consists of units which cross-cut deformational features in both the older suites. These youngest rocks are themselves slightly to nondeformed. The members in the suite have ages of 90 Ma (granodiorite of Claraville), 93 Ma (tonalite stock at Tweedy Creek), and 94 Ma (pegmatite dike at Comanche Point).

Field mapping and petrography have shown a southward continuation of Sierran plutonic and metasedimentary framework rocks to the region of Tejon Creek. The plutons show a constant age spread and overall composition throughout the region, with a greater degree of solidus to hot sub-solidus deformation exhibited southward. The metamorphic septa have a higher grade, and are more strongly deformed southwards, becoming migmatitic. The southern margin of the tonalite of Bear Valley Springs consists of a gradational contact with the hypersthene tonalite of Bison Peak, which is believed to represent the floor or conduit phase of the batholith. Along its southwestern margin, the tonalite of Bear Valley Springs grades into the gneiss complex of the Tehachapi Mountains through a region of tonalitic gneiss that appears to be derived through the mixing of tonalitic magmas and migmatitic melts produced from paragneiss components in the gneiss complex. Paleomagnetic and structural restoration of the southwestern margin of the tonalite indicates that it may represent the uptilted floor of the batholith that originally spread out over its gneissic substrate.

The crystalline rocks of the southernmost Sierra Nevada represent the deepest exposed levels of the Sierra Nevada batholith. Saleeby and others (1986a) indicate a continual increase in depth of exposure from the central to southern part of the batholith. Elan (1985) shows metamorphic conditions of 3.0 kb and 700°C in the south-central Sierras, while Sharry (1981b) has suggested that parts of the gneiss complex have a deep-seated (8 kb) origin with rapid late-Cretaceous

uplift. Granulitic nodules of similar character to parts of the gneiss complex have been described by Domenick and others (1983) as originating from a similar depth beneath the central Sierra. Gneissic granitoids have numerous lenses of mafic to ultramafic cumulates showing igneous crystallization under granulite facies conditions. The domains of "granulite" in the gneiss complex of the Tehachapi Mountains are believed to be hot, relatively dry zones in a crystallizing and deforming batholithic complex. Magmatic epidote-bearing tonalites and late stage subsolidus autometamorphic garnet growth are further indicators of a deep (≥6 kb) level of origin for the region.

The "granulites" (metagabbro of Tunis Creek and hypersthene tonalite of Bison Peak) are interpreted to be of an igneous origin. Evidence for this interpretation consists of: relict olivine grains and cumulate textures; foliation believed to be the result of igneous flow; zoned plagioclase necessitating the presence of a magma; tonalites that contain epidote that is interpreted to be of magmatic origin; $\delta^{18}O$ and Rb/Sr isotopic values in the igneous range; abundance of retrograde but paucity of prograde mineral reactions; gradational contacts between plutonic units; and observed intrusive contacts. Pyroxene within the "granulites" is believed to be of a pyrogenic origin. The rocks typically have a retrograde assemblage that consists of olivine → orthopyroxene and pyroxene → amphibole. The mineral assemblages all point to a downward P-T path.

Simple two-component mixing models have been constructed for samples from the southernmost Sierra Nevada, and involve incorporation of partial to complete melts of metasedimentary material into "primitive" upper mantle orogenic mafic magmas prior to crystallization. The two possible end-members are the quartzite-paragneiss of Comanche Point and the hypersthene tonalite of Bison Peak-metagabbro of Tunis Creek. Initial $^{87}Sr/^{86}Sr$ correlates directly with $\delta^{18}O$,

and generally correlates inversely with Sr content for most of the samples. Simple isotopic mixing models indicate incorporation of up to 33% metasedimentary material in the granitic rocks, and up to 15% in the tonalites, with younger and more easterly samples requiring a larger metasedimentary component. The non-correlation of Sr_o with Sr content for some of the Pastoria Creek samples indicates an oceanic-affinity source with little interaction with continental crustal material. A number of samples appear to require a third, probable lower continental crustal and/or oceanic crustal-upper mantle component that may have a Paleozoic age.

Based on Rb/Sr and K/Ar age systematics, the region was uplifted in a regional cooling event at ~85 Ma perhaps as part of regional thrusting event(s) in southern California. The crystalline rocks were subsequently exposed and unconformably overlapped by Eocene marine sediments. Paleomagnetic data suggest about 45-60° of clockwise rotation between 80 and 16 Ma for the southern end of the Sierras, possibly as the result of the thrusting event responsible for the regional uplift.

Saleeby and others (1986c) have suggested that the lower crust beneath the Sierra Nevada batholith is comprised in part by granulitic and mafic intrusive rocks. Experimental studies by Christensen and Fountain (1975) also suggest the presence of granulites in the lower continental crust. The interpretation that the study area represents the deepest exposed level of the southernmost Sierra Nevada batholith leads to the implication that granulitic-affinity rocks comprise the lower part of the continental crust. Therefore, this study provides some degree of confirmation to the aforementioned hypotheses.

III. GEOCHRONOLOGY

III. U/PB ZIRCON GEOCHRONOLOGY AND THE PETROTECTONIC SIGNIFICANCE OF THE GNEISS COMPLEX OF THE TEHACHAPI MOUNTAINS

VI. APPENDIX - GEOCHRONOLOGY

LIST OF FIGURES

Plates

LIST OF TABLES

I. INTRODUCTION

I.1. Nature of the problem

Detailed geochronological, petrologic, and geochemical data on the crystalline rocks of the southernmost Sierra Nevada is vital to the understanding of the geologic history of the area, and for regional correlations. The crystalline rocks of the southern Sierra have yet to be traced south of the Garlock fault. This is due in part to structural complexity, and the lack of geochronological control and detailed geochemical studies. It is usually assumed that the Tehachapi Mountains are the southward continuation of similar rocks in the southern Sierras, but this has not been previously demonstrated. Detailed information regarding these rocks is required for comparison and possible correlations with rocks in the Mojave, Salinian, and Transverse Ranges blocks.

The southernmost Sierra Nevada crystalline terrane (shown in Figures 1-3) is characterized by thin metamorphic septa and voluminuous Cretaceous plutonic rocks (Saleeby and others, 1978; Sams and others, 1983). Structures are steeply dipping, and have an overall northwest trend, except for the southernmost "tail" end of the Sierras, where northeast and east trends are found. The map pattern of the Sierra Nevada batholith curves around parallel to the Garlock fault, which truncates the batholith.

Recent work (Ross 1985, 1986; Sams and others, 1983) shows the Sierran batholith grading into a gneiss complex in the Tehachapi Mountains. Work by Sharry (1981a,b) emphasized the presence of pyroxene and garnet in some of the gneiss units, and their resemblance to granulites. He speculated a deep-seated metamorphic origin for the "granulites", and their subsequent rapid late-Cretaceous uplift. Work by Saleeby and others (1986a), Elan (1985), Elan and Thomas (1984), and Saleeby (1981) in the south-central Sierra Nevada suggests that the

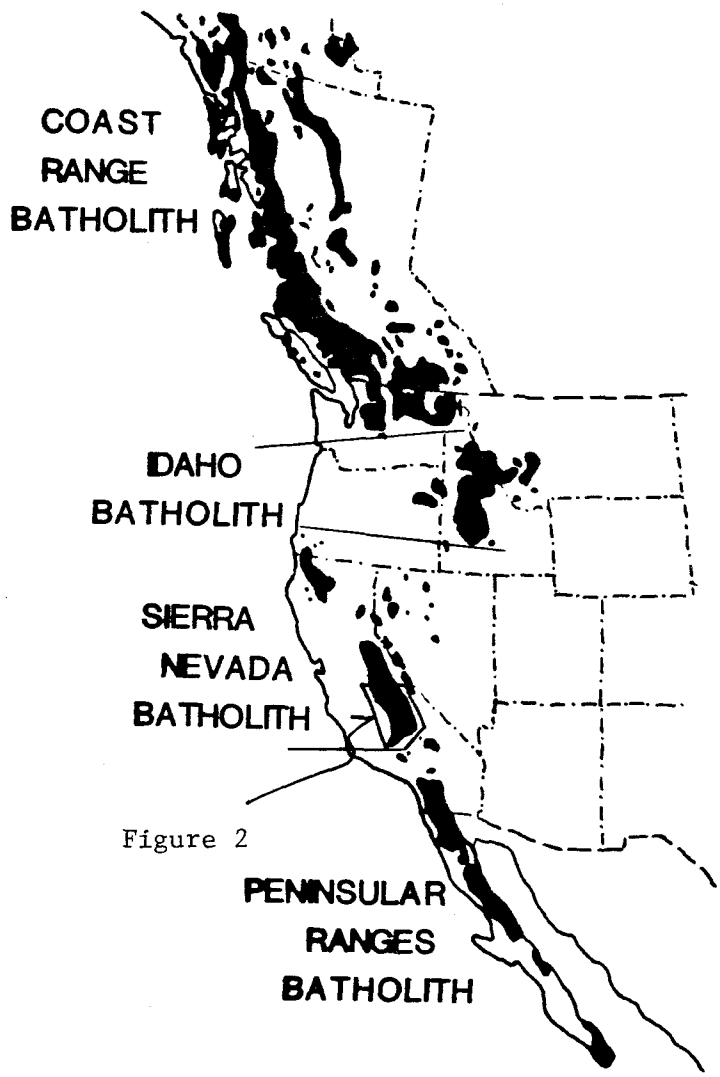

Figure 2

Figure 1. Map of Mesozoic Cordilleran batholithic belt, showing the relationship of the Sierra Nevada batholith to the Coast Range, Idaho, and Peninsular Ranges batholiths. All these batholiths have large components of Cretaceous plutons. After Hill (1984).

Figure 2. Map showing general geology of the south-central Sierra Nevada including major batholithic belts and wallrock domains (map distribution after Saleeby, 1986; initial $^{87}Sr/^{86}Sr$ isopleth after Kistler and Peterman, 1978, except for southernmost Sierra Nevada, which is after Sams and others, 1986). Major Cretaceous batholiths are shown, as is the gneiss complex of the Tehachapi Mountains. Note the lack of pre-Cretaceous batholithic rocks in the southernmost Sierra Nevada, and the overall continuity of the metasedimentary framework rocks in the south-central Sierra.

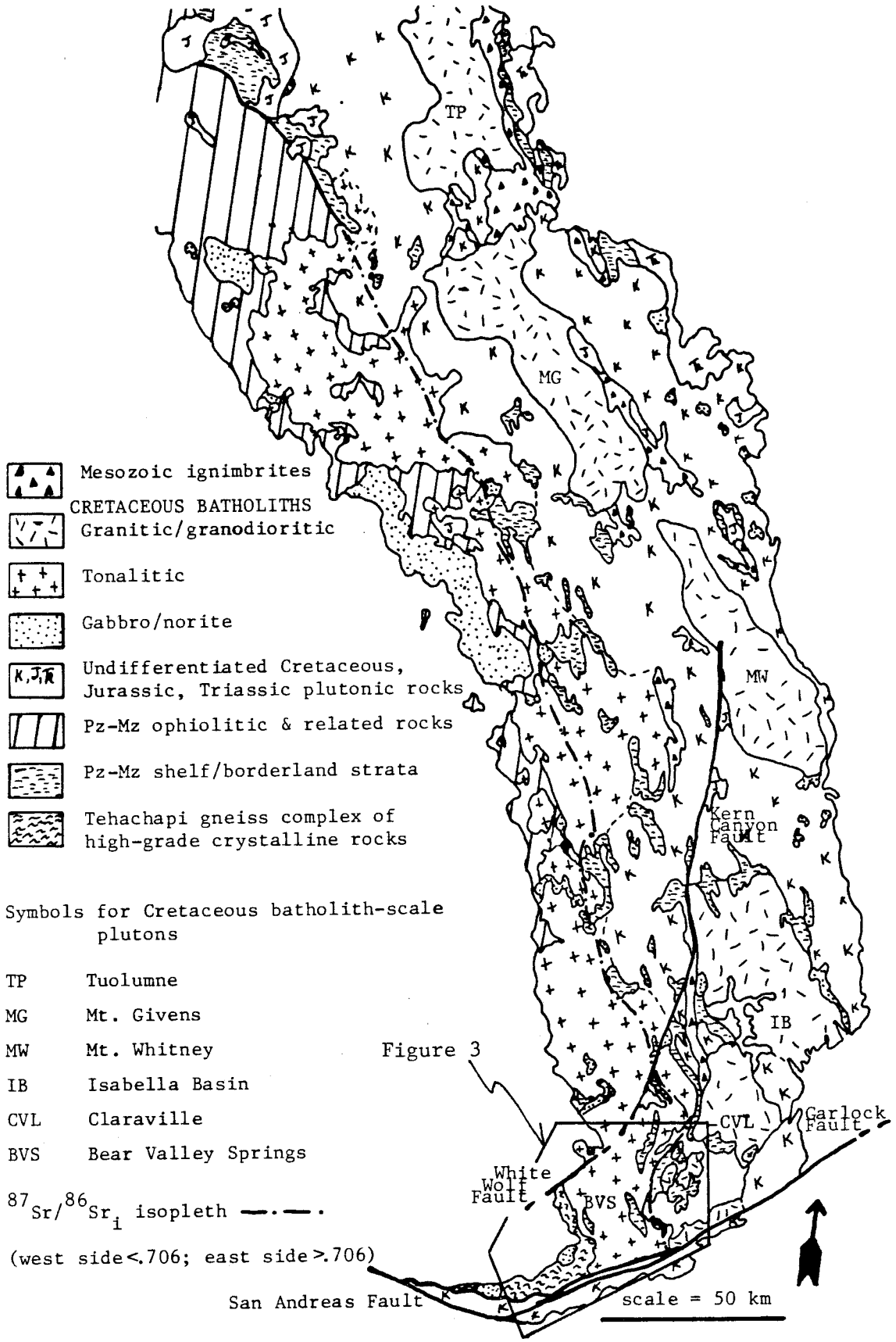
Mesozoic ignimbrites
CRETACEOUS BATHOLITHS
Granitic/granodioritic
Tonalitic
Gabbro/norite
Undifferentiated Cretaceous, Jurassic, Triassic plutonic rocks
Pz-Mz ophiolitic & related rocks
Pz-Mz shelf/borderland strata
Tehachapi gneiss complex of high-grade crystalline rocks
Symbols for Cretaceous batholith-scale plutons
TP Tuolumne
MG Mt. Givens
MW Mt. Whitney
IB Isabella Basin
CVL Claraville
BVS Bear Valley Springs
87Sr/86Sri isopleth
(west side<.706; east side>.706)
Figure 3
TP
MG
MW
IB
CVL
BVS
Kern Canyon Fault
Garlock Fault
White Wolf Fault
San Andreas Fault
scale = 50 km

KEY TO BASE MAPS - SOUTHERNMOST SIERRA NEVADA

UNITS

QT Quaternary/Tertiary cover

UPPER CRETACEOUS

gr undifferentiated granitic plutons
CVL granodiorite of Claraville
MAd tonalite of Mount Adelaide
peg pegmatite dike swarm
Bear Valley Springs igneous suite
BVS tonalite of Bear Valley Springs
BP hypersthene tonalite of Bison Peak
TC metagabbro of Tunis Creek
SS metagabbro of Squirrel Spring

MID-CRETACEOUS

gneiss complex of the Tehachapi Mountains
TJ tonalite gneiss of Tejon Creek
WO diorite gneiss of White Oak
PC quartzo-feldspathic gneiss of Pastoria Creek
CP paragneiss of Comanche Point
ag augen gneiss of Tweedy Creek

PRE-CRETACEOUS

ms metasedimentary septa
RS Rand Schist

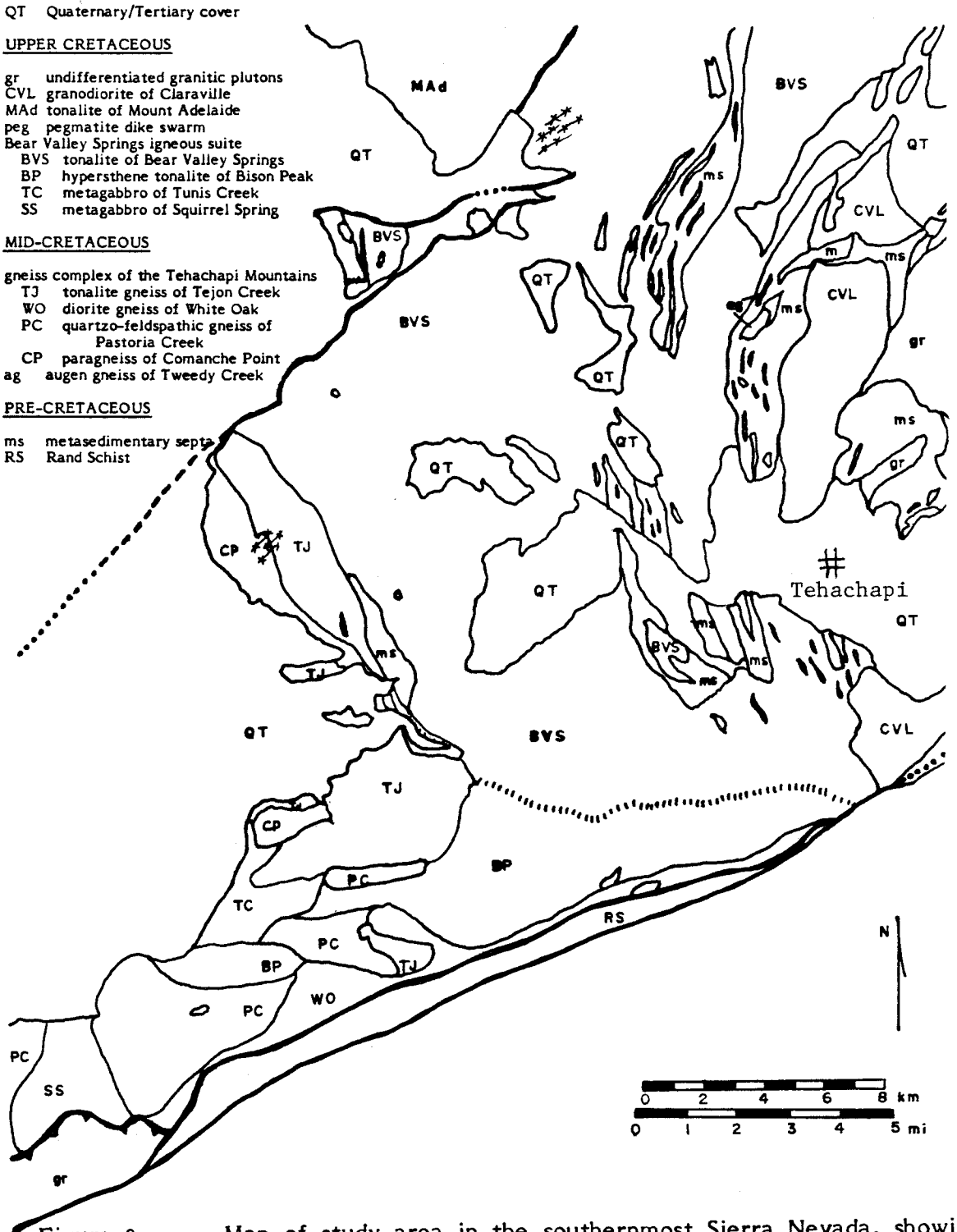

Figure 3. Map of study area in the southernmost Sierra Nevada, showing major crystalline rock units (from Plate 1). Study area is southeast of Bakersfield.

depth of exposure of the Sierra Nevada batholith increases southward from mesozonal levels (about 10 km depth) in the Lake Isabella area to catazonal levels (20 to 25 km) in the gneiss complex. U/Pb age dating on plutonic rocks, and on "granulitic" and amphibolitic gneiss bodies exhibit zircon populations with systematics most suggestive of mid-Cretaceous igneous crystallization (Sams and Saleeby, 1986; Sams and others, 1983). The zircon systematics are for the most part similar to those from mesozonal-epizonal type batholithic plutons of the south-central Sierras (Chen and Moore, 1982; Saleeby and Sharp, 1980).

Zircon studies were initiated in 1981 in order to investigate two major topics: 1) the possible remnants of Proterozoic sialic material within the Sierra Nevada crystalline framework, and 2) structural relations between the Sierra Nevada batholith and gneissic rocks reported in reconnaissance studies by Ross (1980). Geochemical studies by DePaolo (1981b) and Kistler and Peterman (1973, 1978) indicate that Proterozoic sialic material should be a major component in the materials that gave rise to the Sierran batholithic rocks. This material has not been found in the central or southern Sierra Nevada, although zircon U/Pb isotopic signatures indicative of its existence are seen in the southern and central Sierra Nevada batholith (Tobisch and others, 1985; Chen and Moore, 1982; Chen and Tilton, 1978).

The Pelona schist in southern California occurs as the lower thrust plate beneath a varied crystalline terrane, which in part contains Precambrian gneiss (Haxel and Dillon, 1978; Ehlig, 1981, 1968). A similar situation is seen in the Rand Mountains, where the Rand schist occurs below a thrust fault whose upper plate rocks contain Cretaceous granitoids and possible Precambrian gneiss (Silver and Nourse, 1986; Nourse and Silver, 1986; Silver and others, 1984). Ross (1985, 1986) and Sharry (1981b) show the gneiss complex of the Tehachapi Mountains as com-

prising the upper plate structurally above the Rand schist block which occurs between strands of the Garlock fault. Accepting the interpretation that the gneiss complex of the Tehachapi Mountains represents the southern continuation of Sierran bedrock, and accepting the general view that the Rand schist is part of the Pelona schist terrane, then the aforementioned tectonic contact represents the only known pre-Neogene contact between Sierran and southern Californian basement regimes.

A critical question which this study has answered is whether the gneiss complex of the Tehachapi Mountains represents the deepest exposed levels of the Sierra Nevada batholith. This is in fact shown to be the case, and thus this region should provide insights into mesozonal-catazonal transitions and the phenomena of catazonal levels in batholithic belts. The study also provides support for the hypothesis that granulites comprise part of the lower continental crust (Saleeby and others, 1986b; Christensen and Fountain, 1975). A further question is whether the "granulites" represent vestiges of older sialic crust, high-grade metasedimentary or metavolcanic rocks, or merely hot dry zones in a crystallizing and deforming plutonic complex. As discussed below, the latter is suggested by the findings of this study.

This study shows that the crystalline rocks of the southern Sierra Nevada underwent intense mid-Cretaceous deformation. Eocene strata lie unconformably on the crystalline bedrock in the Tehachapi Mountains (Nilsen and Clarke, 1975; Harris, 1954), which along with age (this report; Sams and others, 1983) and geobarometric data (Sharry, 1981a) suggest a rapid uplift of the gneiss terrane. The uplift and exposure of the probable deep-seated crystalline rocks may be related to a southern California thrusting event (Silver, 1982, 1983; Haxel and Dillon, 1978), and/or a major Cretaceous deformational episode as recognized in the

central Sierras (Nokleberg and Kistler, 1980; Tobisch and Fiske, 1982). Investigations were performed to establish the duration, areal extent, style, cause, and significance of the deformational episode in the southern Sierras.

I.2. Scope of thesis investigations and goals of study

This study encompasses much of the crystalline rocks of the southernmost Sierra Nevada and Tehachapi Mountains. Work has extended from just east of Grapevine Canyon (Interstate Route 5) on the west and the Garlock fault on the south, to lines running approximately east-west about 15 km north of Tehachapi (around Caliente and Loraine) and running north-south about 10 km east of Tehachapi. It investigates the petrography, field relations, geochemistry, and zircon geochronology of the crystalline rocks of the region. In addition, it addresses many of the questions posed in the preceding section in a topical manner. The goals of this study were the following: 1) to characterize the major and critical plutonic and gneissic units by field relations, petrography, and U/Pb zircon geochronology; 2) to study the proposition that the region is the deep and locally dry level of the Sierra Nevada batholith as suggested by the presence of granulite-affinity rocks and other garnet- and magmatic epidote-bearing granitoids; 3) to study a major deformation as expressed in mid-Cretaceous blastomylonitic augen gneisses and deformed granitoid dikes; 4) to determine whether the crystalline rocks of the Tehachapi Mountains are the southward continuation of similar rocks in the Sierra Nevada, or if a major tectonic break separates the two; and 5) to help provide a geochronological and petrologic basis for the testing of possible correlations between the crystalline rocks of the southernmost Sierra Nevada-Tehachapi Mountains and the Salinian, Transverse Ranges, and Mojave blocks.

The ultimate aim was to establish the fundamental nature of the gneiss complex of the Tehachapi Mountains and associated plutonic rocks. Clarification

of the age and character of the crystalline terrane in the southernmost Sierra Nevada and Tehachapi Mountains will contribute to our understanding of the Sierra Nevada batholith and its metamorphic framework, and to the understanding of the tectonic development of the southwestern Cordillera.

A summary of the field, petrographic, and geochronological data available for the various units present in the southern Sierra Nevada and Tehachapi Mountains is presented in this chapter. More detailed information regarding each unit is given in a sequential fashion in Chapter II. The results of the geochronological investigations are given in Chapter III. The conclusions of this study are presented in Chapter IV, and address the topics listed under goals of study. Detailed zircon U/Pb geochronology analytical techniques are found in the Appendix.

I.3. Summary of geology

The western North American Cordilleran Mesozoic batholithic belt is depicted in Figure 1, illustrating the relation of the Sierra Nevada batholith to the Coast Range, Idaho, and Peninsular Ranges batholiths. Figure 2 shows the general geology of the south-central Sierra Nevada, with emphasis on the major Cretaceous batholith-scale plutons and various wallrock domains. Note the voluminuous Cretaceous batholiths, and relative paucity of pre-Cretaceous batholithic material in the southern Sierra. A map of the study area in the southernmost Sierra Nevada and Tehachapi Mountains is shown in Figure 3, which is generalized from Plate 1. Topographic map coverage of the study area is shown in Figure 4, while notable landmarks are found in Figure 5. Major geographic features are the San Joaquin, Cummings, and Tehachapi Valleys, Bear and Cummings Mountains, Tejon and Grapevine Canyons, and the cities of Bakersfield and Tehachapi.

The area of interest consists of the southern end of the Sierra Nevada, with a regional north-northwest trend that swings around to an east-northeast orienta-

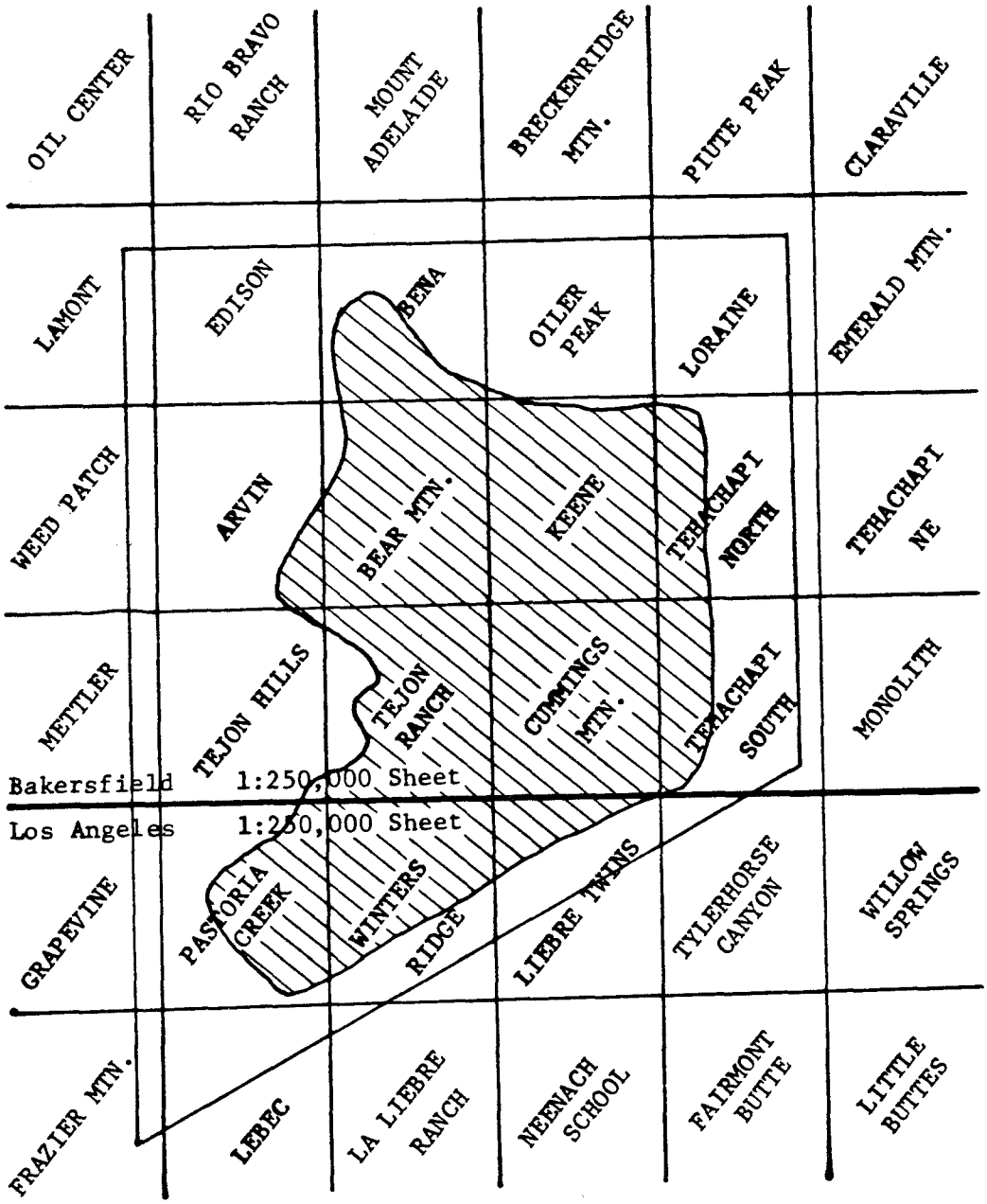

Figure 4. Map of U.S.G.S. topographic sheets (7.5' quadrangles) covering area of Figure 3 (polygon), and area of primary interest (ruled).

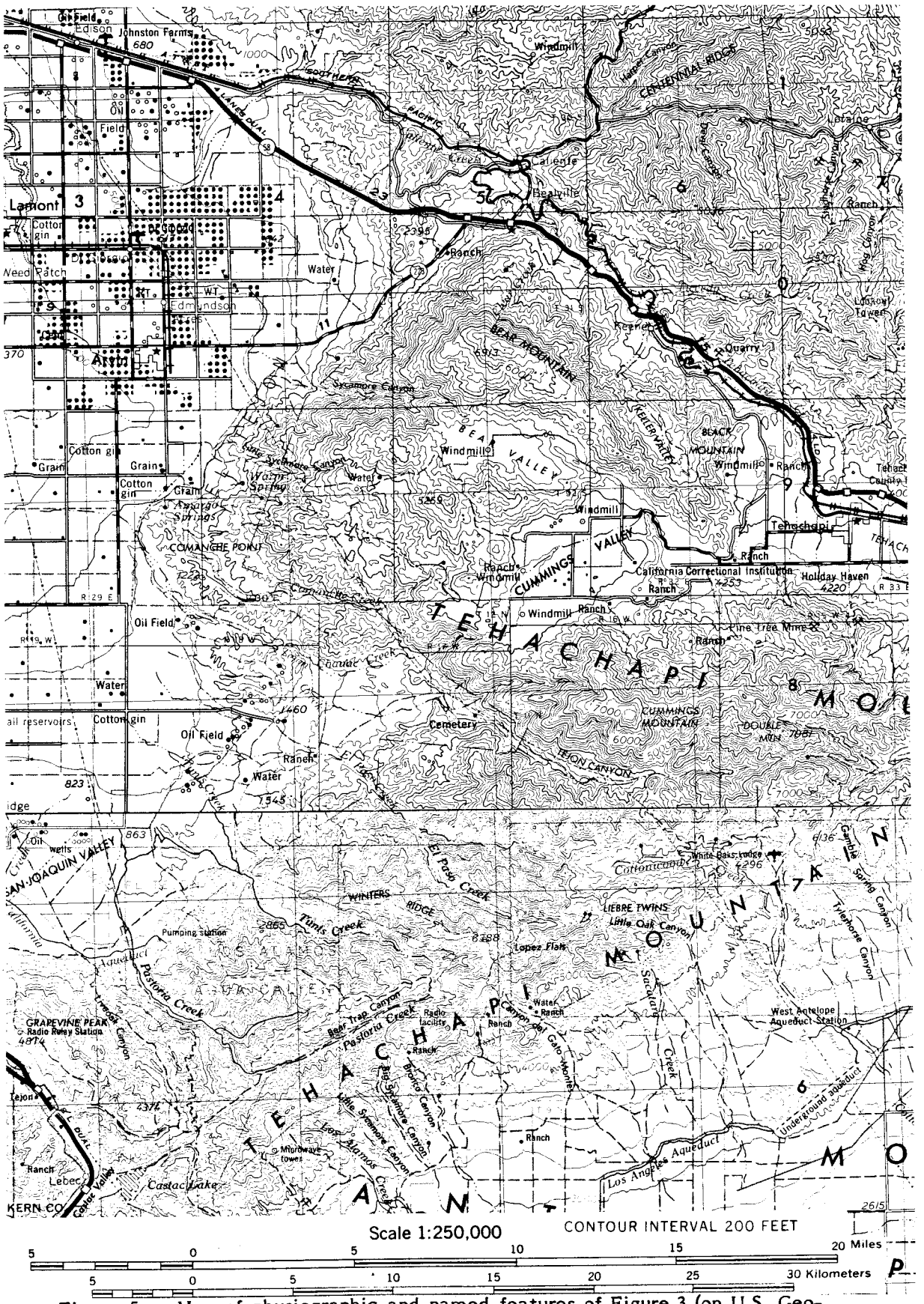

Figure 5. Map of physiographic and named features of Figure 3 (on U.S. Geological Survey 1:250,000 Los Angeles and Bakersfield base maps).

tion in the Tehachapi Mountains (the Sierran "tail" of Ross, 1980, 1986). The area of study exceeds 1000 km^2, of which some 300 km^2 are in the Tehachapi Mountains. The mountainous regions are underlain primarily by crystalline rock. Eocene to Holocene strata overlap the crystalline basement along the southern and southeastern margins of the San Joaquin Valley. The strata has moderate to shallow dips towards the valley.

Elevations range from less than 1000' to slightly lower than 8000'. The mountaintops are rounded, rolling masses with steeply incised canyons. The uplands suggest an old erosional surface due to their topographic expression and near even altitudes. Northern slopes are densely vegetated, while southern slopes are more open. Weathering for the most part has been deep, forming a thick soil horizon. Fresh outcrops are scarce; primitive roads form the best observable outcrops, although small hillside outcrops are present.

Access is moderately thorough via private primitive roads of widely varying conditions; a large portion of the area, especially the gneiss complex, is owned by the Tejon Ranch Company. Only a small percentage is public land. Public access is through Interstate Route 5 on the western extremity, California Route 58 across the northern half of the area, and along Comanche Point Road, a moderately well maintained primitive road running from Cummings Valley to the floor of the San Joaquin Valley.

Faults within the study area are the Garlock, White Wolf, Pastoria, and Pleito faults. The Garlock fault is an east-northeast trending fault that has steep dips. It has been described as an intra-continental transform that separates the Basin and Range-Sierra Nevada provinces from the Mojave province (Davis and Burchfiel, 1973). It has approximately 50 km of left-lateral basement offset (Ross, 1986). Within the study area, the Garlock fault has two branches that

encase a horse of Rand schist (Sharry, 1981b; Ross, 1986). The northern branch may represent reactivation of a moderate to low angle north dipping fault thought to represent thrusting of the Rand schist under the crystalline terrane of the Tehachapi Mountains (Sharry, 1981b). The White Wolf fault is a northeast trending active fault. In 1952 the 7.7 magnitude Tehachapi-Arvin earthquake was centered on the fault. The surface trace and aftershock foci indicate a southeast dipping reverse fault that has components of left slip (Buwalda and St. Armand, 1955; Ross, 1986). The Pleito fault is an active(?), southeast dipping low angle fault that places crystalline rock over Cenozoic strata west of Grapevine Canyon (Hall, 1984). The Pastoria thrust is a southeast dipping, low angle fault that places the granodiorite of Lebec over the gneiss complex of the Tehachapi Mountains (Ross, 1986; Crowell, 1952), and may represent the westward extension of the northern branch of the Garlock fault (Ross, 1986; Crowell, 1952).

The southernmost Sierra Nevada and Tehachapi Mountains consist primarily of crystalline rocks that are overlain unconformably by middle to upper Eocene marine strata (Nilsen and Clarke, 1975; Harris, 1954). Prevailing structures within the crystalline rocks are foliation surfaces and lithologic contacts. These are generally northwest trending north of Tehachapi (Figure 3), and northeast to south trending to the south. Typical Sierran batholithic rocks can be traced southward to the vicinity of Tejon Creek, a prominent east-west canyon, where they grade into the gneiss complex of the Tehachapi Mountains. Metasedimentary pendants within the batholith, whose structures parallel those in the batholith, are also traceable to Tejon Creek, where they terminate. However, small bodies of quartzite, marble, and calc-silicate rock can be found south of Tejon Creek. The southernmost Sierran plutonic and metasedimentary rocks resemble analagous rocks to the north, and have been traced in reconnaissance fashion north to the

Lake Isabella area (Ross, 1980; Saleeby and others, 1978; Saleeby and Sams, unpublished field work).

The gneiss complex of the Tehachapi Mountains is herein defined as a collection of gneisses that have U/Pb ages of between 110 and 120 Ma, and contain high-grade deformational fabrics (transposition of internal contacts, gneissic banding consisting of mylonitic and crystalloblastic textures). It is comprised of an assortment of heterogeneous gneisses that range in composition from diorite/tonalite to granite. The gneisses consist of mafic to felsic meta-igneous rocks, with subordinate paragneiss, quartzite, marble, and calc-silicate lenses.

Within the gneiss complex of the Tehachapi Mountains, several units have been distinguished based on field, petrographic, and age relations. Their contacts are typically obscure, but where observed, are generally concordant and gradational. Sharp, intrusive contacts are infrequent, and are restricted to units interpreted to belong to late-stage intrusive bodies within the complex. Much of the gneiss complex appears to have been derived from magma mixing of gabbroic and tonalitic melts, and by mixing of these magmas with migmatitic melts derived from paragneiss enclaves in the complex. The rocks show evidence of residence at high-grade conditions of upper amphibolite to lower granulite facies. Migmatites and apparent complete melts have been produced at least locally. Recrystallization textures are common, and range from blastomylonitic to annealed. Evidence for retrograde reactions involving the replacement of olivine by orthopyroxene and the replacement of pyroxenes by amphiboles can be found, while evidence for prograde reactions is sparse.

It is possible to divide the crystalline rocks of the southernmost Sierra Nevada into three major suites based on age, structural relations, and deformational fabrics. The first suite, herein termed the Tehachapi suite, and dated at

110-120 Ma, includes the gneiss complex of the Tehachapi Mountains and the augen gneiss of Tweedy Creek. It consists of rocks that show a major deformational fabric exhibited by gneissic banding, high-grade recrystallization, and blastomylonitic to local mylonitic fabrics. The fabrics appear to be the result of pervasive deformation under high temperature conditions. Many of the bodies in this suite consist of lenses of varying composition that have been strongly transposed. The fabrics are occasionally overprinted by textures developed in or as the result of intrusion of the second suite. These rocks have lost any remnant of previous textures.

The second suite, defined here as the Bear Valley Springs intrusive suite, consists of the tonalite of Mount Adelaide, the tonalite of Bear Valley Springs, the hypersthene tonalite of Bison Peak, and the metagabbros of Tunis Creek and Squirrel Spring. The members of this suite have ages of 100±2 Ma. The tonalite of Bear Valley Springs has as its southern margin a gradational contact with the Bison Peak unit whose structures parallel those within the pluton. The western margin of the pluton is a gradational(?) contact with tonalite gneiss of the gneiss complex of the Tehachapi Mountains. Structures and foliations within the tonalite gneiss parallel those within the batholith. The metagabbros are ovoid bodies with little internal sub-solidus structure, and often have gradational contacts with dioritic to tonalitic gneisses.

The rocks of the Bear Valley Springs suite locally cross-cut the deformational fabric of the older suite, and contain planar ductile deformation fabrics developed under solidus to hot subsolidus conditions within the tonalitic members, while the gabbroids contain igneous-flow, compositional layering, and crystal accumulation features. They may be distinguished from rocks within the older suite on the basis of local intrusive relations and a lack of gneissic banding. This

intrusive suite is interpreted as the culmination of the high temperature environment represented by the gneiss complex. Deformational fabrics are developed to a much lesser degree than in the preceeding suite. Recrystallization and blastomylonitization fabrics are present, but less pervasive and less well developed compared to those developed in the Tehachapi suite. Mylonitic fabrics are rare.

The third suite (late deformational intrusive suite, dated at 90 to 94 Ma) comprises rocks that frequently cross-cut and postdate the major deformational fabrics in both of the preceding suites. These rocks include the granodiorite of Claraville, a small tonalitic stock intrusive into the augen gneiss of Tweedy Creek, and cross-cutting dikes including pegmatite dike swarms and a garnet granite dike within the Pastoria Creek gneiss. Except for the pegmatites, these rocks show local ductile deformational fabrics in the vicinity of metasedimentary septa, suggesting differential movement localized along or within the septa. The pegmatites lack a strong deformational fabric, and are seen to clearly cross-cut major structures in the first two suites.

I.4. Previous Work

Most of the study area was mapped by Dibblee and Louke (1970), Dibblee and Warne (1970), Dibblee and Chesterman (1953), Crowell (1952), and Wiese (1950) on a scale of 1:62,500 (fifteen minute quadrangles). Their works were generally of a reconnaissance nature, and contained brief petrographic descriptions. They showed the major plutonic units, and the regional similarities of the hornblende biotite quartz diorite batholith (tonalite of Bear Valley Springs) that dominates the region. Their works also showed the general continuity of metasedimentary framework rocks from the vicinity of Lake Isabella to Tejon Creek. They did little work on the gneisses other than to show "more gneissic rocks" from other "plutonic" rocks. Their contacts between the metamorphic septa and plutonic rocks are for the most part the same as those on the compilation map (Plate 1).

One of the earliest works in the area was by Weise (1950), who mapped the Neenach 15' quadrangle in the Tehachapi Mountains. His was a rough, first attempt to create order in the gneissic terrane. He broke out plutonic gabbro and diorite units, a gneiss unit, and described the region as having either a plutonic or ultrametamorphic origin. Most of his units have not been retained, but much of his gabbro-gneiss contact is reflected in the shape of the Tunis Creek unit.

A reconnaissance map of the crystalline rocks of the region was created by Ross (1980, 1986), who compiled the individual works from the previous authors. Ross's work consisted mainly of reconciling the various units into a coherent "stratigraphy" and into a more unified framework. He did reconnaissance traverses throughout the region. A major contribution of his work is a large body of petrographic data and the compilation of previous field and geochemical investigations (Ross, 1980, 1983a,b,c,d, 1986). In his earlier works (Ross, 1980), he did not emphasize the high-grade nature of the Tehachapi Mountain complex. Ross broke out two primary units in the gneiss complex, felsic and amphibolitic gneisses (some garnet-bearing), a transitional-mixed zone between the tonalite of Bear Valley Springs and the gneiss complex, and a number of minor metasedimentary bodies. His gneissic units have not been retained, but his transitional zone between the gneiss complex and the tonalite of Bear Valley Springs essentially corresponds to the tonalite gneiss of Tejon Creek and paragneiss of Comanche Point units.

Further work in the crystalline rocks along both sides of the Garlock fault was done by Sharry (1981b). Sharry was the first to emphasize the high-grade nature of the Tehachapi Mountain gneisses, and he mapped two granulite units (one garnet-bearing) on the basis of the presence of pyroxenes, a quartzofeldspathic gneiss unit, and a cataclastically deformed diorite gneiss unit probably

derived from a Tunis Creek-affinity protolith. He performed geobarometric and geothermometric studies that suggested metamorphic conditions for the gneiss complex of approximately 750°C and 8 kb. Many of Sharry's units have been retained, but have been reinterpreted in light of new data obtained in this work. Many of Sharry's (1981b) contacts within the gneiss complex of the Tehachapi Mountains have been revised, although his basic division of units and their gross shapes have been retained. He did not work in the gneissic rocks in the Tejon Creek area, in the vicinity of the foothills just south of the old Tejon Ranch headquarters, or in the Comanche Point area, thus not approaching the northern edge of the gneiss complex.

I.5. Method of Study

I have mapped the area in a reconnaissance nature, making a number of traverses. In a number of strategic areas (for example Tweedy Creek, Pastoria Creek, Winters Ridge, Plates 2-4), due to the presence of exceptional outcrops, or because of geochronological considerations, I have mapped in much greater detail. Most of the mapping was done on portions of 7.5 minute quadrangles (see Figure 4 for a summary of topographic map coverage). Detailed areas were mapped at that scale, and the Tweedy Creek area was mapped at 1:12,000.

The compilation map (Plate 1) shows the major units, and the important petrography, structure, and deformational fabrics within each unit. These are given as symbols accompanying the conventional attitude symbols. Units have been mapped by petrography most frequently in the gneiss complex of the Tehachapi Mountains, where exposures are infrequent and contacts between units are rare or nondefinitive. The compilation map is shown in a generalized form in Figure 3. Plate 1 is a compilation from several sources: the bedrock geology is taken from this investigation; metamorphic septa-pluton and pluton-pluton con-

tacts north of Tehachapi Pass, and east and southeast of Tehachapi (except for the Tweedy Creek region), are from Ross (1980, 1986); and contacts within and south of the Garlock fault are from Ross (1980, 1986) and Sharry (1981b). Quaternary and Tertiary contacts are from Nilson and Clarke (1975) and Harris (1954).

The description of the major mapped units in Chapter II includes the location, size and extent of the unit; units bounding the described unit, as well as the nature of their contacts (concordant, intrusive, gradational, etc.), textures, structures, and a description of the mineralogy of the unit, including variations and special features. In the discussion, the petrographic classification scheme of Streckeisen (1973, 1976) has been followed. The field relations and petrography of the map units shown in Plate 1 will be described in a sequential fashion. The mineralogy and fabrics of each unit are summarized in a series of Tables (1-11). In particular, the mineralogy containing pyroxene, olivine, and/or garnet; and the textures revealing relict igneous or sedimentary structures, annealing or lower temperature tectonic overprinting, retrograde mineral reactions, and brittle or ductile deformation will be described. An attempt will be made to note the relation between mineralogy and texture, and the interrelations between rock types. In addition, an attempt will be made to speculate on possible origins and protoliths wherever possible. Relevant geochemical data will be explored where such data exists. Plagioclase anorthite content was determined using the method of Michel-Levy (1877) with the petrographic microscope.

Textural terms have been defined in the following manner (after Wise and others, 1984; Bates and Jackson, 1980). Cataclastic textures are produced by mechanical crushing and differential movement within the rock, and are characterized by granular, fragmented, deformed, or strained crystals, with a low recovery to strain ratio. Mylonitic textures are produced by crystal-plastic processes

that produce extreme granulation and diminuation of grain size, with an intermediate recovery to strain ratio. Blastomylonitic textures occur in mylonitic rocks in which some recrystallization or neomineralization has taken place. Blastomylonitic textures have a high recovery to strain ratio, with extensive recovery including annealing. Crystalloblastic textures are produced by recrystallization under conditions of high viscosity and directed pressure. Annealed textures consist of the formation of new grains in the rock after solid-state deformation, while the temperature is still high.

Granulites and granulite facies rocks have been the subject of widely varied definitions, and have lost much of their descriptive purpose. Since the rocks in the area of study have been described as granulites or granulite facies rocks (Sams and others, 1983; Ross, 1983b,c; 1985; 1986; Sharry, 1981a,b), the following definition of granulites is used in this work (after Best, 1982; Williams and others, 1982). A granulite is a metamorphic rock that experienced granulite facies (high-grade regional) metamorphic conditions. Granulites are characterized by the occurrence of two metamorphic pyroxenes. The mineral assemblage is clinopyroxene (augite) + orthopyroxene (hypersthene) + plagioclase ± garnet ± sillimanite or kyanite ± quartz. Primary muscovite is absent. The mafic minerals are often predominantly anhydrous, and typically contain only scarce amounts of amphibole and biotite. The textures are predominantly crystalloblastic or granoblastic. It is suggested below that parts of the gneiss complex of the Tehachapi Mountains experienced upper amphibolite or perhaps lower granulite facies conditions during and immediately following igneous crystallization, but all pyroxenes observed are thought to be pyrogenic.

II. SUMMARY OF FIELD AND PETROGRAPHIC STUDIES

II.1 Order of coverage

The units in this chapter are discussed in a generally northeast to southwest fashion. This is to emphasize the transition from "normal" Sierran crystalline rocks into the gneissic rocks of the Tehachapi Mountains. In particular, the order is: metamorphic framework rocks, rocks of the Bear Valley Springs suite, rocks of the late deformational intrusive suite, and rocks of the gneiss complex of the Tehachapi Mountains. The metamorphic rocks form the structural framework for the igneous and meta-igneous rocks, and include rocks of the Kings sequence and paragneiss of Comanche Point. The augen gneiss of Tweedy Creek was intruded into and shared much of the deformation of the Kings sequence rocks, placing age constraints on the timing of the deformation, and thus it will be discussed in that section. The Bear Valley Springs suite of rocks (tonalite of Mount Adelaide, tonalite of Bear Valley Springs, hypersthene tonalite of Bison Peak, and meta-gabbros of Tunis Creek and Squirrel Spring) are members of a major batholith-scale igneous suite that comprise the most voluminous rocks in the study area, and also provide a basis for an understanding of the rocks within the gneiss complex. Late-deformational intrusive suite rocks (granodiorite of Claraville, tonalite stock, pegmatite and garnet granite dikes) place time constraints on the intrusive and deformational history of the area. Finally, rocks of the gneiss complex of the Tehachapi Mountains (diorite gneiss of White Oak, tonalite gneiss of Tejon Creek, and quartzo-feldspathic gneiss of Pastoria Creek) are discussed.

II.2 Metamorphic framework rocks

Metamorphic rocks occur as remnants of the structural and stratigraphic framework into which igneous and meta-igneous rocks were emplaced. One of the main metamorphic framework assemblages for the southern part of the batholith

is the Jura-Triassic Kings sequence (Saleeby and others, 1978), which consists of marble- and quartzite-bearing psammitic to pelitic schists. Rocks described as Kings sequence extend from the southern part of the study area northward for over 200 km (Saleeby and others, 1978). Metamorphic framework rocks that resemble rocks identified as Kings sequence in the Lake Isabella area (Saleeby and others, 1978; Saleeby and Busby-Spera, 1986) form semi-continuous septa from Tejon Creek to areas north of the study area. These septa are therefore described in this report as Kings sequence rocks. A second assemblage is the paragneiss of Comanche Point, which will be discussed after the Kings sequence rocks. The Comanche Point gneiss may be related to the Kings sequence, or it may represent a different basement assemblage, based on its isotopic characteristics relative to the Kings sequence rocks as discussed in Chapter IV.

The basement rocks for the metamorphic framework rocks in the southernmost Sierra are unknown. The only observed basement to Kings sequence rocks is to the north, where there is a probable westward onlapping of Kings sequence rocks over Paleozoic ophiolitic rock in the Kaweah River area (Saleeby, 1979). Thus the only observed pre-batholithic rocks of the study area are early-Mesozoic (?) continental-derived clastic rocks, shallow water carbonates, ensimatic argillaceous rocks, and possible volcanic rocks.

II.2.1 Kings sequence rocks

Metamorphic framework rocks form semi-continuous septa from Tejon Creek to beyond the northern boundary of the study area (Plate 1). The septa have a maximum width of 3 km, with an average width of 2 km. They extend discontinuously for several tens of kilometers in length, and can be traced continuously for up to 10 km. They may be traced into and beyond the Lake Isabella region (Saleeby and Busby-Spera, 1986).

Two major septa are of concern here. The eastern septum separates the Claraville and Bear Valley Springs plutonic units along most of their entire contact. It is continuously exposed from the vicinity of Tehachapi Peak to beyond the northern limits of study. It is concordantly intruded by both plutonic units, and shows a cross-cutting relation only in the Tweedy Creek area, where it is intruded by both the augen gneiss of Tweedy Creek and a tonalite stock (Plate 2, and discussion below). The second septum forms a screen about one-third of the way into the tonalite of Bear Valley Springs from the east, and separates its eastern marginal and mixed phases. It is concordantly intruded by the tonalite; no cross-cutting relations were noted. This screen is structurally and petrographically similar to the first, but with a seemingly lower quartzite and marble content. It is similar in size, but less continuous than the eastern septum, being more engulfed by the tonalite. A third small septum forms part of the southwestern margin of the tonalite of Bear Valley Springs. It can be distinguished from the paragneiss of Comanche Point to the west on the basis of its containing marble, quartzite, and sillimanite-bearing pelite, and by its sharp intrusive relations (versus diffuse, migmatitic, lit-par-lit contacts of the paragneiss) with the tonalite. This distinction may not be significant, as it may only represent differing degrees of metamorphism and partial melting affecting the paragneiss and metamorphic septum.

Internal schistose fabrics and gross lithologic layering are oriented subparallel to the external contacts of the septa, which are concordant with their outcrop pattern. Foliation surfaces in the metamorphic framework rocks have steep to vertical dips. Foliations (Figure 6) are dominantly steeply east dipping, and northeast to northwest trending. Very few surfaces dip west. The west dips are all very steep, and may in fact be tight to isoclinal folds. The map pattern of the septa (Figure 3) helps define the regional trends of foliation, and describes a

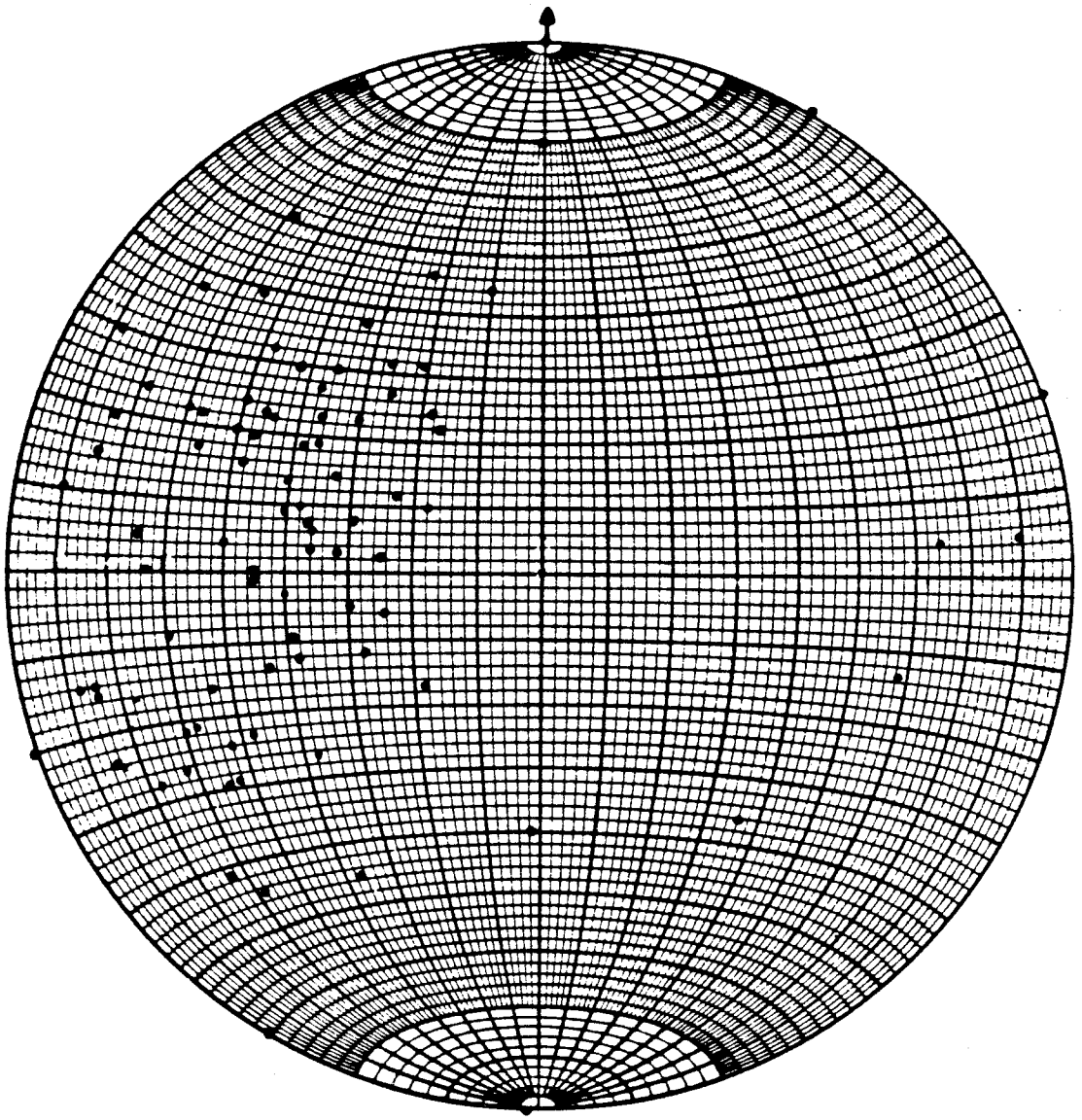

Figure 6. Lower hemisphere projection, equal-area stereoplot of poles to foliation for Kings sequence metamorphic septa rocks.

broad, open z-shape. Tight to isoclinal folds are most commonly seen within marble and calc-silicate layers. Fold axes and stretching lineations plunge moderately to steeply southeast. Sedimentary structures and fossils have not been found in the southernmost Sierra Nevada south of the Lake Isabella area.

The deformational fabrics within the septa at Tweedy Creek are cut by both the augen gneiss of Tweedy Creek and tonalite intrusive stock, and are shared with the orthogneiss. The fabrics define a gneissic foliation and consist of strong coarse crystalloblastic schistosity in the metamorphic rocks and blastomylonitic banding in the orthogneiss. The compositional layering in the metasediments is cut at shallow angles by the intrusive bodies, but the overall fabrics and contacts are concordant. At least part of the fabric in the septum predates the intrusion of the orthogneiss. It appears that the metamorphic framework rocks were deformed, folded into open folds, and had bedding disrupted prior to intrusion of the orthogneiss. The entire assemblage was then flattened and stretched in a moderate to steep southeast plunge, and folds in the metamorphic rocks were tightened into tight to isoclinal folds. The Tweedy Creek orthogneiss has a zircon age of 114±3 Ma. Thus, the relations at Tweedy Creek are important to the regional structural chronology. Deformations involving the folding of metasedimentary septa prior to and after intrusion of mid-Cretaceous plutons have also been seen in the Lake Isabella area (Saleeby and others, 1986a; Saleeby and Busby-Spera, 1986; Saleeby and Sams, unpublished field work).

The metamorphic rocks appear to have had a continental-affinity sedimentary protolith, and consist of a sequence of impure quartzites (~5-10 volume percent), dirty carbonates (~20%), and calc-silicates (≤5%) in a quartz mica schist matrix of psammitic composition (Figure 7). Granofels and gneiss are locally present, especially in the vicinity of Cummings Valley. The marbles and quartz-

Figure 7. Photographs of field relations of gneiss and marble in Kings sequence metasedimentary septum, Tweedy Creek area. Tight to isoclinal folds and steep, southeast-plunging fold axes are well illustrated. The rocks have been strongly transposed, and relict sedimentary features (except for possible compositional layering) have been strongly transposed and obliterated. Photograph (a) is of gneiss, while (b) is marble. Field of view is approximately 45 cm wide in (a) and 2 m in (b).


a

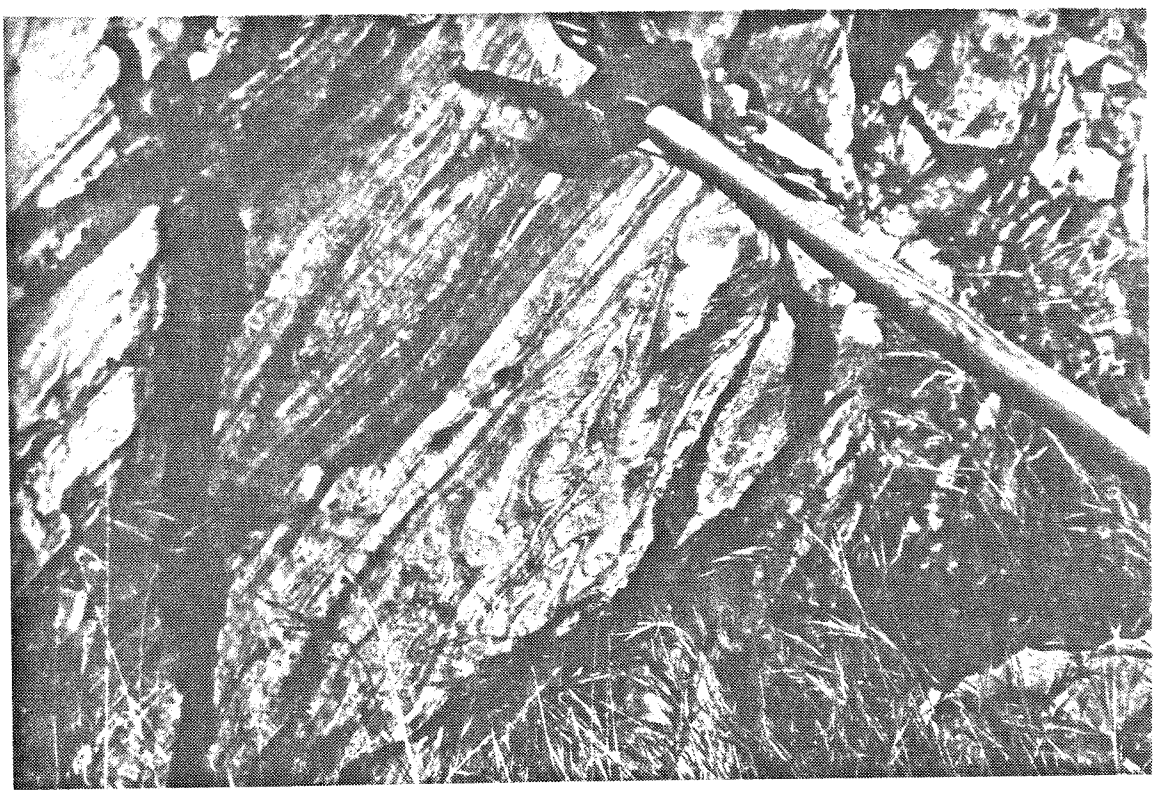

ites are typically massive to faintly banded, range from ~5-500 m in width, and can be traced for up to 10 km in extent. Marble is sometimes found completely encased in plutonic rocks. Quartzite may be found to grade into psammitic schist of the host matrix. Within the southern portion of the septum west of Cummings Valley, and in the small westernmost septum, the schistose rocks commonly contain sillimanite ± garnet. Coarse tectonitic schists with local migmatitic structures, granofels, and gneisses are commonly found there, giving the impression of an overall higher metamorphic grade as compared to rocks at locations to the north and east. These higher grade rocks may in fact grade into the migmatitic paragneiss of Comanche Point. Andalusite is not found in the study area. Psammitic schists predominate over those of pelitic composition. The low abundance and discontinuous appearance of aluminosilicates indicates the lack of proper bulk chemistry to produce such minerals in the metasedimentary material.

The metamorphic rocks show an overall uniformity in texture and mineralogy throughout the study area (Table 1). The marble is predominantly a calcite marble. It is medium- to very coarse-grained, completely recrystallized, white to blue-gray, banded on a centimeter scale, and contains stringers of graphite, and less commonly, siliceous material, probably derived from chert, with subordinate calc-silicate minerals. Quartzites (Figure 8) range from about 60 to 90 percent quartz. Plagioclase, K-feldspar, muscovite, biotite, and clinopyroxene are the most common accessories. Other less common minerals are garnet, graphite, and detrital zircon. Concentrations of accessories in the quartzites frequently occur in lenses that may represent transposed sedimentary bedding. Probable protoliths for the quartzites are orthoquartzites and arkosic sandstones. Calc-silicate layers are associated with the marble, and contain pale green clinopyroxene, plagioclase, hornblende, garnet, and epidote. The quartz mica schist matrix is coarse-grained,

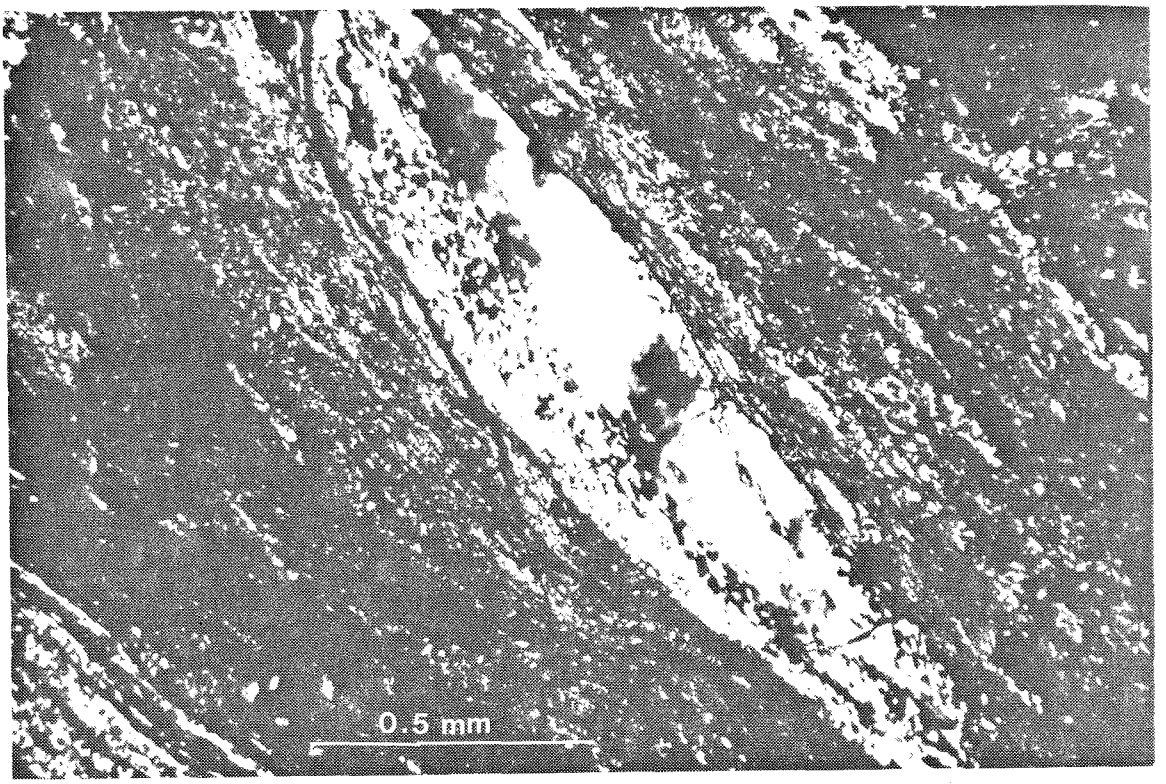

Figure 8. Photomicrograph of quartzite in Kings sequence metasedimentary septum, Tweedy Creek area. Light mineral in pod is quartz, light minerals in groundmass are quartz and feldspar, dark mineral is biotite. Note the high degree of deformation and recrystallization. Field of view is approximately 2 mm wide.

TABLE 1. SUMMARY OF PETROGRAPHY OF KINGS SEQUENCE METASEDIMENTARY FRAMEWORK ROCKS†

HAND SAMPLE	ROCK NAME	CI	QTZ	PLG	(An)	KSP	HBL	BIO	CPX	OPX	GAR	SPH	APA	ZIR	OPQ	EPI	CHL	MUS	OTH	TEXTURES ANL	RXL	MYL	CST	RTR
CM2	qf gneiss	5	20	35	x	40		5													x	x		
CM3b	qf gneiss	10	20	40	20	30		10														x		
CM3c	qf gneiss	10	25	50	x	15		10																
CM6	qf schist	10	30	40	x	20		10																
CM20	qf schist	15	45	25	x	0		15										10						
TC7	quartzite	8	70	25	40			8										1			x	x		
TC8	qf gneiss	10	40	25	40	20		2			8							3			x	x		
TC9	qf schist	10	50	15	x										10			25			x	x		
TC10	hornfels	5	20			70												10			x	x		
TC16	qf schist	20	20	40	x	20		20										10			x	x		
TC17	qf schist	25	25	50	x			25										2			x	x		
TC18	qf gneiss	5	30	40	30	25		5										2			x	x		
CM162a	qf gneiss	20	50	30	x			20												x				
PM540	qf schist	18	35	35	x			15							3			15						
CM640§	quartzite	18	50	10	x	20			15			x		2	3			1	graph					
CM653	qf gneiss	25	40	15	x			25										5	sill15					

† key to abbrevations:
CI = color index; QTZ = quartz; PLG (An) = plagioclase with Anorthite content after Michel-Levy (1887); KSP = K-feldspar; HBL = hornblende; BIO = biotite; CPX = clinopyroxene; OPX = orthopyroxene; GAR = garnet; SPH = sphene; APA = apatite; ZIR = zircon; OPQ = opaques; EPI = epidote; CHL = chlorite; MUS = muscovite; OTH = other; cumm = cummingtonite; graph = graphite; oliv = olivine; scap = scapolite; ser = sericite; sill = sillimanite; ANL = annealed; RXL = recrystallized; MYL = mylonitic or protomylonitic; CST = cataclastic; RTR = retrograded; qz = quartz; grdiorite = granodiorite; qf = quartzo-feldspathic; Ca-silc = calc-silicate; pxhbdite = pyroxene hornblendite. Rock names after Streckeisen (1976, 1973).

§ U/Pb zircon geochronology sample.

and contains quartz, plagioclase, K-feldspar, red to brown biotite, muscovite, and garnet (Figure 9). Sillimanite is present only where pelitic schist occurs.

The eastern septum displays a crystalloblastic schistosity, while the same lithologies in the western septum have experienced a greater degree of metamorphic recrystallization. The small septum along the southwestern margin of the tonalite of Bear Valley Springs has the same assemblage as the other two septa, but has experienced a higher degree of metamorphism. It typically is a granofels or gneiss.

Overall, the metamorphic framework rocks are very similar in lithology and structure to the metamorphic Triassic to early Jurassic Kings sequence rocks identified by Saleeby and others (1978) in the south-central Sierras. Stratigraphic relations and protolith structures have been preserved in the Lake Isabella area (Saleeby and Busby-Spera, 1986), where the assemblage consists of orthoquartzite, arkosic sandstone, marble, calc-silicate layers, and psammitic to quartz-rich schist with pelitic intervals. Similar appearing metamorphic rocks form continuous screens southward from the Lake Isabella area into the Tehachapi Mountains, where they appear to terminate at Tejon Creek. However, impure quartzites, calc-silicates, and marbles are found, although in a very small proportion, even in the gneiss complex of the Tehachapi Mountains.

Metavolcanic rocks have not been observed south of Piute Mountain, although felsic and basaltic volcanic rocks form part of the assemblage at Lake Isabella. Mid-Cretaceous silicic tuffs can be traced to within 15 km of the study area (Saleeby and Kistler, unpublished data; Sams and others, 1983), while older silicic tuffs can only be found as close as Mineral King (150 km north). Mafic to intermediate volcanics occur only as near as 200 km (Tule River area) within the Sierra Nevada.

Figure 9. Photomicrographs of quartz mica schist (top) and gneiss (bottom) in Kings sequence metasedimentary septum. Location is in Tweedy Creek area. Light minerals are quartz and feldspar, dark mineral is biotite. Note the high degree of deformation, and the isoclinal folding. Field of view is approximately 2 mm wide.

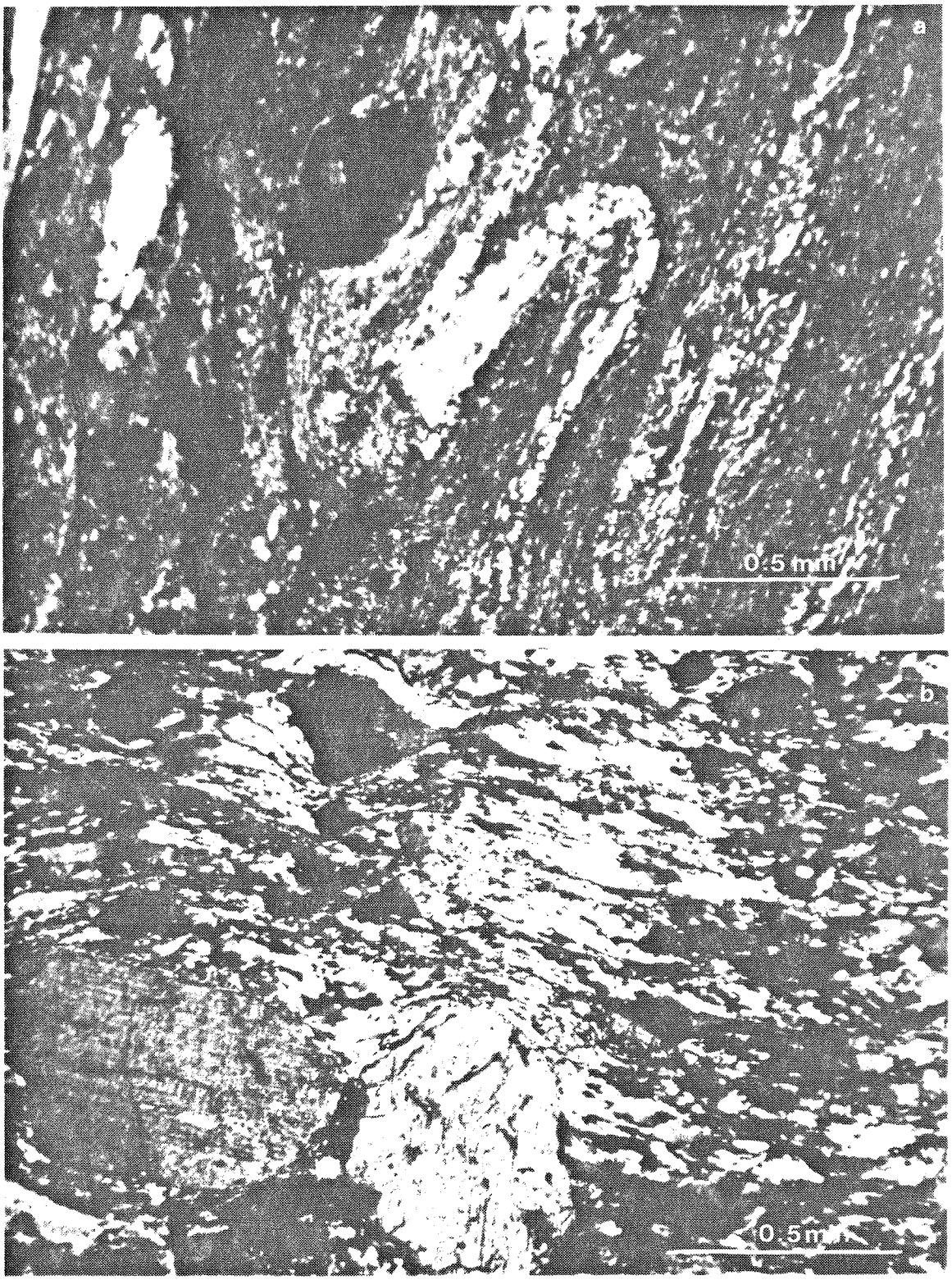
a
0.5 mm
b
0.5 mm

Zircon age determinations on a quartzite in the metamorphic rocks suggest a detrital zircon component derived from an upper-Proterozoic crystalline source terrane (see Chapter III). The nearest fossil locality to the study area is at Lake Isabella, where Saleeby and Busby-Spera (1986) and Saleeby and others (1978) describe a late Triassic to early Jurassic bivalve. Similar aged fossils have been found in the Kings sequence further north (Saleeby and others, 1978).

II.2.2 Augen gneiss of Tweedy Creek

In the Tweedy Creek area (about 20 km northwest of Tehachapi), a strongly mylonitized and recrystallized orthogneiss intrudes the Kings sequence metamorphic framework rocks (Plate 1,2). The orthogneiss is strongly mylonitic with conspicuous 1-2 cm K-feldspar megacrysts set in a foliated groundmass (Figure 10). The orthogneiss consists of two lenticular bodies with an overall outcrop area of ≤ 5 km^2 that are bisected by Tweedy Creek. The gneiss is homogeneous within and between the two bodies. The northern body has an outcrop pattern that resembles a dike concordantly intruding the septum, while the larger southern body has a lensoidal outcrop pattern. The orthogneiss shows intrusive relations where it cross-cuts deformational fabrics in the septum, but it has an overall concordant contact with septum rocks (as discussed above). It has a very strongly developed foliation oriented parallel to that in the metasediments, and shares much of the deformational fabric with the septum. The foliation is restricted to northeast trends, with moderate east dips (Figure 11). The augen gneiss is in turn concordantly and discordantly intruded by the tonalite stock described below. The orthogneiss has an apparent 114±3 Ma igneous crystallization age.

The augen gneiss (Table 2) has a blastomylonitic texture that is characterized by porphyroclasts of pink to red K-feldspar that range in size from one-half to four cm in greatest dimension (Figure 10b,12). The augen are set in a ductilely

Figure 10. Field photograph and thin section photomicrograph of augen gneiss of Tweedy Creek. (a) shows conspicuous K-feldspar augen visible in the field, with a strongly developed foliation. Field of view is about 0.8 m. (b) shows recrystallized quartz and biotite, rounded and brittlely deformed feldspars, and blastomylonitic fabric. Field of view is approximately 2 mm wide in photomicrograph. Minerals are qz=quartz, pg=plagioclase, Kf=K-feldspar, bi=biotite.

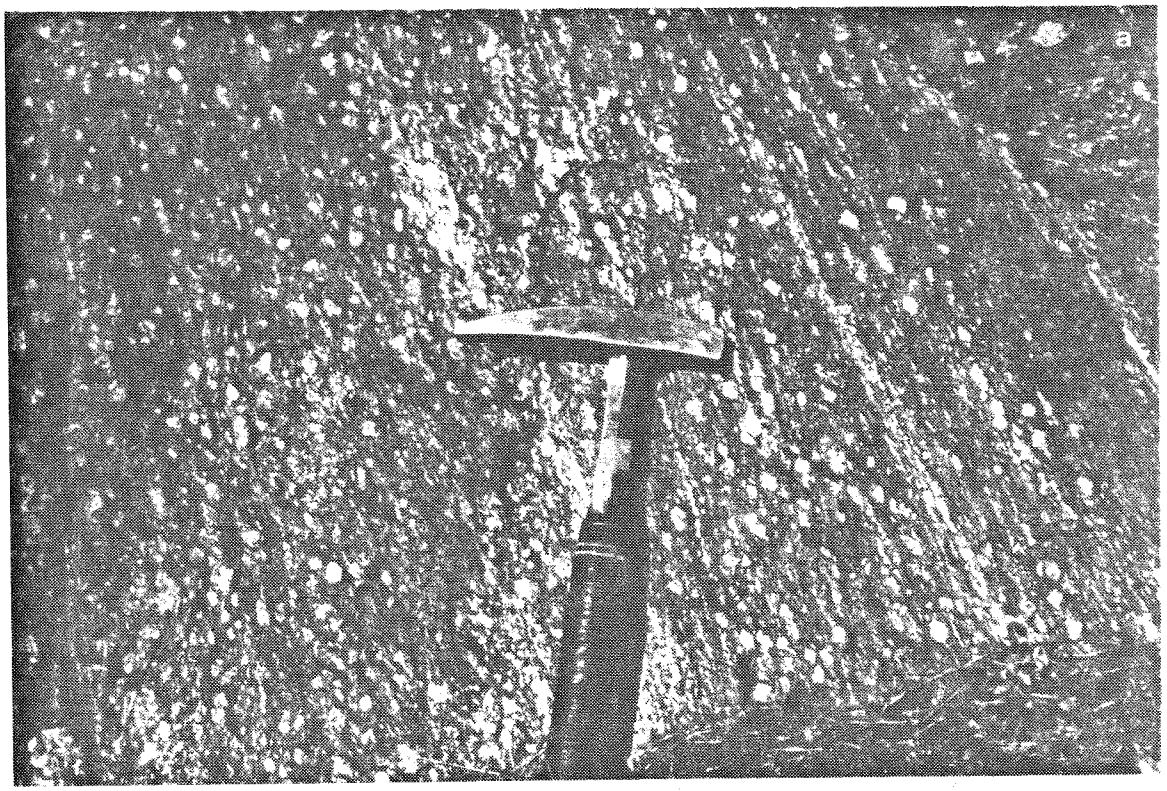
a

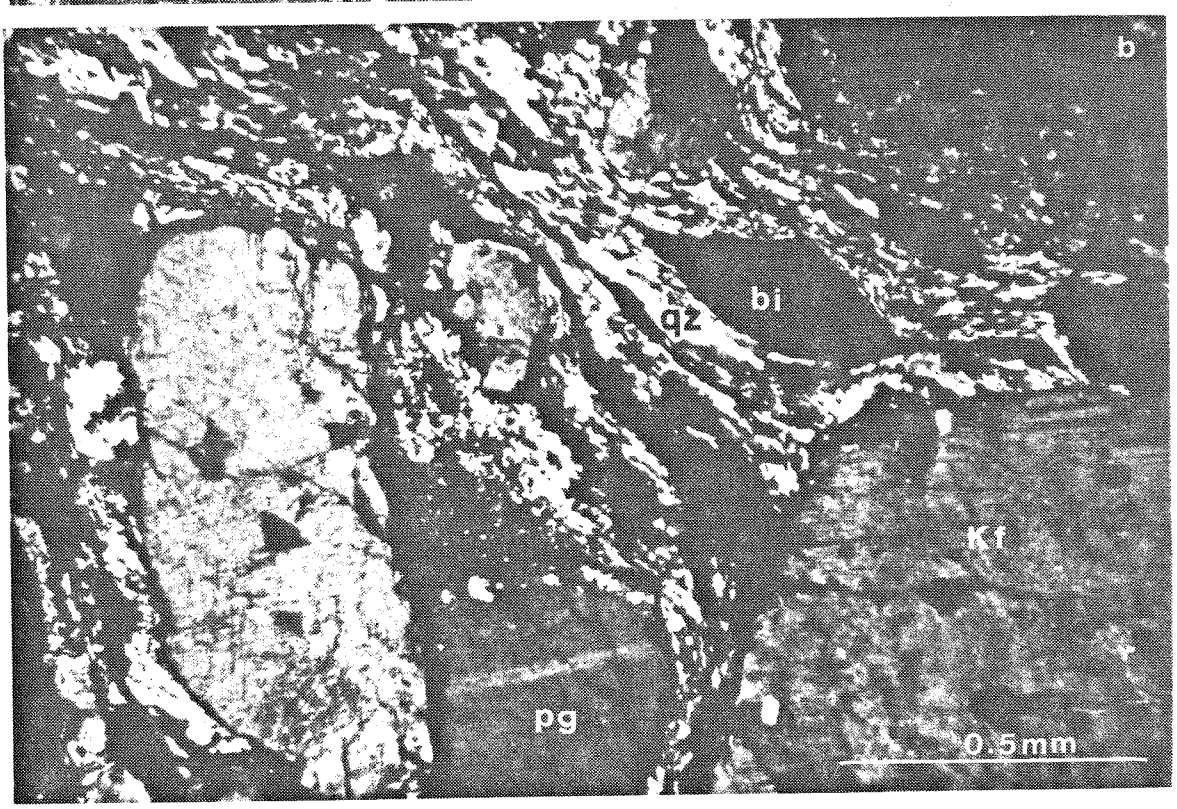
b
bi
qz
Kf
pg
0.5mm

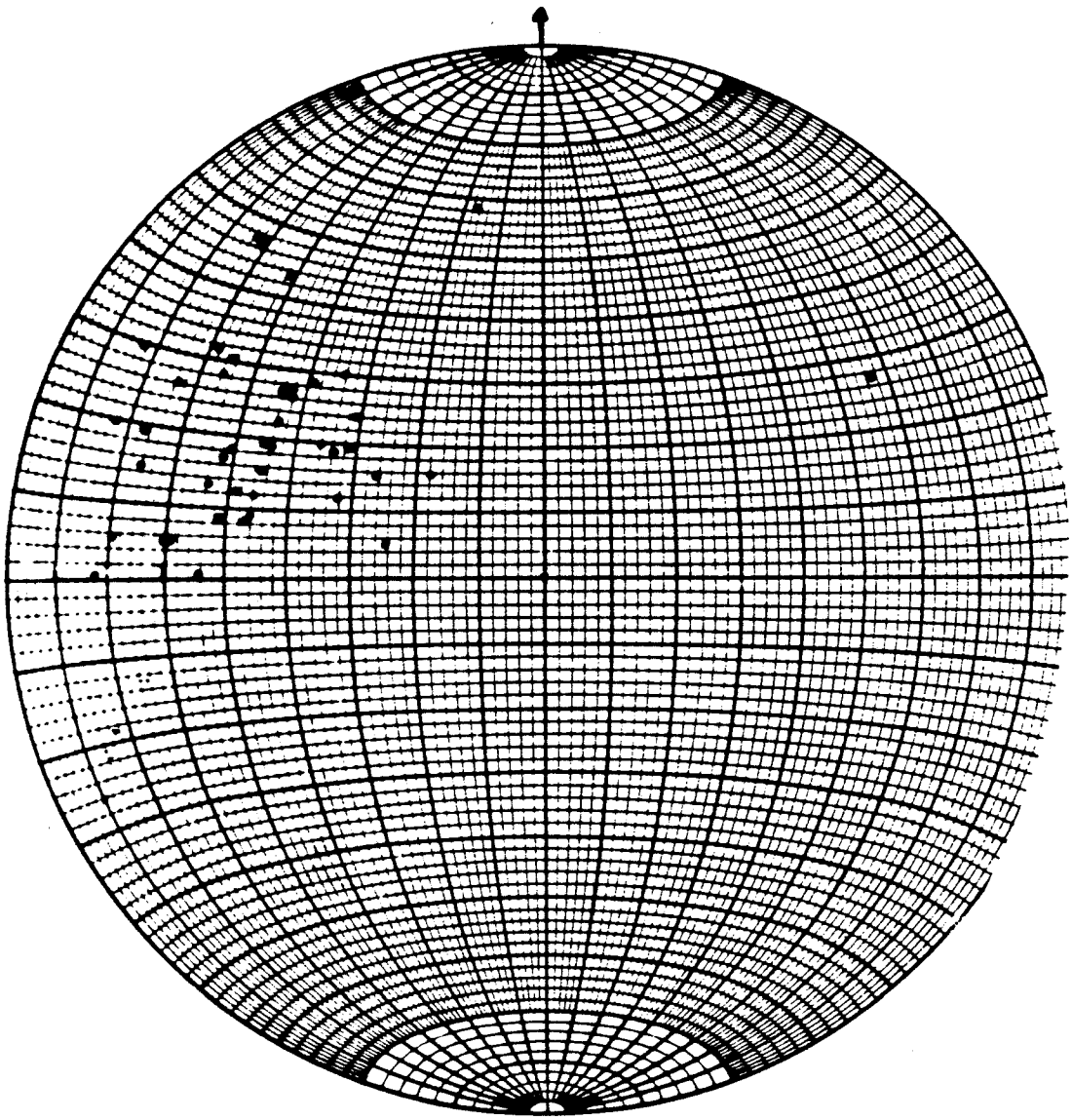

Figure 11. Lower hemisphere projection, equal-area stereoplot of poles to foliation for augen gneiss of Tweedy Creek.

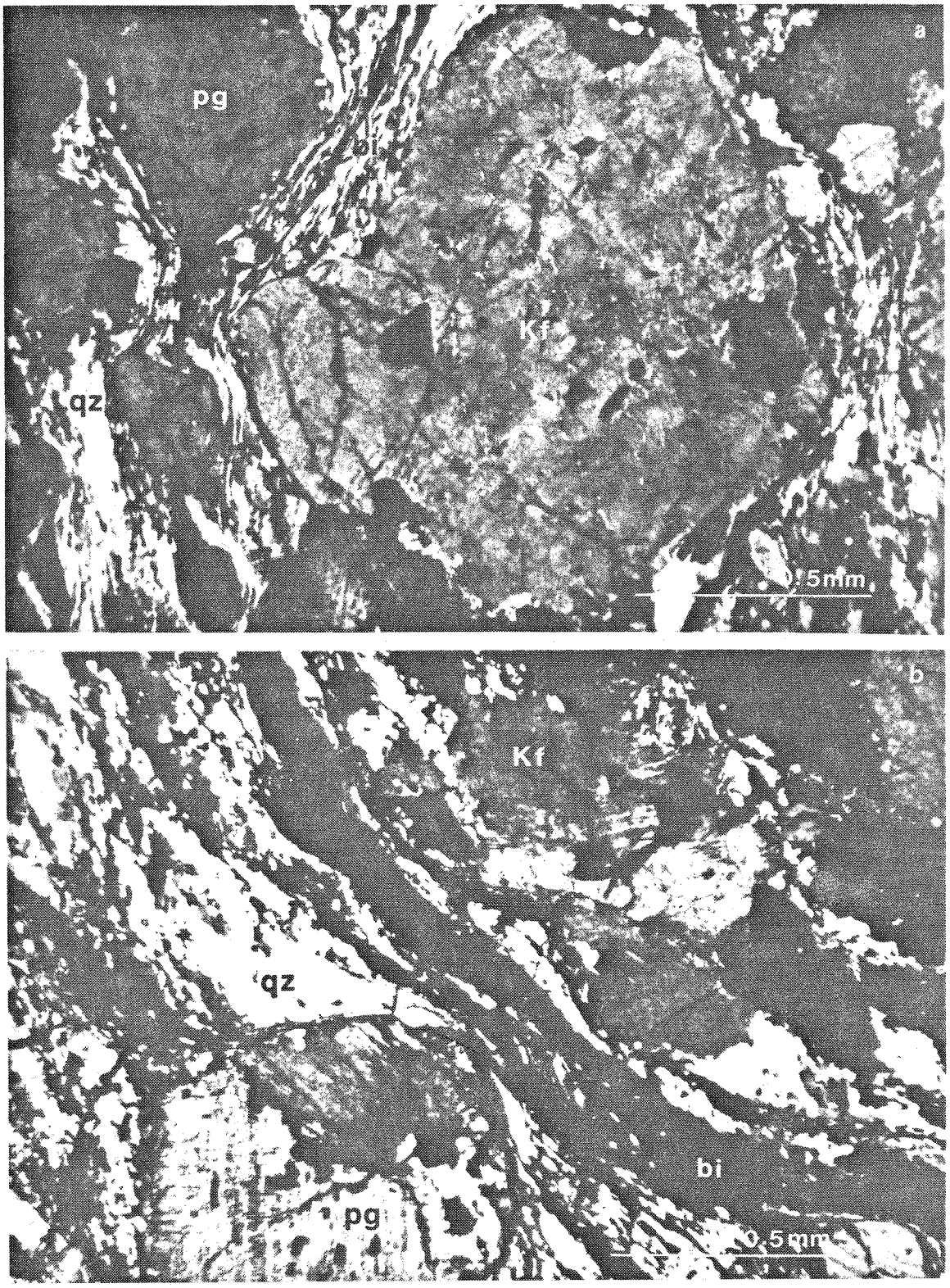

Figure 12. Photomicrographs of augen gneiss of Tweedy Creek showing brittle behavior of feldspar and ductile behavior of quartz. Width=2 mm. Minerals are qz=quartz, pg=plagioclase, Kf=K-feldspar, bi=biotite.

TABLE 2. SUMMARY OF PETROGRAPHY OF THE AUGEN GNEISS OF TWEEDY CREEK†

HAND SAMPLE	ROCK NAME	CI	QTZ	PLG	(An)	KSP	HBL	BIO	CPX	OPX	GAR	SPH	APA	ZIR	OPQ	EPI	CHL	MUS	OTH	TEXTURES ANL	RXN	MYL	CST	RTR
TC0	grdiorite	10	40	35	20	15		10													x	x		
TC1a	grdiorite	12	40	35	25	10		10					x		2		2				x	x		
TC1b	granite	10	30	20	x	40		10				x					x		ser		x	x		
TC2	tonalite	17	20	60	30	4		12							5				ser		x	x		
TC3	granite	10	30	20	x	40		10													x	x		
TC5	grdiorite	12	30	25	30	40		8							4						x	x		
TC11	tonalite	15	45	40	40			15													x	x		
TC12a§	grdiorite	14	35	30	30	20		10							2		2				x	x		
TC13	grdiorite	15	25	45	x	15		15													x	x		
TC20a	tonalite	15	30	50	30	2		15									x		ser		x	x		
TC38	granite	10	20	25	30	45		8							2				ser		x	x		
TC41	grdiorite	10	40	40	x	10		10											ser					
MAFIC INCLUSIONS																								
TC12b§	amphibolite	46	10	45	50		25	15				2	2							x				

† key to abbrevations:
CI = color index; QTZ = quartz; PLG (An) = plagioclase with Anorthite content after Michel-Levy (1887); KSP = K-feldspar; HBL = hornblende; BIO = biotite; CPX = clinopyroxene; OPX = orthopyroxene; GAR = garnet; SPH = sphene; APA = apatite; ZIR = zircon; OPQ = opaques; EPI = epidote; CHL = chlorite; MUS = muscovite; OTH = other; cumm = cummingtonite; graph = graphite; oliv = olivine; scap = scapolite; ser = sericite; sill = sillimanite; ANL = annealed; RXL = recrystallized; MYL = mylonitic or protomylonitic; CST = cataclastic; RTR = retrograded; qz = quartz; grdiorite = granodiorite; qf = quartzo-feldspathic; Ca-silc = calc-silicate; pxhbdite = pyroxene hornblendite. Rock names after Streckeisen (1976, 1973).

§ U/Pb zircon geochronology sample.

deformed quartz, biotite, and plagioclase groundmass that is deflected around the augen. The augen vary from 10 to 30 volume percent of the rock. Most K-feldspar is microcline, with subordinate orthoclase. K-feldspar is concentrated in the augen, but can also be found in the groundmass. The K-feldspar megacrysts are brittlely deformed by internal fracturing and attrition of grain edges. Quartz is frequently ductilely deformed and recrystallized into a ribbon flow fabric that commonly forms flaser structures. Plagioclase is almost as common as quartz in the groundmass, rarely forms augen, and varies from An_{20} to An_{40}. Biotite is the most common mafic mineral. It occurs in thin plates and aggregates of stringers, which, along with the quartz ribbons, imparts a strong foliation to the rock. Accessory minerals are euhedral zircon, sphene, and apatite.

Feldspar augen are rounded, and show a brittle granularity along the corners of the grains and internal fracturing. Quartz, on the other hand, is recrystallized and shows ductile deformation and undulatory extinction. According to Tullis and Yund (1977), at pressures between 2 and 5 kb, the brittle to ductile transition occurs in quartz at 300-400°C, and in feldspar at 500-650°C. Thus, the development of the augen gneissic fabric probably occurred at between 400 and 500°C.

Mafic inclusions (Table 2) form lenses and bodies from 10 to 100 cm in width that are concordant with the foliation in the gneiss. The inclusions are dioritic to tonalitic in composition. They are distributed evenly throughout the gneiss, and are uniform in appearance. They are composed primarily of equal amounts of equidimensional hornblende and plagioclase, with minor amounts of quartz, biotite, and opaques. The inclusions have almost completely annealed textures.

II.2.3 Paragneiss of Comanche Point

The paragneiss of Comanche Point is a near homogeneous, migmatitic gneiss of psammitic composition. It occurs as enclaves within the other units of the

gneiss complex in a belt southwest of the tonalite gneiss of Tejon Creek in the western foothills of the Bear Mountain massif (Comanche Point area), in the low foothills south of the old Tejon Ranch Headquarters as a lenticular body bounded by the metagabbro of Tunis Creek and the tonalite gneiss of Tejon Creek, and as lenses within the Pastoria Creek and Tejon Creek units. It is typically intimately associated with the tonalite gneiss, and their field relations will be discussed in the section that pertains to the Tejon Creek gneiss. The paragneiss is part of Ross's (1980, 1986) transitional-mixed unit in the Comanche Point area, and occurs as undifferentiated gneiss elsewhere. The gneiss contains lenses of calc-silicate rock and less common marble and quartzite. Granitic leucosomes are present throughout the unit. Protolith structures have not been preserved.

The paragneiss can be distinguished from the Kings sequence metasedimentary framework rocks on the basis of diffuse, migmatitic contacts, a paucity of marble, and a lower K-feldspar content. The distinction between these metasedimentary units may represent two different metasedimentary assemblages, or they could represent parts of the same assemblage at different metamorphic grades.

Along Comanche Point road, the paragneiss appears to have been intruded by the tonalite gneiss of Tejon Creek in a lit-par-lit fashion that has local migmatitic structures, with leucosomes locally seen gradational with the tonalite gneiss. The paragneiss is best exposed in this area, thus the informal name for the unit.

The paragneiss consists of alternating segregated cm-scale bands of quartzo-feldspathic and biotite-rich mafic material (Figure 13). The bands are defined by variations in felsic and mafic mineral content, with occasional distinct calc-silicate lenses. Quartz and biotite form stringers which are parallel to the planar fabric of the rock. The quartzo-feldspathic bands contain quartz, K-feldspar, and plagioclase in granite minimum compositions, with subordinate biotite, muscovite,

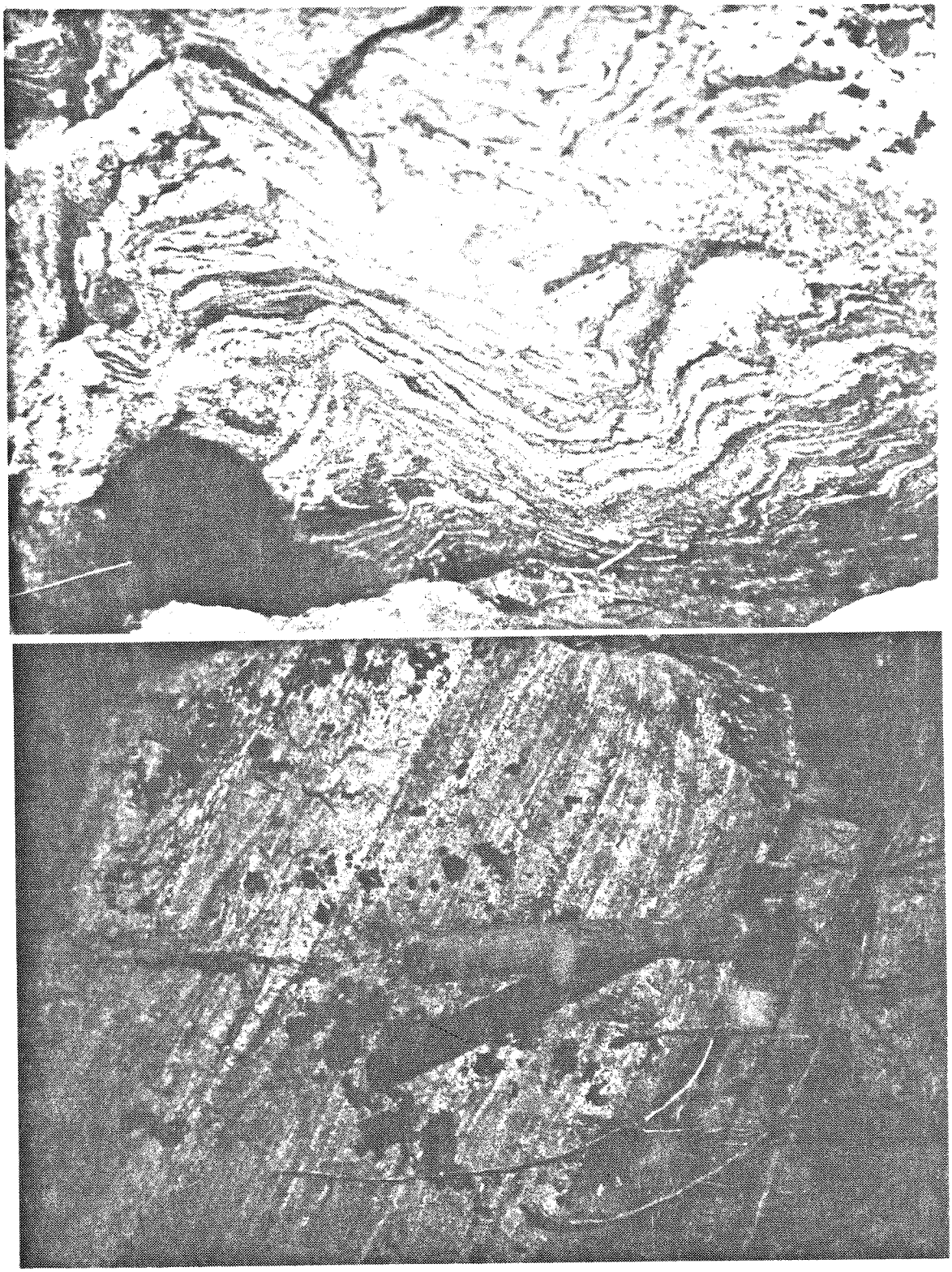

Figure 13. Photographs of field relations in the paragneiss of Comanche Point, showing granofels and gneissic segregation (a) and layers of garnet-bearing gneiss, granofels, and calc-silicates (b).

and garnet. The calc-silicate bands contain these minerals, plus green hornblende, diopside, and scapolite, while the dark layers within the calc-silicate bands contain graphite. The biotite-rich bands have the quartzo-feldspathic assemblage, but with lower modal K-feldspar and higher modal biotite.

Texturally, the quartzo-feldspathic and calc-silicate bands are granoblastic, with K-feldspar and garnet porphyroblasts. The biotite-rich bands are moderately to strongly schistose. Crystalloblastic textures predominate. A mylonitic fabric was found in one section as an overprinting texture oriented subparallel to the gneissic banding.

The banding appears to have resulted from partial melting and transposition of the paragneiss, as seen by cross-cutting dikelets and veins. In other locations, the banding may mimic earlier or primary compositional layering. Meter-scale domains of intensely banded gneiss may represent incompletely digested paragneiss. Evidence for this conclusion may be seen in field relations in the low foothills near the old ranch headquarters. There, a gradational contact between the metagabbro of Tunis Creek and paragneiss is seen. This contact zone involves a continuous transition from hornblende gabbro → quartz diorite → mafic tonalite → inclusion-rich granodiorite → paragneiss over an interval that encompasses about 100 meters. The gabbro has apparantly facilitated melting in the paragneiss, which in turn contaminated the margins of the gabbro.

The paragneiss is complexly folded. In the vicinity of Comanche Creek there is a progression of metasedimentary megaliths within the western margin of the various tonalites that appear to grade from migmatitic paragneiss to high grade metasedimentary rocks found in screens further to the east. Foliations in the paragneiss (Figure 14) are randomly oriented. Premetamorphism structures and fabrics developed prior to the high-grade deformation of the area have not

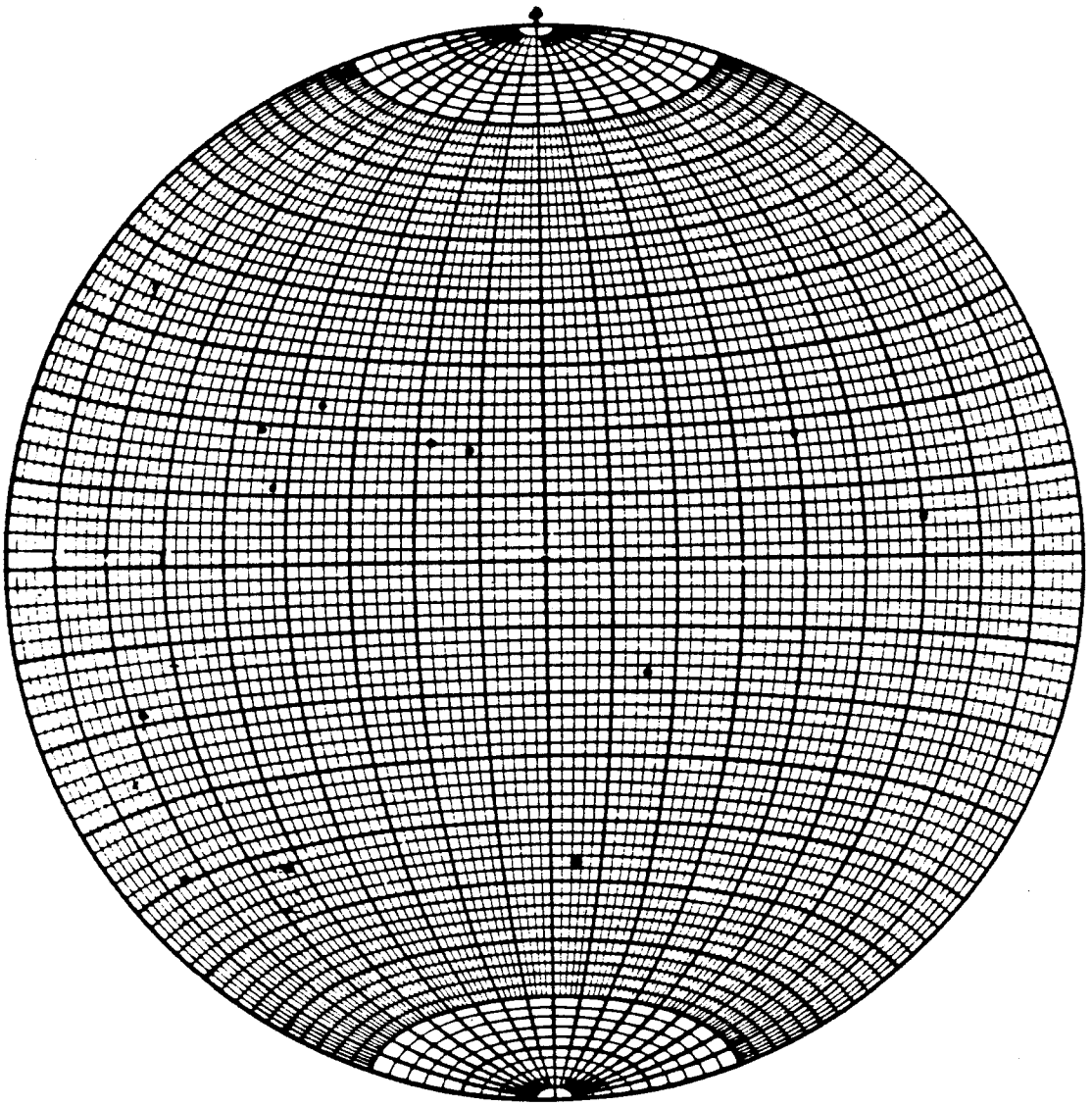

Figure 14. Lower hemisphere projection, equal-area stereoplot of poles to foliation for paragneiss of Comanche Point.

been recognized. They are not likely to have been preserved, due to the high degree of metamorphism, recrystallization, gneissic segregation, migmatism, and transposition that the unit underwent.

The paragneiss has an overall psammitic composition (Table 3). It is composed of quartz, plagioclase, and biotite, with minor amounts of potassium feldspar, garnet, graphite, muscovite, clinopyroxene, hornblende, and opaques. Scapolite was found in one thin section in the Comanche Point area. Aluminosilicate minerals are absent, probably as a result of compositional control. The quartz occurs as fine granular grains. Plagioclase is weakly twinned, anhedral, and about An_{20} to An_{30}. Biotite occurs as red to brown pleochroic subhedral grains. Potassium feldspar is anhedral to subhedral and frequently porphyroblastic.

The bulk chemistry of the paragneiss of Comanche Point approximates that of an immature graywacke, a relatively K-feldspar poor assemblage. A possible protolith for the gneiss may be seen in the Lake Isabella area. In that area, the entire southern Sierran association (paragneiss, marble, quartzite, calc-silicate, and mid-Cretaceous plutonic rock) is found, only at shallower levels of exposure (Saleeby and others, 1986a; Saleeby and Busby-Spera, 1986). The tonalites at Lake Isabella also contain upper-Proterozoic zircon (Saleeby and Busby-Spera, 1986). At Lake Isabella, the paragneiss represents immature greywackes that are relatively K-feldspar poor, with very immature feldspar populations.

In the Klamath Mountains, a similar situation is found. Slates and greywackes represent immature sediments derived from volcanic plagioclase detritus, and contain 1400 to 1800 Ma zircon (Saleeby and others, 1986b). Thus, melts derived from paragneiss material would have a granodioritic composition. Their incorporation into a tonalitic would alter the melt's composition only slightly. Assimilation of the paragneiss material into tonalitic melts would leave calc-silicates, marbles, and quartzites as refractory residual, as observed locally.

TABLE 3. SUMMARY OF PETROGRAPHY OF THE PARAGNEISS OF COMANCHE POINT - GNEISS COMPLEX OF THE TEHACHAPI MOUNTAINS†

HAND SAMPLE	ROCK NAME	CI	QTZ	PLG	(An)	KSP	HBL	BIO	CPX	OPX	GAR	SPH	APA	ZIR	OPQ	EPI	CHL	MUS	OTH	TEXTURES ANL	RXL	MYL	CST	RTR
CM110§	qf gneiss	20	25	40	20	15		15			x				3			2	graph			x		
CM650a	qf gneiss	12	25	48	25	15	5	5		2														
CM650b	Ca-Silc	24	45	25	25	3			15		9								scap3					
CM651b	qf gneiss	20	30	35	30	15		15			5													

† key to abbrevations:
CI = color index; QTZ = quartz; PLG (An) = plagioclase with Anorthite content after Michel-Levy (1887); KSP = K-feldspar; HBL = hornblende; BIO = biotite; CPX = clinopyroxene; OPX = orthopyroxene; GAR = garnet; SPH = sphene; APA = apatite; ZIR = zircon; OPQ = opaques; EPI = epidote; CHL = chlorite; MUS = muscovite; OTH = other; cumm = cummingtonite; graph = graphite; oliv = olivine; scap = scapolite; ser = sericite; sill = sillimanite; ANL = annealed; RXL = recrystallized; MYL = mylonitic or protomylonitic; CST = cataclastic; RTR = retrograded; qz = quartz; grdiorite = granodiorite; qf = quartzo-feldspathic; Ca-silc = calc-silicate; pxhbdite = pyroxene hornblendite. Rock names after Streckeisen (1976, 1973).

§ U/Pb zircon geochronology sample.

II.3 Bear Valley Springs intrusive suite

Rocks of the Bear Valley Springs suite consist of a number of intrusive bodies dated in this study at 100±2 Ma, as well as similar appearing undated stocks and intrusive bodies (such as the metagabbro of Squirrel Spring). The members of this suite can be distinguished from rocks of the gneiss complex by the presence of local intrusive relations with the gneiss complex rocks, and an overall lack of gneissic banding. However, the less mafic rocks in this suite frequently contain a planar fabric that resulted from ductile deformation under solidus to hot sub-solidus conditions. The more mafic rocks contain igneous flow and/or crystal accumulation fabrics.

The tonalite of Bear Valley Springs is a voluminuous batholith-scale pluton. It is possible to divide the batholith into four phases based on field, petrographic, geochronological, and geochemical evidence. The four phases are the tonalite of Mount Adelaide (previously considered as a separate pluton), a "main" phase, a "mixed" phase, and an "eastern marginal" phase. These last three phases were all mapped as the "tonalite of Bear Valley Springs" by previous workers (Ross, 1980, 1985, 1986; Sams and others, 1983), and will be discussed together below.

II.3.1 Tonalite of Mount Adelaide

The tonalite of Mount Adelaide is found in the northwesternmost part of the study area (Plate 1), and extends for several kilometers to the north. It was mapped as biotite quartz diorite by Dibblee and Chesterman (1953), and as the biotite tonalite of Mount Adelaide by Ross (1980, 1986). The contacts on Plate 1 follow those of Ross (1986).

The Mount Adelaide pluton has intrusive contacts with the main phase of the tonalite of Bear Valley Springs in the northwest part of the study area, and north of the study area. It cross-cuts and grades into the eastern marginal phase of the

Bear Valley Springs pluton north and east of the map area. The Mount Adelaide pluton has a moderately deformed eastern margin that has both intrusive and concordant contacts with metamorphic framework rocks of Kings sequence (Ross, 1986). The pluton is cross-cut by a swarm of pegmatites north of Caliente (Plate 1) that are thought to be related to the Comanche Point pegmatite swarm.

The tonalite of Mount Adelaide can be distinguished from the bulk of the tonalite of Bear Valley Springs on the presence of a higher biotite to hornblende ratio, euhedral books of biotite, the presence of fewer mafic inclusions, and a less deformed appearance. It may represent a higher level phase of the tonalite of Bear Valley Springs, due to the lack of strong deformational fabrics, and normal plagioclase zonation and twinning.

The tonalite of Mount Adelaide is a medium- to coarse-grained, hypidiomorphic granular, biotite tonalite (Table 4). It is weakly to moderately foliated. Quartz, 25-40 volume percent, is sutured and has undulatory extinction. Plagioclase, An_{25} to An_{30}, is subhedral, with normal oscillatory zoning and distinct albite twins. Biotite, about 10-15%, occurs as euhedral grains up to 1 cm in size, and is a pleochroic medium to dark brown. Hornblende comprises no more than 5% of the rock. It occurs as subhedral, pleochroic olive to green grains. Accessory minerals are zircon, sphene, apatite, K-feldspar, and opaques.

II.3.2 Tonalite of Bear Valley Springs

The tonalite of Bear Valley Springs is an elongate northwest-trending batholith-scale pluton that extends at least 50 km northward from Tejon Creek (Ross, 1980, 1986) (Plate 1). It is bounded on the west by onlapping Eocene to Quaternary strata (Nilsen and Clarke, 1975; Harris, 1954), the tonalite of Mount Adelaide, and the White Wolf fault. Its eastern contacts are a series of metasedimentary septa into which it is concordantly intrusive. Contacts with younger Creta-

TABLE 4. SUMMARY OF PETROGRAPHY OF THE TONALITE OF MOUNT ADELAIDE†

HAND SAMPLE	ROCK NAME	CI	QTZ	PLG	(An)	KSP	HBL	BIO	CPX	OPX	GAR	SPH	APA	ZIR	OPQ	EPI	CHL	MUS	OTH	TEXTURES ANL	RXL	MYL	CST	RTR
CM136	tonalite	10	40	50	25		2	7							1									
PM510	tonalite	15	35	50	30		5	10							x						x			
BM520	tonalite	23	25	55	30		3	20							x									
BM683	tonalite	10	50	40	25			10				x	x	x	x									
BM684§	tonalite	15	45	40	30			12				x	x	x	1	2								

† key to abbrevations:
CI = color index; QTZ = quartz; PLG (An) = plagioclase with Anorthite content after Michel-Levy (1887); KSP = K-feldspar; HBL = hornblende; BIO = biotite; CPX = clinopyroxene; OPX = orthopyroxene; GAR = garnet; SPH = sphene; APA = apatite; ZIR = zircon; OPQ = opaques; EPI = epidote; CHL = chlorite; MUS = muscovite; OTH = other; cumm = cummingtonite; graph = graphite; oliv = olivine; scap = scapolite; ser = sericite; sill = sillimanite; ANL = annealed; RXL = recrystallized; MYL = mylonitic or protomylonitic; CST = cataclastic; RTR = retrograded; qz = quartz; grdiorite = granodiorite; qf = quartzo-feldspathic; Ca-silc = calc-silicate; pxhbdite = pyroxene hornblendite. Rock names after Streckeisen (1976, 1973).

§ U/Pb zircon geochronology sample.

ceous plutons are poorly defined, but appear for the most part to be subparallel to foliation. It is intruded by the tonalite of Mount Adelaide northeast and southwest of Caliente, and by the granodiorite of Claraville south of Tehachapi. Cross-cutting contacts are for the most part absent, but are present for a small distance near the Garlock fault, where the Claraville intrudes the Bear Valley Springs.

The tonalite of Bear Valley Springs grades into the hypersthene tonalite of Bison Peak in the upper Tejon Creek area. This contact is poorly exposed and characterized, and represents a major geochemical jump, perhaps across two distinct basement assemblages (Chapter IV). The tonalite of Bear Valley Springs is distinguished from the hypersthene tonalite on the basis of a more pervasive foliation, higher modal quartz and biotite, less common hypersthene, and the lack of clinopyroxene. The Bison Peak unit is believed to represent a deeper-level phase of the tonalite of Bear Valley Springs, possibly the floor of the batholith.

Along lower Tejon Creek and in the vicinity of Comanche Point (along the southern and southwestern margins of the tonalite), the tonalite has a concordant, apparent gradational contact with the gneiss complex of the Tehachapi Mountains through a region of tonalite gneiss (Tejon Creek unit) that appears to have been derived through the mixing of older tonalitic magmas and migmatitic melt products of paragneiss enclaves in the gneiss complex. This contact is in a region of discontinuous but fairly well-exposed bedrock. The contact is a broad 2-3 km wide zone of increasing gneissosity, diminution in grain size, and increase in K-feldspar content towards the tonalite gneiss, as well as the local occurrence of garnet ± muscovite in the Tejon Creek unit. The clear distinction in zircon systematics between the two units indicates two distinct episodes of magma intrusion.

The tonalite of Bear Valley Springs falls into the Buddington (1959) classification scheme as a catazonal, concordantly bounded pluton. It has an apparent

igneous crystallization age of 100±2 Ma. It is pervasively foliated, oriented subparallel to its eastern and western margins, with increasing foliation towards the margins and south towards the gneiss complex of the Tehachapi Mountains. The foliation (Figure 15) is northeast to northwest trending, and moderately to steeply east dipping. The foliation trends west-northwesterly in the Tejon Creek region, becoming more northwesterly throughout much of the pluton, except northwest of Tehachapi, where it is north-northeast trending.

The foliation consists of aligned mafic tabular and platy igneous minerals, distorted mafic inclusions, and schlieren (Figure 16). Near the contact with the septa, the tonalite of Bear Valley Springs is very strongly foliated, with a moderate ductile deformation texture including streaked out mafic and quartz grains. Here the foliation is believed to have developed as a result of the differential movement between the pluton and the metamorphic framework rocks. At locations away from the margins of the pluton, the tonalite has an igneous flow foliation with little evidence of additional tectonic deformation. This foliation appears to have developed synplutonically under solidus to hot sub-solidus conditions, as evidenced by the alignment of tabular and platy igneous mafic minerals, schlieren, and inclusions, as well as the strongly elongated nature of the mafic inclusions. In addition, the cross-cutting contacts of the Mount Adelaide pluton constrain the time of formation of the foliation. Further, gradational contacts with the tonalite gneiss of Tejon Creek and the parallel orientation of deformational fabrics in the tonalite with high-grade metamorphic fabrics in the tonalite gneiss and the metamorphic framework rocks indicate synplutonic deformation.

The tonalite of Bear Valley Springs is a medium- to coarse-grained, hypidiomorphic to allotriomorphic granular, biotite hornblende tonalite (Table 5). Quartz, 20-40 volume percent, is strained and sutured, with local undulose extinc-

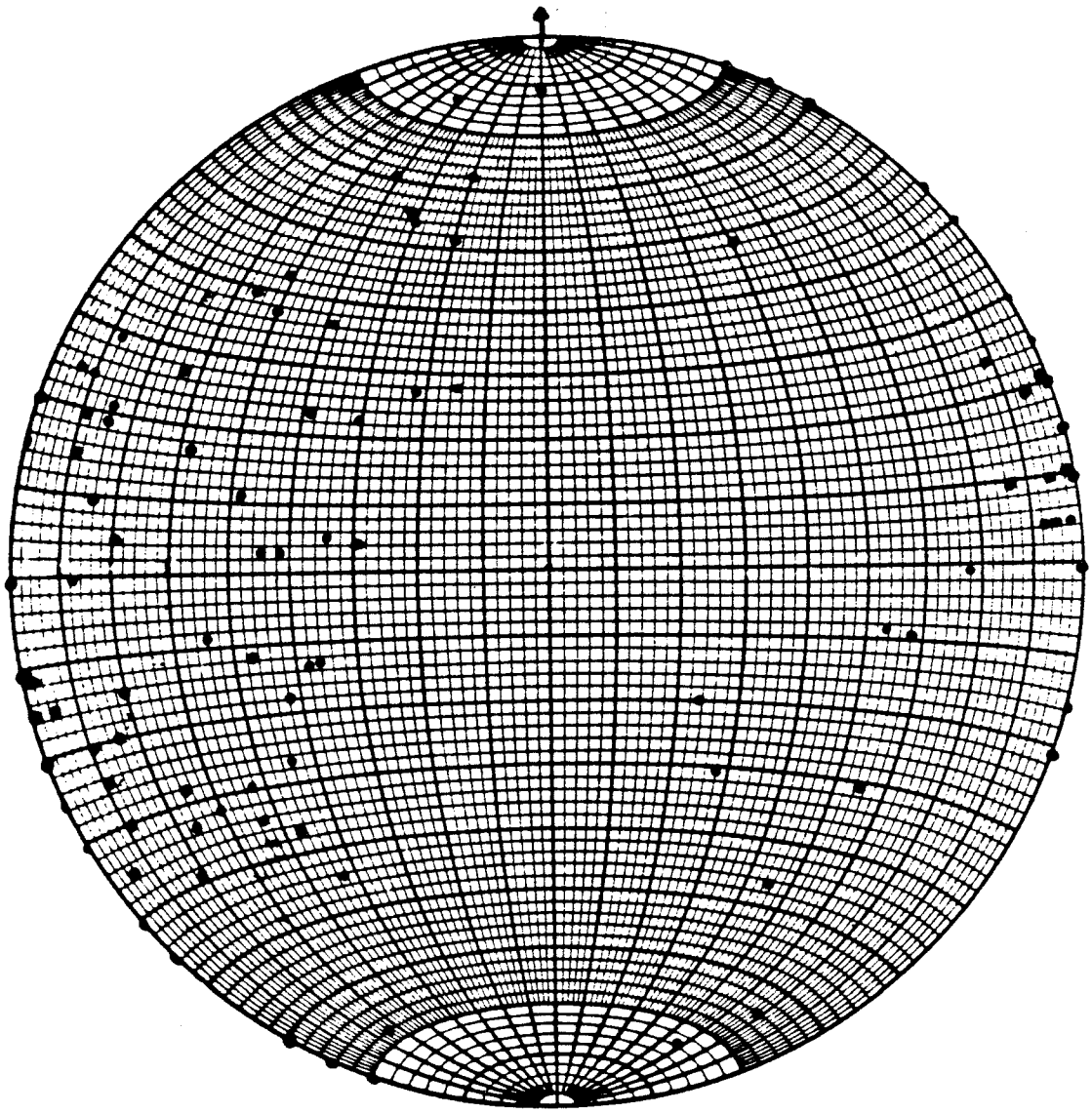

Figure 15. Lower hemisphere projection, equal-area stereoplot of poles to foliation for tonalite of Bear Valley Springs.

Figure 16. Photographs of field relations of the tonalite of Bear Valley Springs in the Bear Mountain area. Visible in (a) is a swarm of mafic inclusions, which are both strongly oriented and elongated parallel to the foliation in the tonalite of Bear Valley Springs. Person on left for scale, width of view about 6 m. White streaks are drill holes for roadcut, irregular dark patches are colluvium. (b) illustrates close-up of mafic inclusions and mafic clots. Field of view approximately 30 cm. Note the continuity of the felsic groundmass of the host rock with the mafic inclusion at the pen, and the sharp margins of the inclusion at the lower right corner.

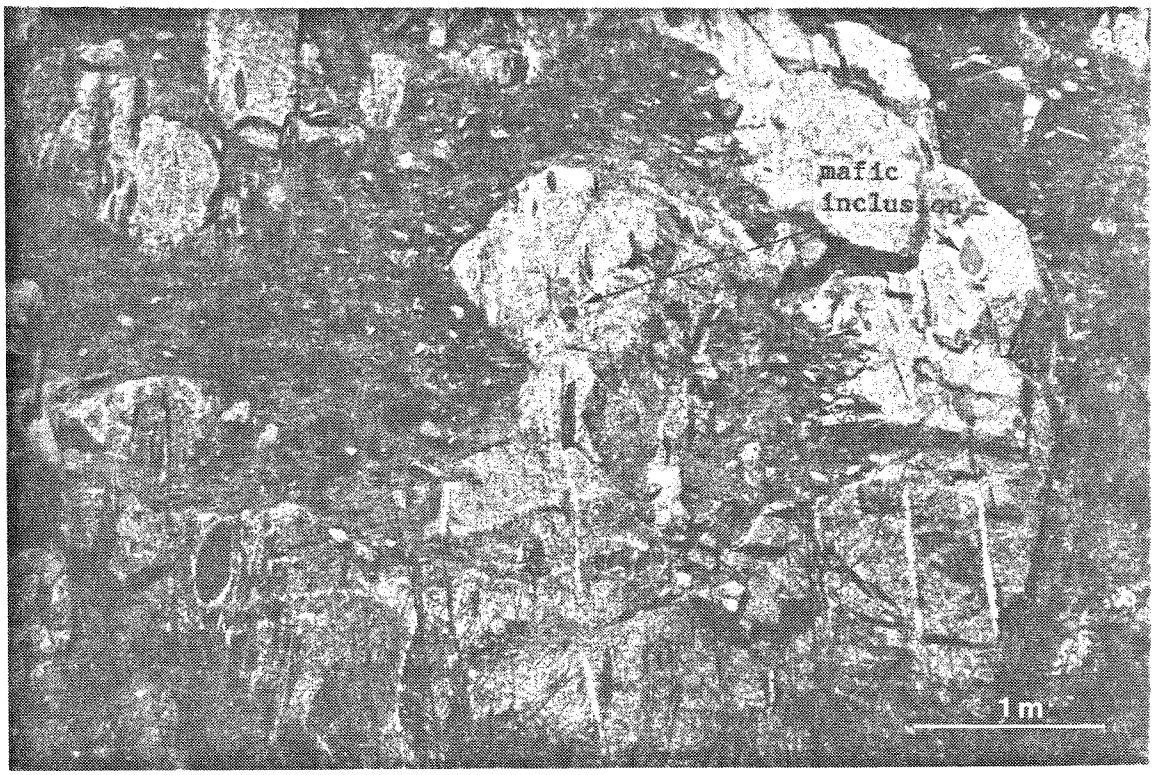
mafic
1m

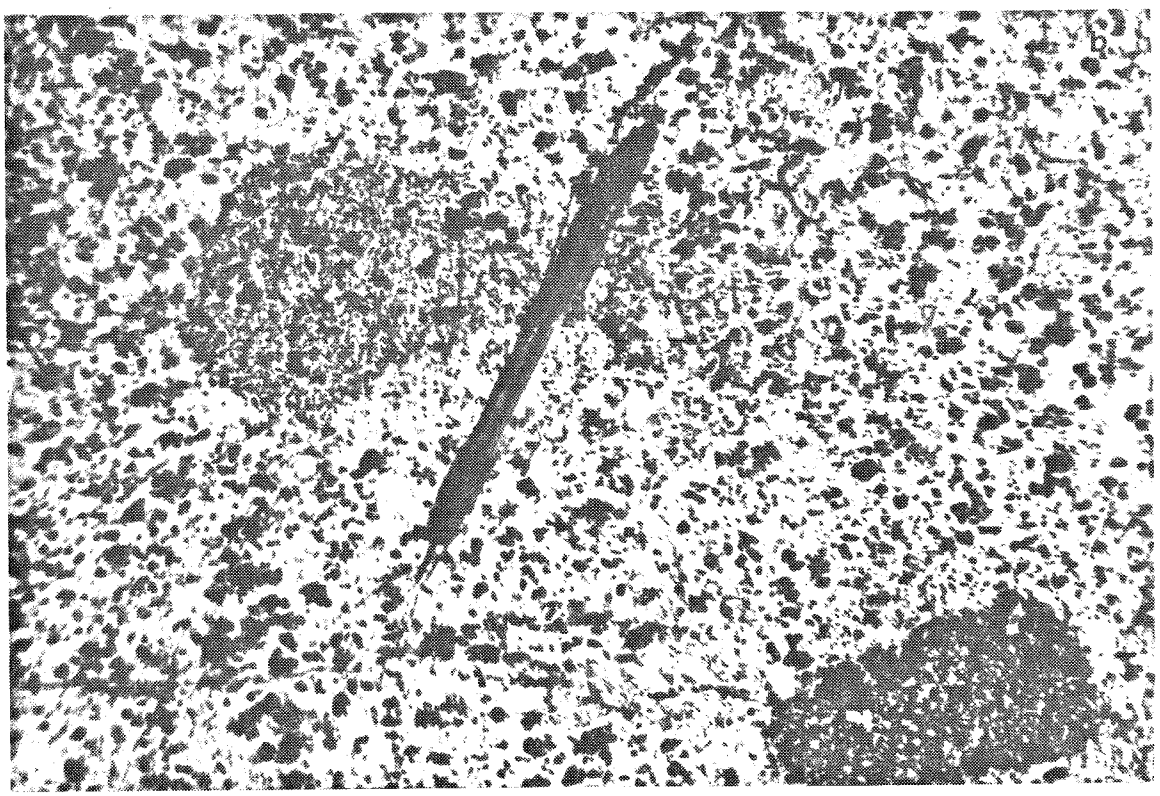

TABLE 5. SUMMARY OF PETROGRAPHY OF THE TONALITE OF BEAR VALLEY SPRINGS†

HAND SAMPLE	ROCK NAME	CI	QTZ	PLG	(An)	KSP	HBL	BIO	CPX	OPX	GAR	SPH	APA	ZIR	OPQ	EPI	CHL	MUS	OTH	TEXTURES ANL	RXL	MYL	CST	RTR
CM1	tonalite	20	30	50	25		13	6							1							x		
CM4	diorite	62		40	40		60								2									
CM5	tonalite	30	30	50	25		20	10																
CM8	tonalite	25	25	40	25	10	15	10													x			
CM9§	tonalite	35	20	45	30		20	15				x				x			ser		x			
CM11	tonalite	21	30	50	30		10	10							1									
CM12	tonalite	15	40	45	30		5	10														x		
CM13b	tonalite	16	30	30	30	25	2	13							1							x		
CM14a	tonalite	21	25	55	30		5	15							1									
CM14b	tonalite	20	30	55	30			10			3				2									
CM15	tonalite	25	25	50	30		5	18							2									
CM19	tonalite	16	35	50	20	5	9	6							1			1						
CM21	tonalite	25	35	40	35		11	7		5					2									
CM22	tonalite	15	35	50	35		4	10							1									
CM25§	tonalite	35	20	45	40		20	15				x			x									
CM26§	tonalite	27	20	55	50		15	10		2		x	x		x		x	x						
CM30	tonalite	22	35	45	30		10	10						1	1						x			
CM31	tonalite	21	35	40	20		8	12							1									
TC15§	tonalite	25	25	50	40		17	8																
TC19	tonalite	18	25	50	45			18													x			
TC20b	tonalite	20	25	50	x	2		20													x	x		
TC21	tonalite	26	25	50	40		15	10				1					x		ser		x	x		
TC42§	tonalite	22	20	50	40		12	8				1			2		9		ser		x	x		
CM139	tonalite	21	30	50	25		10	10							1									
BM144	tonalite	21	30	50	40		8	12							1				ser					
BM149	tonalite	28	25	45	40	2	17	10							1									
BM514	diorite	38		60	35		35	2							1									
BM527	tonalite	34	30	40	25		15	15						x	2	2	x							
CM568	tonalite	25	25	45	x		20	5									x		ser					
CM569	tonalite	25	30	45	40		20	5									x		ser				x	
MAFIC INCLUSIONS																								
CM22b§	amphibolite	53	10	40	25		40	10				x			3	x				x				

† key to abbreviations:
CI = color index; QTZ = quartz; PLG (An) = plagioclase with Anorthite content after Michel-Levy (1887); KSP = K-feldspar; HBL = hornblende; BIO = biotite; CPX = clinopyroxene; OPX = orthopyroxene; GAR = garnet; SPH = sphene; APA = apatite; ZIR = zircon; OPQ = opaques; EPI = epidote; CHL = chlorite; MUS = muscovite; OTH = other; cumm = cummingtonite; graph = graphite; oliv = olivine; scap = scapolite; ser = sericite; sill = sillimanite; ANL = annealed; RXL = recrystallized; MYL = mylonitic or protomylonitic; CST = cataclastic; RTR = retrograded; qz = quartz; grdiorite = granodiorite; qf = quartzo-feldspathic; ca-silc = calc-silicate; pxhbdite = pyroxene hornblendite. Rock names after Streckeisen (1976, 1973).

§ U/Pb zircon geochronology sample.

tion and granularity. It is ductilely deformed and partially recrystallized in the southern portion of the batholith. Plagioclase, An_{20} to An_{45}, is anhedral to subhedral. It shows a weak compositional zonation around Cummings Valley that becomes stronger north in the pluton, and is prominent in the pluton north of Tehachapi. Sharp albite twinning is common. The twinning and zonation are believed to be the result of normal magmatic processes. The more common occurrence and sharper twinning and zonation suggest shallower levels of exposure in the northern part of the batholith.

The mafic minerals consist of subequal amounts of biotite and hornblende, with a color index of 15-30. Anhedral to subhedral hornblende is present in all sections, and is most frequently a pleochroic blue-green to brown. Biotite is subordinate to subequal in occurrence to hornblende. It is a pleochroic yellow to brown, rarely red-brown, anhedral to subhedral, and frequently intergrown with hornblende, forming mafic clots. Pale red hypersthene is found locally in and south of the Cummings Valley area as an early liquidus phase. It is typically surrounded by hornblende ± biotite clusters. It occurs in equilibrium textures with the mafics, or less commonly is retrograded to hornblende. Potassium feldspars are occasionally present, but always less than 5 percent. They are interstitial, untwinned, weakly perthitic, and infrequently microcline. Brown sphene is the most common accessory mineral. Zircon, apatite, and opaques are less common accessory minerals. Chlorite is a common secondary mineral.

The tonalite retains an igneous texture throughout, although it is ductilely deformed, especially as it extends southward. Figure 17 shows a progression of increasing deformation from near normal igneous textures (a,b) north of Cummings Valley, to deformed textures (c,d) south of Cummings Valley. The tonalite exhibits some degree of retrograde granoblastic and recrystallization fabrics,

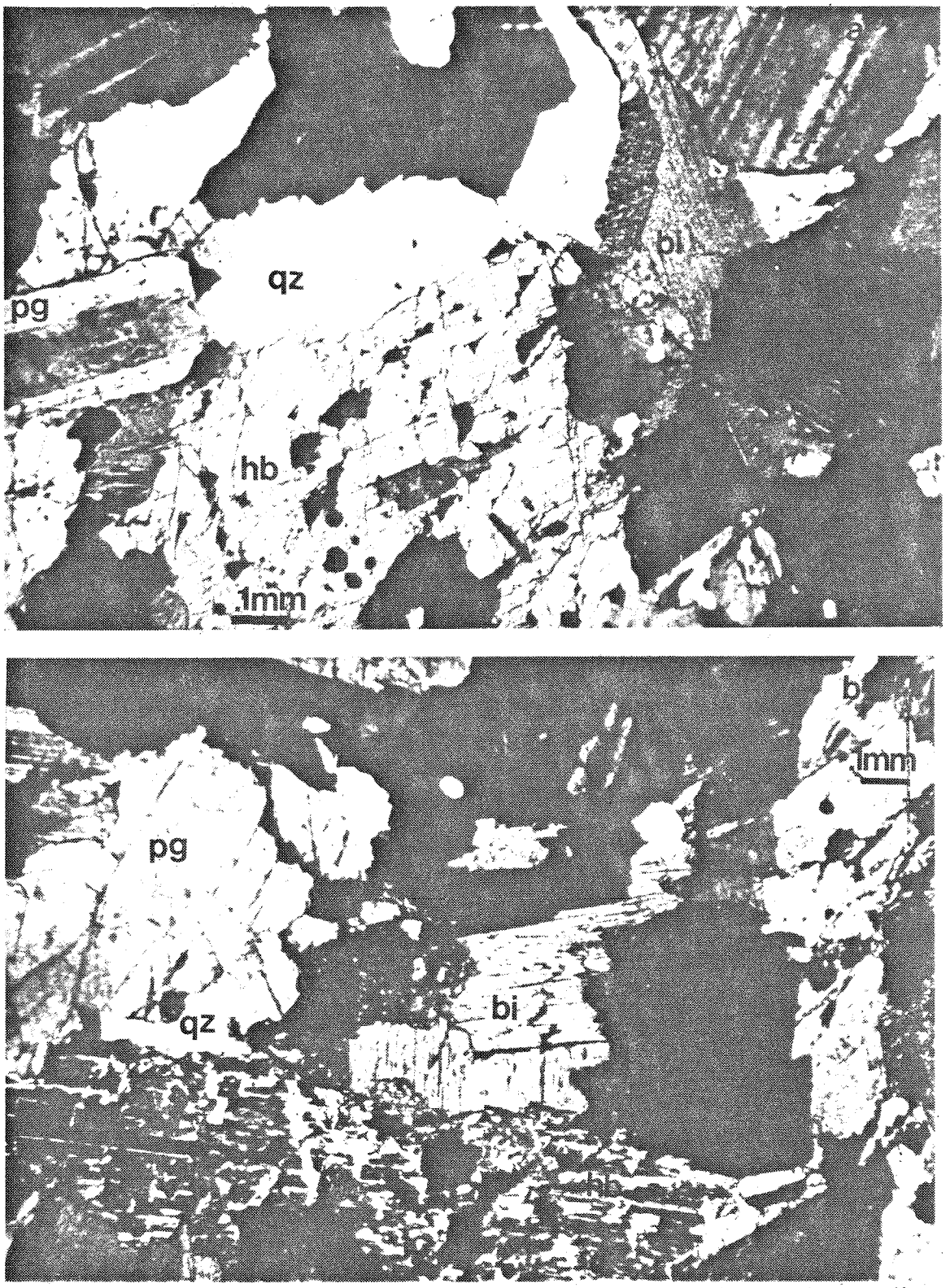

Figure 17. Photomicrographs showing progressive deformation of the tonalite of Bear Valley Springs. (a,b; width=2 mm) illustrate normal igneous textures in the Bear Mountain area,

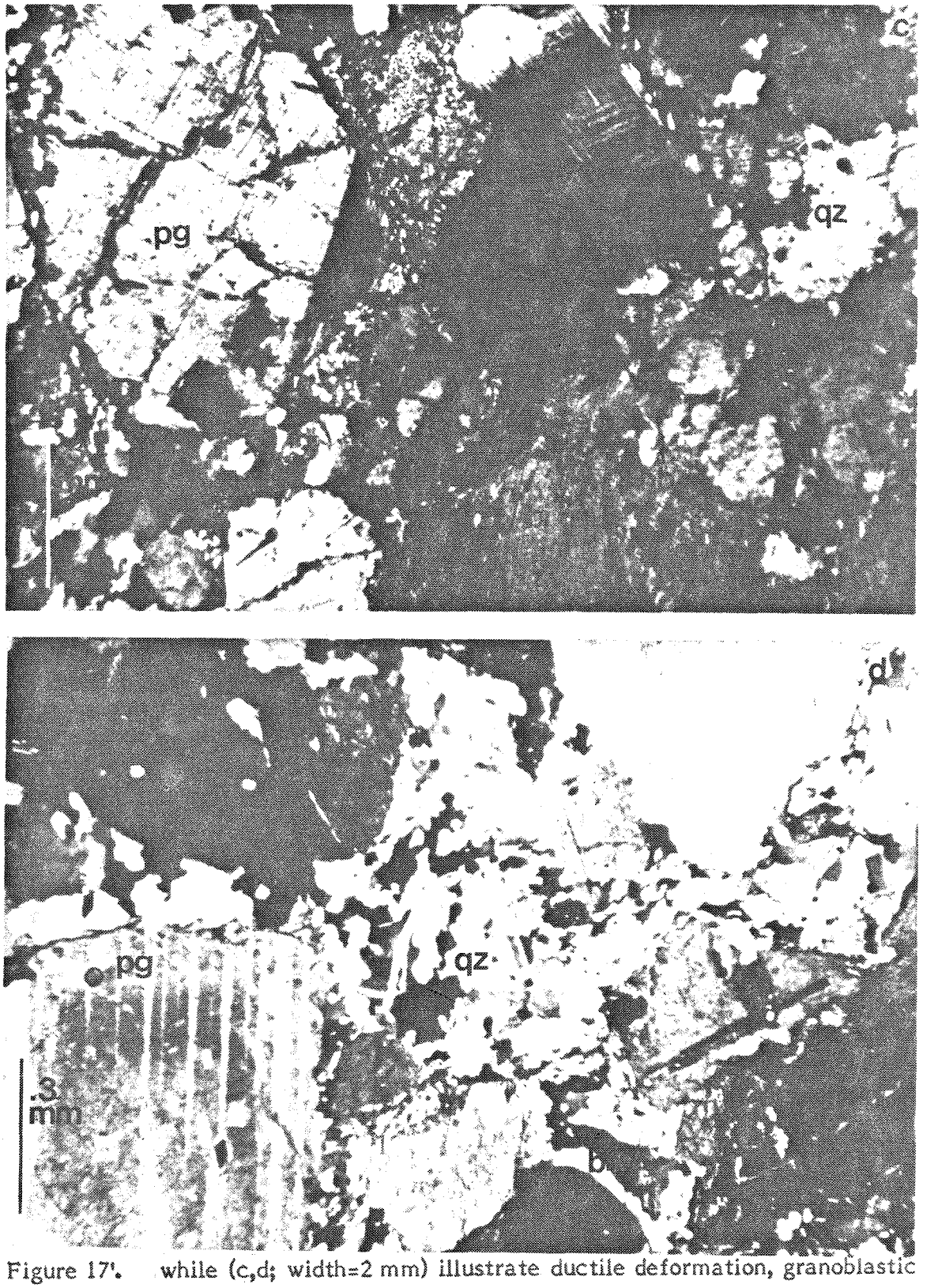

Figure 17. while (c,d; width=2 mm) illustrate ductile deformation, granoblastic and blastomylonitic textures in the Cummings Mountain area. Minerals are pg=plagioclase, qz=quartz, bi=biotite, hb=hornblende.

normally in the quartz. In addition, the tonalite becomes slightly gneissic, formed by stringers of thin biotite and stretched out quartz grains. Mylonitic fabrics are locally present near metamorphic septa, in particular along the eastern margin phase of the batholith (Figure 17d). Retrograde granoblastic and very local cataclastic fabrics overprint the earlier high-grade fabrics.

The tonalite is characterized by abundant dark minerals, mafic inclusions, and schlieren that occur in clumps and streaks throughout the pluton (Figure 16). The mafic inclusions vary from 10 to greater than 75 volume percent, range in size from 10 cm to a few meters in greatest dimension, from 10-50 cm in width, are elliptical in shape, and are concordant with the foliation in the tonalite. They have aspect ratios of 1:2 to greater than 1:25. The inclusions are elongate parallel to the foliation in the tonalite, help to define the foliation, and form distinct inclusion "trains". The inclusions frequently occur as screens in the tonalite, typically near its margins. They are found, however, throughout the pluton. The constituent minerals are generally aligned parallel with the long dimension of the inclusions. The interpretation of solidus to sub-solidus deformation in the tonalite is due in part to the alignment, deformation, and high aspect ratios of the mafic minerals and inclusions in the tonalite. Bateman and others (1963) ascribe these processes as the result of emplacement and magmatic flow.

Mafic inclusions in the tonalite (Table 5) have a composition of mafic tonalite to gabbro, with diorite to quartz diorite dominant. They have a granoblastic texture that is rarely annealed, and are composed of equigranular plagioclase (An_{25}) and olive-green hornblende, with minor brown biotite, interstitial quartz, brown hornblende, and sphene. Hypersthene can be found in mafic inclusions in the southern portion of the batholith in a textural setting analoguous to that in the tonalite. The mineralogy of the inclusions is more mafic than the host rock. The

margins of the inclusions are both sharply defined and diffuse with respect to the host tonalite. The mafic grain clusters and mafic inclusions with diffuse margins have a continuity of the felsic groundmass with the host (Figure 16b). In addition, U/Pb and Rb/Sr systematics are nearly identical to those of the tonalite. Thus, the mafic inclusions appear to be mineralogically, geochemically, and geochronologically equilibrated with the host tonalite. Clearly, the mafic inclusions are not xenoliths of metasedimentary material, due to the incompatibility in bulk chemistry and lack of Proterozoic zircon.

The mafic inclusions could represent either a residuum or restite transported from the source region with the tonalite, or be the result of magma mixing between tonalitic and gabbroic end members. The second possibility is preferred. On the east side of Cummings Mountain within the mixed phase of the batholith, the tonalite shows a mixed and continuous gradation into hundred meter sized lenticular bodies of mafic tonalite to diorite. These bodies are similar in texture and mineralogy to the mafic inclusions in the rest of the tonalite, and are compositionally and texturally similar to parts of the hypersthene tonalite of Bison Peak and the metagabbro of Tunis Creek. The mafic inclusions have structural relations with the host tonalite suggestive of a synplutonic origin with the tonalite. Disrupted mafic dikes and pillow structures have been described in a setting of more obvious magma mixing (Marshall and Sparks, 1984). The existance of such structures in the tonalite further supports a mixed magma origin for the inclusions. Their poor preservation within the tonalite is most likely due to the large volume of the tonalite and deformation due to synplutonic flow.

It is possible that the tonalite of Bear Valley Springs as described herein represents a composite batholith made up of a number of lithologically similar yet discrete tonalite plutons or batches of magma that were intruded in a narrow span

of time, rather than one single large plutonic mass, although the field relations do not require this. Age relations within the batholith as investigated in this study are indistinguishable (all ages are within analytical uncertainty). The tonalite however can be divided into four phases, the tonalite of Mount Adelaide (discussed above), and main, mixed, and eastern marginal phases. The main, mixed, and marginal phases are intergradational, and very similar in appearance.

The mixed phase has a dominantly north-trending foliation, a high proportion of mafic inclusions and schlieren, and is hypersthene-bearing in the southern part of the phase. It ranges in composition from tonalite to leucotonalite and granodiorite. It is found along the discontinuous metasedimentary septum at Cummings Valley. It grades into the eastern and main phases by decreasing amounts of mafic inclusions, and the disappearance of hypersthene and granodioritic compositions. The eastern phase is distinguished by the development of local deformation fabrics related to movement with respect to metamorphic framework rocks. It is bounded by the two Kings sequence septa. The eastern phase is lithologically similar to the main phase. The main phase comprises the bulk of the tonalite, and is fairly uniform in appearance. It occurs west of the eastern and mixed phases.

The eastern phase may be younger than the main phase by 1-2 my, although the ages are all analytically identical (see discussion on geochronology below). Similarly, the Mount Adelaide phase may be younger than the eastern and main phases, with cross-cutting field relations to support this. Thus, age and structural relations suggest the following intrusive sequence. The mixed and main phases were the earliest phases of tonalite to be emplaced, with considerable interaction and assimilation of metasedimentary framework rock into the mixed phase. The eastern phase was intruded next, but sufficiently close in time that cross-cutting relations with the other phases were absent or not preserved. The intrusion of the

Mount Adelaide phase was sufficiently later (or at a higher structural level) that cross-cutting relations were preserved. Most of the deformation in the batholith took place prior to emplacement of the Mount Adelaide phase.

The intrusion of the tonalite into the lower crust was accompanied by coeval gabbros (metagabbro of Tunis Creek). Mixing of silicic (tonalitic) and mafic magma is believed to have been a dominant process with mineralogically equilibrated vestiges of the mafic magma represented by the mafic inclusions in the tonalite. Reaction and differential movement of the tonalite with the country rock led to strong deformational fabric development in the margins, floor, and root zone of the tonalite (hypersthene tonalite of Bison Peak, eastern marginal phase). The entire set of magmatic bodies involved in the 100 Ma event has been termed herein the Bear Valley Springs intrusive suite.

The trend of coeval gabbro to tonalite (metagabbro of Tunis Creek, hypersthene tonalite of Bison Peak, tonalite of Bear Valley Springs) is similar to relations seen in parts of the Cretaceous Sierra Nevada batholith to the north (Emigrant Gap pluton, James 1971; Bear Mountain Intrusive complex, Snoke and others, 1981). There, the relations are gabbros along the outer wall of a conduit, with tonalites in the central part of the conduit. This view may be similar to that of the southernmost Sierra Nevada, where the metagabbro of Tunis Creek and the hypersthene tonalite of Bison Peak may occupy the root or conduit of the tonalite of Bear Valley Springs. The map pattern of the region can be shown to represent a cross-sectional view of the study area (Chapter IV). Thus, the southernmost Sierra Nevada may represent a deeper view of analoguous relations.

II.3.3 Hypersthene tonalite of Bison Peak

The hypersthene tonalite of Bison Peak comprises the eastern majority of the Tehachapi Mountains. It forms a large, continuous mass that makes up much

of the high ridges around the Bison Peak lookout (north of Twin Lakes, Plate 1). The tonalite also underlies much of the northern part of Winters Ridge, where it forms 1-5 km masses. It has been mapped as diorite by Weise (1950), hornblende biotite quartz diorite by Dibblee and Louke (1970), dark amphibolite gneiss by Ross (1980, 1986), and Bison granulite by Sharry (1981b). The hypersthene tonalite of Bison Peak comprises most of Sharry's Bison "granulite", except for the area around the mouth of Tejon Creek where the tonalite gneiss of Tejon Creek has been differentiated in this study from Sharry's Bison unit. The unit as considered in this study follows most of the contacts of Sharry (1981b).

The hypersthene tonalite is in contact with the quartzo-feldspathic gneiss of Pastoria Creek and metagabbro of Tunis Creek on the west. The larger body extends from near the Garlock fault where it is in gradational contact with the White Oak unit (Plate 3), to a gradational contact with the tonalite of Bear Valley Springs in upper Tejon Creek, and a gradational(?) contact with the tonalite gneiss of Tejon Creek along the northern foothills of Winters Ridge. It is considered a part of the Bear Valley Springs intrusive suite, and postulated to be a phase of the tonalite of Bear Valley Springs, but with significant geochemical differences.

The gradational contact between the tonalite of Bear Valley Springs and the hypersthene tonalite of Bison Peak has been discussed above. The contact with the metagabbro of Tunis Creek is typically poorly exposed, but consists of both mixed to gradational and sharp co-intrusive contacts. Gradational contacts along the north slopes of Winters Ridge consist of a smooth(?) mineralogical and textural transition from foliated hypersthene-bearing hornblende biotite tonalite to nonfoliated hornblende gabbro-diorite. In particular, the transition consists of the gradual elimination of quartz and biotite, and an increase in modal hornblende and plagioclase. Planar deformational fabrics are lost for the most part. Along Tunis

Creek the two units have both a gradational contact, and also intrude one another. The two units are believed to be synplutonic, based on their mutual diking of one another, their gradational contacts, and identical zircon ages.

The contacts of the hypersthene tonalite of Bison Peak with the quartzofeldspathic gneiss of Pastoria Creek and the diorite gneiss of White Oak are for the most part obscure. Along the margins of the selvage-like body near Pastoria Creek and along the western part of the larger mass north of Winters Ridge, the tonalite intrudes the Pastoria Creek unit both concordantly and discordantly. The contacts are both diffuse and sharp. The tonalite is seen to rarely intrude the White Oak unit near the Cottonwood area, but the contact is not well characterized elsewhere, due to the poor exposure and superimposed fabrics from the Garlock fault. The contact with the tonalite gneiss of Tejon Creek is obscure. The distinguishing features of the hypersthene tonalite of Bison Peak from the tonalite gneiss of Tejon Creek are the occurrence of hypersthene, a greater amount of hornblende, lesser amount of biotite, lessor degree of foliation and deformation, and a lack of K-feldspar.

The tonalite has an interpreted zircon igneous age of 101±2 Ma, indistinguishable from the age of the tonalite of Bear Valley Springs. Foliation within the unit (Figure 18) is generally west to northwest trending, with a moderate to steep north dip. The foliation is not strongly oriented, except near the Garlock fault, where it is subparallel to the fault.

Mafic inclusions and schlieren are found within the hypersthene tonalite, but not to the extent as in the tonalite of Bear Valley Springs. They appear to be identical to those within the batholith, and resemble deformed dikes of diorite or gabbro from Tunis Creek-affinity rocks. In addition, xenoliths of obvious metasedimentary nature can be found enclosed in the tonalite. These contain quartz-

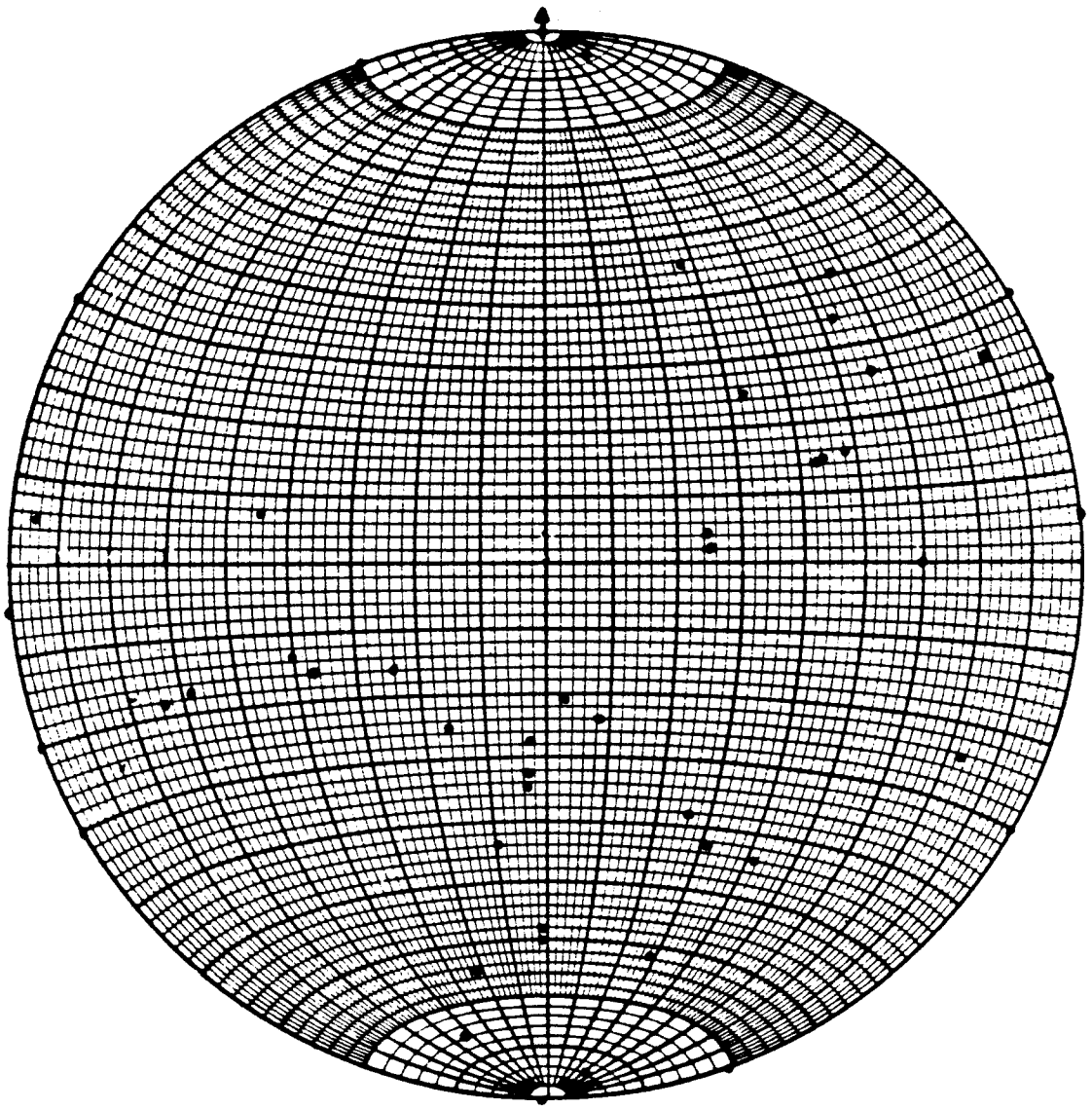

Figure 18. Lower hemisphere projection, equal-area stereoplot of poles to foliation for tonalite of Bison Peak.

ite, marble, paragneiss, calc-silicate rock, and psammitic schist. They may represent large xenoliths or infolded masses into the tonalite, and range in size from a few meters to several hundred meters in width, and up to one kilometer in length. Their long axes, external contacts and internal fabrics are aligned with the foliation of the host rock. The metasedimentary xenoliths are compositionally distinct from the mafic inclusions and schlieren.

The hypersthene tonalite of Bison Peak is an orthopyroxene-bearing hornblende biotite tonalite. It is not a true metamorphic granulite produced by prograde metamorphism of metasedimentary material (as was suggested by Sharry, 1981b) due to the high abundances of hydrous minerals and a probable igneous origin. Rather, it is believed to have crystallized from a magma within upper amphibolite to perhaps lower granulite facies conditions. An igneous origin is suggested by field relations, mineralogy, retrograde fabrics, igneous $\delta^{18}O$ values, and zircon age systematics. Similar appearing but shallower level hypersthene-bearing tonalites can be found in the western Cretaceous part of the Sierran batholith to the north, where an igneous origin for the tonalites is clear.

The tonalite of Bison Peak is a medium- to coarse-grained, hypidiomorphic granular, massive to moderately, but not pervasively, foliated rock (Table 6). It ranges in composition from a tonalite to a quartz diorite. Local gneissosity is defined by ductilely deformed quartz and feldspar aggregates interleaved with streaked-out mafic grain aggregates, but pervasive gneissic banding is absent. It has the appearance of a deformed igneous rock, and is often difficult to distinguish from the tonalite of Bear Valley Springs. Hypersthene-bearing domains within the tonalite of Bear Valley Springs are in fact nearly identical to the hypersthene tonalite of Bison Peak. It is distinguished from the tonalite of Bear Valley Springs on the basis of a lower quartz and biotite content, the presence of clinopyroxene, and a lesser degree of pervasive deformation.

TABLE 6. SUMMARY OF PETROGRAPHY OF THE HYPERSTHENE TONALITE OF BISON PEAK†

HAND SAMPLE	ROCK NAME	CI	QTZ	PLG	(An)	KSP	HBL	BIO	CPX	OPX	GAR	SPH	APA	ZIR	OPQ	EPI	CHL	MUS	OTH	TEXTURES ANL	RXL	MYL	CST	RTR
WR191	tonalite	17	30	55	40		8	7		1					1									
TL194	tonalite	35	30	35	30		15	8		6		x			1				cumm5					x
TL197§	tonalite	30	30	40	25		18	2	3	6					1	x			cumm/ser					x
TL199	tonalite	20	40	50	25		10	5		4					1	x					x	x		
TL201	tonalite	20	25	55	25		15	4							1							x		
TL204	tonalite	16	30	50	25		10	4		1					1									
TL212	tonalite	25	35	40	40		10	5		2					2				cumm6					
TL213	tonalite	25	20	55	30		10	4		10					1									
TL215	tonalite	31	25	45	30		10	10		10					1		x		ser					x
TL216	tonalite	25	25	50	25		18	5							2		x		ser			x		
TL218	tonalite	20	30	45	30	5	10	10									x		ser			x		
PC223	tonalite	20	40	45	25		10	10																

† key to abbrevations:
CI = color index; QTZ = quartz; PLG (An) = plagioclase with Anorthite content after Michel-Levy (1887); KSP = K-feldspar; HBL = hornblende; BIO = biotite; CPX = clinopyroxene; OPX = orthopyroxene; GAR = garnet; SPH = sphene; APA = apatite; ZIR = zircon; OPQ = opaques; EPI = epidote; CHL = chlorite; MUS = muscovite; OTH = other; cumm = cummingtonite; graph = graphite; oliv = olivine; scap = scapolite; ser = sericite; sill = sillimanite; ANL = annealed; RXL = recrystallized; MYL = mylonitic or protomylonitic; CST = cataclastic; RTR = retrograded; qz = quartz; grdiorite = granodiorite; qf = quartzo-feldspathic; Ca-silc = calc-silicate; pxhbdite = pyroxene hornblendite. Rock names after Streckeisen (1976, 1973).

§ U/Pb zircon geochronology sample.

The main mineral assemblage in the hypersthene tonalite is quartz, plagioclase, biotite, and hornblende. Quartz is typically interstitial, 10-20 volume percent, and has undulose extinction. Plagioclase has a composition of An_{25} to An_{55},and commonly has local weak to very weak zonation and sharp albite twins. Hornblende, 20-40%, is commonly poikilitic, pleochroic pale to olive-brown or blue-green, and anhedral in habit. Biotite, ≤5%, is a pleochroic medium-brown to red-brown. Hypersthene, pleochroic clear to pale pink, is a common minor mineral, and is present as subhedral grains contained within hornblende. Garnet and clinopyroxene are less common accessory minerals, and are not found together. Hypersthene and clinopyroxene occur locally together as early igneous phases, often poikilitically enclosed by hornblende in an equilibrium setting (Figure 19a). Cummingtonite is also locally present, typically as a reaction rim between hypersthene and hornblende.

The rock commonly shows a recrystallized, blastomylonitic texture that is rarely annealed. These textures overprint the original hypidiomorphic granular texture of the tonalite. Retrograde reactions are common. These involve the replacement of pyroxene (normally hypersthene) with amphibole (both cummingtonite and hornblende, Figure 19b). No textural evidence for prograde reactions was observed. Mylonitic textures were rarely seen. Cataclastic textures are found locally near the contact with the White Oak unit in the vicinity of the Garlock fault.

II.3.4 Metagabbro of Tunis Creek

The metagabbro of Tunis Creek forms a conspicuous dark, roughly circular mass on the north and west slopes of Winters Ridge, approximately centered on Tunis Creek (see Plate 1). It also occurs as several small stocks within the quartzo-feldspathic gneiss of Pastoria Creek (Plate 3). It was originally mapped

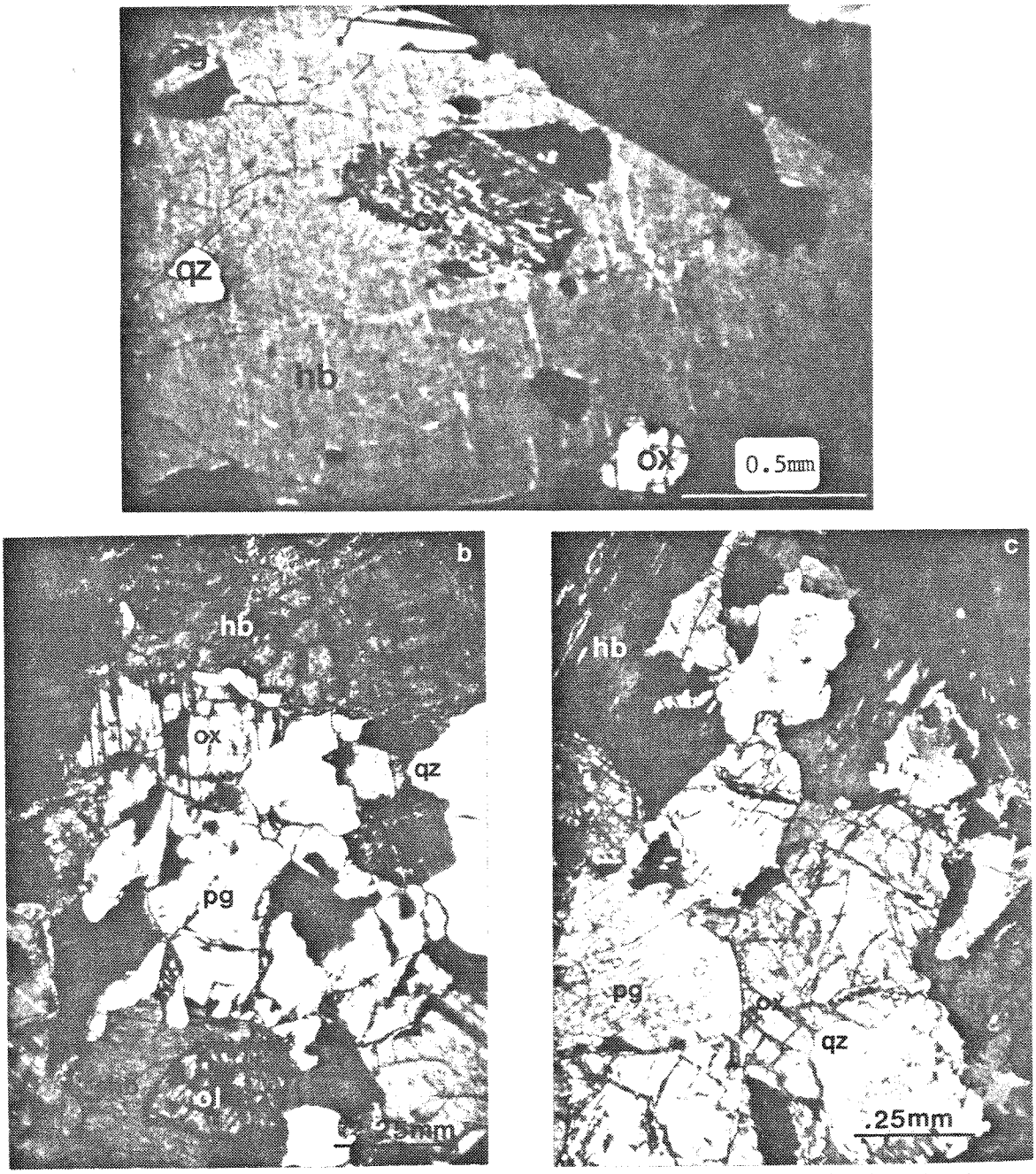

Figure 19. Photomicrographs of hypersthene tonalite of Bison Peak, with hornblende poikilitically enclosing hypersthene and clinopyroxene in equilibrium textures (a); and retrograde reactions of olivine to hypersthene ± cummingtonite, and hypersthene to cummingtonite ± hornblende (b,c). Field of view is 2 mm (a) and 0.8 mm (b,c). Minerals are qz=quartz, pg=plagioclase, ol=olivine, ox=orthopyroxene, cx=clinopyroxene, hb=hornblende, cu=cummingtonite.

as gabbro by Weise (1950), and was included as part of the dark amphibolite gneiss of Ross (1980, 1986). Sharry (1981b) called it the Tunis Creek granulite on the basis of the presence of orthopyroxene, garnet, and "relict" compositional banding. The current map distribution of the unit approximates that of Sharry (1981b) and Weise (1950).

The main mass is surrounded on the south and west by poorly exposed intrusive contacts with the quartzo-feldspathic gneiss of Pastoria Creek, on the east by gradational contacts with the Bison Peak unit, and on the north by gradational contacts with the tonalite gneiss of Tejon Creek and the paragneiss of Comanche Point, and by overlying Tertiary strata. Contacts with the surrounding quartzo-feldspathic gneiss of Pastoria Creek are sharp, concordant or intrusive contacts, while those with the hypersthene tonalite of Bison Peak are both gradational and sharp, where observable. The sharp contacts resemble intrusive contacts, while the gradational contacts appear to originate from magma mixing (as discussed above). The contact with the tonalite gneiss of Tejon Creek is a near continuous transition in terms of mineralogy and deformation, going from gabbro to tonalite gneiss.

The metagabbro is dominantly a two pyroxene, plagioclase hornblende gabbro with occasional remnants of olivine. The metagabbro of Tunis Creek is not a true granulite (Sharry, 1981b) following similar arguments given in the above section. It is most likely part of a gabbroic intrusive complex that crystallized under upper amphibolite to lower granulite conditions.

The gabbro typically occurs as dark grey to black, massive unfoliated outcrops. It lacks a pervasive foliation (Figure 20) and other notable deformational features. The foliations that are observed resemble igneous flow foliations and compositional layering, along with local cumulate layering. Foliations are also

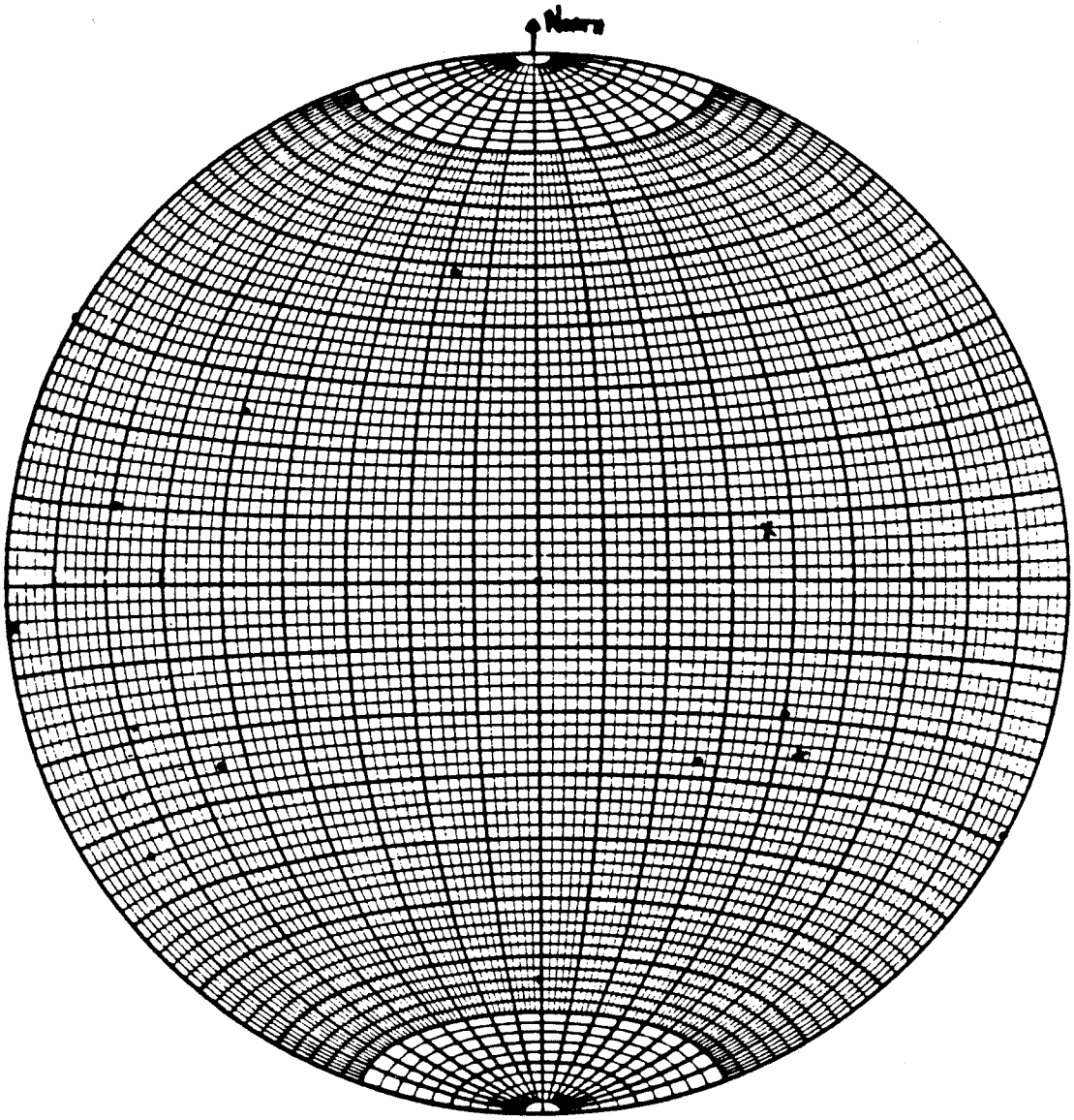

Figure 20. Lower hemisphere projection, equal-area stereoplot of poles to foliation for metagabbros of Tunis Creek(.) and Squirrel Spring(x).

present locally where hornblende shows a preferred orientation. Typically, however, the rock has randomnly oriented polygonal grains. The metagabbro contains relict olivines of probable igneous origin. It is probably the most easily distinguishable rock in the gneiss complex due to the lack (or low content) of quartz and biotite, which appear in all of the other units that make up the gneiss complex; its dark, massive appearance; and its lack of a deformational fabric. It has a zircon age of about 101 Ma.

The metagabbro is a dark, even, fine- to coarse-grained, weakly to nonfoliated, hypidiomorphic to allotriomorphic granular rock (Table 7). It ranges in composition from a two-pyroxene hornblende diorite to gabbro, with scattered porphyroblastic garnet, and contains small bodies of ultramafic and intermediate composition. It consists dominantly of sub-equal portions of plagioclase (often zoned) and poikilitic hornblende. Minor amounts of garnet, opaques, reddish hypersthene, clinopyroxene, cummingtonite, and quartz are found. Plagioclase is anhedral, with a composition of around An_{30} to An_{50}. It is well twinned, and sometimes shows a weak zoning. Hornblende is anhedral to subhedral, dark green to olive or brown pleochroic, and poikilitically encloses pyroxene and plagioclase (Figure 21a,b). It occurs as millimeter-sized prisms to centimeter-scale oikiocrysts. Olivine remnants were found as cores rimmed by orthopyroxene or amphibole (Figures 21a,22). Hypersthene is anhedral, and moderately pleochroic. The textural settings of the pyroxenes indicate a pyrogenic origin as an early liquidus phase, and/or as an olivine reaction product. The assemblage two pyroxenes + garnet was not seen. Secondary cummingtonite is a lighter green color, and occurs as a rim around orthopyroxene.

Red almandine garnets in disequilibrium settings occur as euhedral to subhedral porphyroblasts up to 5 cm in diameter that contain plagioclase inclusions.

TABLE 7. SUMMARY OF PETROGRAPHY OF THE METAGABBROS OF TUNIS CREEK AND SQUIRREL SPRING†

HAND SAMPLE	ROCK NAME	CI	QTZ	PLG	(An)	KSP	HBL	BIO	CPX	OPX	GAR	SPH	APA	ZIR	OPQ	EPI	CHL	MUS	OTH	TEXTURES ANL	RXL	MYL	CST	RTR
METAGABBRO OF TUNIS CREEK																								
WR30/1	diorite	55		40	40		50		x						5					x				
WR84a§	diorite	48	3	50	40		35		1	x	1		1		10				cumm					x
WR84b	diorite	38	2	50	40		30			2	x				6		x		cumm					
WR85	qz diorite	53	3	44	40		50								3									
WR86§	diorite	50		50	35		45		x	x	x				5					x	x			
WR87	diorite	48	2	50	40		40								8					x				
PC172	diorite	51		40	40		x		10						1				cumm40	x				
PC173	diorite	46		30	35		x		5						1				cumm40					x
PC174	gabbro	76		15	50		25		15	10					1				oliv10/cumm15					x
PC175	gabbro	66		30	45		20		10	8					x				oliv15/cumm10					x
WR189	diorite	45		50	40		40		x						5					x				
WR190§	diorite	53		35	45		40		3	x					5				oliv1/cumm3					x
PC224	gabbro	53		45	35		50								3						x			
PC225	diorite	50		50	35		40		5						5					x				x
PC226	gabbro	58		40	55		55								3									x
PC227§	gabbro	44		60	45		10		25	x					5				oliv2/cumm2	x				x
WR655	qz diorite	50	5	45	35		45								5					x				
METAGABBRO OF SQUIRREL SPRING																								
PC62b	qz diorite	40	5	50	25		40										5			x				
PC64b	diorite	45		55	35		45										x		ser/cumm					
PC74	diorite	55		45	35		25								10	10	10		ser					
PC78	qz diorite	50	5	45	35		45								5									
PC102	diorite	55		45	40		45								10				ser/cumm					
PC105	qz diorite	35	3	60	30		35				x								ser					
MISCELLANEOUS OTHERS, Kern Mesa Area																								
CM134	diorite	60		40	45		15		5	15									oliv10/cumm15					x
CM138	px hbdite	99					70		29						1									

† key to abbrevations:
CI = color index; QTZ = quartz; PLG (An) = plagioclase with Anorthite content after Michel-Levy (1887); KSP = K-feldspar; HBL = hornblende; BIO = biotite; CPX = clinopyroxene; OPX = orthopyroxene; GAR = garnet; SPH = sphene; APA = apatite; ZIR = zircon; OPQ = opaques; EPI = epidote; CHL = chlorite; MUS = muscovite; OTH = other; cumm = cummingtonite; graph = graphite; oliv = olivine; scap = scapolite; ser = sericite; sill = sillimanite; ANL = annealed; RXL = recrystallized; MYL = mylonitic or protomylonitic; CST = cataclastic; RTR = retrograded; qz = quartz; grdiorite = granodiorite; qf = quartzo-feldspathic; Ca-silc = calc-silicate; pxhbdite = pyroxene hornblendite. Rock names after Streckeisen (1976, 1973).

§ U/Pb zircon geochronology sample.

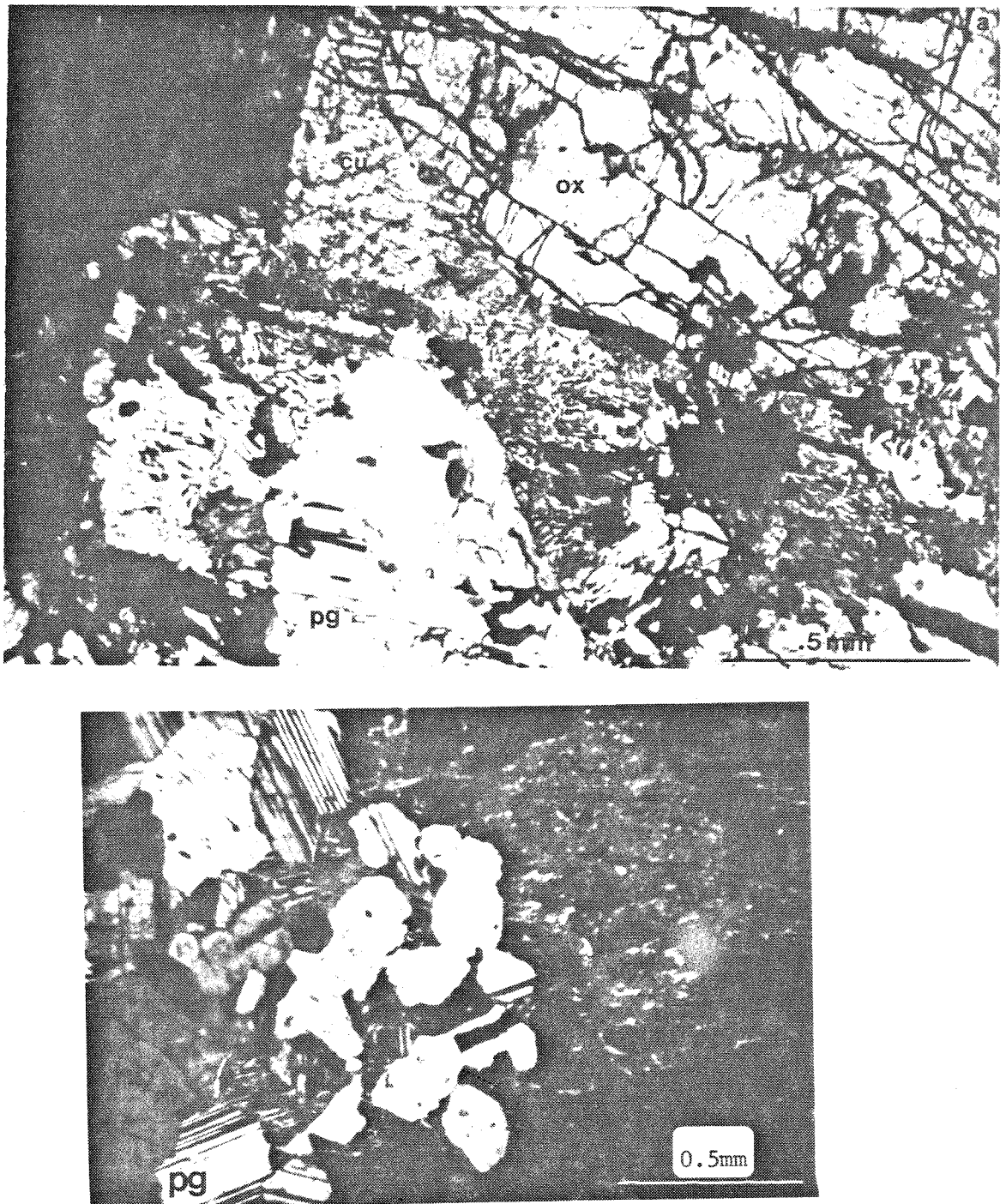

Figure 21. Photomicrographs of the metagabbro of Tunis Creek showing hornblende oikiocryst enclosing hypersthene and plagioclase (a), and retrograde reactions of olivine to orthopyroxene ± cummingtonite, and orthopyroxene to hornblende ± cummingtonite. Field of view is 2 mm. Minerals are pg=plagioclase, ox=orthopyroxene, ol=olivine, hb=hornblende, cu=cummingtonite.

Figure 22. Photomicrographs illustrating retrograde reactions in the metagabbro of Tunis Creek. These reactions involve olivine to orthopyroxene ± amphibole, and orthopyroxene to cummingtonite ± hornblende. Field of view is 2 mm. Minerals are pg=plagioclase, am=amphibole, cu=cummingtonite, ox=orthopyroxene, ol=olivine.

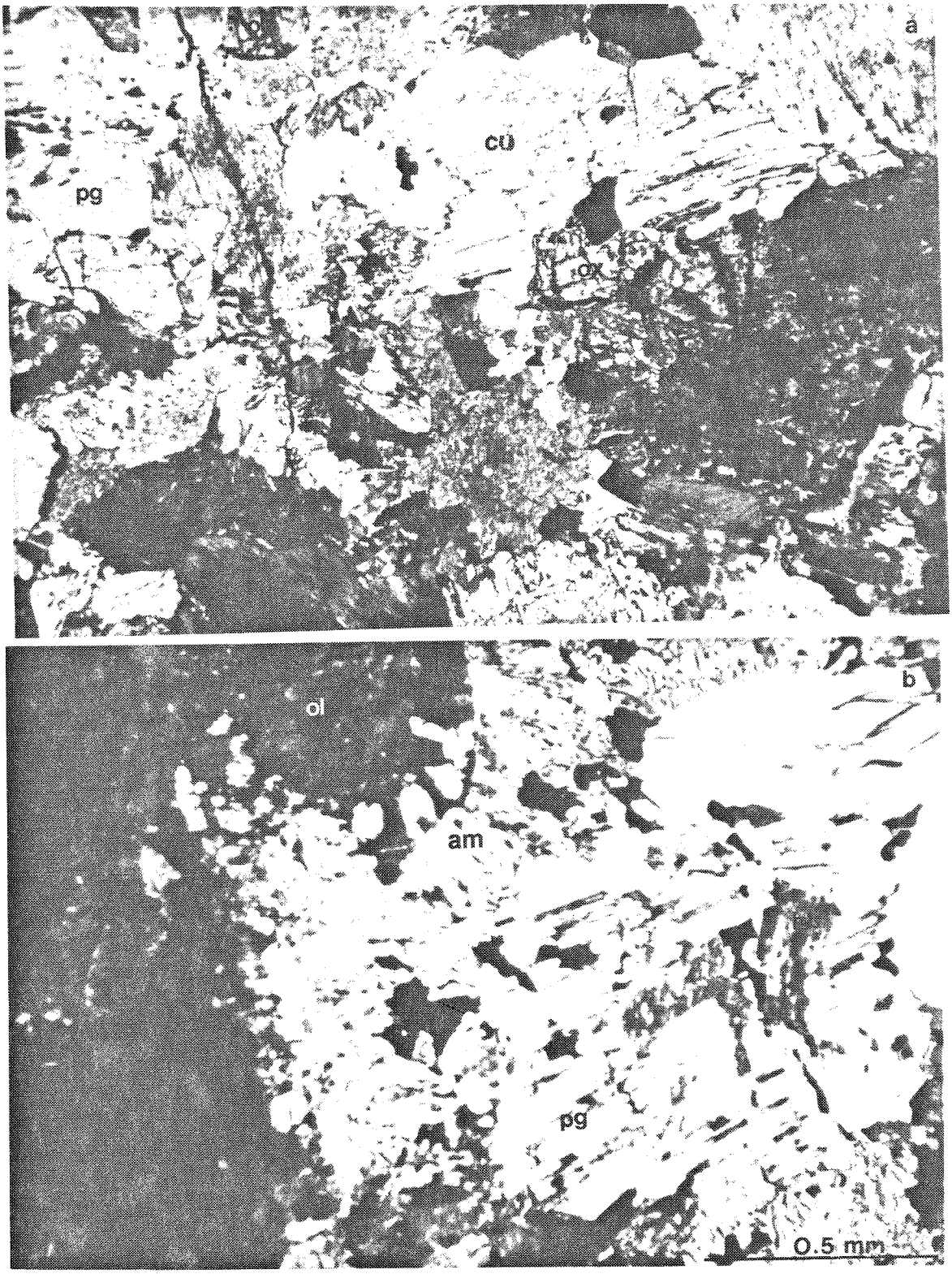
a
pg
cü
cx
b
ol
am
pg
0.5 mm

The garnet is most often seen granoblastically growing across earlier apparent igneous textures and structures and occasionally across ductile deformation fabrics (Figure 23), and occurs as chains of porphyroblasts locally along fractures and veins. The garnet is often seen to have grown clearly at the expense of hornblende in bleached, plagioclase-rich halos and zones. This may represent local dehydration reactions under static conditions that occured after cessation of magmatic flow. The garnet in the Tunis Creek unit is texturally distinct from the garnet that is in equilibrium settings in the quartzo-feldspathic gneiss of Pastoria Creek.

Annealed, retrograde, and remnant cumulate textures are found. Evidence of annealed textures (Figure 24b,c;25) can be seen in the recrystallization of grains into polygonal shapes, commonly with 120° angles between crystal faces. Cumulate textures (Figure 21b) are seen in optically aligned, polygonally shaped crystals, planar rythmic variations in modal hornblende, allotriomorphic textures in poikilitic hornblende and zoned plagioclase, and compositional layering. Remnant cumulate textures suggest a cumulate pyroxenite as a protolith. Retrograde reactions (Figures 21a,22) involve the replacement of olivine, present as remnant grains, by orthopyroxene, and pyroxenes by amphiboles. Evidence for prograde reactions was not observed. Recrystallized textures are common (Figures 24a, 25b), while ductile deformational fabrics are rare and concentrated along the margins of the unit.

Ultramafic rocks occur as centimeter to hundred-meter sized patches of hornblendite, hornblende orthopyroxenite, hornblende-plagioclase clinopyroxenite, and cumulate wehrlite. They are locally present as intrusive "plugs" into the gneiss of Pastoria Creek. Similar ultramafic rocks are found in the tonalite of Bear Valley Springs in the Kern Mesa area southwest of Caliente.

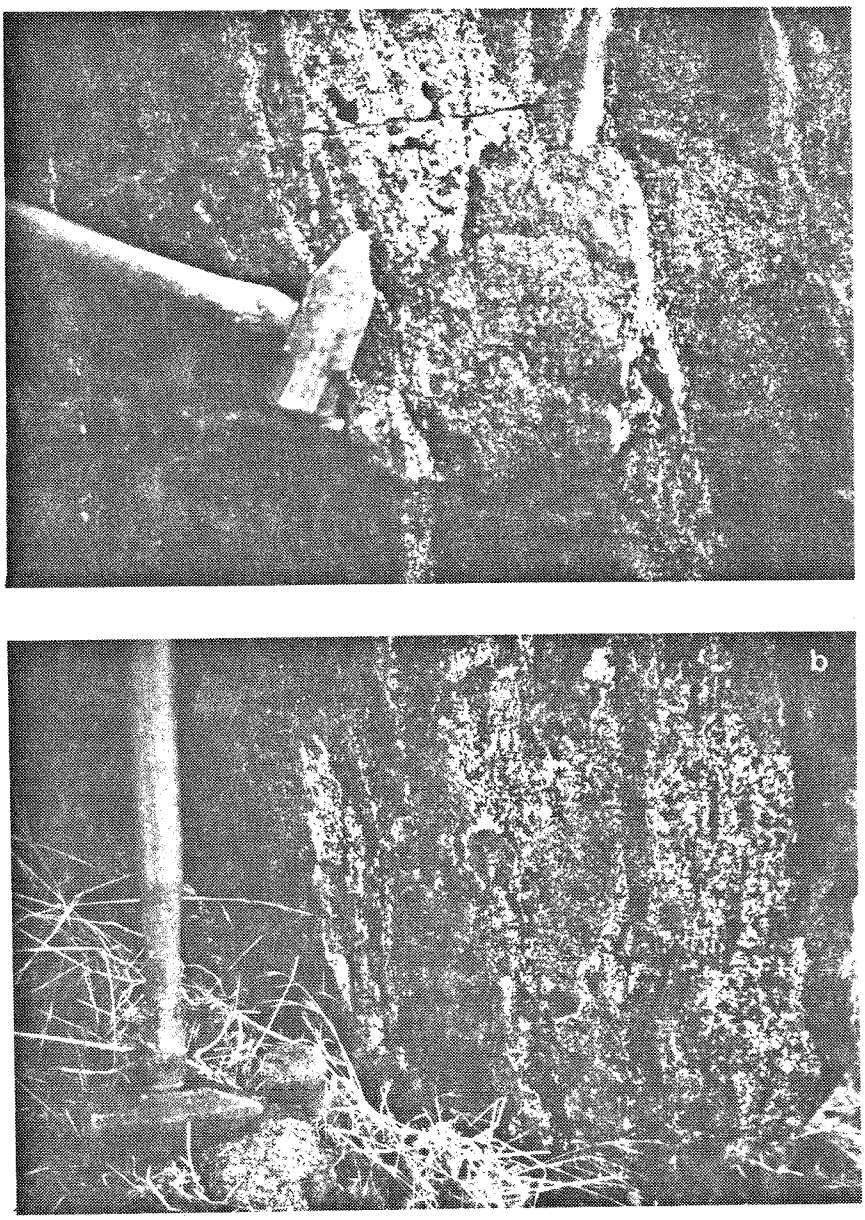

Figure 23. Photographs of field relations in metagabbro of Tunis Creek. Large porphyroblastic garnets are seen to be growing across earlier igneous flow foliation in the rock, and to be filling cross-cutting veins, at arrow in (a). Note the bleached halos (mafic mineral free zones) around the garnets.

Figure 24. Photomicrographs of metagabbro of Tunis Creek showing recrystallized textures (polygonally shaped minerals) (a), and annealed textures (120° triple junctions) (b). Field of view is 2 mm (a), 0.8 mm (b). Minerals are pg=plagioclase, bi=biotite, hb=hornblende.

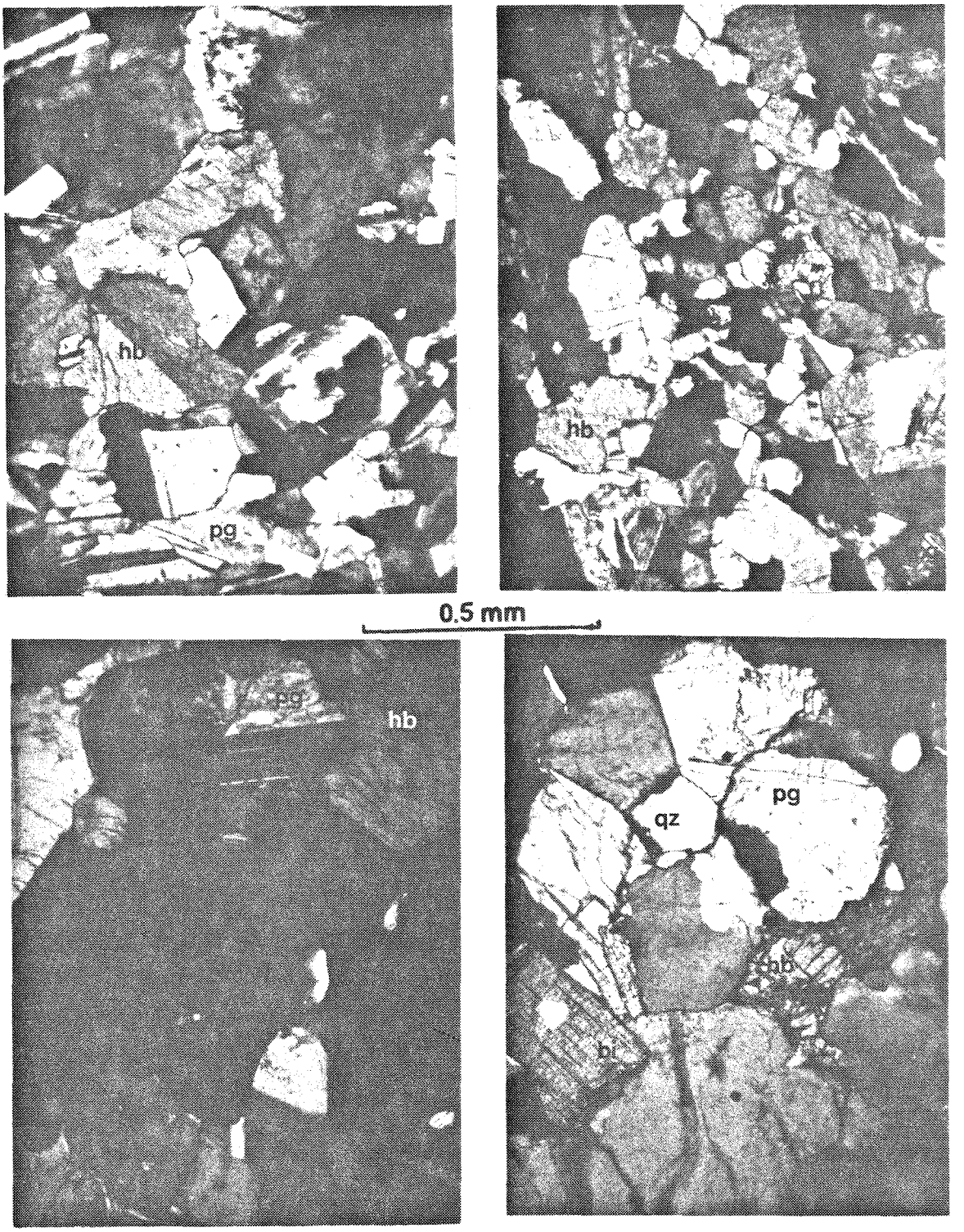

Figure 25. Photomicrographs of metagabbro of Tunis Creek showing annealed textures (confined to hornblende and plagioclase), with some recrystallization (plagioclase and biotite) (b). Field of view is 1 mm. Minerals are qz=quartz, pl=plagioclase, hb=hornblende.

II.3.5 Metagabbro of Squirrel Spring

A gabbroid body similar to the metagabbro of Tunis Creek forms much of the area west of Pastoria Creek (Plate 1), but was not studied in detail. It is informally named the metagabbro of Squirrel Spring after Squirrel Spring in Live-oak Canyon, near the center of the mass. The metagabbro is bounded by the Garlock fault on the south, and overlain by Tertiary strata on the north. It has poorly defined contacts with the quartzo-feldspathic gneiss of Pastoria Creek to the east and west that appear in places to be intrusive. It is very similar to the metagabbro of Tunis Creek mineralogically and texturally. The Squirrel Spring unit has been broken out of the previously undifferentiated amphibolitic gneisses of Ross (1980, 1986).

The metagabbro of Squirrel Spring (Table 7) appears to be less mafic than the metagabbro of Tunis Creek. It is most commonly a hornblende diorite to quartz diorite. It is composed dominantly of plagioclase, An_{25} to An_{40} and weakly zoned, and pleochroic green to brown hornblende. Quartz is uncommon. Cummingtonite is a secondary mineral, but pyroxene, olivine, and cumulate textures are not found. Garnet is present as a local, static phase. Prograde reactions are absent. The Squirrel Spring unit has textures similar to those of the Tunis Creek unit, but not as varied, and not exhibiting crystal accumulation processes.

II.4 Late deformational intrusive suite

It is thought that most of the high temperature fabrics in the Bear Valley Springs and Tehachapi suites were developed contemporaneously with deep crustal magmatism that culminated in the Bear Valley Springs intrusive event. These deformational fabrics are cross-cut by a number of weakly to nondeformed intrusive bodies. Zircon ages on these intrusives of between 90 and 100 Ma provide age constraints on the development of the high temperature fabrics. Major plutons

that exhibit such cross-cutting relations are the tonalite of Mount Adelaide and the granodiorite of Claraville. The Mount Adelaide pluton has been discussed above along with the Bear Valley Springs batholith, and was shown to be the latest phase of Bear Valley Springs plutonism and to share a synplutonic origin with the batholith. The Claraville is discussed below, along with a number of smaller intrusives.

II.4.1 Granodiorite of Claraville

The granodiorite of Claraville is exposed in several areas north and east of Tehachapi that are separated by Tertiary volcanic rocks. The granodiorite extends from the Garlock fault south of Tehachapi northward to the vicinity of Walker Basin, and eastward to the Mojave Desert (where the Garlock fault again is the boundary). The granodiorite has a total area approaching that of the tonalite of Bear Valley Springs (Plate 1). The granodiorite lies east of the Kings sequence metamorphic septum forming the east wall of the tonalite of Bear Valley Springs. It typically has concordant contacts with the septum, and locally cross-cuts the major deformational fabrics within the metamorphic framework rocks. The contacts of the granodiorite with the tonalite of Bear Valley Springs parallel the foliation within the tonalite. The granodiorite concordantly intrudes and cuts the penetrative fabric of the tonalite for a few kilometers just north of the Garlock fault. The relatively nondeformed state and low color index distinguish the Claraville body from the tonalite of Bear Valley Springs and the gneiss complex of the Tehachapi Mountains. The granodiorite has a zircon age of 90±2 Ma.

The granodiorite of Claraville was only studied along upper Tweedy Creek (north of Tehachapi). It is a homogeneous, medium- to coarse-grained, hypidiomorphic granular, biotite granodiorite (Table 8). It has a well preserved granular igneous texture, and has a salt and pepper appearance. It is generally nonde-

TABLE 8. SUMMARY OF PETROGRAPHY OF THE LATE DEFORMATIONAL INTRUSIVE SUITE†

HAND SAMPLE	ROCK NAME	CI	QTZ	PLG	(An)	KSP	HBL	BIO	CPX	OPX	GAR	SPH	APA	ZIR	OPQ	EPI	CHL	MUS	OTH	TEXTURES ANL	RXL	MYL	CST	RTR
GRANODIORITE OF CLARAVILLE																								
TC40§	tonalite	22	20	50	x		15	5				2					3		ser			x		
TC45	tonalite	31	30	40	x	5		25							1						x			
PM542	grdiorite	5	20	55	x	20		5																
TONALITE STOCK AT TWEEDY CREEK																								
TC24	tonalite	20	30	45	40	5		15									1		ser		x	x		
TC27§	grdiorite	15	15	55	30	12		12							2		3				x	x		
PEGMATITE DIKES																								
CM620§	granite	5	35	35	20	25		3			2													
GARNET GRANITE DIKE AT PASTORIA CREEK																								
PC35§	granite	15	20	15	40	50		5			5				5			x	ser		x			

† key to abbrevations:
CI = color index; QTZ = quartz; PLG (An) = plagioclase with Anorthite content after Michel-Levy (1887); KSP = K-feldspar; HBL = hornblende; BIO = biotite; CPX = clinopyroxene; OPX = orthopyroxene; GAR = garnet; SPH = sphene; APA = apatite; ZIR = zircon; OPQ = opaques; EPI = epidote; CHL = chlorite; MUS = muscovite; OTH = other; cumm = cummingtonite; graph = graphite; oliv = olivine; scap = scapolite; ser = sericite; sill = sillimanite; ANL = annealed; RXL = recrystallized; MYL = mylonitic or protomylonitic; CST = cataclastic; RTR = retrograded; qz = quartz; grdiorite = granodiorite; qf = quartzo-feldspathic; Ca-silc = calc-silicate; pxhbdite = pyroxene hornblendite. Rock names after Streckeisen (1976, 1973).

§ U/Pb zircon geochronology sample.

formed and weakly foliated, primarily along its margins, and lacks a pervasive foliation. The foliation is north-northwest trending with moderate east dips (Figure 26). The foliation is somewhat discordant with regional trends in the Tweedy Creek area (Plate 2). Mafic inclusions in the granodiorite are rare to nonexistent. The Claraville mass is similar to plutons which comprise most of the south-central Sierra Nevada east of the $^{87}Sr/^{86}Sr$ = 0.7060 isopleth (Ross, 1980, 1986).

Within the granodiorite, biotite consists of 5-10% of the rock, and is a pleochroic yellow to brown. Hornblende is rarely seen. Quartz ranges up to 15%, and is slightly strained and sutured. Plagioclase is well twinned, faintly zoned, and has a composition of between An_{30} and An_{40}. K-feldspar is rarely twinned, and ranges from 5 to greater than 15 volume percent. The granodiorite shows a slight to moderate deformational fabric in the vicinity of the metamorphic septum, where it contains recrystallized quartz and has a local protomylonitic texture.

II.4.2 Tonalite stock at Tweedy Creek

A small tonalitic stock intrudes the Kings sequence metamorphic framework rocks and the augen gneiss of Tweedy Creek (Plate 1,2). It locally cross-cuts the gneissic fabric of the augen gneiss and the metamorphic septum (Figure 27). The stock is comprised of two discrete masses, about one by two km, that are elongate in a northeasterly fashion. The long axis of the tonalite stocks are concordant with the regional fabrics and outcrop pattern of the augen gneiss and metamorphic septum. The tonalite is strongly foliated with sheared mafic and quartz grains, and has a moderate blastomylonitic to cataclastic texture (Figure 28). The foliation is steeply east dipping along northeast trends that are concordant with the margins of the stock, and with regional trends. The foliation is probably due to differential movement accompanying the diking nature of the intrusion of the stock. The stock has an age of 93±3 Ma.

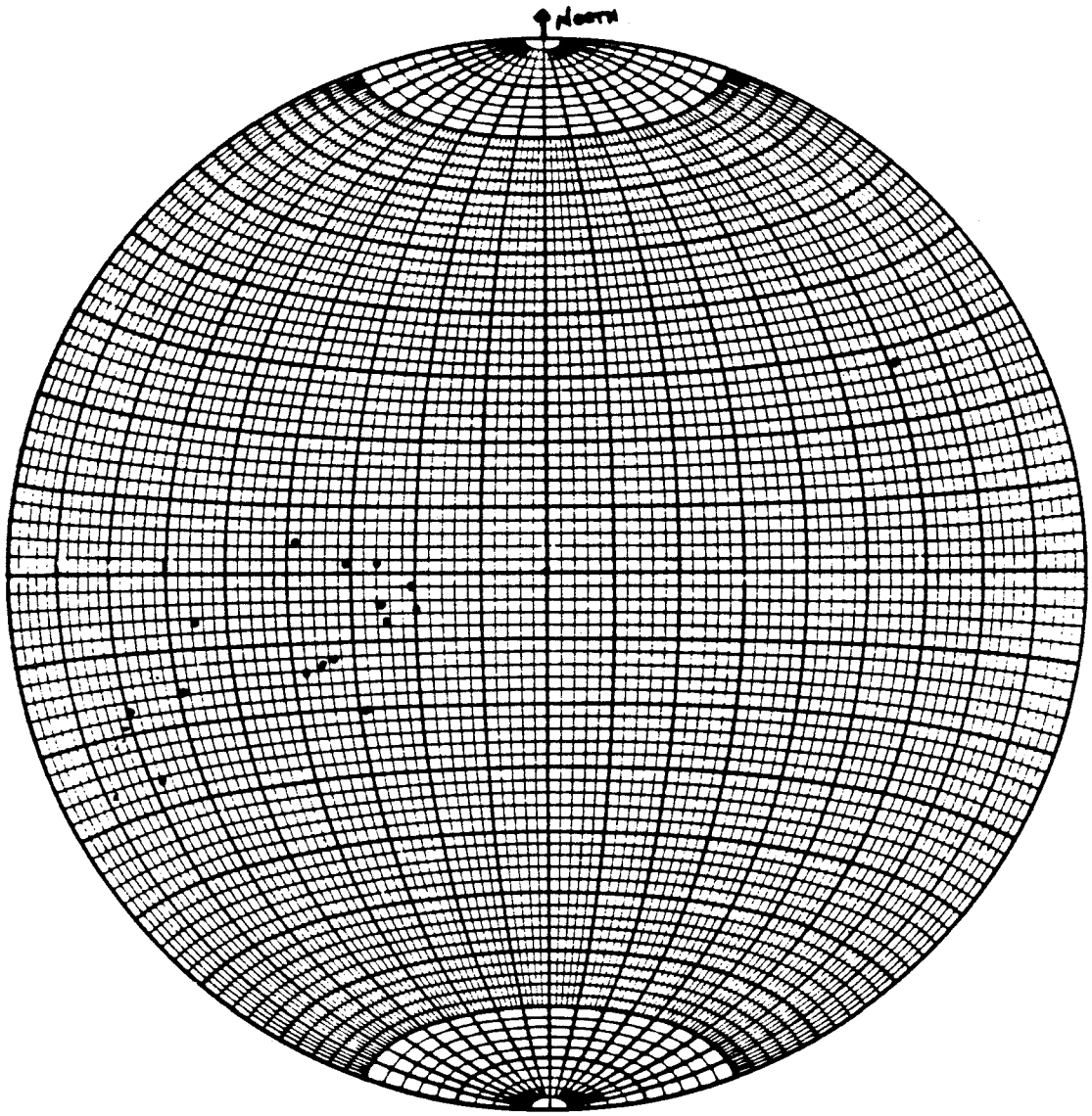

Figure 26. Lower hemisphere projection, equal-area stereoplot of poles to foliation for granodiorite of Claraville.

Figure 27. Field photographs of tonalitic stock intruding augen gneiss of Tweedy Creek. (a) shows tonalite (at pencil) cross-cutting foliation in the orthogneiss, which is oriented parallel to the Brunton. A chill margin about 0.4 cm wide can be seen on both sides of the tonalite dike. Field of view is 1 m. (b) shows a close-up of diking of the tonalite into the gneiss. Field of view is 25 cm wide.

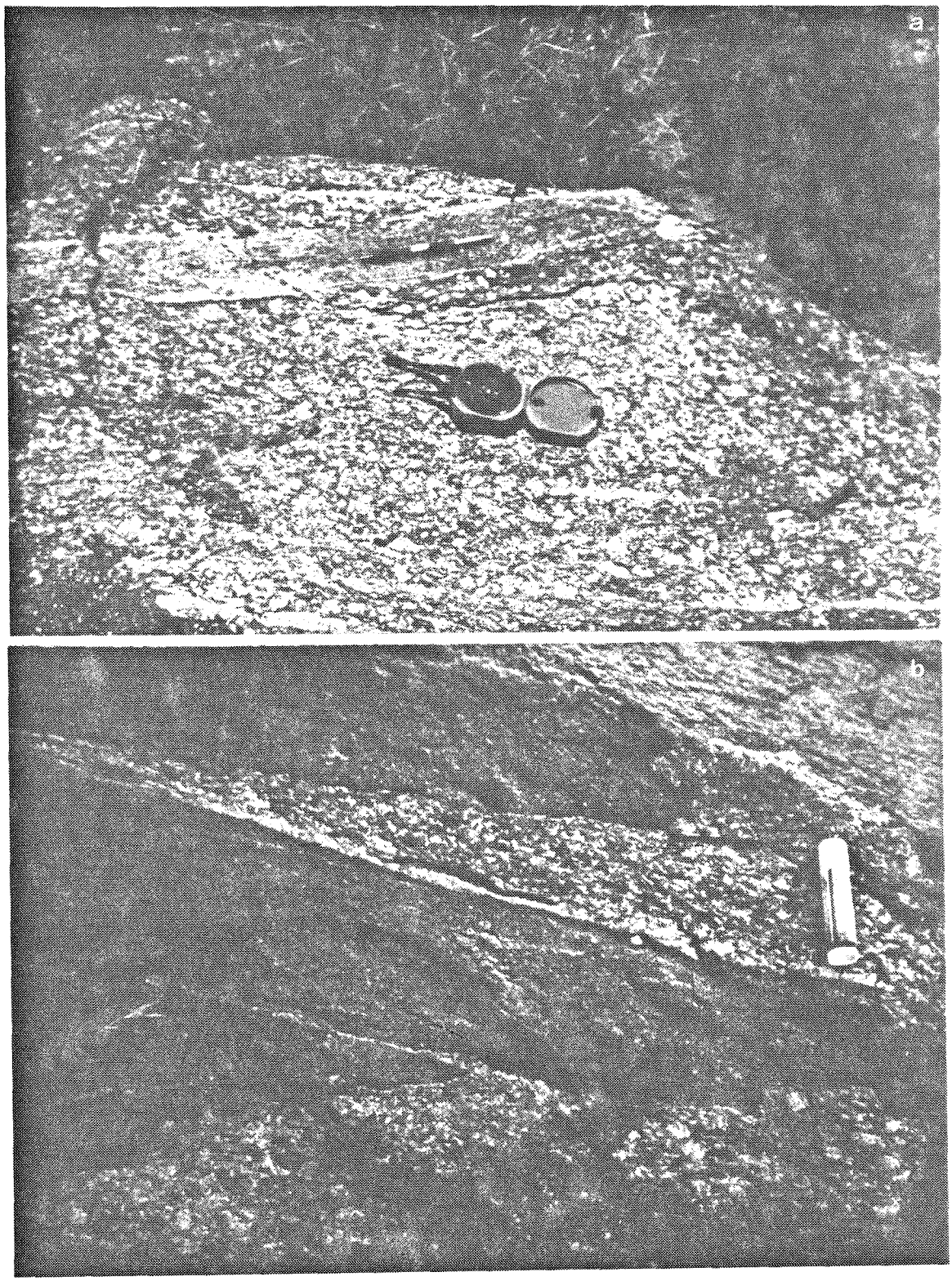
a
b

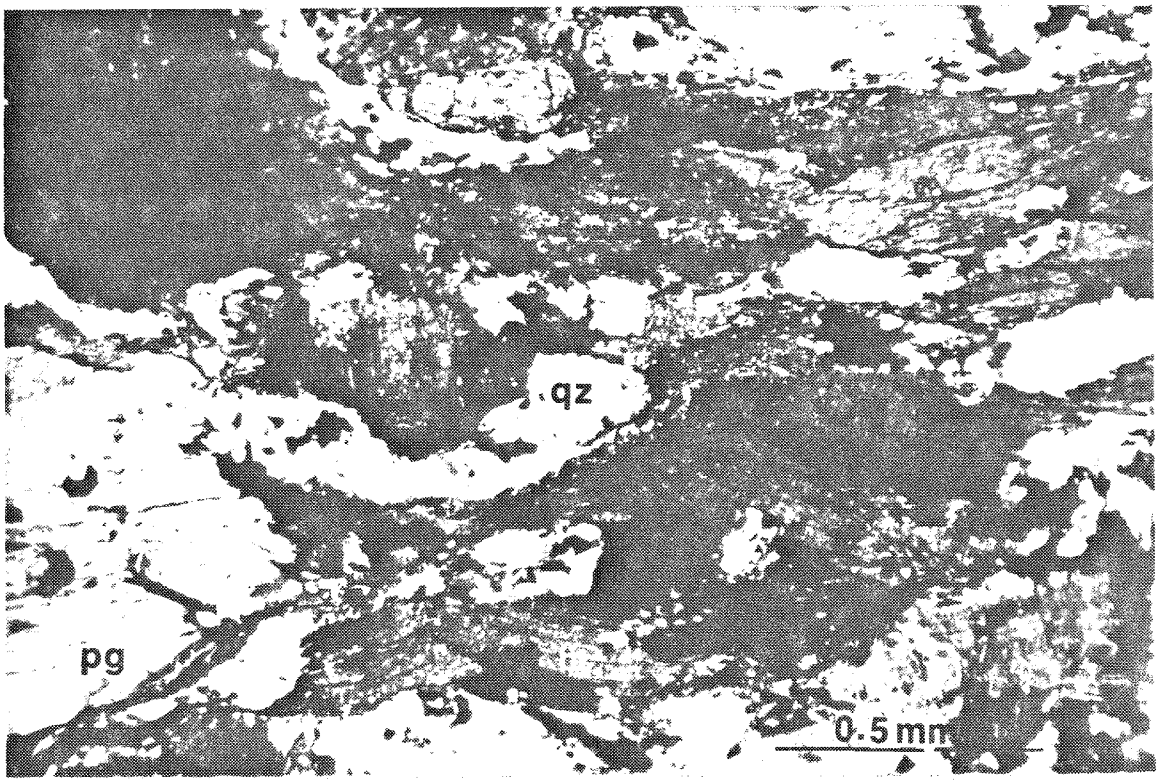

Figure 28. Photomicrograph of the tonalite stock that intrudes the augen gneiss and Kings sequence metamorphic rocks at Tweedy Creek. Field of view is approximately 2 mm wide. Minerals are qz = quartz, pg = plagioclase, bi = biotite.

The tonalite stock is a moderately foliated, medium-grained, biotite hornblende tonalite (Table 8). It is composed of quartz, plagioclase, and biotite. Quartz is strained, recrystallized, and forms ribbon structures. Plagioclase occurs as porphyroblasts with rounded edges. Biotite forms stringers that impart a foliation to the rock. The gneiss has a moderate blastomylonitic fabric intermediate in degree between the fabric in the augen gneiss and the margins of the granodiorite of Claraville.

II.4.3 Pegmatite dike swarms

West of Cummings Valley in the vicinity of Comanche Point and north of Caliente there are swarms of northeast trending pegmatite dikes (Plate 1). These dikes range from a few centimeters to ten meters in thickness, and average one to two meters in width. They have a near vertical dip, and rarely intersect one another. Some can be followed for up to two kilometers, but most are only traceable for a few hundred meters. Their width does not vary much along strike. These dikes cross-cut the foliation in the 100 Ma tonalite of Bear Valley Springs and those gneisses of the 110 to 120 Ma gneiss complex of the Tehachapi Mountains (tonalite gneiss of Tejon Creek, paragneiss of Comanche Point) at Comanche Point (Figure 29). They also cross-cut the foliation in the tonalite of Bear Valley Springs and the tonalite of Mount Adelaide north of Caliente. The dikes themselves show little to no deformation, and hence form a lower age limit to the formation of the main deformational fabrics in the tonalite and gneisses. Zircons from a pegmatite near Comanche Point yielded a concordant age of 94±2 Ma.

The pegmatite dikes (Table 8) have a granitic composition that is composed almost entirely of quartz, K-feldspar, and plagioclase (An_{20}). Small pink garnets, biotite, muscovite, and tourmaline are occasionally present, but always as accessories. Grains range in size up to several centimeters. They differ from pegma-

Figure 29. Field photographs of pegmatite dikes cross-cutting fabric in the tonalite gneiss of Tejon Creek, and paragneiss of Comanche Point. Fabric consists of a foliation and gneissosity in both the tonalite and the paragneiss. Pegmatite dikes are undeformed, and trend northeast. Field of view for upper photograph is about 2 m, and for lower photograph is approximately 0.5 m. Location along Comanche Point road.

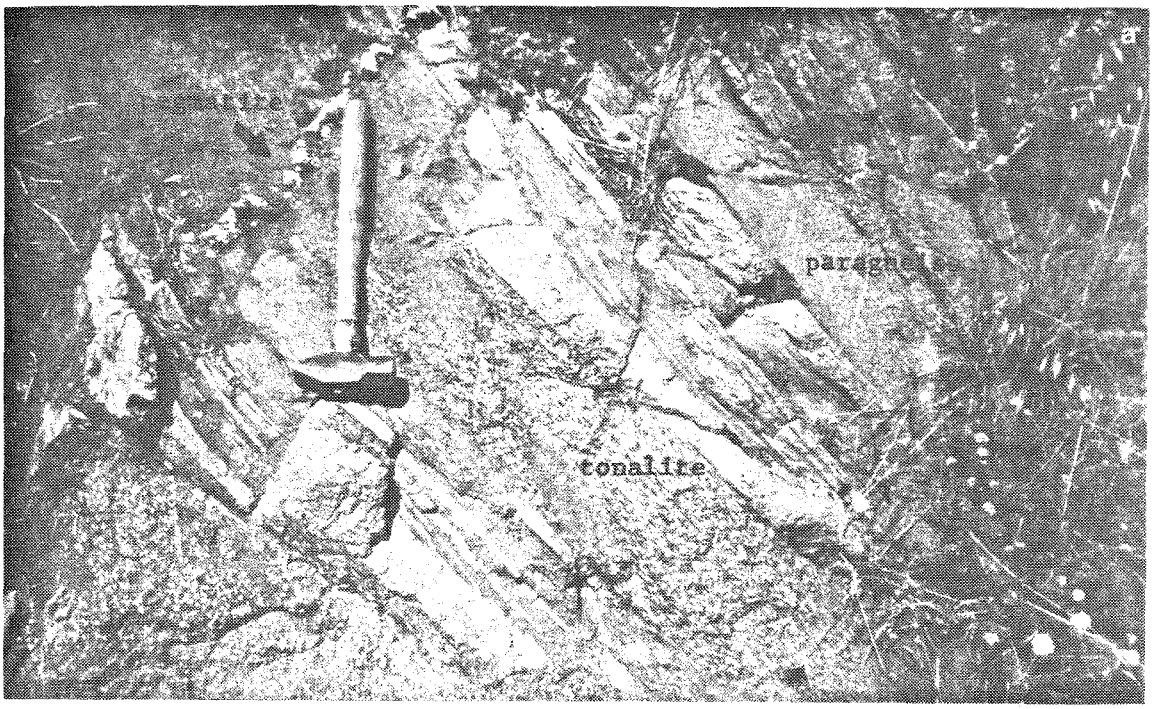
a
paragneiss
tonalite


b
hand lens for scale
pegmatite dike
interlayered paragneiss
and tonalite gneiss

tites in the quartzo-feldspathic gneiss of Pastoria Creek by considerably less deformation.

II.4.4 Garnet granite dike within Pastoria Creek gneiss

A granite dike can be found to locally cross-cut the major deformational fabric within the quartzo-feldspathic gneiss of Pastoria Creek in the Pastoria Creek area (Plates 1,3). The dike is found within granitic gneiss, and is strongly foliated and considerably deformed itself. The dike is about fifty meters thick, and can be traced for less than one kilometer. The external contacts and internal fabrics of the dike parallel those of the gneiss. The dike is not linked to pegmatites found within the Pastoria Creek unit, which are typically found in the more mafic varieties of the gneiss. It resembles the leucosomes found within the tonalite gneiss of Tejon Creek and paragneiss of Comanche Point, and may have been formed as a partial melt product from the Pastoria Creek gneisses. The age of the dike has been assigned as 97 (+20/-2), based on zircon systematics and Rb/Sr isotopic characteristics, as discussed in Chapters III and IV.

The granite dike is composed dominantly of plagioclase (An_{40}), K-feldspar, and quartz. Biotite and garnet are minor constituents, with accessory muscovite and opaques. The dike has a strong recrystallized fabric.

II.5 Gneiss complex of the Tehachapi Mountains

The gneiss complex of the Tehachapi Mountains underlies most of the Tehachapi Mountains from the Comanche Point and Tejon Creek areas west into the San Emigdio Hills (Plate 1; Ross, 1980, 1986). Grapevine Canyon is the southwestern limit of the gneiss complex as studied in this report. The complex is a heterogeneous suite of penetratively deformed meta-igneous rocks consisting of mafic to felsic gneisses, with subordinate ultramafic pods, and lenses of metasedimentary psammitic paragneiss, calc-silicate, quartzite, and marble.

The gneiss complex is overlain on the north by Eocene volcanic and sedimentary units (Nilson and Clarke, 1975; Harris, 1954) and younger Tertiary strata of the San Joaquin Valley. These strata have steep to shallow dips towards the valley. The complex is bounded by the Garlock fault on the south. From about Pastoria Creek to Cottonwood Creek the gneiss complex forms the upper plate rocks to the "Rand schist" sliver that is between two strands of the Garlock fault (Ross, 1980, 1986; Sharry, 1981b; Weise, 1950). Along its eastern and northeastern borders (in the lower Tejon Creek area) it grades into the tonalite of Bear Valley Springs through a region that Ross (1980, 1986) terms mixed and transitional. This contact is described in greater detail in a later section, and appears to be a region of probable mixing and gradational contacts.

The gneiss complex consists dominantly of plagioclase-rich amphibolites; augen, dioritic, ortho-, and para- gneisses; and local patches of pyroxene- or garnet-bearing granulite affinity rocks. Many of the rocks appear to be granitic or tonalitic orthogneisses; some are of a metasedimentary origin. Many of the rocks in the gneiss complex of the Tehachapi Mountains are very similar to rocks exposed in small bodies encompassed in plutonic rocks to the north (see Ross, 1983d, 1985, 1986; for one interpretation). One example of the similarity would be the augen gneiss exposed on Winters Ridge which very closely resembles the augen gneiss of Tweedy Creek in composition, texture, and age, and may share a similar history with the orthogneiss.

Samples from the gneiss complex of the Tehachapi Mountains have a narrowly defined age range despite such a diverse set of lithologies. Many zircon populations have systematics suggestive of igneous crystallization in the 110 to 120 Ma range, with signs of zircon inheritance or entrainment only in the vicinity of metasedimentary screens (Ch. III). Only one sample shows strong discordance.

The paragneiss of Comanche Point has a lower intercept with concordia at 108 Ma, and an upper intercept of 1450 Ma. Only one sample has an age exclusive of the 110 to 120 Ma range, a 97 Ma garnet granite dike intrusive into the gneiss complex that is included as part of the late deformational intrusive suite based on field and petrographic considerations. The zircon age systematics are discussed in Chapter III.

The main units found within the gneiss complex are: the diorite gneiss of White Oak and the quartzo-feldspathic gneiss of Pastoria Creek (after Sharry, 1981b), the tonalite gneiss of Tejon Creek, and the paragneiss of Comanche Point. The Comanche Point unit has been discussed above as part of the metamorphic framework for the region, although its joint field relations with the Tejon Creek unit will be discussed along with the latter. Cross-cutting relations between units are absent for the most part within the gneiss complex. Contacts between the various gneiss units are concordant with the overall shapes and internal fabrics of the units. Thus, an intrusive chronology relating the components in the gneiss complex could not be established.

The rocks within the gneiss complex of the Tehachapi Mountains display a range of textures, including relict igneous features, various degrees of annealing, retrograde mineral reactions, moderately rare migmatitic features, cataclastic, and mylonitic deformation, and local spaced schistosity developed under retrograde conditions. Evidence for prograde mineral reactions was observed only in obvious metasedimentary rocks (marble, quartzite, paragneiss). Sharry (1981b) has suggested that parts of the gneiss complex of the Tehachapi Mountains have a deep seated (8 kb or 27 km) origin. Granulitic nodules of a similar character have been described by Domenick and others (1983) as originating from a similar depth beneath the central Sierra. Gneissic granitoids have numerous lenses of mafic to

ultramafic rocks with apparent cumulate textures showing igneous crystallization, followed by partial annealing under upper amphibolite to granulite facies conditions. It is possible that the granulitic rocks represent hot dry spots in an otherwise upper amphibolite grade assemblage. The petrographic and geochemical evidence suggests that the gneiss complex of the Tehachapi Mountains represents the deepest exposed levels of the Sierra Nevada batholith. The field and petrographic descriptions of the individual units of the gneiss complex of the Tehachapi Mountains are described below.

II.5.1 Diorite gneiss of White Oak

The diorite gneiss of White Oak forms a narrow strip up to two km in width parallelling the Garlock fault from the vicinity of Pastoria Creek to White Oak (Twin Lakes) area (Plate 1). It was originally included as part of the diorite unit of Weise (1950). Sharry (1981b) separated it from the other units in the gneiss complex, primarily on the basis of its sheared nature.

The diorite gneiss is pervasively sheared parallel to the Garlock fault, with brittle deformation and granulation increasing towards the fault. It has poorly exposed contacts with the Bison Peak and Pastoria Creek units (Plates 3,4). These contacts are concordant with compositional and structural layering. Some of the contacts with the Bison Peak unit appear to be gradational. The diorite gneiss is distinguished from the Bison Peak and Pastoria Creek units on the basis of a lower quartz, biotite and pyroxene content, and its pervasive mylonitic to cataclastic foliation. It may have been derived from a protolith similar to the metagabbro of Tunis Creek, as suggested by Sharry (1981b). Foliation within the unit is generally oriented parallel to the Garlock fault (Figure 30), and consists of oriented plagioclase and hornblende grains.

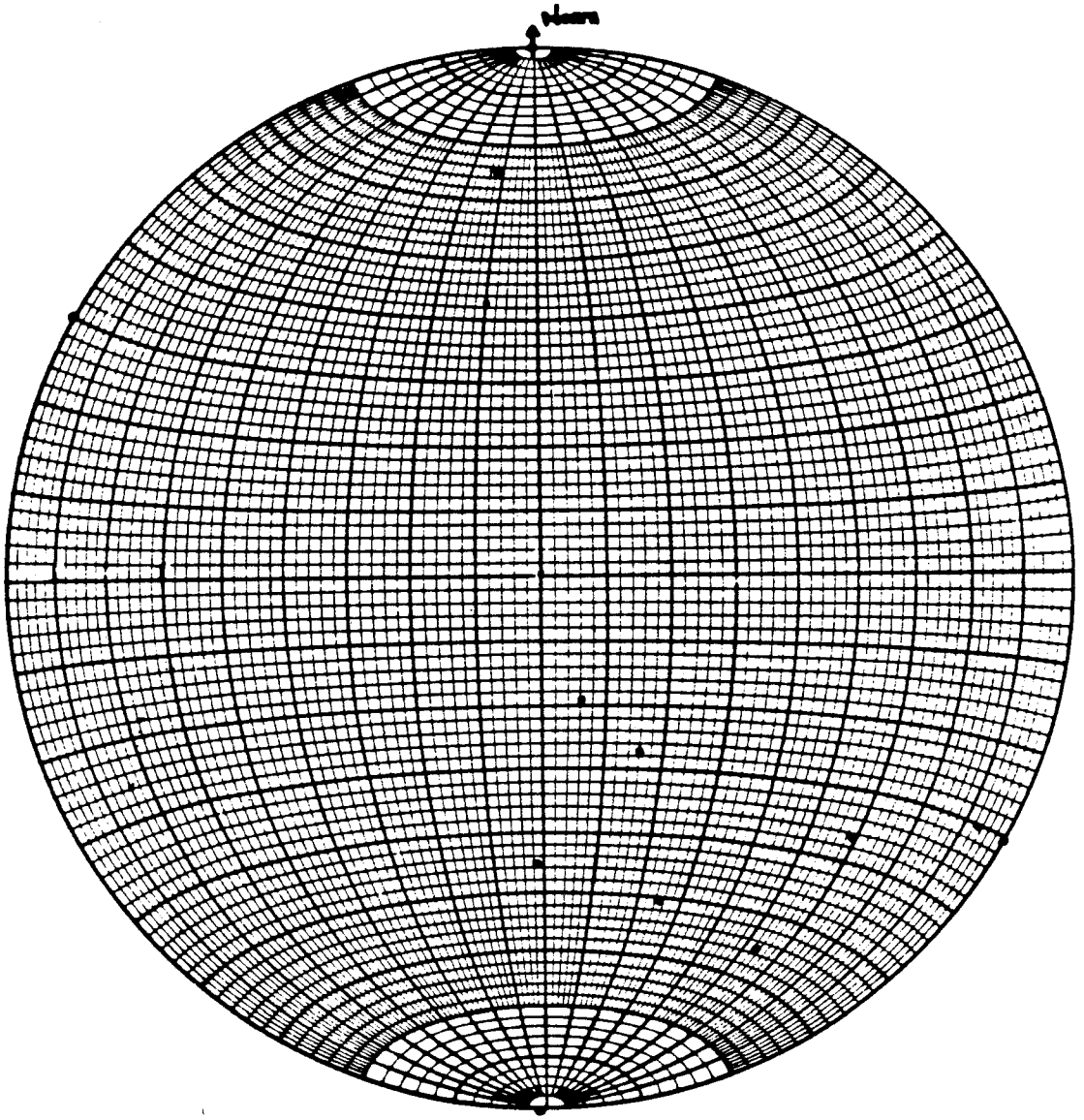

Figure 30. Lower hemisphere projection, equal-area stereoplot of poles to foliation for diorite gneiss of White Oak.

The diorite gneiss of White Oak (Table 9) is a medium- to coarse-grained, allotriomorphic granular, hornblende diorite to quartz diorite gneiss. It consists of approximately subequal portions of hornblende and plagioclase. The plagioclase, An_{25} to An_{50}, is a milky white, and rarely has a subhedral form. It commonly shows indistinct twinning, with weak zonation. It occurs in equidimensional and elongated laths, all of which show some rounding of corners. The hornblende occurs as anhedral elongate grains, and is frequently zoned. The grains have dark green to brown or olive pleochroic centers, with lighter green rims. The alignment of hornblende and plagioclase grains imparts a moderate foliation to the rock. Quartz is a minor constituent, occurring as interstitial, granulated grains. Biotite is rarely found; where found it is a pleochroic red-brown. Clinopyroxene and garnet were each found in one thin section. Chlorite is a very common alteration mineral. Considerable retrograde reactions are evident, involving biotite and hornblende going to chlorite. The rock has an overall sheared texture to it, which is commonly proto- to mylonitic. The mylonitic to cataclastic textures overprint and obliterate the earlier fabrics. Annealed textures are rare.

II.5.2 Tonalite gneiss of Tejon Creek

The tonalite gneiss of Tejon Creek is a heterogeneous collection of metaigneous appearing gneisses, and is for the most part a tonalitic orthogneiss. It is named after Tejon Creek which flows through the center of the unit. The gneiss extends in an arcuate shape around the southwestern edge of the Bear Valley Springs batholith in the Comanche Point area, occurring between the tonalite and the paragneiss of Comanche Point (Plate 1). It also forms much of the lower slopes and foothills on the north side of the gneiss complex west of Tejon Creek, where it is bounded on the south by the hypersthene tonalite of Bison Peak, and is situated between the metagabbro of Tunis Creek and paragneiss. It is commonly

TABLE 9. SUMMARY OF PETROGRAPHY OF THE DIORITE GNEISS OF WHITE OAK - GNEISS COMPLEX OF THE TEHACHAPI MOUNTAINS†

HAND SAMPLE	ROCK NAME	CI	QTZ	PLG	(An)	KSP	HBL	BIO	CPX	OPX	GAR	SPH	APA	ZIR	OPQ	EPI	CHL	MUS	OTH	TEXTURES ANL	RXL	MYL	CST	RTR
PC14	tonalite	27	15	25	35		10	15	x							x	30					x		
WR23a	diorite	39		50	50		35				1				3	2	10		ser		x			
WR23b	diorite	37		55	50		35								2	3	5		ser					
WR178	diorite	43		50	40		40								3	7						x		
WR183	qz diorite	51	4	45	30		50								1					x				
TL203	tonalite	31	25	45	25		20	10							1	x			ser			x		

† key to abbrevations:
CI = color index; QTZ = quartz; PLG (An) = plagioclase with Anorthite content after Michel-Levy (1887); KSP = K-feldspar; HBL = hornblende; BIO = biotite; CPX = clinopyroxene; OPX = orthopyroxene; GAR = garnet; SPH = sphene; APA = apatite; ZIR = zircon; OPQ = opaques; EPI = epidote; CHL = chlorite; MUS = muscovite; OTH = other; cumm = cummingtonite; graph = graphite; oliv = olivine; scap = scapolite; ser = sericite; sill = sillimanite; ANL = annealed; RXL = recrystallized; MYL = mylonitic or protomylonitic; CST = cataclastic; RTR = retrograded; qz = quartz; grdiorite = granodiorite; qf = quartzo-feldspathic; Ca-silc = calc-silicate; pxhbdite = pyroxene hornblendite. Rock names after Streckeisen (1976, 1973).

§ U/Pb zircon geochronology sample.

intimately associated with the paragneiss, and their joint field relations are discussed here. The tonalite gneiss corresponds to portions of the transitional/mixed unit of Ross (1980, 1986). It has U/Pb ages at least 10 my above those of the Bear Valley Springs suite.

The contact with the tonalite of Bear Valley Springs appears to be gradational in terms of mineralogy and texture, with an apparent smooth transition from the hornblende biotite tonalite to the K-feldspar-bearing, hornblende biotite tonalite gneiss. Intrusive relations between the two units were not observed. The contact with the hypersthene tonalite of Bison Peak was not readily observable. The contact with the metagabbro of Tunis Creek appears to be transitional in terms of mineralogy and texture, from a tonalite gneiss into a gabbro. Compared to the tonalite of Bear Valley Springs and the Bison Peak unit, the tonalite gneiss of Tejon Creek is more felsic, richer in quartz and potassium feldspar, lacks pyroxene, and contains scattered garnet and muscovite. It is also finer grained and more pervasively deformed and gneissic (Figure 31a). The tonalite gneiss has sharp concordant and intrusive contacts with the Kings sequence septum west of Cummings Valley. There is a low abundance of migmatitic structures in the septum, perhaps as a result of compositional controls (a higher silica content) relative to the paragneiss of Comanche Point.

Along much of the northern flanks of the Tehachapi Mountains, and along the power line in the Comanche Point area, the tonalite gneiss has an intimate intergradational and intrusive contact with the paragneiss of Comanche Point. Fabrics in both units are subparallel, and appear to have developed at least in part at the same time. Near the contacts with the paragneiss, the tonalite gneiss grades into a muscovite- and garnet-bearing granodiorite. Granitic leucosomes, dikes, and veins derived from migmatitic paragneiss are seen to flow or grade into

Figure 31. Photographs of field relations of tonalite gneiss of Tejon Creek. (a) shows "swirly" foliation and fine-grained nature of the tonalite gneiss, with some concentration of mafic minerals. (b) shows the tonalite gneiss of Tejon Creek intruding the paragneiss of Comanche Point. Also shown are small masses of leucocratic migmatitic material being produced from the paragneiss, and their incorporation into the tonalite gneiss. The tonalite gneiss along the contact with the paragneiss contains garnet. Field of view is approximately 0.6 m wide in (a), and 1 m in (b). Locations are in low hills northeast of the mouth of Tejon Creek.

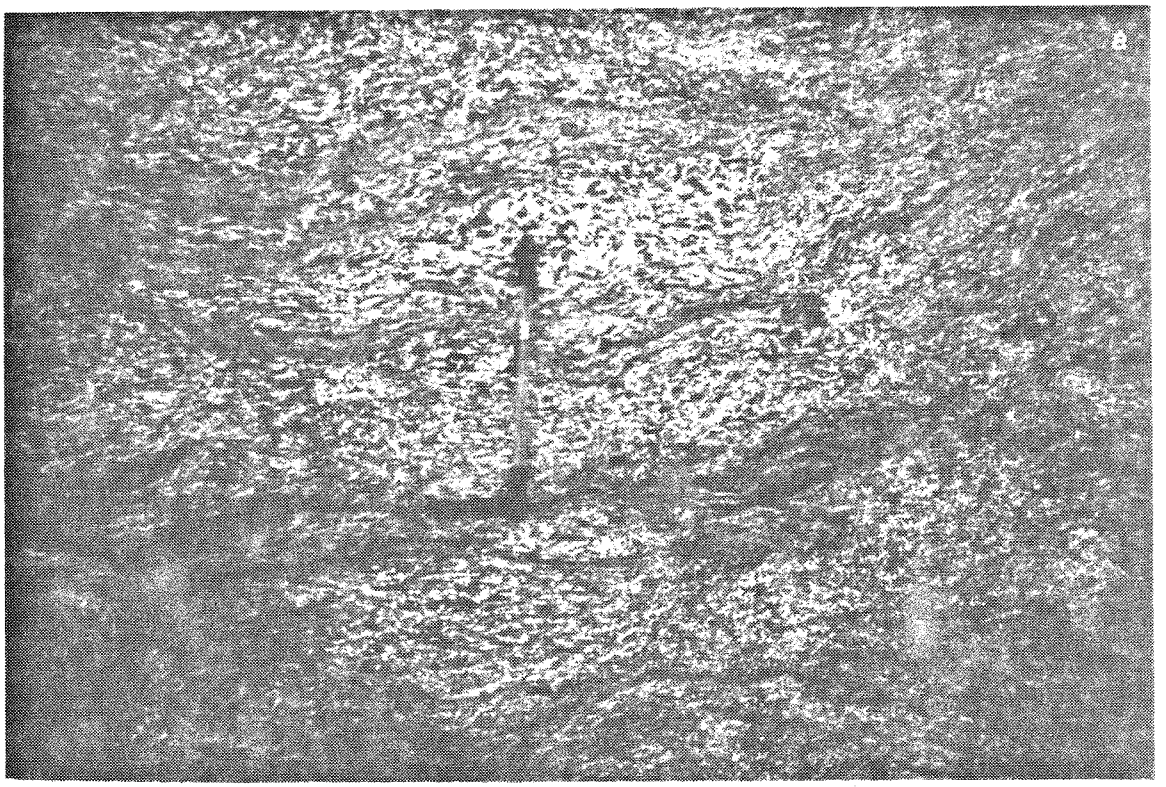
a

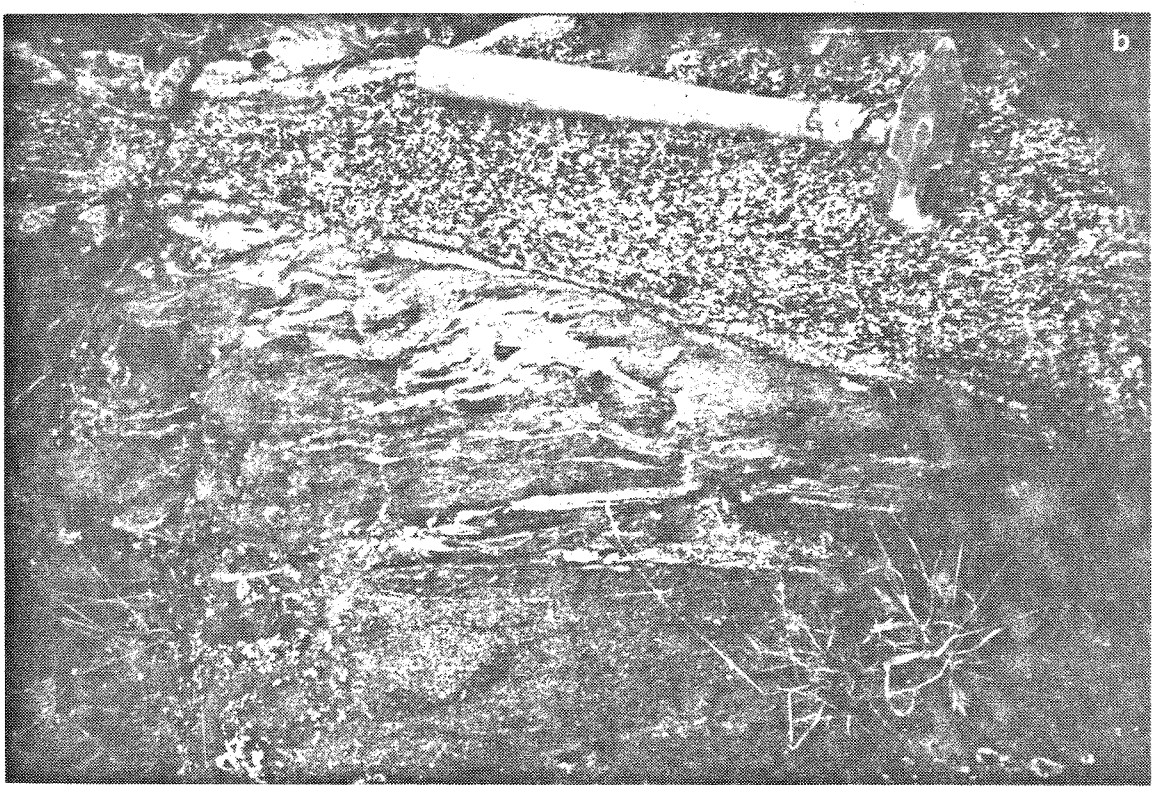
b

the tonalite gneiss (Figures 31b,32). These structures have a granodioritic composition, and are frequently transposed where they enter the gneiss. In other locations, the tonalite gneiss intrudes the paragneiss of Comanche Point (Figures 31b, 33), typically in a lit-par-lit fashion. Partly transposed apophyses of tonalite are seen to intrude the paragneiss. These apophyses are seen typically concordant with the fabric in both units. The margins of the apophyses are both sharp and diffuse, illustrating varying degrees of assimilation of the paragneiss into the tonalite gneiss. This melt production and assimilation is believed to be responsible for the mineralogy of the tonalite gneiss near its margins with the paragneiss.

Scattered throughout the tonalite are smaller paragneiss enclaves (from 10 to 100 meters in maximum dimension). The tonalite gneiss in the vicinity of paragneiss enclaves is a granodiorite in composition. The material incorporated into the gneiss from the paragneiss was not a granite, but more granodioritic in composition, due to the overall psammitic composition of the paragneiss.

Within the tonalite gneiss of Tejon Creek mafic lenses are found locally. Mafic lenses and mafic inclusions are less common in the tonalite gneiss compared to the Bear Valley Springs unit. They are concentrated along and within the gneissic fabrics, and are concordant with the foliation within the surrounding gneiss. Compositionally, they are mafic tonalites to diorites that are mineralogically equilibrated with their host rock. A mafic lens near the mouth of El Paso Creek has a $\delta^{18}O$ value of $+8.5°/_{\infty}$ (Taylor, unpublished data). Clearly, the mafic bodies in the tonalite gneiss are not metasedimentary or paragneiss xenoliths. The lenses may represent basaltic intrusive material coeval with magmas of the Bear Valley Springs intrusive epoch, or may be restite material from the formation of the tonalite gneiss of Tejon Creek.

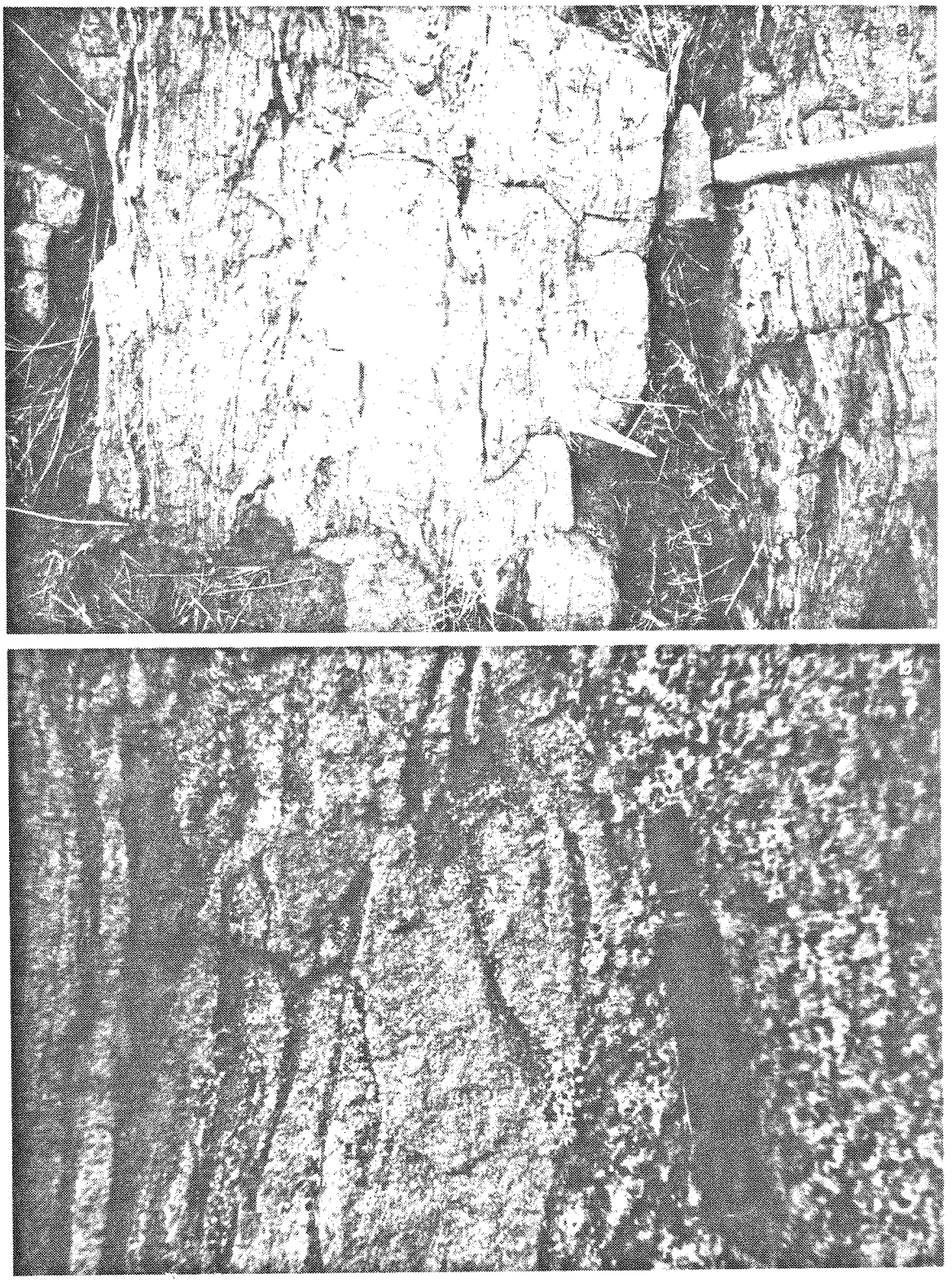

Figure 32. Photographs of field relations showing leucosome material derived from the paragneiss of Comanche Point, and tonalite gneiss of Tejon Creek incorporating same. Field of view is 1 m for (a), and 25 cm for (b). Locations are in foothills southeast of Comanche Point.

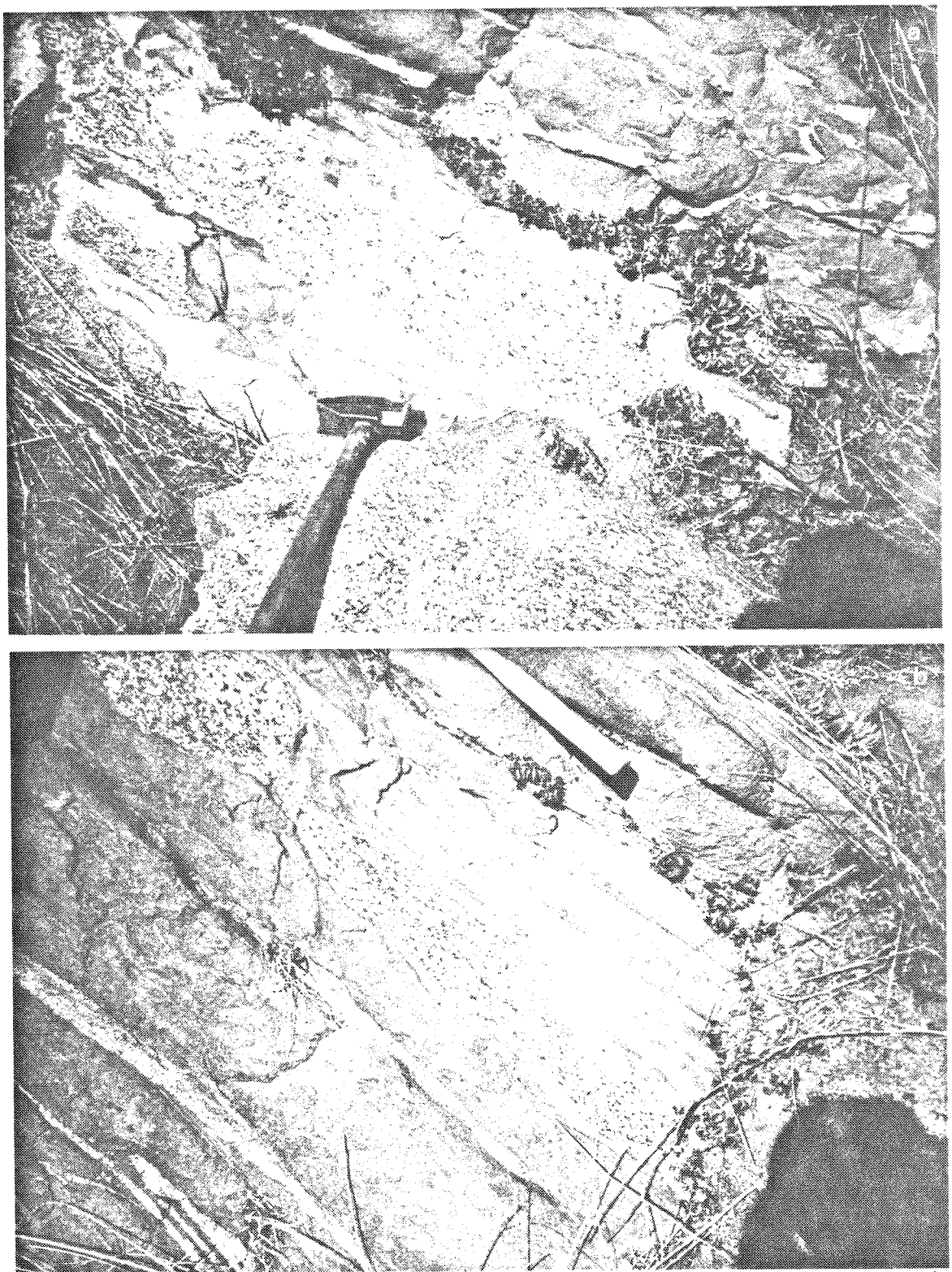

Figure 33. Photographs of field relations of the tonalite gneiss of Tejon Creek intruding the paragneiss of Comanche Point. Migmatitic behavior of the paragneiss is evident. Field of view is 1.4 m wide for (a,b). Location is in foothills southeast of Comanche Point.

The tonalite gneiss of Tejon Creek appears to be the product of magma mixing between tonalitic melts analoguous to those of the Bear Valley Springs pluton and paragneiss leucosomes. Foliation within the tonalite gneiss (Figure 34) is strongly oriented in a steeply dipping, northwest trending pattern that parallels the contact with the tonalite of Bear Valley Springs. The foliation is defined by the alignment of aggregates of feldspars and ductilely deformed quartz, interleaved with aligned mafic grain aggregates.

The tonalite gneiss of Tejon Creek (Table 10) is a well-foliated, medium-grained, allotriomorphic to hypidiomorphic granular tonalite orthogneiss that resembles a complexly deformed Bear Valley Springs unit. The foliation is defined by feldspar and ductilely deformed quartz aggregates interleaved with aligned mafic grain aggregates. It is composed of quartz, plagioclase, biotite, and hornblende, with minor amounts of garnet. The quartz is about one-third by volume, anhedral, sutured, and commonly defines a flaser texture. Plagioclase is anhedral, twinned and occasionally zoned, with an approximate An_{20} to An_{40} content. It typically has recrystallized rims. Mafic minerals consist of subequal parts biotite and hornblende, with a color index of 15 to 25. Biotite is a brown to red-brown pleochroic, and occurs as small anhedral grains that form a stringy foliation in the rock. Hornblende is anhedral to subhedral, and a pleochroic olive to blue-green or brown. Muscovite and garnet are found locally adjacent to paragneiss enclaves. Garnet is subhedral to euhedral, in small discrete grains. Potassium feldspar is a minor constituent, anhedral, and commonly microcline. Clinopyroxene and orthopyroxene are mutually exclusive minor minerals, and are infrequently seen as cores in hornblende. Zircon, opaques, and epidote are accessory minerals. In the vicinity of paragneiss, the tonalite gneiss grades into a garnet- and muscovite-bearing granodiorite by variations in the plagioclase-potassium feldspar modes.

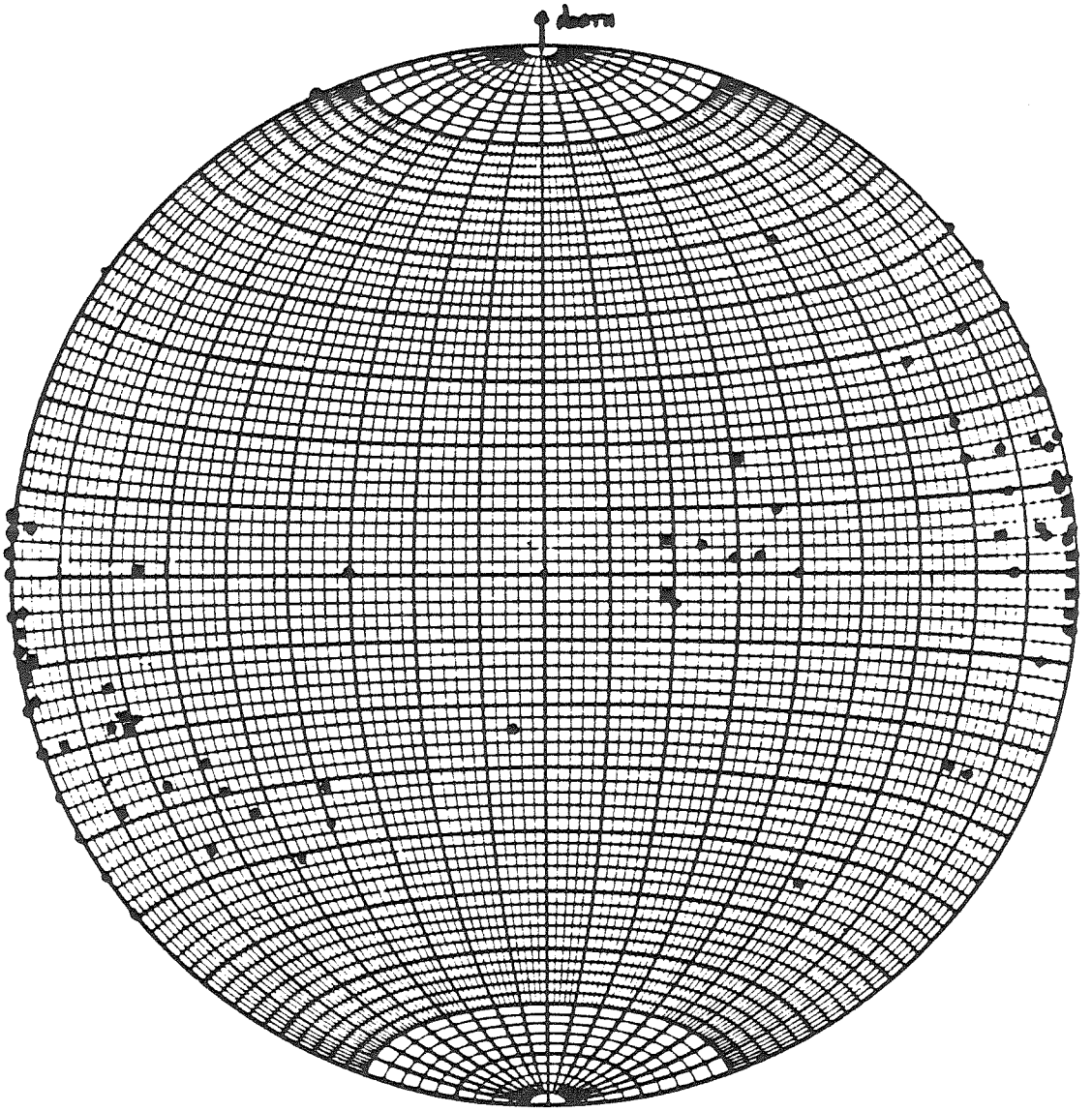

Figure 34. Lower hemisphere projection, equal-area stereoplot of poles to foliation for tonalite gneiss of Tejon Creek.

TABLE 10. SUMMARY OF PETROGRAPHY OF THE TONALITE GNEISS OF TEJON CREEK - GNEISS COMPLEX OF THE TEHACHAPI MOUNTAINS†

HAND SAMPLE	ROCK NAME	CI	QTZ	PLG	(An)	KSP	HBL	BIO	CPX	OPX	GAR	SPH	APA	ZIR	OPQ	EPI	CHL	MUS	OTH	TEXTURES ANL	RXL	MYL	CST	RTR
CM17b	tonalite	16	30	55	35		12	3			x				1									
CM34	tonalite	30	30	40	40		15	5		10														
CM36	tonalite	30	30	40	30		10	15		5														
CM38	tonalite	25	30	45	25		18	7																
CM40b	tonalite	16	25	60	30		10	5		1														
CM41	tonalite	15	30	55	35		14								1									
CM42	tonalite	15	35	50	25		5	10																
CM45	tonalite	15	35	55	25		7	8												x				
WR24	tonalite	18	25	25	x		15				3						x		ser		x	x		
WR25a	tonalite	35	15	45	40		15			15	x				5	4			ser		x	x		
WR25b	tonalite	30	20	35	40		20			10	x				5	7			ser		x	x		x
WR26	tonalite	24	30	40	40		20								4	6			ser		x	x		
WR27a	tonalite	25	30	45	25	2	15	10								2			ser		x			
WR27b	tonalite	35	20	40	40		15	10		3					7	7			ser		x			
WR28	tonalite	25	50	25	30		5	15	5													x		
WR29	tonalite	31	25	45	30		15	6		6					2									x
WR30/2§	qz diorite	40	5	50	30		30	x	3						5	7								x
WR38	gabbro	58		40	55		50								8				ser					
WR39§	tonalite	32	30	30	30		25	x	3						4	4			ser		x	x		
WR41	diorite	62	1	35	30		40	12	2		x				8							x		
WR46	tonalite	25	30	40	30		20	3							2	5						x		
WR50	tonalite	40	20	40	30		30	8							2							x		
WR53	tonalite	17	25	55	25		1	15								2								
WR54b	granite	10	25	35	35	25		10														x		
WR56	granite	11	30	45	30	25		10										1						
CM58	tonalite	18	40	40	35	2	3	15												x				
WR82	grdior	15	20	50	30	15	4	10	1									x						
WR83	diorite	50		50	40		40								10									
WR98	diorite	50		50	x		40				x				5		5	cumm/ser						

TABLE 10. SUMMARY OF PETROGRAPHY OF THE TONALITE GNEISS OF TEJON CREEK - GNEISS COMPLEX OF THE TEHACHAPI MOUNTAINS†

(cont'd)

HAND SAMPLE	ROCK NAME	CI	QTZ	PLG	(An)	KSP	HBL	BIO	CPX	OPX	GAR	SPH	APA	ZIR	OPQ	EPI	CHL	MUS	OTH	TEXTURES ANL	RXL	MYL	CST	RTR
CM109	tonalite	35	20	45	40		30			2					3									
CM110b	tonalite	15	40	45	20		7	8						x										
CM111	tonalite	12	35	55	25			10			2													
CM112	tonalite	22	35	45	20		10	10							2									
CM113	tonalite	21	30	50	20		10	10							1									
CM114a	tonalite	20	30	50	30		12	6							2									
CM114c	tonalite	10	35	55	30		4	5							1									
WR169	tonalite	15	35	50	30		8	6							1									
WR171§	tonalite	15	30	55	30		9	6							1					x				
WR181	tonalite	32	25	40	25		25								2		x	cumm5/ser				x	x	
CM614b	tonalite	16	25	60	30		7	8							1									
CM614c	tonalite	11	35	55	25		4	6						x	1									
CM630§	tonalite	10	35	55	30	x	x	10								x								
WR643§	tonalite	13	35	55	25	x	x	10		2						x		1						
CM651a	tonalite	30	40	30	30		6	8	8		8													
CM652a	tonalite	20	20	60	25		10	7	3															
CM652b	granite	5	20	35	20	40		5																
WR654	tonalite	21	25	55	25			15	1							5								
WR656	tonalite	25	25	50	30		15	5	5							x								
WR657	tonalite	15	30	55	25	3	3	10	1						1									
WR663	tonalite	40	15	45	25		20	15							5					x				

† key to abbrevations:
CI = color index; QTZ = quartz; PLG (An) = plagioclase with Anorthite content after Michel-Levy (1887); KSP = K-feldspar; HBL = hornblende; BIO = biotite; CPX = clinopyroxene; OPX = orthopyroxene; GAR = garnet; SPH = sphene; APA = apatite; ZIR = zircon; OPQ = opaques; EPI = epidote; CHL = chlorite; MUS = muscovite; OTH = other; cumm = cummingtonite; graph = graphite; oliv = olivine; scap = scapolite; ser = sericite; sill = sillimanite; ANL = annealed; RXL = recrystallized; MYL = mylonitic or protomylonitic; CST = cataclastic; RTR = retrograded; qz = quartz; grdiorite = granodiorite; qf = quartzo-feldspathic; Ca-silc = calc-silicate; pxhbdite = pyroxene hornblendite. Rock names after Streckeisen (1976, 1973).

§ U/Pb zircon geochronology sample.

The tonalite gneiss has a poorly preserved igneous texture; it contains a dominantly gneissic fabric and/or overprint. Annealed textures are occasionally found, while mylonitic textures are rare.

II.5.3 Quartzo-feldspathic gneiss of Pastoria Creek

The quartzo-feldspathic gneiss of Pastoria Creek consists of several similar heterogeneous gneiss bodies that range in size from 1-10 km. It is informally named for Pastoria Creek which flows through much of the largest body. It incorporates most of Sharry's (1981b) quartzo-feldspathic gneiss unit, and continues into the undifferentiated gneiss of Ross (1980, 1986). It is distinguished from the metagabbros, tonalite gneiss, and paragneiss by its uniform heterogeneity over the scale of centimeters to kilometers, its wider compositional range, higher quartz and biotite modes, and its more intense deformational characteristics. The Pastoria Creek gneisses form the western part of the gneiss complex in the area studied, extending from Interstate Route 5 in Grapevine Canyon east to Winters Ridge (Plate 1). The gneisses are bounded by the Garlock fault and diorite gneiss of White Oak on the south, onlapping Tertiary (Eocene) deposits on the north (Nilsen and Clarke, 1975; Harris, 1954), and by parts of the metagabbro of Tunis Creek and hypersthene tonalite of Bison Peak on the east. It forms the eastern and western contacts of the metagabbro of Squirrel Spring west of Pastoria Creek.

Contacts between the Pastoria Creek and other units are typically obscure or covered. Where seen, they are concordant with respect to compositional and structural layering, or consist of intrusion of the surrounding unit into the quartzo-feldspathic gneiss of Pastoria Creek. A number of instances of intrusive contacts (diking?) involving the Bison Peak and Tunis Creek units occur. These contacts are typically sharp, and where exposed frequently involve these darker tonalites or gabbros discordantly intruding and cross-cutting deformational fabrics

in the gneiss. The contacts with the gabbro occurs in the western part of Winters Ridge, while the intrusive contacts with the Bison Peak unit are found on the north slope of Winters Ridge, and in the Tunis Creek area. In addition, small plugs of mafic to ultramafic rock of Tunis Creek affinity are seen intruding the Pastoria Creek gneiss just east of the Edmonston (Pastoria Creek) road.

The quartzo-feldspathic gneiss of Pastoria Creek is an assemblage of gneisses ranging in composition from diorite and gabbro through tonalite banded orthogneiss to granodioritic and granitic banded and augen gneisses. The various components of this unit form discontinuous, phacoidal masses (Figure 35), with lenses and complex contacts between the various compositions (Plate 3). Banding within the gneiss consists of transposed biotite- and hornblende-rich aggregates and partially recrystallized domains with both planar and linear fabrics. Foliations within the gneiss (Figure 36) are most commonly east trending and moderately north dipping, although there is a large scatter in the orientation of the foliation, with no associated regional pattern.

Quartz-rich granitoids (quartz + plagioclase + hornblende + biotite ± K-feldspar ± garnet gneisses) are the most common rock type, showing coarsely recrystallized and blastomylonitic to locally mylonitic fabrics (Figures 37,38). The rocks frequently show evidence for mylonitic and blastomylonitic deformational fabrics that developed by varying degrees of recrystallization and annealing. Areas containing deformed pegmatites (quartz + plagioclase + K-feldspar + biotite + muscovite ± garnet) that are concordant to slightly discordant with the surrounding foliation can be found (Figure 39a), but the pegmatites are not abundant. These pegmatites may represent partial melt material similar to the production of leucosomes in the paragneiss of Comanche Point.

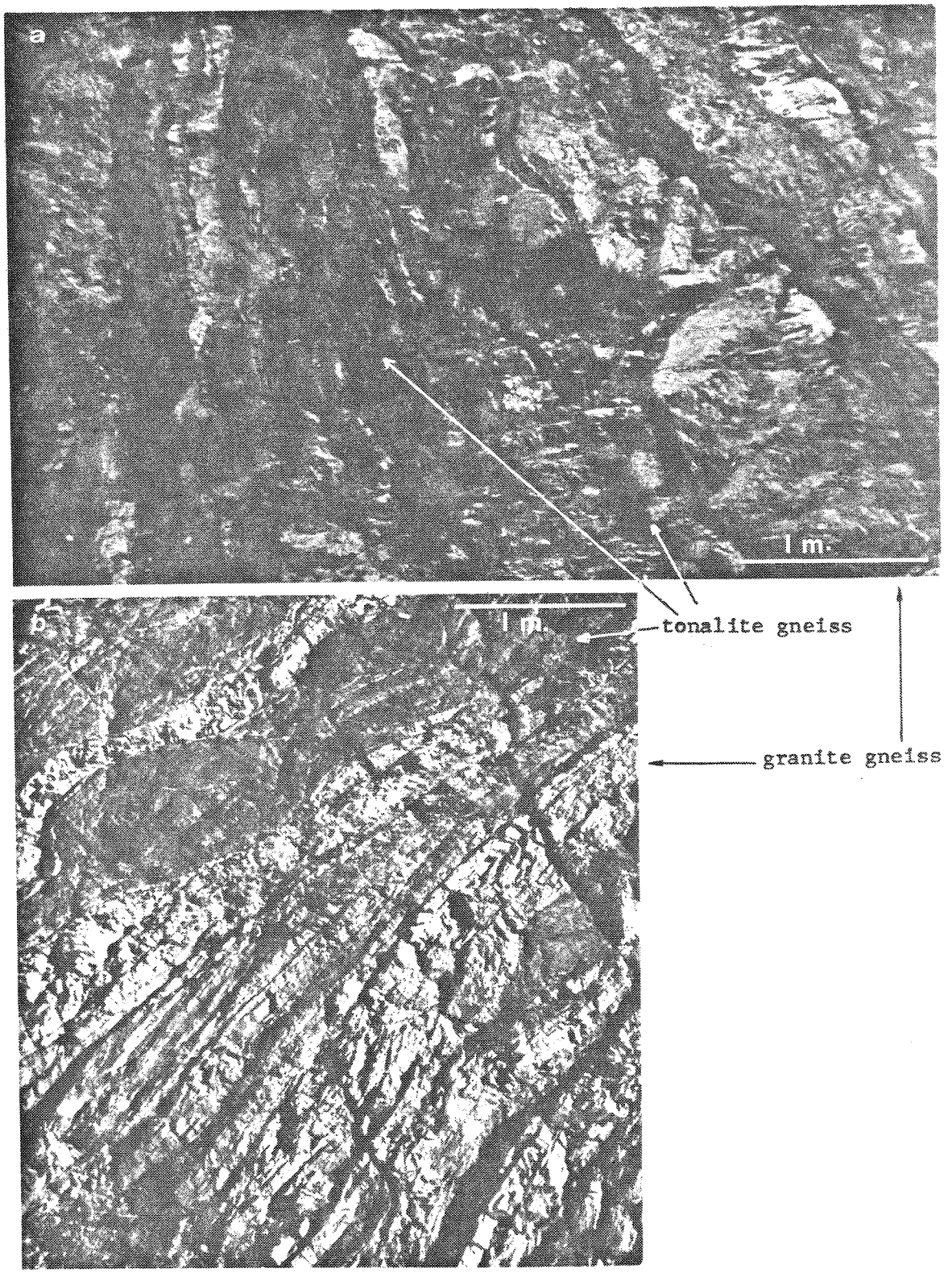

Figure 35. Field photographs showing phacoidal relations within the Pastoria Creek gneiss. Dark material is tonalitic gniess, lighter material is granitic gneiss. Field of view is 5 m in (a), and 4 m in (b).

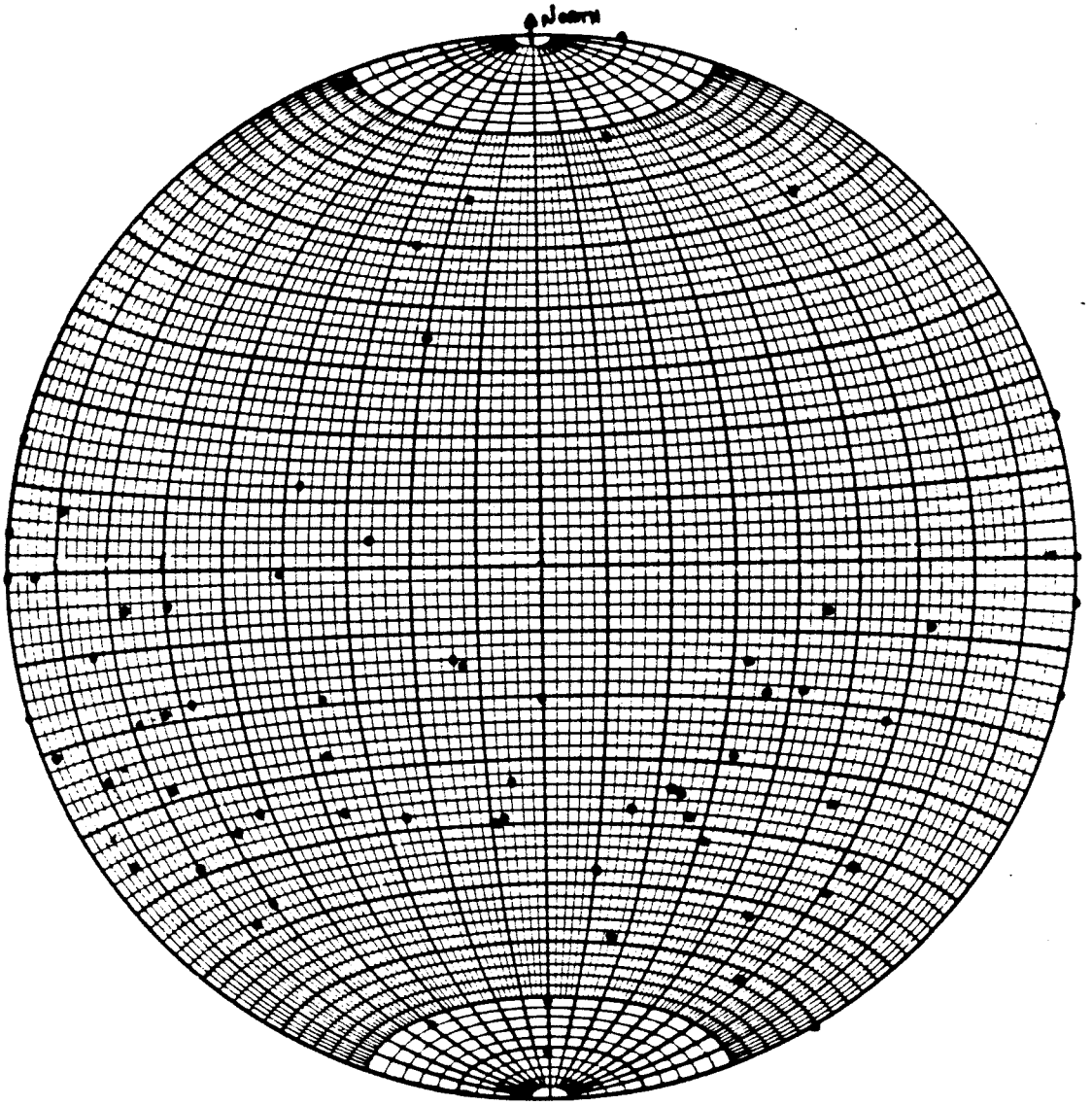

Figure 36. Lower hemisphere projection, equal-area stereoplot of poles to foliation for quartzo-feldspathic gneiss of Pastoria Creek.

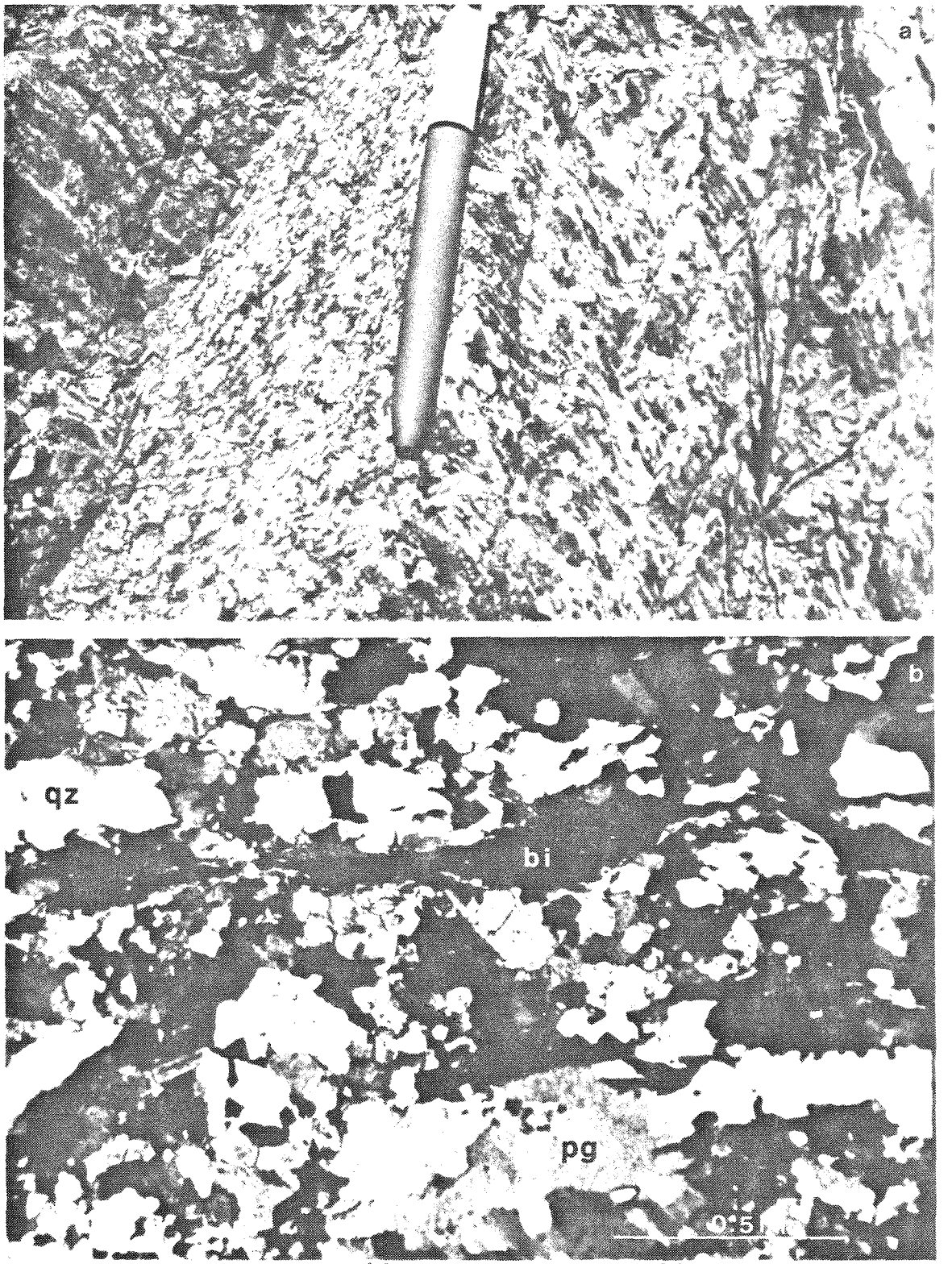

Figure 37. Field photograph (a) and photomicrograph (b) of tonalite gneiss in Pastoria Creek gneiss showing deformation involving large amounts of stretching but little flattening. Field of view is 20 cm (a) and 2 mm (b). Minerals are qz=quartz, pg=plagioclase, bi=biotite.

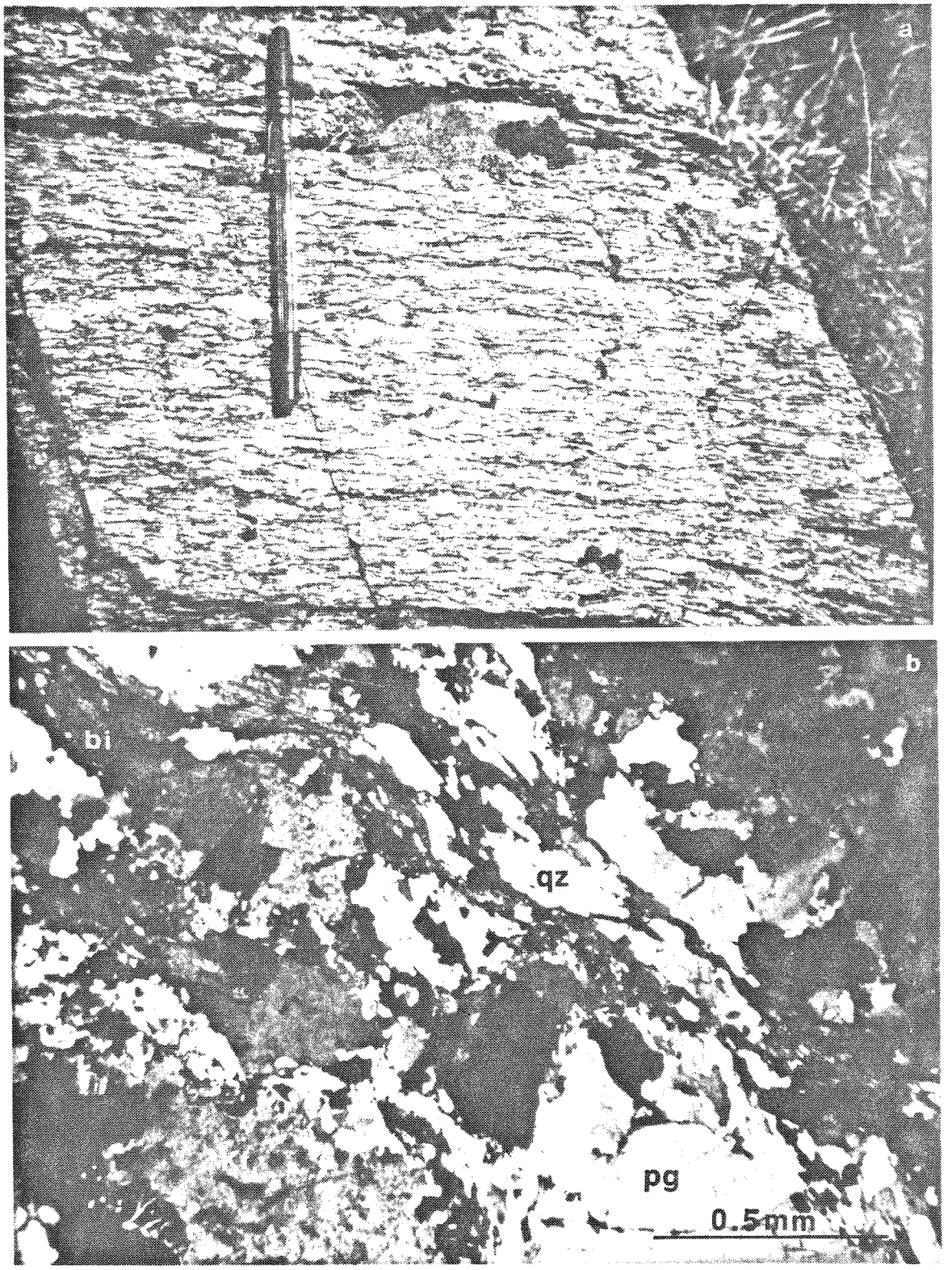

Figure 38. Field photograph (a) and photomicrograph (b) of augen gneiss within Pastoria Creek gneiss. Field of view is 50 cm (a) and 2 mm (b). Minerals are qz=quartz, pg=plagioclase, Kf=K-feldspar, bi=biotite.

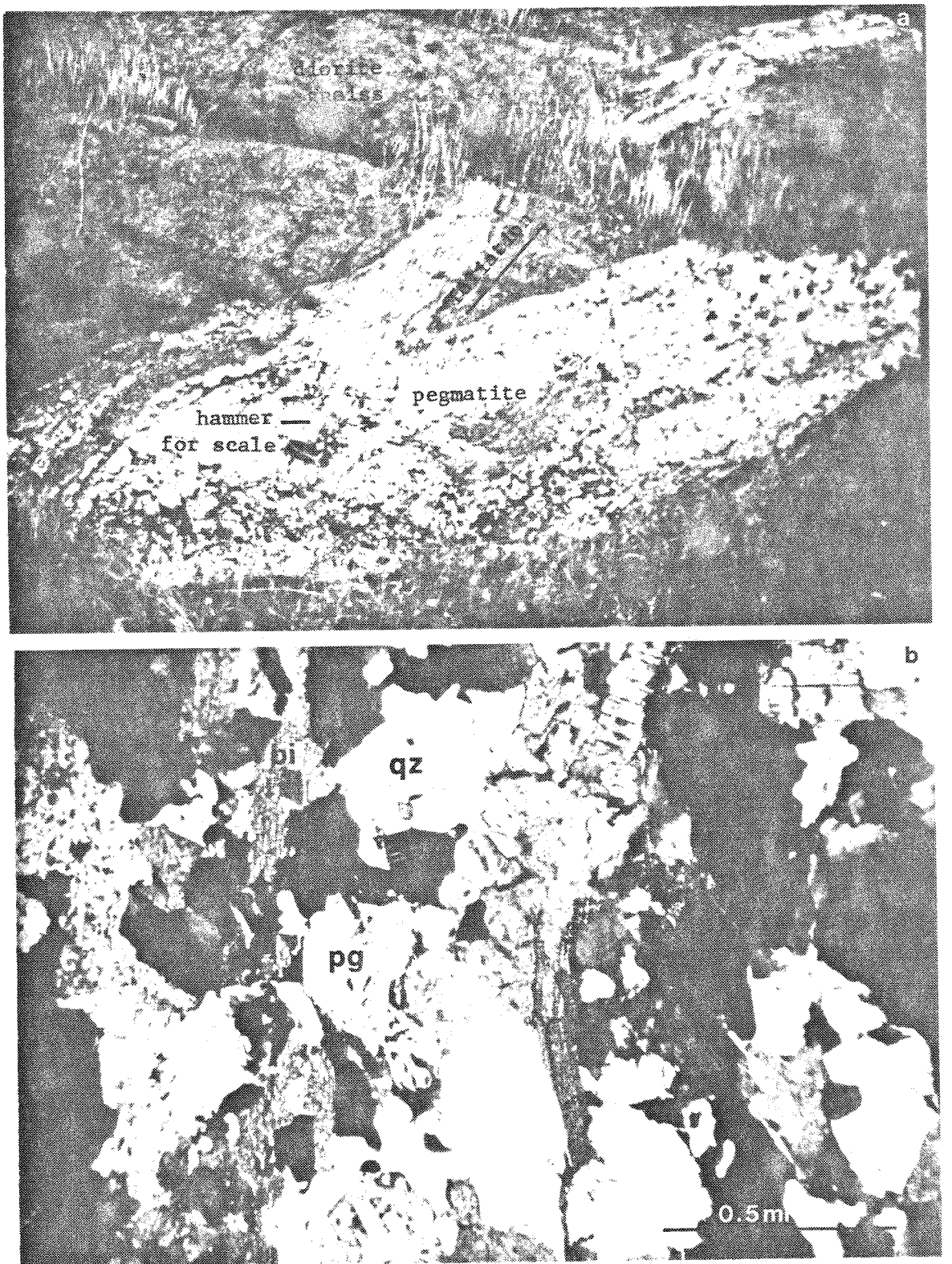

Figure 39. Field photograph (a) and photomicrograph (b) of deformed pegmatite in tonalitic gneiss in Pastoria Creek gneiss. Field of view is 8 m (a), and 2 mm (b). Minerals are qz=quartz, pg=plagioclase, bi=biotite.

The gneiss has been subdivided into granitic and tonalitic members (Table 11). The two subdivisions have been shown separately on Plate 1. Tonalitic and granitic gneisses occur in subequal amounts. They are locally gradational between varieties due to differences in modal plagioclase and K-feldspar. Generally speaking, the tonalite gneisses are tonalitic to dioritic in composition, while the granites range in composition from granite to granodiorite.

The tonalites are richer in hornblende, less deformed, and have a more "igneous" appearance. They are comprised of two feldspars, quartz, green hornblende, deep-red to brown biotite, and occasionally garnet. The garnet occurs as 1-5 cm grains that are seen to grow statically across deformational fabrics, and at the expense of hornblende. This may represent local dehydration conditions.

The granite gneisses are richer in biotite, quartz, and garnet, and typically lack hornblende. They are comprised of two feldspars, quartz, biotite, and garnet, with and without hornblende. The garnet occurs as fine, 1-2 cm sized grains in equilibrium textures with the rest of the rock. The granite gneisses frequently have been deformed into augen gneisses, and have a strong crystalloblastic texture. The augen gneisses show a protracted history of deformation, with overprinting blastomylonitic fabrics.

A survey of photomicrographs illustrating the varied compositions and textures within the quartzo-feldspathic gneiss of Pastoria Creek can be seen as the lower halves of Figures 36-39. The upper half of the figure illustrates the associated field relations. The textures illustrated are typical for the gneisses, and show strained and recrystallized quartz and feldspar, flaser structures in quartz, and ribbon structures in biotite. Quartz is anhedral, strained, and sutured, typically granular or recrystallized, and commonly ductilely deformed and transposed into a flaser structure. Plagioclase is anhedral and twinned, with a compo-

TABLE 11A. SUMMARY OF PETROGRAPHY OF TONALITE GNEISSES, GNEISS OF PASTORIA CREEK-GNEISS COMPLEX OF THE TEHACHAPI MOUNTAINS†

HAND SAMPLE	ROCK NAME	CI	QTZ	PLG	(An)	KSP	HBL	BIO	CPX	OPX	GAR	SPH	APA	ZIR	OPQ	EPI	CHL	MUS	OTH	TEXTURES ANL	RXL	MYL	CST	RTR
PC1a	tonalite	44	20	25	35		35	5				x	x		4		x		ser	x				
PC1b	tonalite	37	20	35	30		20	15					x		3		x		ser	x				
PC6a	tonalite	52	30	25	35		30	5	15						2	x					x			
PC6b	tonalite	47	20	35	40		45					2	x	x						x				x
PC7	tonalite	30	15	50	40		5	20	2			1			2	3			ser		x	x		
PC8	tonalite	50	20	35	40		35	8	2		1	x	x		2	2			ser		x	x		
PC9a	tonalite	50	10	40	55		45	3				x	x		2		3		ser					
PC9b	tonalite	30	30	35	55		20		10				x			x					x			
PC10	tonalite	12	30	50	40	7		10	5							x			ser		x	x		
PC12b	tonalite	13	50	35	30	2		10	3		x					x			ser		x			
PC13	tonalite	21	35	45	35			10	3		8					x			ser		x	x		
PC30	diorite	71		25	30		70								1		x							
PC33	tonalite	62	10	25	50		60	2							2		x							
PC34§	tonalite	43	15	40	40		30	5	5						5	x	x				x	x		
PC36§	tonalite	15	35	50	30	2		10	2		x				2	x		x			x			
PC43	tonalite	38	16	45	30		30	5							3		x		ser			x		
WR88	tonalite	30	20	50	25		22	8													x			
WR90c	tonalite	10	45	45	25			10													x			
WR91a§	tonalite	15	25	60	25	x	x	7			8													
WR94	tonalite	15	30	60	25		5	8			2										x	x		
WR95	tonalite	18	35	40	25	7	15	3													x	x		
WR100	tonalite	25	25	50	25		6				15				4		x		ser		x			
PC106	tonalite	9	35	55	20			5							1	1		2			x	x		
PC107	tonalite	17	30	50	20		6	6			3				2									
PC108	tonalite	20	30	50	25		10	10			x													
PC127	tonalite	11	40	50	25			10							1									
PC129§	tonalite	15	25	60	30			12			2				1									
PC130b	tonalite	15	40	45	30			10			4				1									
PC176	tonalite	20	40	40	30		10	10													x	x		

† key to abbrevations:
CI = color index; QTZ = quartz; PLG (An) = plagioclase with Anorthite content after Michel-Levy (1887); KSP = K-feldspar; HBL = hornblende; BIO = biotite; CPX = clinopyroxene; OPX = orthopyroxene; GAR = garnet; SPH = sphene; APA = apatite; ZIR = zircon; OPQ = opaques; EPI = epidote; CHL = chlorite; MUS = muscovite; OTH = other; cumm = cummingtonite; graph = graphite; oliv = olivine; scap = scapolite; ser = sericite; sill = sillimanite; ANL = annealed; RXL = recrystallized; MYL = mylonitic or protomylonitic; CST = cataclastic; RTR = retrograded; qz = quartz; grdiorite = granodiorite; qf = quartzo-feldspathic; Ca-silc = calc-silicate; pxhbdite = pyroxene hornblendite. Rock names after Streckeisen (1976, 1973).

§ U/Pb zircon geochronology sample.

TABLE 11B. SUMMARY OF PETROGRAPHY OF GRANITE GNEISSES, GNEISS OF PASTORIA CREEK - GNEISS COMPLEX OF THE TEHACHAPI MOUNTAINS†

HAND SAMPLE	ROCK NAME	CI	QTZ	PLG	(An)	KSP	HBL	BIO	CPX	OPX	GAR	SPH	APA	ZIR	OPQ	EPI	CHL	MUS	OTH	TEXTURES ANL	RXL	MYL	CST	RTR
PC2	granite	12	55	15	30	15	1	10					x						ser	x				
PC3	granite	5	50	5	30	40		5											ser			x		
PC4	granite	5	40	2	x	40		5											ser			x		
PC5	granite	13	30	30	30	35		10		2									ser	x				
PC11	granite	10	25	25	30	40		10											ser		x	x		
PC12a	granite	20	30	30	30	40		15	3							x	x		ser		x	x		
PC31§	granite	14	20	25	30	40	2	12									x				x			
PC32§	granite	10	30	10	25	50		8	1						1	.			ser		x	x		
PC37§	granite	20	30	25	20	25		16	2						2	x					x	x		
WR40§	granite	10	30	20	x	35		10								3					x	x		
PC44	granite	10	20	30	30	40		7										3				x		
PC45	granite	11	30	30	30	30		10										1	ser			x		
WR48	granite	11	20	30	x	40		10	1												x	x		
WR49	granite	11	25	30	x	35		10	1												x	x		
PC51	granite	12	30	30	30	30		10							2						x	x		
PC52	granite	11	30	25	x	35		10								1					x	x		
WR89a	quartzite	8	90	8	x			7							1						x	x		
WR93	granite	24	25	20	25	35		15			x				4									
WR99	granite	10	30	30	x	30		5										5			x	x		
PC125c	qf schist	30	50	20	25			15							5			10						
PC126	qf schist	20	35	45	30			10							2			8						
CM135	quartzite	19	60	20	25		10		5			2			2					x				
WR187	quartzite	10	60	30	25			9							1							x		
TL206	qf gneiss	18	60	25	30		5	2		1							x	cumm9/ser				x		
GNEISS COMPLEX OF THE TEHACHAPI MOUNTAINS WEST OF GRAPEVINE CANYON																								
LB117c	tonalite	22	35	40	40			10		5					1	3		6						
LB118	granite	3	20	25	20	45		3																
LB131	tonalite	30	20	50	20		20	10																
LB132	quartzite	16	80					8			4							4				x		
LB133	tonalite	11	30	60	40		7	2			1				1						x	x		

† key to abbrevations:
CI = color index; QTZ = quartz; PLG (An) = plagioclase with Anorthite content after Michel-Levy (1887); KSP = K-feldspar; HBL = hornblende; BIO = biotite; CPX = clinopyroxene; OPX = orthopyroxene; GAR = garnet; SPH = sphene; APA = apatite; ZIR = zircon; OPQ = opaques; EPI = epidote; CHL = chlorite; MUS = muscovite; OTH = other; cumm = cummingtonite; graph = graphite; oliv = olivine; scap = scapolite; ser = sericite; sill = sillimanite; ANL = annealed; RXL = recrystallized; MYL = mylonitic or protomylonitic; CST = cataclastic; RTR = retrograded; qz = quartz; grdiorite = granodiorite; qf = quartzo-feldspathic; Ca-silc = calc-silicate; pxhbdite = pyroxene hornblendite. Rock names after Streckeisen (1976, 1973).

§ U/Pb zircon geochronology sample.

sition of about An_{20} to An_{55}. It occasionally has fuzzy pericline twinning, and less commonly a weak zonation that is more common in tonalitic varieties. Occasionally quartz and plagioclase form myrmekite and/or graphic intergrowths.

The gneisses have a color index of 5-50. Biotite is anhedral, red-brown to brown pleochroic, and forms stringers running through the rock. Hornblende is pleochroic green, brown, or olive, and occurs as anhedral masses. Garnet usually is subhedral to euhedral, and occurs as grains ≤10 cm in diameter that frequently have a bleached, mafic (hornblende) free zone or halo surrounding them. The garnets contain inclusions of quartz and plagioclase, and are in an apparent equilibrium setting. Potassium feldspar is restricted primarily to augen gneisses and garnet granites that appear to be dikes. It is porphyroclastic, and frequently occurs as microcline. Clinopyroxene is an uncommon accessory mineral, with orthopyroxene rarely seen. Cummingtonite was found in one section. Sphene, apatite, zircon, opaques, and muscovite are all found as accessory minerals.

Subhedral to euhedral epidote occurs as a replacement product of hornblende in a number of tonalitic gneisses. Zen and Hammarstrom (1984) and Zen (1985) interpret the existence of epidote in some tonalites as a late crystallization product of a magma at lower crustal levels. They suggest that epidote crystallizes just above the solidus at about 600-800°C and 6-8 kb. Their evidence for the magmatic nature of the epidote is in the resorbed nature of hornblende into a magmatic fluid, euhedral nature of epidote in relation to biotite, and the vermicular contacts of epidote with plagioclase and quartz. They cite the occurrence of nonzoned plagioclase as common in tonalites that contain magmatic epidote as contrasted to shallower-level tonalites. The epidote-bearing tonalites in the quartzo-feldspathic gneiss of Pastoria Creek exhibit all of the preceeding relations (Figure 40), and are therefore interpreted to have had an igneous origin.

Figure 40. Photomicrographs of epidote-bearing tonalites in the quartzo-feldspathic gneiss of Pastoria Creek. Epidote is vermicular with plagioclase (a,d); hornblende is resorbed and embayed by epidote (b,d); epidote euhedral against biotite (c,d). Field of view is 0.2 mm Minerals are pg=plagioclase, bi=biotite, hb=hornblende, ep=epidote.

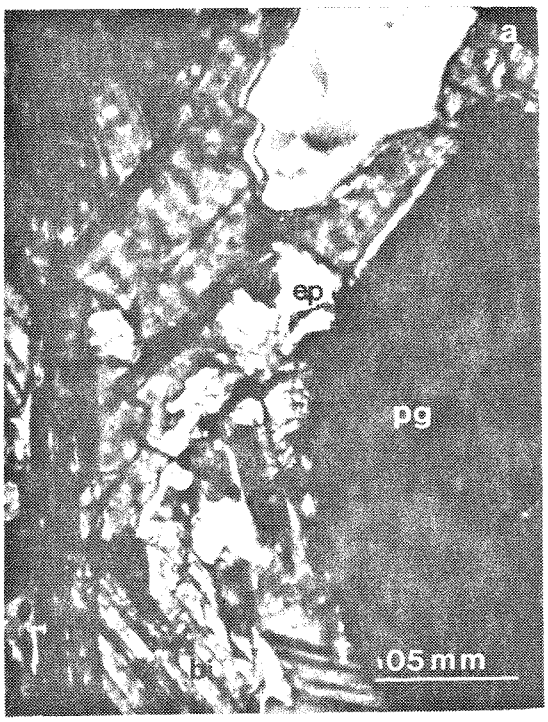
a
ep
pg
.05mm

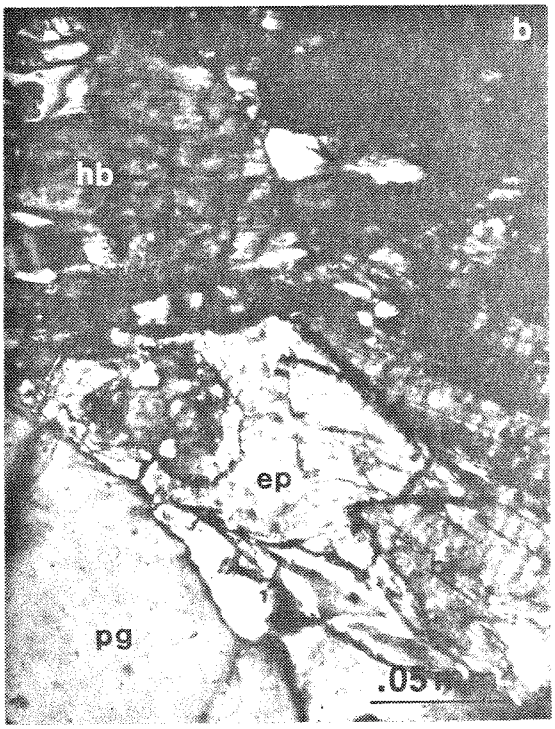
b
hb
ep
pg

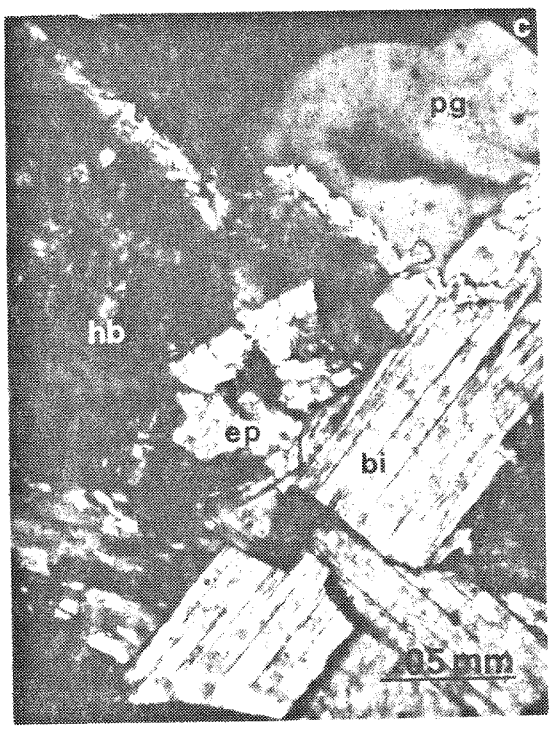
c
pg
hb
ep
bi
.05mm

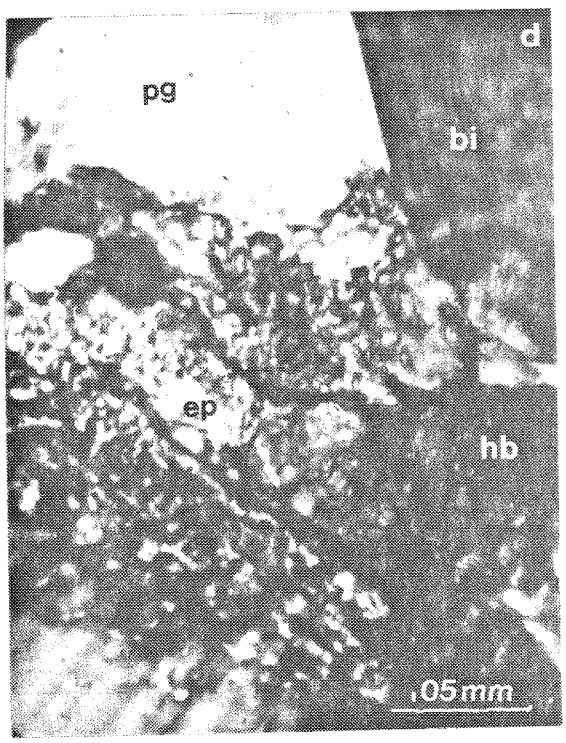
d
pg
bi
ep
hb
.05mm

They also provide evidence for mid- to lower-crustal levels of emplacement for the orthogneisses.

The bulk composition of the Pastoria Creek gneisses would probably approximate a granodiorite, and much of the unit is believed to have an orthogneiss protolith. Rocks interpreted as having an igneous protolith consist of diorites and tonalites, as well as local lenses of gabbroic to ultramafic rock, and are distinguished by the remnants of igneous textures, and igneous $\delta^{18}O$ values. These rocks are more strongly deformed relative to the Tunis Creek and Bison Peak units. The deformation is typical or slightly less than that within other rocks in the Pastoria Creek unit. The meta-igneous rocks are interpreted as small masses that were intruded into the lower crust prior to the Bear Valley Springs intrusive epoch, and deformed prior to and during the Bear Valleys Springs thermal event.

Metasedimentary rocks in the gneiss complex consist of lenses of grey-white marble, impure quartzite, psammitic paragneiss, granofels, granulites, and thin calc-silicates that contain pale-green clinopyroxene. The granofels often exhibit annealed textures and local granulite facies mineral assemblages. The granulites occur as diffuse zones of massive to weakly gneissic rock within the granitic gneiss, and are denoted by the symbol "u" on Plate 1. The granulites contain quartz, two feldspars, red biotite, and hornblende, with subordinate hypersthene and graphite, or clinopyroxene, graphite, and garnet. A metasedimentary origin is postulated for the granulites, based on observed gradations into psammitic paragneiss, the occurrence of graphite, and high $\delta^{18}O$ values ($\geq +14^{\circ}/_{\circ\circ}$, Ross, 1983c). The granulites may represent ultrametamorphosed sediments, while the lenses appear to represent refractory residual material.

III. GEOCHRONOLOGY

III.1 Introduction and background

Previous geochronological work on the southernmost Sierra Nevada and Tehachapi Mountains consists of seven K/Ar age and two Rb/Sr age determinations, of which only three K/Ar ages were performed on the gneiss complex of the Tehachapi Mountains (summarized in Ross, 1986). The data show a restricted range of ages from 77-88 Ma. The tonalite of Bear Valley Springs yielded ages from 80-88 Ma, while the gneiss complex yielded ages between 77 and 87 Ma. There are no recognizable patterns of age with respect to isotopic system. With the exception of the 77 Ma age in the gneiss complex, the older ages (86-88 Ma) are south of the younger ages (80-81 Ma).

Zircon studies were initiated in 1981 in order to investigate two major topics: 1) the possible remnants of Proterozoic sialic material within the gneiss complex of the Tehachapi Mountains, and 2) structural relations between the Sierra Nevada batholith and gneissic rocks reported in reconnaissance studies by Ross (1980). Geochemical studies by DePaolo (1981b) and Kistler and Peterman (1973, 1978) suggest that Proterozoic sialic materials constituted a major component of the Sierran batholithic source materials. Their results indicate that the southern and central Sierra Nevada batholith is isotopically comprised of homogenized Proterozoic sialic source material and mantle-derived island arc material. The gneiss complex of the Tehachapi Mountains occupies a structural position analagous to Precambrian crystalline terranes of southern California. Sharry (1981b) has suggested that the gneiss complex of the Tehachapi Mountains comprises the upper plate structurally above the Rand schist block which occurs between strands of the Garlock fault. The Pelona schist in southern California occurs as the lower thrust plate beneath a varied crystalline terrane, which in part

contains Precambrian gneiss (Haxel and Dillon, 1978; Ehlig, 1968, 1981). A similar situation is seen in the Rand Mountains, where the Rand schist occurs below a thrust fault whose upper plate rocks contain Cretaceous granitoids and possible Precambrian gneiss (Silver and Nourse, 1986; Nourse and Silver, 1986; Silver and others, 1984). The Pelona and Rand schists, along with their associated thrust faults, are considered by many workers to be part of an extensive southern California schist terrane (Haxel and Dillon, 1978; Ehlig, 1968). If this interpretation of the tectonic setting of the gneiss complex of the Tehachapi Mountains is correct, then the gneiss complex would be a prime area to search for the existence of old sialic material. This Proterozoic source material has not been found in the southern Sierra Nevada, although zircon U/Pb isotopic signatures indicative of its existence are seen in the southern and central Sierra Nevada batholith (this study; Tobisch and others, 1985; Chen and Moore, 1982; Chen and Tilton, 1978).

This investigation was undertaken to test the hypotheses outlined above by applying zircon U/Pb dating methods to the rocks of the southernmost Sierra Nevada and Tehachapi Mountains. Additional goals of the geochronological investigations were to characterize the age of the southernmost Sierra Nevadan crystalline rocks, to develop an absolute chronology in the development of the high-grade deformational fabrics, and to characterize the isotopic systematics of detrital zircon in metasedimentary protoliths as contaminate populations to the magmas.

III.2 Procedure and Theory

This investigation consists of zircon U/Pb age determinations on thirty-three samples in the southernmost Sierras, thirteen of which are from the gneiss complex. Samples were selected to provide as broad a selection of rock types as possible, and to represent each of the major rock units in the compilation map

(Plate 1). Samples were also selected to place age constraints on deformational fabrics. Sample descriptions, field settings and localities, petrographic descriptions, and zircon yield data are given in Table 12. Sample preparation followed the technique of Saleeby (1982) and Saleeby and Sharp (1980), modified from Krogh (1973). Detailed discussions of analytical procedures, error analysis, and concordia intercept theory for interpreting discordant data are given in the Appendix - Geochronology.

In a U/Pb analysis, most of the errors are in the determination of the spike concentration and composition (systematic error), and in the working characteristics of the mass spectrometer (random error). The most precisely determined age is the $^{206}Pb^*/^{238}U$ age, and this is what is referred to as the "age" of a concordant sample. The uncertainty in the age is based on the uncertainties in the ^{206}Pb and ^{238}U concentration determinations and in the reproducibility of ages. The $^{207}Pb^*/^{235}U$ age has a greater degree of uncertainty due to the difficulty in measuring the ^{207}Pb concentration. Based on the errors due to analytical error, reproducibility of results, analysis of Pb and U standards, and common and initial lead compositions, the uncertainty in the $^{206}Pb^*/^{238}U$ age is given as ±1.0 to 1.5% of the quoted age, while the uncertainty in the $^{207}Pb^*/^{235}U$ age is given as ±1.5 to 2.0% of the quoted age (see Appendix).

The uncertainty in the $^{207}Pb^*/^{206}Pb^*$ age is based on the long-term reproducibility of NBS standards, common and initial lead compositional uncertainties, and agreement between the ages determined for both the spiked and unspiked aliquots (see Appendix). The uncertainty is dependent on the amount of common lead; samples with a larger measured $^{206}Pb/^{204}Pb$ ratio have a smaller error. There is considerable disagreement in $^{207}Pb^*/^{206}Pb^*$ ages between the two aliquots, most likely due to the operating characteristics of the mass spec-

TABLE 12. GEOCHRONOLOGY SAMPLE LOCATIONS, PETROGRAPHY, AND ZIRCON YIELD DATA

Sample Number	Field Setting and Location	Petrography and Special Comments	mg Zircon /kg Rock
LATE DEFORMATIONAL INTRUSIVE SUITE			
GRANODIORITE OF CLARAVILLE			
#1 TC27	Massive bouldery outcrops about 0.6 km from metamorphic septa, along Tweedy Creek road 5.6 km E. of junction at spring at 4050' elev., 0.2 km N. of Tweedy Creek; Lat. 35° 13' 06" N., Long. 118° 27' 40" W., Tehachapi North 7.5' quad.	Biotite granodiorite: weakly foliated, porphyritic, medium to coarse grained, hypidiomorphic granular rock, C.I.=15; dominantly plagioclase (An_{30}), with sutured quartz, K-feldspar, and biotite, accessory opaques, secondary chlorite.	327/18
TONALITE STOCK AT TWEEDY CREEK			
#2 TC40	Stock into metamorphic septa and orthogneiss, bouldery outcrops along Tweedy Creek at 3550' elev., 1.7 km E. of road junction at spring; Lat. 35° 13' 28" N., Long. 118° 28' 58" W., Tehachapi North 7.5' quad.	Biotite hornblende tonalite: moderately foliated, coarse grained, hypidiomorphic granular rock, C.I.=22; dominantly plagioclase, with abundant sutured, veiny quartz and blue-green to brown hornblende, and minor brown biotite, accessory sphene, secondary chlorite and sericite. Rock has a protomylonitic, recrystallized texture.	1293/18
PEGMATITE DIKE SWARM			
#3 CM620	0.5 m thick pegmatite crosscutting foliation in gneiss and tonalite (BVS); along Comanche Point Road at 2800' elev., 0.8 km W. of BM 2756; Lat. 35° 07' 26" N., Long. 118° 44' 21" W., Tejon Ranch 7.5' quad.	Garnet biotite granite: fine grained, unfoliated, hypidiomorphic granular rock, C.I.=5; plagioclase (An_{20}), quartz, and K-feldspar, accessory brown biotite and red garnet.	124/27
GARNET GRANITE DIKE AT PASTORIA CREEK			
#4 PC35	Dike intruding gneiss in roadcut along California Aqueduct access road, 7.6 km S. of Edmonston Pumping Plant; Lat. 34° 55' 10" N., Long. 118° 47' 46" W., Pastoria Creek 7.5' quad.	Biotite garnet granite gneiss: Moderately foliated, fine to medium grained, allotriomorphic granular rock, C.I.=15; K-feldspar, microcline, quartz, and plagioclase (An_{40}) in a sutured, granular mass, accessory garnet, stringy biotite, muscovite, and opaques, secondary sericite. Recrystallized, mylonitic texture.	100/28

TABLE 12. GEOCHRONOLOGY SAMPLE LOCATIONS, PETROGRAPHY, AND ZIRCON YIELD DATA continued

Sample Number	Field Setting and Location	Petrography and Special Comments	mg Zircon /kg Rock
BEAR VALLEY SPRINGS INTRUSIVE SUITE			
TONALITE OF MOUNT ADELAIDE			
#5 BM684	Massive outcrops in Telephone Canyon at 2120' elev., along road 1.0 km SE. of Baker Grade road, 2.3 km N. of Caliente, 5.5 km SW. of Oiler Peak; Lat. 35° 18' 47" N., Long. 118° 39' 23" W., Oiler Peak 7.5' quad.	Biotite tonalite: unfoliated, porphyritic, medium to coarse grained, hypidiomorphic granular rock, C.I.=15; dominantly well twinned and moderately zoned plagioclase (An_{20}-An_{35}) and sutured quartz, with euhedral books of yellow to red pleochroic biotite, minor opaques, accessory zircon, apatite, and sphene, secondary chlorite.	340/14
TONALITE OF BEAR VALLEY SPRINGS			
#6 TC15	Bouldery outcrops at edge of metamorphic septa along Tweedy Creek at 3350' elev., 0.4 km E. of road junction at spring; Lat. 35° 13' 47" N., Long. 118° 29' 29" W., Tehachapi North 7.5' quad.	Biotite hornblende tonalite: moderately foliated, coarse grained, hypidiomorphic granular rock, C.I.=25; abundant plagioclase (An_{40}), sutured quartz, and brown-green hornblende, lesser biotite. Rock has an overall slight recrystallized texture.	1835/18
#7 TC42	Massive bouldery outcrops 0.3 km from metamorphic septa, along Tweedy Creek at 3300' elev., just NW. of road junction at spring; Lat. 35° 13' 42" N., Long. 118° 29' 46" W., Tehachapi North 7.5' quad.	Biotite hornblende tonalite: moderately foliated, coarse grained, hypidiomorphic granular rock, C.I.=22; abundant plagioclase (An_{40}), sutured quartz, and blue-green to brown hornblende, lesser biotite, accessory sphene and opaques, secondary chlorite and sericite. Rock has a protomylonitic, recrystallized texture.	1729/16
#8 CM25	Massive bouldery rock along west shoulder of Bear Mountain; Lat. 35° 12' 38" N., Long. 118° 39' 47" W., Bear Mountain 7.5' quad.	Biotite hornblende tonalite: moderately foliated, coarse grained, hypidiomorphic granular rock, C.I.=35; plagioclase (An_{40}), quartz, blue-green to olive hornblende, and brown biotite, accessory sphene and opaques.	3585/40
#9 CM26	Massive bouldery rock atop ridge south of Bear Valley; Lat. 35° 08' 23" N., Long. 118° 37' 03" W., Keene 7.5' quad.	Biotite hornblende tonalite: moderately foliated, coarse grained, hypidiomorphic granular rock, C.I.=27; plagioclase (An_{50}), quartz, blue-green hornblende, and brown biotite, accessory sphene, apatite, orthopyroxene, and opaques, secondary chlorite and white mica.	2486/32
#10 CM9	Massive bouldery rock atop Cummings Mountain; Lat. 35° 02' 27" N., Long. 118° 34' 06" W., Cummings Mountain 7.5' quad.	Biotite hornblende tonalite: strongly foliated, heterogeneous to slightly gneissic, medium grained, hypidiomorphic granular rock, C.I.=35; plagioclase (An_{30}), recrystallized quartz and brown biotite, brown to blue-green hornblende, and accessory sphene, secondary epidote and sericite. Rock shows some mylonitic overprinting.	4257/43

TABLE 12. GEOCHRONOLOGY SAMPLE LOCATIONS, PETROGRAPHY, AND ZIRCON YIELD DATA **continued**

Sample Number	Field Setting and Location	Petrography and Special Comments	mg Zircon /kg Rock
#11 CM22b	Mafic inclusion in massive tonalite (BVS) in roadcut 2.5 km SSW. of Bear Mountain on Deer Trail Road, 0.8 km N. of junction with Paramount Road; Lat. 35° 11' 02" N., Long. 118° 38' 45" W., Bear Mountain 7.5' quad.	Amphibolite: fine to medium grained, unfoliated, hypidiomorphic granular rock, C.I.=53; dominantly fine equigranular plagioclase (An_{25}) and olive green hornblende, minor medium grained plagioclase, brown biotite, interstitial quartz, and brown hornblende, accessory sphene and opaques, secondary epidote. Rock has an annealed texture.	1309/36
HYPERSTHENE TONALITE OF BISON PEAK			
#12 TL197	Blocky, rubbly outcrops of massive appearing rock along powerline access road, elev. 5500', 2.5 km WNW. of Twin Lakes; Lat. 34° 59' 27" N., Long. 118° 32' 16" W., Liebre Twins 7.5' quad.	Hypersthene, hornblende, biotite tonalite gneiss: weak to moderately foliated, medium to coarse grained, hypidiomorphic granular rock, C.I.=30; dominantly plagioclase (An_{25}), interstitial quartz, and pale to olive brown hornblende, minor red hypersthene, red-brown biotite and interstitial quartz, accessory brown biotite, clinopyroxene, and opaques, secondary fibrous pale green cummingtonite. Pyroxene cored amphiboles.	418/74
METAGABBRO OF TUNIS CREEK			
#13 WR84a	Massive blocky rock in roadcut along road about 10.5 km S. from old Tejon Ranch Headquarters at 3300' elev.; Lat. 34° 58' 59" N., Long. 118° 43' 17" W., Winters Ridge 7.5' quad.	Diorite: medium grained, unfoliated, hypidiomorphic granular rock, C.I.=48; abundant plagioclase (An_{40}) and fine green hornblende, minor red hypersthene, accessory coarse garnet, clinopyroxene, quartz, apatite, and opaques, secondary cummingtonite. Pyroxene cored amphiboles.	203/36
#14 WR86	Massive bouldery outcrops along road about 12.7 km S. from old Tejon Ranch Headquarters at elev. 3840'; Lat. 34° 58' 27" N., Long. 118° 43' 45" W., Winters Ridge 7.5' quad.	Diorite: dark, even, fine to medium grained, hypidiomorphic granular rock, C.I.=50; dominantly plagioclase (An_{35}) and hornblende, with minor red hypersthene, accessory clinopyroxene, garnet, and opaques. Slightly annealed texture.	78/41
#15 WR190	Massive bouldery outcrops along road atop ridge N. of Tunis Creek, at 2700' elev. 75 m SE. of "oil well"; Lat. 34° 58' 40" N., Long. 118° 45' 44" W., Pastoria Creek 7.5' quad.	Diorite: dark, even, medium grained, unfoliated, hypidiomorphic granular rock, C.I.=53; abundant dark green hornblende and plagioclase (An_{45}), minor red-green pleochroic hypersthene, accessory clinopyroxene and opaques, secondary cummingtonite, remnant olivine. Retrograded texture: olivine has gone to orthopyroxene, pyroxenes to amphiboles, remnant cores of olivine in pyroxene, pyroxene in amphibole.	<1/41

TABLE 12. GEOCHRONOLOGY SAMPLE LOCATIONS, PETROGRAPHY, AND ZIRCON YIELD DATA **continued**

Sample Number	Field Setting and Location	Petrography and Special Comments	mg Zircon /kg Rock
#16 PC227	Massive blocky rock along Tunis Creek at 1750' elev., 0.8 km E. of road end; Lat. 34° 58' 16" N., Long. 118° 46' 42" W., Pastoria Creek 7.5' quad.	Diorite: Unfoliated, medium grained, allotriomorphic granular rock, C.I.=44; abundant plagioclase (An_{40}), clinopyroxene, and green hornblende, minor yellow hypersthene and opaques, secondary cummingtonite, remnant olivine. Olivine cored pyroxene, pyroxene cored amphibole. Olivine retrograded to pyroxenes, pyroxenes to amphiboles. Annealed.	<1/41
TEHACHAPI SUITE			
TONALITE GNEISS OF TEJON CREEK - GNEISS COMPLEX OF THE TEHACHAPI MOUNTAINS			
#17 CM630	Massive bouldery outcrops of a plutonic appearance 0.3 km N. of Comanche Point Road at BM 2937; Lat. 35° 07' 30" N., Long. 118° 43' 22" W., Tejon Ranch 7.5' quad.	Biotite tonalite gneiss: weakly foliated to gneissic, medium grained, coarse hypidiomorphic granular rock, C.I.=10; plagioclase (An_{30}) and quartz, with lesser amounts of brown biotite, minor K-feldspar and olive-green hornblende, accessory epidote.	2918/29
#18 WR643	Massive bouldery outcrops along road 1 km E. of Tejon Reservoir #2 at 2150' elev.; Lat. 35° 01' 28" N., Long. 118° 42' 24" W., Tejon Ranch 7.5' quad.	Biotite tonalite gneiss: moderately foliated to banded, fine grained, hypidiomorphic granular rock, C.I.=13; abundant plagioclase (An_{25}), quartz, and brown biotite, minor orthopyroxene, accessory green hornblende and K-feldspar, epidote, and muscovite.	2750/34
#19 WR171	Massive bouldery outcrop 8 km S. along road from old Tejon Ranch Headquarters at 2700' elev.; Lat. 34° 59' 31" N., Long. 118° 43' 44" W., Winters Ridge 7.5' quad.	Biotite hornblende tonalite gneiss: weakly foliated, fine to medium grained, hypidiomorphic granular, plutonic appearing rock, C.I.=15; abundant plagioclase (An_{30}), quartz, green hornblende, and red-brown biotite, accessory opaques. Foliation is due to felsic and mafic zones. Has an annealed texture.	3080/35
#20 WR30/2	Small outcrop in outcrop along road about 9.5 km S. from old Tejon Ranch Headquarters, at elev. 3360'; Lat. 34° 59' 04" N., Long. 118° 43' 29" W., Winters Ridge 7.5' quad.	Hornblende quartz diorite gneiss: weakly foliated, medium to coarse grained, hypidiomorphic granular rock, C.I.=40; abundant plagioclase (An_{30}) and green hornblende, minor biotite, and granular, recrystalline quartz, accessory clinopyroxene and opaques, secondary epidote. Clinopyroxene cores hornblende.	2457/27

TABLE 12. GEOCHRONOLOGY SAMPLE LOCATIONS, PETROGRAPHY, AND ZIRCON YIELD DATA **continued**

Sample Number	Field Setting and Location	Petrography and Special Comments	mg Zircon /kg Rock
#21 WR39	Massive bouldery outcrops along road about 23.5 km S. from old Tejon Ranch Headquarters at 6250' elev., 0.4 km WSW. of elev. 6388' along E. Winters Ridge;, Lat. 34° 56' 38" N., Long. 118° 39' 48" W., Winters Ridge 7.5' quad.	Hornblende tonalite gneiss: well foliated to banded, medium grained rock, C.I.=32; abundant fluxiony coarse blue-green hornblende, plagioclase (An_{30}), and veiny, granular quartz, minor biotite, accessory clinopyroxene and opaques, secondary epidote and sericite. Has a recrystallized, mylonitic texture.	3957/30
QUARTZO-FELDSPATHIC GNEISS OF PASTORIA CREEK - GNEISS COMPLEX OF THE TEHACHAPI MOUNTAINS			
#22 PC31	Massive banded rock in roadcut of California Aqueduct access road, 0.7 km S. of Edmonston Pumping Plant; Lat. 34° 56' 29" N., Long. 118° 49' 32" W., Pastoria Creek 7.5' quad.	Hornblende biotite granite gneiss: strongly foliated to banded, fine grained, allotriomorphic granular rock, C.I.=14; K-feldspar, plagioclase (An_{30}), quartz, with books of biotite and accessory blue-green hornblende, secondary chlorite.	1977/33
#23 PC32	Massive banded rock in roadcut of California Aqueduct access road, 3.0 km S. of Edmonston Pumping Plant; Lat. 34° 56' 13" N., Long. 118° 49' 08" W., Pastoria Creek 7.5' quad.	Biotite granite gneiss: strongly foliated and lineated, fine grained, allotriomorphic granular rock, C.I.=10; fluxiony quartz and stringy biotite in a mass of granular K-feldspar/microcline, plagioclase (An_{25}), and quartz, accessory clinopyroxene and opaques, secondary sericite. Recrystallized, mylonitic (augen gneissic) texture.	856/31
#24 PC34	Massive rock in roadcut along California Aqueduct access road, 7.4 km S. of Edmonston Pumping Plant; Lat. 34° 55' 40" N., Long. 118° 48' 04" W., Pastoria Creek 7.5' quad.	Biotite hornblende tonalite gneiss: moderately foliated to faintly banded, medium grained rock, C.I.=43; ragged subhedral olive to blue-green poikilitic hornblende in an allotriomorphic mass of plagioclase (An_{40}), granular quartz, and stringy biotite, accessory clinopyroxene, epidote, and opaques, secondary green hornblende and chlorite.	1292/32
#25 PC36	Layer in gneiss, roadcut along California Aqueduct access road, 10.9 km S. of Edmonston Pumping Plant; Lat. 34° 54' 59" N., Long. 118° 47' 40" W., Pastoria Creek 7.5' quad.	Biotite tonalite gneiss: strongly foliated and lineated, fine to medium grained, allotriomorphic granular rock, C.I.=15; plagioclase (An_{30}) and strained quartz, stringy biotite, accessory K-feldspar, clinopyroxene, garnet, white mica, epidote, and opaques. Weakly recrystallized and mylonitic.	1006/31

TABLE 12. GEOCHRONOLOGY SAMPLE LOCATIONS, PETROGRAPHY, AND ZIRCON YIELD DATA continued

Sample Number	Field Setting and Location	Petrography and Special Comments	mg Zircon /kg Rock
#26 PC37	Layer in gneiss, roadcut along California Aqueduct access road, 12.5 km S. of Edmonston Pumping Plant; Lat. 34° 54' 30" N., Long. 118° 47' 15" W., Pastoria Creek 7.5' quad.	Biotite granite augen gneiss: strongly foliated to banded, medium grained rock, C.I.=20; coarse porphyroblasts of plagioclase (An_{20}) and K-feldspar in a groundmass of sutured, strained, fluxiony quartz and stringy biotite, with fine granular feldspars, accessory clinopyroxene, epidote, and opaques.	3638/31
#27 PC129	Massive bouldery outcrops along road (not shown on 1974 topo) about 2.5 km S. of California Aqueduct access road, or 1.3 km ESE. of the Grapevine, 100 m SE. of elev. 2395'; Lat. 34° 55' 31" N., Long. 118° 54' 42" W., Grapevine 7.5' quad.	Biotite garnet tonalite: unfoliated, medium to coarse grained, hypidiomorphic granular rock, C.I.=15; dominantly plagioclase (An_{30}), granular quartz, and red-brown biotite, many very coarse (2-5 cm) red garnets, accessory opaques.	1135/36
#28 WR91a	Massive bouldery outcrops at W. end of Winters Ridge, 20 m S. of elev. 5336', about 16 km S. along road from old Tejon Ranch Headquarters; Lat. 34° 57' 30" N., Long. 118° 43' 08" W., Winters Ridge 7.5' quad.	Garnet tonalite gneiss: weakly foliated to banded, fine grained, felsic rock, C.I.=15; abundant plagioclase (An_{25}), quartz, and red-brown biotite, with lesser K-feldspar and hornblende, many coarse (1-3 cm) garnets.	3518/22
#29 WR40	Blocky-flaky outcrops at W. end of E. 1/2 Winters Ridge, 0.4 km W. of elev. 6445', about 22 km S. along road from old Tejon Ranch Headquarters; Lat. 34° 56' 47" N., Long. 118° 40' 41" W., Winters Ridge 7.5' quad.	Biotite granite augen gneiss: strongly foliated, medium grained, felsic rock, C.I.=10; abundant veiny, sutured, granular quartz, porphyroclastic and granular K-feldspar/microcline, and lesser clasts of plagioclase, minor biotite and epidote.	2315/40
AUGEN GNEISS OF TWEEDY CREEK			
#30 TC12a	Small orthogneiss body intrusive into metasedimentary septa, cut by tonalite stock (#2 - TC40); massive outcrops along Tweedy Creek at 3420' elev., 0.7 km E. of road junction at spring; Lat. 35° 13' 39" N., Long. 118° 29' 18" W., Tehachapi North 7.5' quad.	Biotite granodiorite augen gneiss: strongly foliated, fine to medium grained orthogneiss, C.I.=14; abundant fluxiony, partially recrystallized quartz, plagioclase (An_{30}), and K-feldspar, minor microcline, and biotite, accessory opaques, secondary chlorite. Feldspars show brittle deformation, while quartz has undergone ductile deformation.	1220/46

TABLE 12. GEOCHRONOLOGY SAMPLE LOCATIONS, PETROGRAPHY, AND ZIRCON YIELD DATA **continued**

Sample Number	Field Setting and Location	Petrography and Special Comments	mg Zircon /kg Rock
#31 TC12b	Mafic inclusion in augen gneiss of Tweedy Creek, 20 m W. of TC12a locality; Lat. 35° 13' 39" N., Long. 118° 29' 18" W., Tehachapi North 7.5' quad.	Amphibolite: fine, even grained, unfoliated rock, C.I.=46; dominantly fine, equigranular recrystallized plagioclase (to An_{50}) and blue-green to brown hornblende, lesser biotite and quartz, accessory sphene and apatite. Rock has a slightly annealed texture.	121/51
METASEDIMENTARY FRAMEWORK ROCKS			
QUARTZITE - METAMORPHIC SEPTA			
#32 CM640	1-2 m layer in banded gneiss, NE. corner of low hills S. of old Cummings Valley Road, 1 km W. of BM 4089; Lat. 35° 08' 01" N., Long. 118° 33' 46" W., Keene 7.5' quad.	Impure quartzite: fine, even grained rock; dominantly granoblastic, strained quartz, minor K-feldspar, colorless clinopyroxene, and plagioclase, accessory graphite, muscovite, sphene, opaques, and detrital zircon.	1991/61
PARAGNEISS OF COMANCHE POINT - GNEISS COMPLEX OF THE TEHACHAPI MOUNTAINS			
#33 CM110	Massive banded gneiss in low blocky outcrops along Comanche Point Road at BM 1495; Lat. 35° 08' 19" N., Long. 118° 46' 53" W., Arvin 7.5' quad.	Biotite quartzofeldspathic (para)gneiss: Strongly foliated to segregated, fine grained rock, C.I.=20; plagioclase (An_{35}), quartz, and red-brown biotite, minor K-feldspar, graphite, muscovite, garnet, and opaques.	155/40

trometer (variations in multiplier peak shapes, and differences in background on the sides of the ^{204}Pb peak) and the near linearity of concordia for mid-Cretaceous ages. Based on all of the preceding factors, the uncertainties in the $^{207}Pb^*/^{206}Pb^*$ ages are given as ±15 Ma.

A concordant system (Wetherill, 1956; Faure, 1977) is a system that consists of minerals that are closed to uranium, lead, and intermediate daughter product loss or gain throughout its history. A discordant system is one that does not satisfy the above conditions. A U/Pb analysis is considered to be internally concordant if, within analytical uncertainty, the U/Pb ages agree (the error polygons overlap) (Chen and Moore, 1982). On a concordia diagram ($^{206}Pb^*/^{238}U$ vs. $^{207}Pb^*/^{235}U$; Wetherill, 1956), such overlap is shown by the error polygon of an analysis intersecting concordia. A sample is considered to be externally concordant when multiple fractions from the same sample are concordant with one another (again, their error polygons overlap). Externally concordant ages usually are assumed to represent igneous crystallization ages (Chen and Moore, 1982). The uncertainties in the interpreted ages were assigned from agreement of the $^{206}Pb^*/^{238}U$ and $^{207}Pb^*/^{235}U$ ages within a fraction; agreement of $^{206}Pb^*/^{238}U$ ages between fractions; and agreement of $^{207}Pb^*/^{206}Pb^*$ ages between aliquots of a sample.

In well-behaved discordant zircon populations, the normal sequence of ages is $^{206}Pb^*/^{238}U < ^{207}Pb^*/^{235}U < ^{207}Pb^*/^{206}Pb^*$. The dispersion of ages within and between fractions is most likely due to the gain or loss of radiogenic lead or uranium. The first process that could cause discordance is a magma inheriting pre-existing zircon from a magmatic source rock or entraining wallrock material containing zircon. The dated zircons commonly show older cores with overgrowth by new zircon. However, the pre-existing zircon may be completely melted and

incorporated into the magma, in which case there is no visible manifestation of the older zircon. The second process to cause discordance is a post-crystallization disturbance which results in lead loss and/or uranium gain in the dated zircon.

At the deep structural levels as represented by the southernmost Sierra Nevada, there is abundance evidence for migmatism and local melt production and assimilation into intrusive magmas. Hence, the distinction between inheritance and entrainment of zircon becomes blurred and breaks down. Thus, incorporation of pre-existing zircon into magmas is termed "inheritance" for the purpose of this study, and entails both inheritance and entrainment mechanisms. "Entrainment" is only used where there is a clear basis for an actual entrainment mechanism.

The concordia curve is defined by the set of concordant $^{206}Pb^*/^{238}U$ and $^{207}Pb^*/^{235}U$ age pairs. The modern cosmic atomic ratios of $^{235}U/^{238}U$, the ratio of which changes through time (due to differing decay constants), causes the shape of concordia to change through time. By extrapolating a line passing through a set of discordant analyses from a sample (discordia), one can obtain two intersections with concordia. In the case of the first process mentioned above (inheritance or entrainment of pre-existing zircon), the data points most commonly fall on discordia trending away from the lower intercept with concordia. The upper intercept reflects the overall isotopic character of the contaminate zircon, which may be a multi-component system. The lower intercept may represent the igneous crystallization age (Tobisch and others, 1986). In the second case (post-crystallization disturbance), the data points most commonly fall on discordia trending away from the upper intercept. The lower intercept represents the time of lead loss (time elapsed since closure of the U/Pb system), while the upper intercept may represent the igneous crystallization age or overall isotopic character of the zircon population (Faure, 1977). To perform this sort of a concordia intercept theory

investigation, multiple splits of a zircon population into different physical groups (fractions) are required. Multiple fraction analyses were performed on all samples that yielded sufficient zircon to perform such an analysis.

A major difficulty arises in trying to interpret concordance or discordance in Mesozoic samples. This is due to the near linearity of concordia between the origin and 300 Ma. Such linearity could permit a disturbed zircon system to have no resolvable divergence from concordia. In addition, the dispersion of Mesozoic zircon populations is often insufficient to adequately determine upper and lower intercepts with concordia (Saleeby, 1982).

III.3 Results

The results of this investigation are summarized in Table 13. Recorded therein are the sample zircon weight, uranium and radiogenic lead concentrations, and lead isotopic compositions, as well as U/Pb and Pb/Pb ages. Zircons within the selected fractions were generally clear, euhedral, and relatively free of inclusions and visible cores. The interpreted ages and related uncertainties are shown as part of Table 14, along with bulk rock initial $^{87}Sr/^{86}Sr$ and $\delta^{18}O$ data (these isotopic systems are discussed in Chapter IV). The interpreted ages are shown on the base map of the region in Figure 41, and are summarized in the histogram in Figure 42. There is a progressive west to east and a general north to south decrease in ages, especially in the plutonic samples. Note the widespread occurrence of the late deformational intrusive suite of samples, from the southwestern part of the map (Pastoria Creek area) to the west-central (Comanche Point) and then east (Tweedy Creek).

There is a general lack of any ages older than mid-Cretaceous in the southernmost Sierra Nevada; in fact the data exhibit a narrow age range of less than 30 my. Close attention to the age data presented in Table 13 and Figure 42 shows

TABLE 13. U/Pb ZIRCON AGE DATA

FRACTION PROPERTIES††		mg SAMPLE	concentrations ppm 238U	ppm 206Pb*	measured ratios 206Pb/ 204Pb	206Pb/ 207Pb	206Pb/ 208Pb	radiogenic ratios 206Pb*/ 238U	207Pb*/ 235U	207Pb*/ 206Pb*	isotopic ages (Ma) † 206Pb*/ 238U	207Pb*/ 235U	207Pb*/ 206Pb*†††
LATE DEFORMATIONAL INTRUSIVE EPOCH													
GRANODIORITE OF CLARAVILLE													
#1	biotite granodiorite												
	165-120 μ	14.4	509.3	8.057	2811	14.47	10.60	0.018277	0.16112	0.06396	116.8	151.7	740
10/20nm	120-80 μ	34.6	666.3	9.808	1529	14.20	9.970	0.017007	0.14283	0.06094	108.7	135.7	637
	80-45 μ	32.7	787.6	10.45	2867	17.03	12.12	0.015331	0.11330	0.05322	98.1	109.0	338
	<45 μ	26.6	967.2	12.04	1830	17.34	11.63	0.014389	0.09844	0.04964	92.1	95.3	178
TONALITE STOCK AT TWEEDY CREEK													
#2	biotite hornblende tonalite stock into augen gneiss of Tweedy Creek and metasedimentary septum												
	165-120 μ	32.0	248.0	3.425	604	13.26	5.478	0.015959	0.11259	0.05119	102.1	108.3	249
4/20nm	120-80 μ	13.8	310.0	4.191	708	13.75	5.722	0.015622	0.11204	0.05204	99.9	107.8	287
	<45 μ	19.4	265.6	3.598	60.94	3.430	1.369	0.015650	0.11046	0.05121	100.1	106.4	250
PEGMATITE DIKE SWARM CUTTING TEJON CREEK AND COMANCHE POINT GNEISSES													
#3	granite pegmatite crosscutting tonalite gneiss of Tejon Creek												
1/20nm	<165 μ	12.3	906.4	11.57	6498	19.89	6.895	0.014752	0.09762	0.04801	94.4	94.6	99
LEUCOCRATIC DIKE CUTTING PASTORIA CREEK GNEISS													
#4	biotite garnet granite gneiss (dike)												
	120-80 μ	13.0	2352	31.73	5900	19.60	16.64	0.015588	0.10425	0.04852	99.7	100.7	124
2/20nm	80-45 μ	7.2	2469	32.34	4917	19.42	17.40	0.015137	0.10119	0.04850	96.9	97.9	123
BEAR VALLEY SPRINGS INTRUSIVE EPOCH													
TONALITE OF MOUNT ADELAIDE													
#5	biotite tonalite - Mount Adelaide phase of tonalite of Bear Valley Springs(?)												
	80-45 μ	14.8	341.3	4.635	1503	17.18	10.05	0.015660	0.10452	0.04843	100.2	100.9	120
2/20	<45 μ	7.0	350.4	4.709	2458	18.47	5.501	0.015546	0.10319	0.04816	99.5	99.7	106
TONALITE of BEAR VALLEY SPRINGS													
#6	biotite hornblende tonalite near Tweedy Creek - eastern margin phase												
	120-80 μ	33.7	478.4	6.247	771	14.80	7.770	0.015088	0.10086	0.04850	96.6	97.6	123
2/20nm	80-45 μ	27.7	563.0	7.460	1682	17.48	9.167	0.015309	0.10227	0.04847	98.0	98.9	122
#7	biotite hornblende tonalite near Tweedy Creek - east margin phase												
	120-80 μ	45.7	378.7	5.109	2200	18.20	8.194	0.015588	0.10367	0.04826	99.7	100.2	111
2/20nm	80-45 μ	28.2	463.1	6.224	2607	18.75	8.434	0.015529	0.10209	0.04770	99.4	98.7	84

TABLE 13. U/Pb ZIRCON AGE DATA **continued**

FRACTION PROPERTIES††		mg SAMPLE	concentrations ppm 238U	ppm 206Pb*	measured ratios 206Pb/ 204Pb	206Pb/ 207Pb	206Pb/ 208Pb	radiogenic ratios 206Pb*/ 238U	207Pb*/ 235U	207Pb*/ 206Pb*	isotopic ages (Ma) † 206Pb*/ 238U	207Pb*/ 235U	207Pb*/ 206Pb*†††
#8	biotite hornblende tonalite - main phase												
	120-80 μ	21.2	857.8	11.77	4440	19.40	8.253	0.015857	0.10543	0.04824	101.4	101.8	111
1/20nm	80-45 μ	23.2	830.0	11.43	2284	18.24	7.645	0.015913	0.10612	0.04839	101.8	102.4	118
#9	biotite hornblende tonalite - main phase												
	120-80 μ	17.1	566.5	7.631	1432	17.26	7.092	0.015564	0.10220	0.04810	99.6	98.8	104
2/20nm	80-45 μ	22.9	674.9	9.121	1555	17.41	6.787	0.015614	0.10325	0.04798	99.9	99.8	98
#10	biotite hornblende tonalite - main phase												
	120-80 μ	30.5	592.9	8.015	2796	18.61	7.078	0.015619	0.10434	0.04847	99.9	100.8	122
1/20nm	80-45 μ	29.4	635.1	8.499	4686	19.58	7.307	0.015462	0.10213	0.04792	98.9	98.7	96
#11	diorite inclusion in tonalite - main phase												
	120-80 μ	24.1	623.5	8.464	3852	19.23	7.025	0.015685	0.10418	0.04820	100.3	100.6	108
1/20nm	80-45 μ	22.2	709.5	9.697	6166	19.76	6.568	0.015792	0.10497	0.04823	101.0	101.4	110
HYPERSTHENE TONALITE OF BISON PEAK													
#12	hypersthene biotite hornblende tonalite												
	120-80 μ	22.4	296.2	4.070	4567	19.52	7.599	0.015874	0.10503	0.04801	101.5	101.4	100
0/20nm	<80 μ	25.5	318.3	4.443	10170	20.07	8.090	0.016126	0.10754	0.04838	103.1	103.7	118
METAGABBRO OF TUNIS CREEK													
#13	hornblende diorite												
	165-120 μ	24.2	78.39	1.075	2796	18.64	9.790	0.015850	0.10570	0.04813	101.4	102.0	106
1/20nm	120-80 μ	23.5	78.17	1.079	2213	18.33	9.274	0.015943	0.10524	0.04814	102.0	101.6	106
	80-45 μ	12.3	75.64	1.059	2998	18.58	9.060	0.016179	0.10909	0.04893	103.5	105.1	144
#14	hornblende diorite												
	165-120 μ	25.6	64.32	.8980	1226	16.72	6.944	0.016132	0.10629	0.04781	103.2	102.6	90
2/20nm	120-80 μ	22.3	74.78	1.022	547.0	13.25	5.968	0.015790	0.10576	0.04767	101.0	102.1	98
	<80 μ	19.1	74.55	1.279	939.7	13.91	6.743	0.019818	0.15410	0.05642	126.5	145.5	469
#15	hornblende diorite												
	insufficient zircon to date												
#16	hornblende diorite												
	insufficient zircon to date												

TABLE 13. U/Pb ZIRCON AGE DATA continued

FRACTION PROPERTIES††		mg SAMPLE	concentrations ppm 238U	ppm 206Pb*	measured ratios 206Pb/ 204Pb	206Pb/ 207Pb	206Pb/ 208Pb	radiogenic ratios 206Pb*/ 238U	207Pb*/ 235U	207Pb*/ 206Pb*	isotopic ages (Ma) † 206Pb*/ 238U	207Pb*/ 235U	207Pb*/ 206Pb*†††
TEHACHAPI EPOCH													
TONALITE GNEISS OF TEJON CREEK - GNEISS COMPLEX OF THE TEHACHAPI MOUNTAINS													
#17	biotite tonalite gneiss												
	165-120 μ	18.1	1026	16.57	3656	18.84	10.07	0.018670	0.12625	0.04907	119.3	120.7	151
1/20nm	165-120 μ	13.3	1090	16.8	6504	19.51	10.67	0.017806	0.12024	0.04900	113.8	115.3	147
	120-80 μ	19.6	989.2	15.27	11220	19.76	10.74	0.017855	0.12129	0.04929	114.1	116.2	161
	<45 μ	16.8	1019	16.08	11190	19.61	10.11	0.018231	0.12481	0.04967	116.5	119.4	179
#18	biotite tonalite gneiss												
	165-120 μ	24.7	876.9	13.96	5982	19.62	11.79	0.018396	0.12302	0.04852	117.5	117.8	124
1/20nm	<45 μ	18.1	979.4	15.51	7329	19.77	12.09	0.018301	0.12254	0.04859	116.9	117.4	128
#19	biotite hornblende tonalite gneiss												
	165-120 μ	18.2	327.2	5.063	3722	18.61	8.381	0.017879	0.12269	0.04979	114.2	117.5	185
1/20nm	120-80 μ	17.9	332.6	4.848	4656	19.03	8.348	0.016840	0.11464	0.04940	107.7	110.2	166
	80-45 μ	16.7	375.2	5.645	4269	18.94	8.351	0.017384	0.11826	0.04936	111.1	113.5	164
	<45 μ	11.0	248.0	3.827	5196	18.67	8.335	0.017830	0.12470	0.05075	113.9	119.3	229
#20	hornblende quartz diorite												
	120-80 μ	12.8	216.6	3.552	2074	17.66	7.887	0.018945	0.12937	0.05023	121.0	123.5	205
1/20nm	80-45 μ	11.8	227.4	3.615	2142	17.58	7.761	0.018368	0.12665	0.05003	117.4	121.1	196
	<45 μ	4.4	231.9	3.732	875	14.88	5.993	0.018594	0.12928	0.04984	118.8	123.4	187
#21	hornblende tonalite gneiss												
	80-45 μ	27.7	169.3	2.590	5475	19.58	8.306	0.017677	0.11786	0.04818	113.0	113.1	108
-1/20nm	<45 μ	5.1	201.9	3.082	4087	19.04	7.615	0.017631	0.11890	0.04893	112.7	114.1	127
QUARTZO-FELDSPATHIC GNEISS OF PASTORIA CREEK - GNEISS COMPLEX OF THE TEHACHAPI MOUNTAINS													
#22	hornblende biotite granite gneiss												
	120-80 μ	36.7	812.7	12.16	1795	17.70	9.938	0.017290	0.11511	0.04831	110.5	110.6	114
2/20nm	80-45 μ	29.4	917.8	13.93	2077	18.01	9.948	0.017540	0.11713	0.04845	112.1	112.5	121
#23	biotite granite gneiss												
	120-80 μ	29.2	1658	25.08	2069	17.99	12.04	0.017480	0.11678	0.04848	111.7	112.2	122
2/20nm	80-45 μ	28.3	1894	28.63	2475	18.59	13.82	0.017468	0.11519	0.04806	111.6	110.7	102
	<45 μ	6.8	1825	28.00	1869	17.89	14.22	0.017730	0.11736	0.04803	113.3	112.7	101
#24	biotite hornblende tonalite gneiss												
	120-80 μ	33.0	221.5	3.486	3885	19.05	7.544	0.018183	0.12210	0.04872	116.2	117.0	134
1/20nm	80-45 μ	30.2	337.8	5.360	7455	19.60	8.048	0.018335	0.12395	0.04905	117.1	118.6	150
	<45 μ	5.9	405.3	6.270	1372	16.72	6.705	0.017874	0.12092	0.04909	114.2	115.9	152

TABLE 13. U/Pb ZIRCON AGE DATA continued

FRACTION PROPERTIES††		mg SAMPLE	concentrations ppm 238U	ppm 206Pb*	measured ratios 206Pb/ 204Pb	206Pb/ 207Pb	206Pb/ 208Pb	radiogenic ratios 206Pb*/ 238U	207Pb*/ 235U	207Pb*/ 206Pb*	isotopic ages (Ma) † 206Pb*/ 238U	207Pb*/ 235U	207Pb*/ 206Pb*†††
#25	biotite tonalite gneiss												
	120-80 μ	29.1	1221	18.29	8759	19.97	12.02	0.017308	0.11542	0.04837	110.6	110.9	118
1/20nm	80-45 μ	26.1	1393	20.54	3343	19.13	11.75	0.017038	0.11242	0.04817	108.9	108.2	105
#26	biotite granite augen gneiss												
	120-80 μ	16.2	785.9	12.11	6590	19.80	11.63	0.017809	0.11849	0.04827	113.8	113.7	113
1/20nm	80-45 μ	11.2	855.0	13.21	4148	19.14	10.96	0.017858	0.11985	0.04858	114.1	114.9	127
#27	biotite garnet tonalite												
	120-80 μ	14.6	335.1	5.239	1348	16.78	8.350	0.018063	0.12120	0.04868	115.4	116.2	132
0/20nm	80-45 μ	13.8	342.5	5.280	2820	18.71	9.344	0.017811	0.11840	0.04842	113.8	113.6	120
#28	garnet tonalite gneiss												
	80-45 μ	24.5	763.4	11.58	5071	19.56	13.22	0.017522	0.11645	0.04822	112.0	111.8	110
-1/20pm	<45 μ	23.4	814.3	11.99	4880	19.32	12.68	0.017013	0.11433	0.04876	108.8	109.9	136
#29	biotite granite augen gneiss												
	120-80 μ	19.7	911.9	14.49	3715	19.12	10.74	0.018355	0.12228	0.04834	117.3	117.1	116
1/20nm	80-45 μ	17.5	1091	16.93	4658	19.48	11.14	0.017926	0.11904	0.04818	114.6	114.2	108
AUGEN GNEISS OF TWEEDY CREEK													
#30	biotite granite orthogneiss												
	165-120 μ	15.1	896.7	13.80	3374	18.87	12.62	0.017783	0.11918	0.04863	113.6	114.3	129
10/20nm	120-80 μ	8.7	1022	15.55	2227	18.03	11.57	0.017578	0.11840	0.04887	112.3	113.6	141
	80-45 μ	22.8	1132	16.96	3465	18.98	11.74	0.017372	0.11561	0.04846	111.0	111.4	122
	<45 μ	38.4	1206	18.51	4106	19.10	11.80	0.017741	0.11929	0.04879	113.4	114.4	137
#31	mafic inclusion in augen gneiss												
10/20nm				No radiogenic lead									
METASEDIMENTARY FRAMEWORK ROCKS													
QUARTZITE - KINGS SEQUENCE-AFFINITY METAMORPHIC SEPTA													
#32	impure quartzite in metasedimentary septum within tonalite of Bear Valley Springs												
-1/20pm	<45 μ	25.0	512.2	37.95	1999	9.643	8.308	0.085604	1.14200	0.09680	529.6	773.5	1563
PARAGNEISS OF COMANCHE POINT - GNEISS COMPLEX OF THE TEHACHAPI MOUNATINS													
#33	biotite quartzo-feldspathic paragneiss												
	165-120 μ	1.3	364.9	25.09	581	9.221	5.208	0.079455	0.92298	0.08428	493.0	664.0	1299
0/20pm	120-80 μ	8.7	632.6	26.06	2778	11.93	9.478	0.047601	0.51652	0.07873	299.8	422.8	1165
	80-45 μ	20.2	684.4	27.00	2828	12.23	9.378	0.045577	0.48208	0.07675	287.4	399.5	1114
	<45 μ	23.9	876.4	29.70	6332	13.08	11.09	0.039157	0.40042	0.07420	247.6	342.0	1047

TABLE 13. U/Pb ZIRCON AGE DATA **continued**

† The decay constants used for these age calculations were: $\lambda^{238}U = 1.55125 \times 10^{-10}$, $\lambda^{235}U = 9.8485 \times 10^{-10}$ (Jaffey and others, 1971); $^{238}U/^{235}U$ (atom) = 137.8 (Chen and Wasserburg, 1981). Common lead compositions used for non-radiogenic correction were based on blank and initial lead determinations, which were approximated from laboratory measurements and from feldspar determinations of nearby mid-Mesozoic granitoids (Chen and Moore, 1982). Blank lead = Initial lead: $^{206}Pb/^{204}Pb$ = 18.8, $^{207}Pb/^{204}Pb$ = 15.6, $^{208}Pb/^{204}Pb$ = 37.7. Analyses conducted at California Institute of Technology between 1981 and 1984, during which total blank averaged 0.1 ng Pb. Uncertainty in reported Pb/U ages: $^{206}Pb^*/^{238}U \approx 1.0$-$1.5\%$, $^{207}Pb^*/^{235}U \approx 1.5$-$2.0\%$, based on uncertainties in uranium and lead concentrations. Mass spectrometer performance monitored on a regular basis by runs of NBS SRM983 and SRM981 (Pb) and U500 (U) reference standards.

†† Fractions separated by grain size and magnetic properties. Magnetic properties are given as nonmagnetic (nm) or paramagnetic (pm) split at side/front slopes for 1.7 amps on Frantz Isodynamic Separator. Samples hand-picked to >99% purity prior to dissolution. Dissolution and chemical extraction techniques after Saleeby and Sharp (1980); modified from Krogh (1973). Size range is given in microns.

††† $^{207}Pb^*/^{206}Pb^*$ ages were derived from comparison of ages determined from spiked and unspiked aliquots. The relative precisions associated with the ages guided the age selection as follows. If the precision and ages were similar, the unspiked aliquot age was used. If the precision and ages were dissimilar, the ages were weighted according to their associated precision, and an intermediate age was assigned. The spiked aliquot age was used where there was a large error associated with the unspiked aliquot analysis. The uncertainty in the $^{207}Pb^*/^{206}Pb^*$ ages = ± 15, based on agreement of aliquot analyses, mass spectrometer precision, and uncertainty in initial lead compositions.

Table 14. U/Pb zircon ages, $\delta^{18}O$ values, and initial $^{87}Sr/^{86}Sr$ ratios

SAMPLE #	UNIT‡		AGE (Ma)	$\delta^{18}O$‡‡ ‰SMOW	$^{87}Sr/^{86}Sr_o$§
Late deformational intrusive suite					
1	TC27	Claraville granodiorite	90±2/1900	11.34	0.70731
2	TC40	tonalite stock	93±3	10.11	0.70703
3	CM620	pegmatite x-cuts TJ	94±2	n/d	n/d
4	PC35	granite dike xcuts PC	97+20/-2	10.00	0.70776
Bear Valley Springs intrusive suite					
5	BM684	tonalite (BVS-A)	100±2		
6	TC15	tonalite (BVS-e)	98±2	10.08	0.70583
7	TC42	tonalite (BVS-e)	100±2	9.10	0.70570
8	CM25	tonalite (BVS-m)	102±2	8.64	0.70591
9	CM26	tonalite (BVS-m)	100±2	9.63	0.70637
10	CM9	tonalite (BVS-m)	100±2	9.12	0.70677
11	CM22b	mafic inclusion (BVS-m)	100±2	7.82	0.70605
12	TL197	tonalite (BP)	101±2	5.73	0.70496
13	WR84	metagabbro (TC)	101±2	7.19	0.70499
14	WR86	metagabbro (TC)	102±2	8.13	0.70504
15	WR190	metagabbro (TC)	n/d	7.55	0.70499
16	PC227	metagabbro (TC)	n/d	8.61	0.70493
Tehachapi suite					
17	CM630	tonalite gneiss (TJ)	110±10	10.10	0.70472
18	WR643	tonalite gneiss (TJ)	117±2	10.52	0.70518
19	WR171	tonalite gneiss (TJ)	110±15	6.84	0.70467
20	WR30/2	quartz diorite (TJ)	110±10	8.46	0.70478
21	WR39	tonalite gneiss (TJ)	113±2	8.42	0.70499
22	PC31	granite gneiss (PC)	111±2	9.31	0.70519
23	PC32	granite gneiss (PC)	112±2	10.89	0.70510
24	PC34	tonalite gneiss (PC)	117±3	8.61	0.70469
25	PC36	tonalite gneiss (PC)	110±2	9.50	0.70500
26	PC37	granite gneiss (PC)	114±2	9.44	0.70469
27	PC129	tonalite (PC)	115±2	10.27	0.70594
28	WR91a	tonalite gneiss (PC)	113±4	8.74	0.70536
29	WR40	granite gneiss (PC)	113±5	10.68	0.70480
30	TC12a	Tweedy Creek augen gneiss	114±3	10.80	0.70682
31	TC12b	mafic inclusion in above	n/d	n/d	n/d
Metamorphic framework rocks					
32	CM640	quartzite (KS)	100/1700	17.38	0.72434
33	CM110	paragneiss (TGC)	108/1450	18.26	0.71146

‡ BVS=tonalite of Bear Valley Springs (A=Mount Adelaide, e=eastern, m=main), BP=hypersthene tonalite of Bison Peak, TC=metagabbro of Tunis Creek; TGC=gneiss complex of the Tehachapi Mountains, PC=quartzo-feldspathic gneiss of Pastoria Creek, TJ=tonalite gneiss of Tejon Creek; KS=Kings sequence.

‡‡ Uncertainties are ±0.20 per mil.

§ Zircon ages were used to correct for in situ decay of ^{87}Rb and obtain initial $^{87}Sr/^{86}Sr$ ratios. For samples #15,16 101 Ma was used. For the metasedimentary rocks, $^{87}Sr/^{86}Sr$ at zircon lower intercept age is tabulated. $^{87}Sr/^{86}Sr$ observed for the quartzite is 0.72581, and for the paragneiss is 0.71442. Uncertainties are ±0.00010.

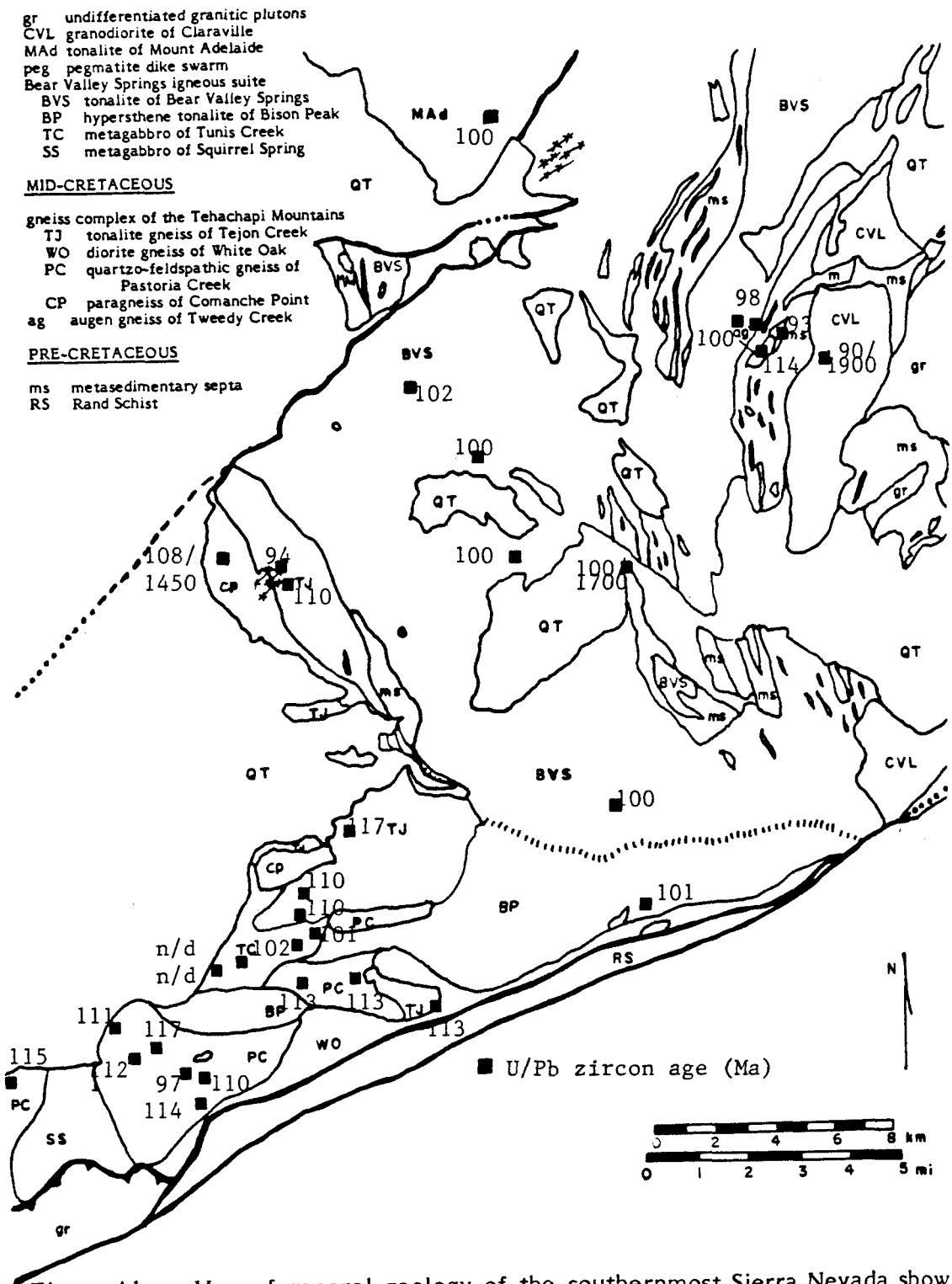

Figure 41. Map of general geology of the southernmost Sierra Nevada showing distribution of interpreted U/Pb zircon ages (this work).

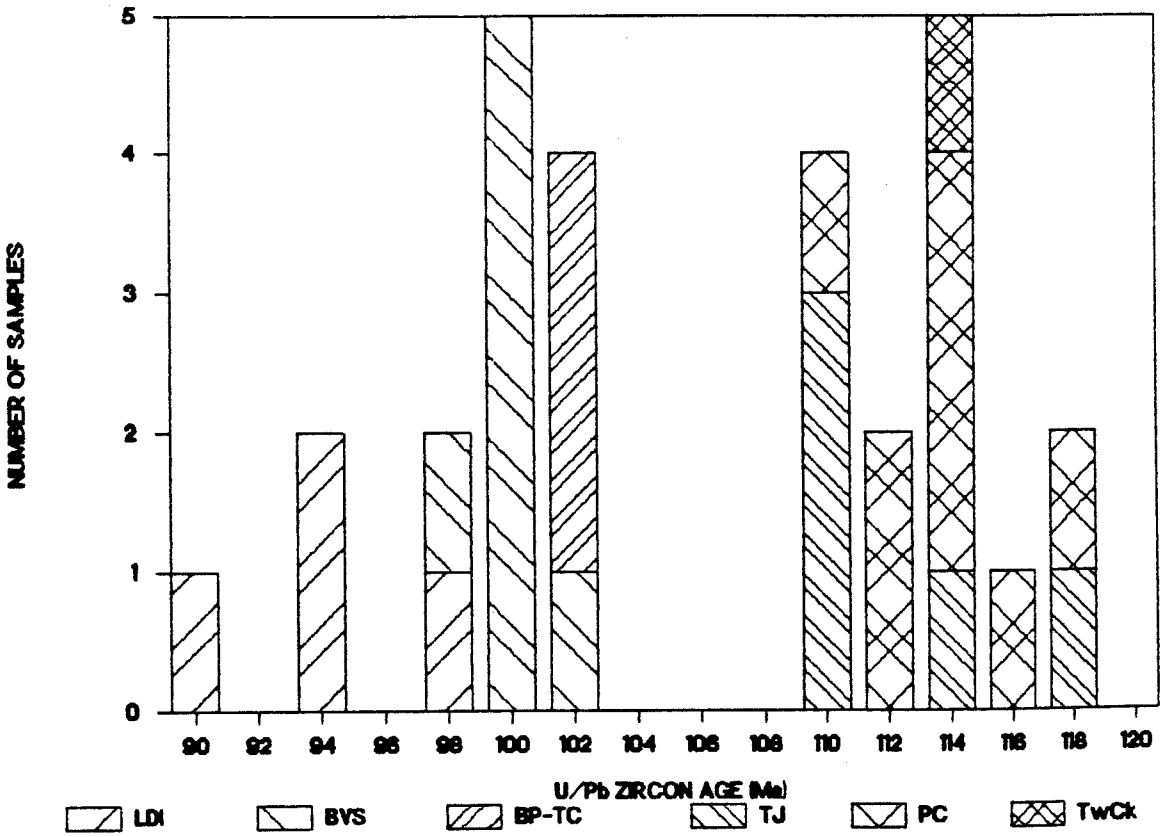

Figure 42. Histogram of U/Pb zircon ages for the crystalline rocks of the southern Sierra Nevada investigated in this report, and shown in Figure 41. There is a strong gap in ages between 102 and 110 Ma. The samples may be grouped into three suites: the Tehachapi, Bear Valley Springs intrusive, and late deformational intrusive suites. Note the overlap of ages within the tonalite gneiss of Tejon Creek and the quartzo-feldspathic gneiss of Pastoria Creek within the Tehachapi suite. LDI=late deformational intrusive rocks; BVS=tonalite of Bear Valley Springs; BP-TC=hypersthene tonalite of Bison Peak-metagabbro of Tunis Creek; TJ=tonalite gneiss of Tejon Creek; PC=quartzo-feldspathic gneiss of Pastoria Creek; TwCk=augen gneiss of Tweedy Creek.

three main suites of ages. There is a clear gap of 8 my between the first and second suites. The first suite has ages that range from 110-117 Ma, and consists of the bulk of the samples in the gneiss complex of the Tehachapi Mountains, and the augen gneiss of Tweedy Creek (defined as the Tehachapi suite). These samples show a much greater degree of deformation, especially under medium to high grade conditions, than the younger samples. The second set has ages of 100±2 Ma, and consists of the samples from the tonalite of Mount Adelaide, the tonalite of Bear Valley Springs, the hypersthene tonalite of Bison Peak and the metagabbro of Tunis Creek (Bear Valley Springs suite). These samples locally cross-cut the above suite, and contain a moderate degree of deformation. The third suite comprises the late deformational intrusive rocks, with ages of between 90 and 97 Ma. Its members are moderately to nondeformed rocks, and consist of the granodiorite of Claraville, a tonalitic stock intrusive into the augen gneiss of Tweedy Creek, a pegmatite dike at Comanche Point, and a garnet granite dike at Pastoria Creek.

The metamorphic framework rocks that were dated for this study are a quartzite within the Kings sequence rocks and a sample from the paragneiss of Comanche Point. The quartzite yielded one very strongly discordant fraction. Both the quartzite and paragneiss consisted primarily of fine to very fine zircon grains (<80 microns), as discussed later. Only three samples show significant discordance, and only two (granodiorite of Claraville, paragneiss of Comanche Point) could be treated by concordia intercept theory.

The following discussion will interpret the zircon isotopic data presented in Table 14 and summarized on plots of various segments of concordia in Figures 43 and 44, in order to derive igneous ages or age constraints on the various units. The Bear Valley Springs suite is discussed first, because its systematics are the most straightforward and simplest to interpret. The metamorphic framework

Figure 43. Concordia diagrams of southernmost Sierra Nevada, with all fractions from Table 14 shown. (a) Metasedimentary samples (quartzite and paragneiss of Comanche Point), which are all strongly discordant; (b) strongly discordant plutonic sample (granodiorite of Claraville); (c) the granodiorite of Claraville and tonalite intrusion into the augen gneiss of Tweedy Creek using the upper intercept from the granodiorite of Claraville, and the discordant fraction from the metagabbro of Tunis Creek using the tonalite of Bear Valley Springs lower intercept; and (d) diagram showing all samples, grouped into three suites (TGC, Tehachapi; BVS, Bear Valley Springs, and LDI, late deformational intrusives).

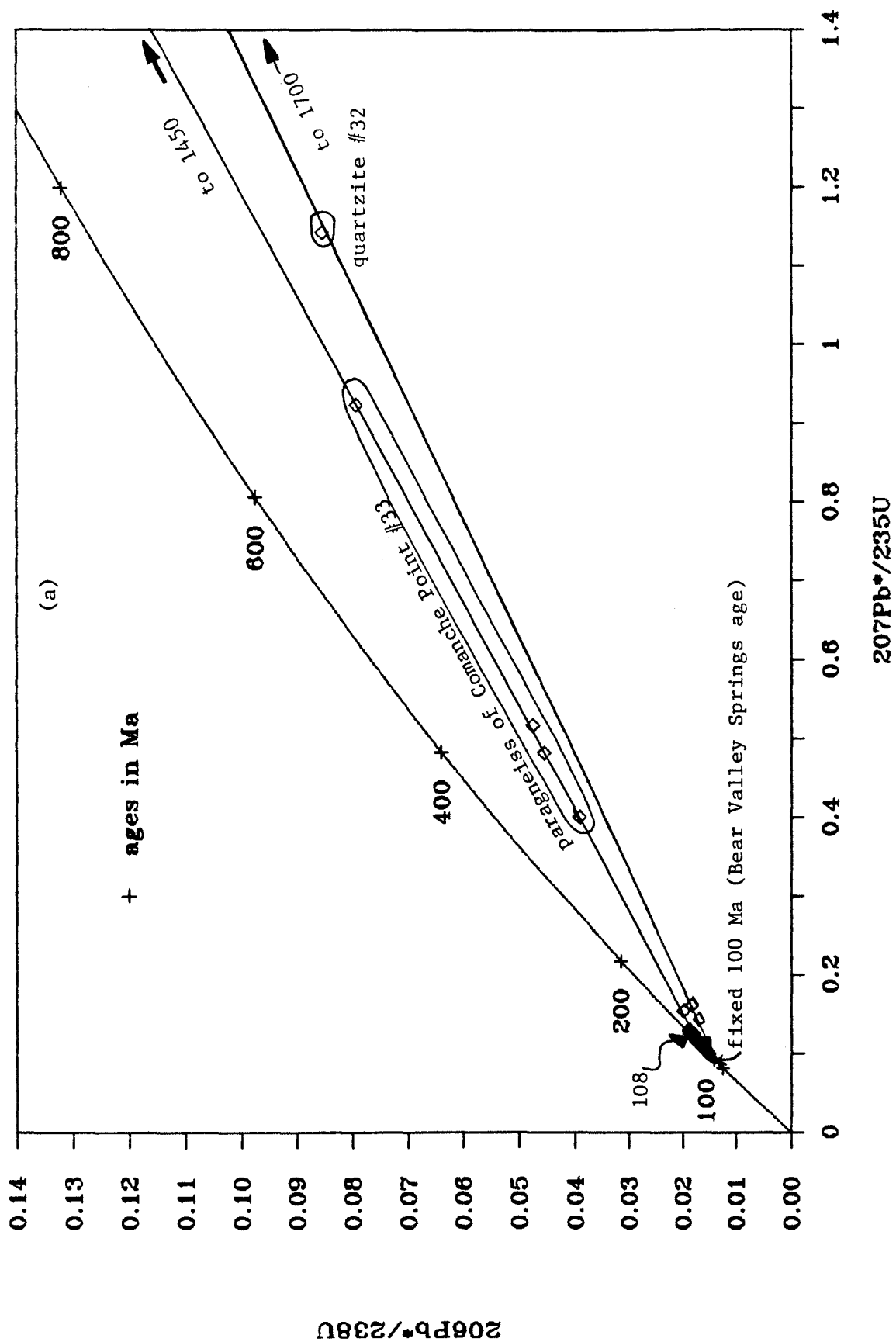
(a)
+ ages in Ma
800
600
400
200
100
to 1450 Ma
to 1700 Ma
quartzite #32
Paragneiss of Comanche Point #23
fixed 100 Ma (Bear Valley Springs age)
108
0.14
0.13
0.12
0.11
0.10
0.09
0.08
0.07
0.06
0.05
0.04
0.03
0.02
0.01
0.00
0
0.2
0.4
0.6
0.8
1
1.2
1.4
206Pb*/238U
207Pb*/235U

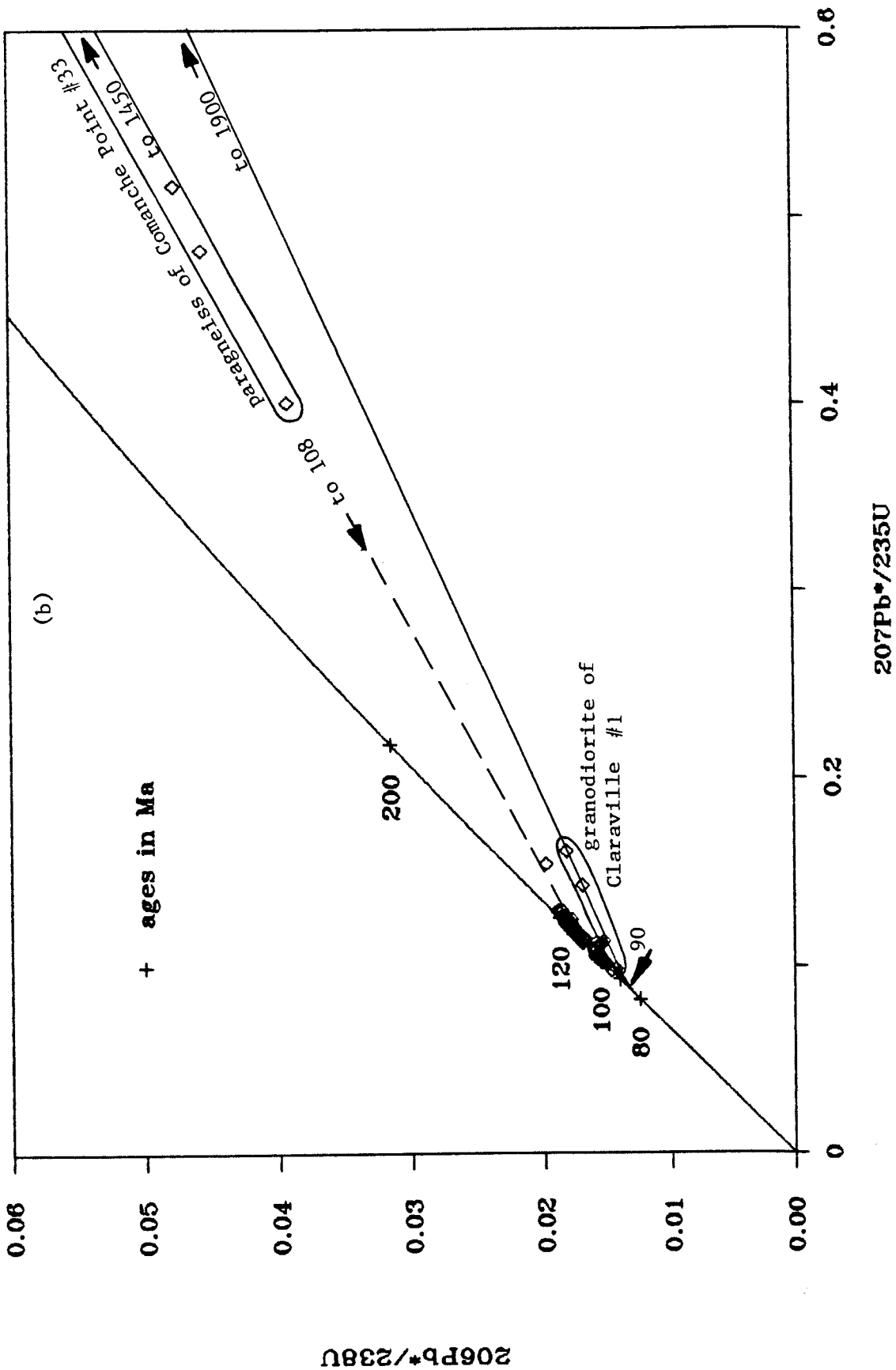
(b)
+ ages in Ma
200
120
100
80
90
granodiorite of
Claraville #1
to 1080
paragneiss of Comanche Point #83
to 1450
to 1900
0.06
0.05
0.04
0.03
0.02
0.01
0.00
0
0.2
0.4
0.6
206Pb*/238U
207Pb*/235U

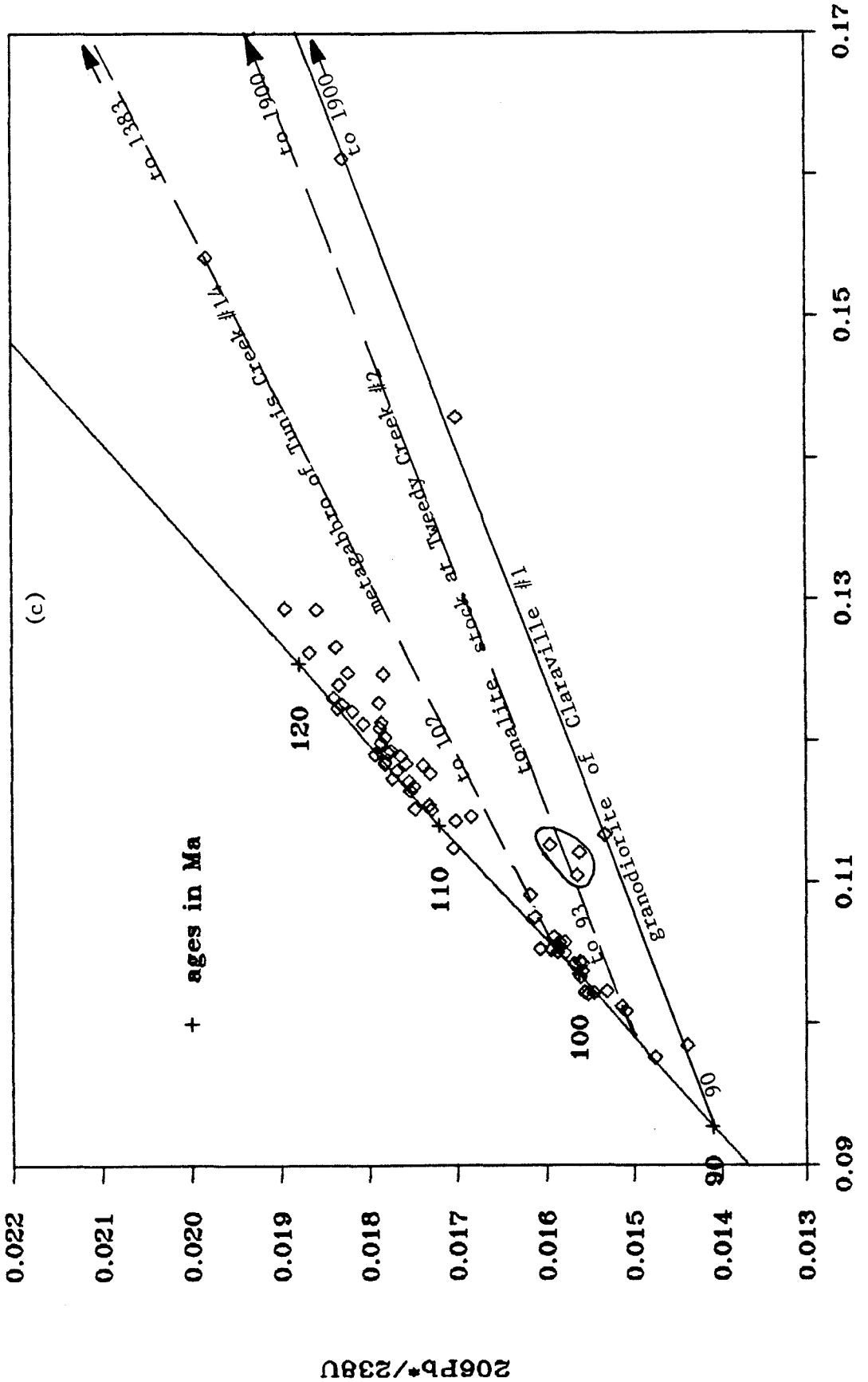
(c)
+ ages in Ma
120
110
100
90
to 1383
to 1900
to 1900
to 102
to 93
to 90
metagabbro of Tunis Creek #1
metagabbro of Tweedy Creek #2
stock at Tweedy Creek #1
tonalite
granodiorite of Claraville #1
0.022
0.021
0.020
0.019
0.018
0.017
0.016
0.015
0.014
0.013
0.09
0.11
0.13
0.15
0.17
206Pb*/238U
207Pb*/235U

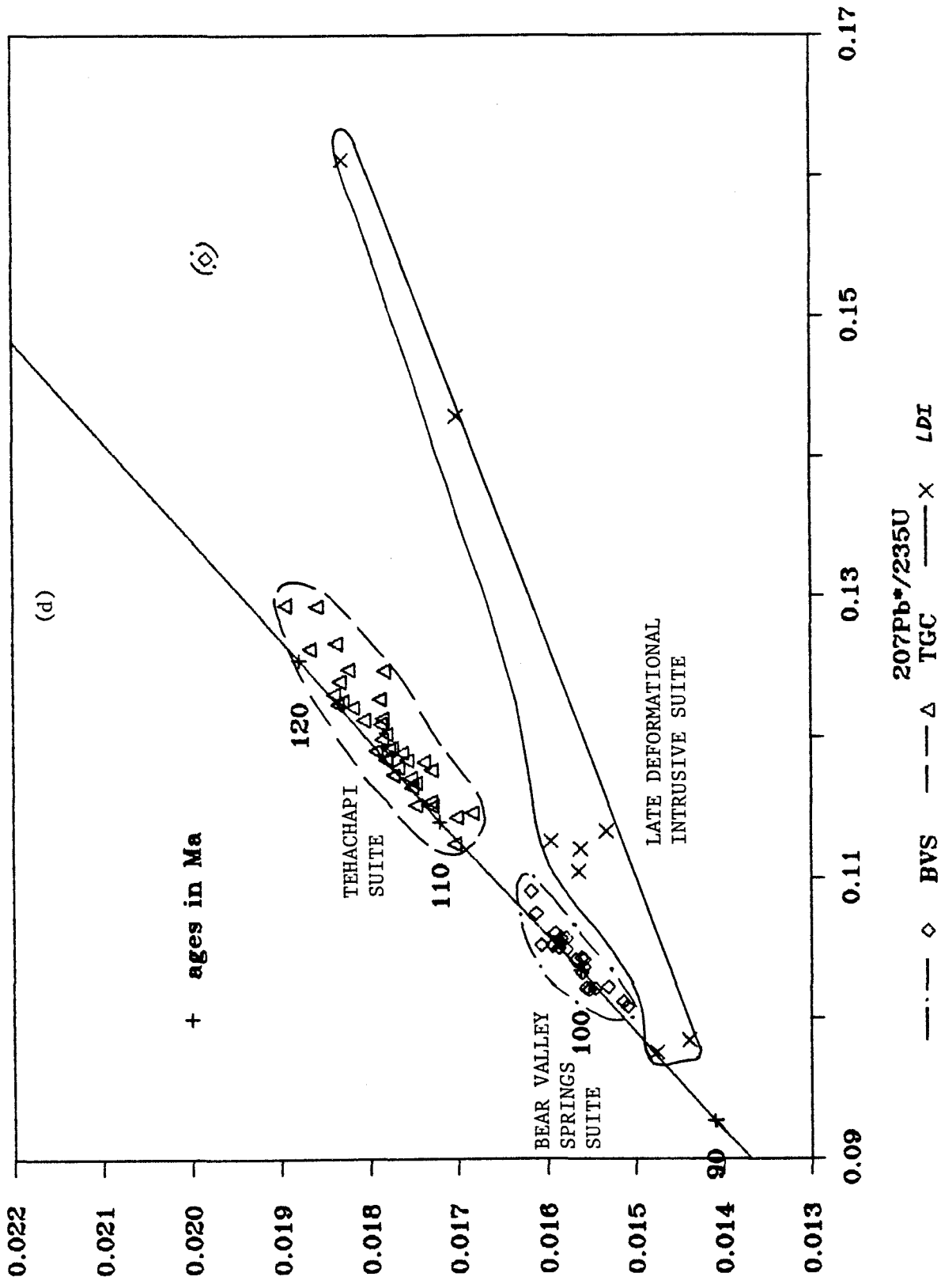
(d)
(o)
+ ages in Ma
120
110
100
90
TEHACHAPI SUITE
BEAR VALLEY SPRINGS SUITE
LATE DEFORMATIONAL INTRUSIVE SUITE
BVS
TGC
LDI
207Pb*/235U
206Pb*/238U
0.022
0.021
0.020
0.019
0.018
0.017
0.016
0.015
0.014
0.013
0.09
0.11
0.13
0.15
0.17

Figure 44. Summary plot of the error polygons and associated segment of concordia for samples from the Bear Valley Springs intrusive suite and the Tehachapi suite. For the tonalite of Bear Valley Springs: MA=Mount Adelaide phase; E=eastern marginal phase; M=main phase; and MM=mafic inclusion within main phase. Note that there are two different segments of concordia, 95 to 105 Ma for the Bear Valley Springs suite, and 105 to 125 Ma for the Tehachapi suite. Also note that concordia is essentially linear.

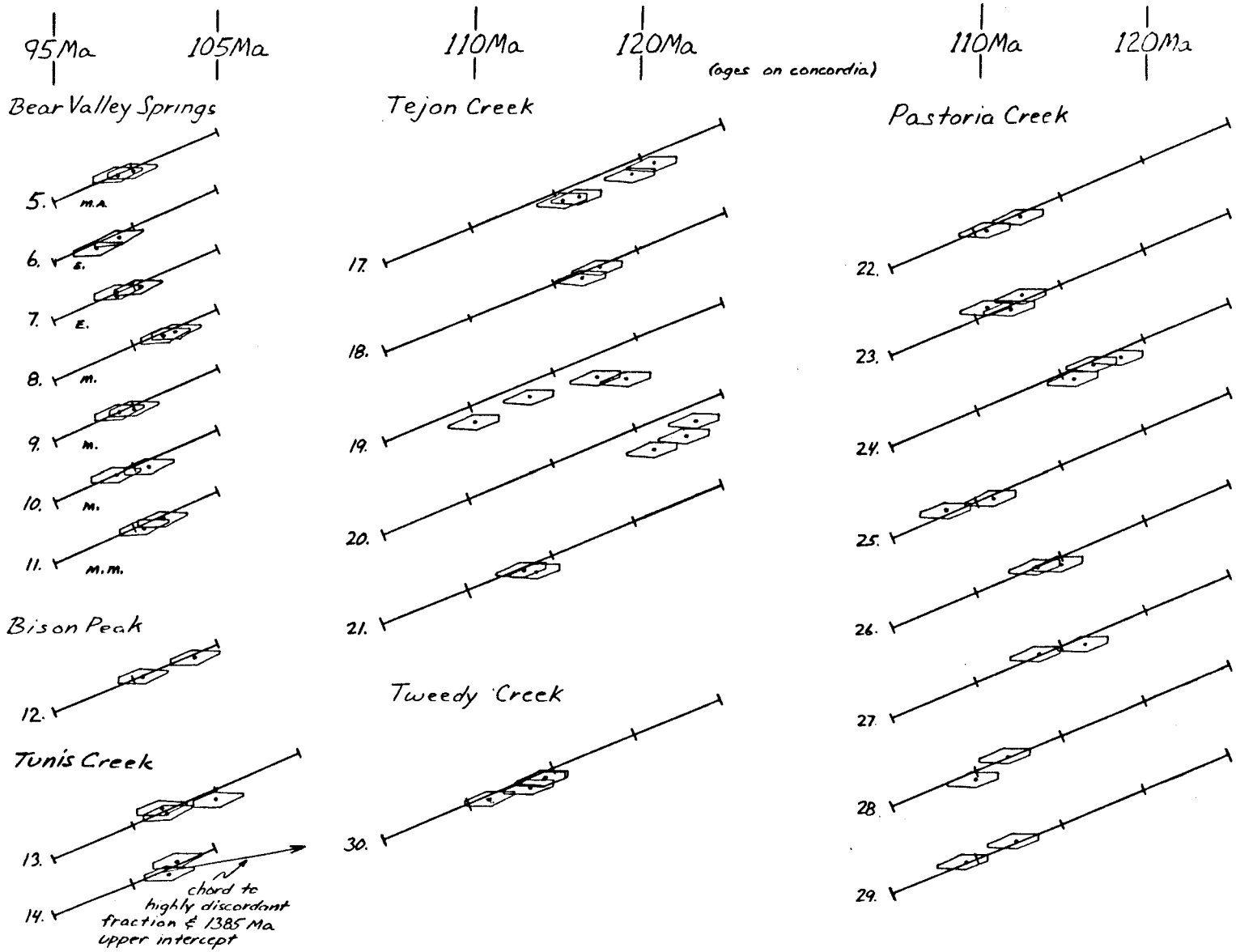
95Ma
105Ma
110Ma
120Ma
(ages on concordia)
110Ma
120Ma
Bear Valley Springs
5.
M.A.
6.
E.
7.
E.
8.
M.
9.
M.
10.
M.
11.
M.M.
Bison Peak
12.
Tunis Creek
13.
14.
chord to highly discordant fraction & 1385 Ma upper intercept
Tejon Creek
17.
18.
19.
20.
21.
Tweedy Creek
30.
Pastoria Creek
22.
23.
24.
25.
26.
27.
28.
29.

rocks will then be discussed. Having formed a basis for igneous ages and possible inheritance populations, the more complex systematics of the late deformational intrusives and gneiss complex of the Tehachapi Mountains will be discussed. Note that concordia in Figure 44 is essentially a straight line.

Bear Valley Springs intrusive suite

Within the Bear Valley Springs suite, the tonalite of Bear Valley Springs has been dated at seven locations (#5-11). Samples cluster within analytical uncertainty about internally and externally concordant ages of 100±2 Ma (Figure 44), which is interpreted as the igneous age of the tonalite. Samples #5-7 may be slightly younger by about 1 my, which is consistent with field observations of the Mount Adelaide and eastern marginal phases of the tonalite. Samples #8-10 are from the main phase of the batholith. A sample from a dioritic inclusion within the tonalite (#11) gave an age identical to that of the tonalite. Its zircon isotopic systematics, as well as strontium and oxygen isotopic concentrations (Table 14) fall within the range of values for the tonalite, which suggests a similar geochemical history, consistent with a synplutonic origin for the mafic inclusions.

The hypersthene tonalite of Bison Peak was dated in one location (#12), and has internally concordant but externally discordant fractions. Its zircon systematics are suggestive of a slight degree of inheritance of zircon in a magma that crystallized at 100-102 Ma (Figure 44). The Bison Peak zircons contain a lower concentration of uranium (300 ppm ^{238}U), and hence radiogenic lead, compared to the tonalite of Bear Valley Springs (480-860 ppm ^{238}U). The low uranium concentrations support an inheritance over a disturbance mechanism to explain the slight discordance in the data. Such low uranium zircon would be less susceptible to lead loss, and also highly sensitive to inheritance of small amounts of older, radiogenic lead-containing zircon (as seen in the Tunis Creek unit). An interpreted age of

101±2 Ma is given to the unit, based in part on field and petrographic relations to the tonalite of Bear Valley Springs.

The metagabbro of Tunis Creek was sampled in four locations, but only two yielded zircon (#13,14), due to the bulk chemistry of the rock. The two samples have both concordant and slight discordant systematics (Figure 44). These samples, especially #14, show a reverse of the expected sequence of ages in a set of fractions. The two coarser fractions are both internally and externally concordant, while the finest-sized fractions are slightly (#13) to strongly (#14) discordant. The zircon systematics are similar to those of the Bison Peak unit (above). The metagabbro has been assigned an interpreted igneous crystallization age of 101±2 Ma, based on the zircon age pattern, in addition to field and petrographic considerations. The Tunis Creek unit has the least uranium-rich population of zircons of any unit in the southernmost Sierra Nevada (64-80 ppm ^{238}U), and is therefore highly susceptible to being effected by inheritance of zircon (as is the case of the Bison Peak unit). In other words, incorporation of a small amount of pre-existing zircon into the metagabbro of Tunis Creek could result in discordant behavior of the metagabbro zircon. This is believed to be the cause of the observed discordances.

Using a lower intercept of 101 Ma (concordant and interpreted unit age), a line passing through the highly discordant fraction from sample #14 intersects concordia at 1383 Ma (Figure 43c), which is similar to the upper intercept of the paragneiss of Comanche Point. It is suggested that inheritance of material from the paragneiss of Comanche Point, where the zircon population is dominantly fine-grained, is responsible for the discordant behavior of this fraction. The intimate, gradational contacts between the Tunis Creek and paragneiss in the northern foothills of Winters Ridge support this conclusion.

Metamorphic framework rocks

Metasedimentary rock samples include the paragneiss of Comanche Point and a quartzite in one of the Kings sequence metamorphic septa. The quartzite (#32) yielded a highly discordant age, indicative of the presence of Proterozoic zircon. Multiple fraction analyses were not possible due to the near-uniformity in the physical characteristics of the zircon population, and the dominance of fine-grained zircon. The quartzite lies within the septum encased by the tonalite of Bear Valley Springs (Plate 1). A discordia chord with a fixed lower intercept of 100 Ma (Bear Valley Springs igneous age) projects to an upper intercept of 1705 Ma (Figure 43a).

The paragneiss of Comanche Point, dated in the Comanche Point area (#33), yielded four strongly discordant fractions (Figure 43a,b). A concordia plot of the data (Figure 45) yields a chord with a lower intercept of about 108 Ma, and an upper intercept of about 1450 Ma. A line regressed through the data has an r-factor of 0.997, where r=1.0 indicates a perfect fit to a straight line. The data points are widely spaced near the center half of the chord. The coarser fractions have older ages and plot nearer to the upper intercept. This pattern is believed to represent lower lead loss in the coarser fractions due to a smaller surface area to volume ratio, and a less metamict structure due to a lower uranium concentration. The paragneiss chord is interpreted to represent the lead loss trajectory of detrital zircon with a 1450 Ma signature being disturbed at ~108 Ma. The disturbance is undoubtably related to the igneous and metamorphic environment of the gneiss complex, with migmatitic stringers produced from the paragneiss clearly becoming incorporated into the tonalite gneiss of Tejon Creek.

The detrital zircon within both the paragneiss and Kings sequence metasedimentary enclaves is dominantly fine- to very fine-grained (<80 microns), well

Figure 45. Concordia diagram of the paragneiss of Comanche Point (sample #33). All fractions (4) from the paragneiss are shown. The intersections of the discordia chord with concordia are at 108±29 and 1450±110 Ma. The location of the data points midway between upper and lower intercepts leads to the interpretation of the array as representing the disturbance of a 1450 Ma component in a thermal event at 108 Ma. The 1450 Ma age is the overall isotopic age of the zircon population, and not its actual age.

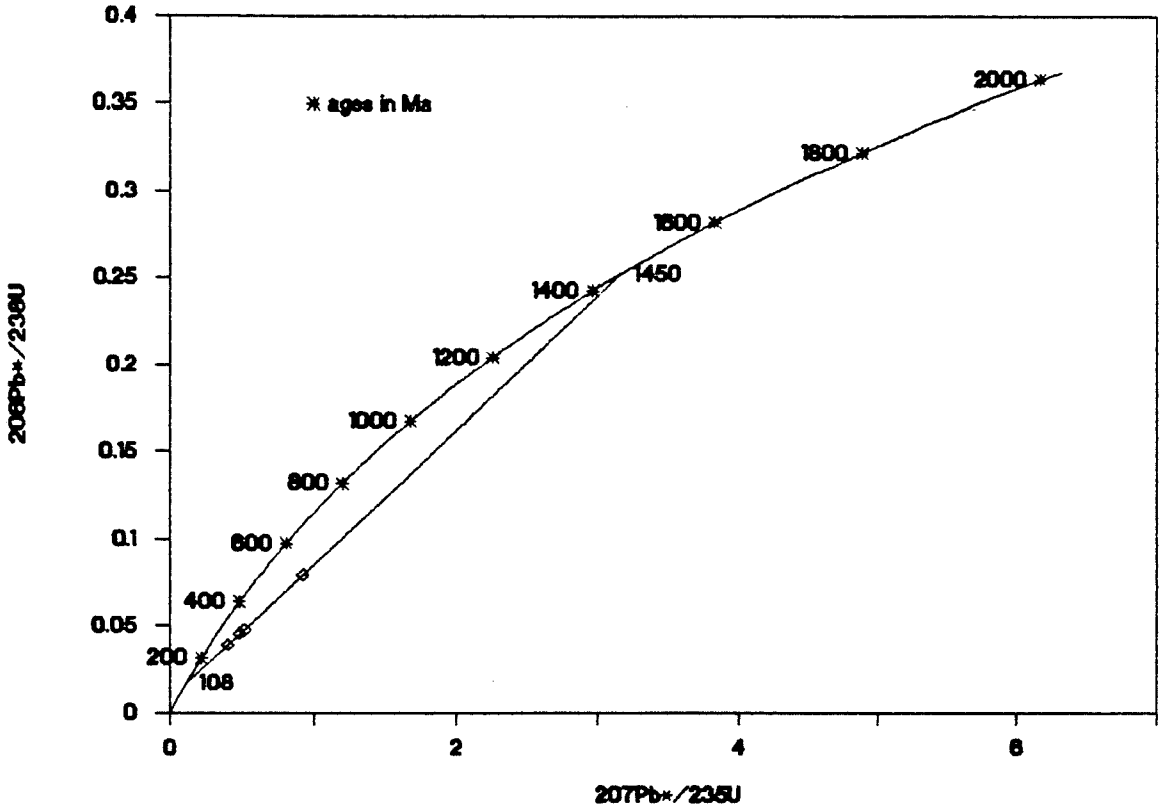
* ages in Ma
2000
1800
1600
1450
1400
1200
1000
800
600
400
200
108
206Pb*/238U
207Pb*/235U
0.4
0.35
0.3
0.25
0.2
0.15
0.1
0.05
0
0
2
4
6

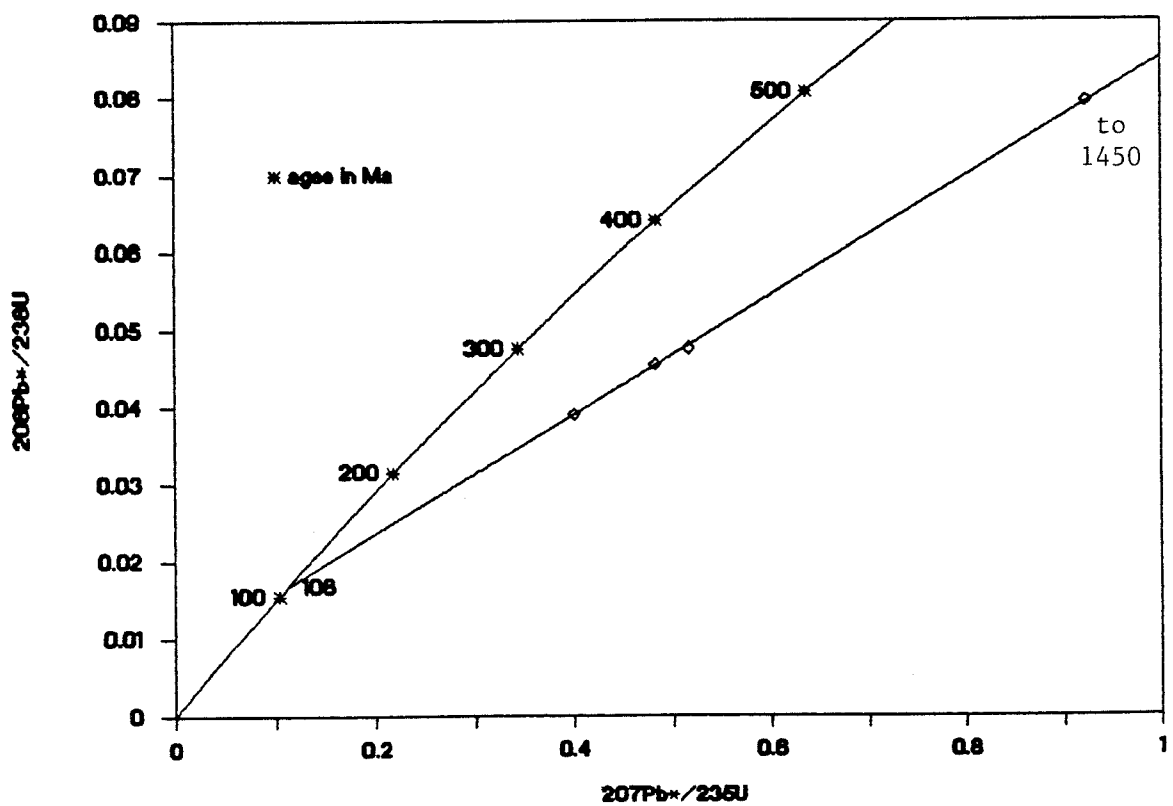
* ages in Ma
500
400
300
200
100
108
to
1450
206Pb*/238U
207Pb*/235U
0.09
0.08
0.07
0.06
0.05
0.04
0.03
0.02
0.01
0
0
0.2
0.4
0.6
0.8
1

rounded, and clearly of a detrital origin. Metamorphic overgrowths were not observed. Such zircon is thought to be the probable and primary sources of discordance in several samples, particularly with regards to the fine-grained zircon fractions. An attempt will be made to discriminate between the paragneiss and quartzite contaminate sources in later discussions. This may be partially justified on the basis of a difference in geographic distribution and upper intercept ages of the two populations.

Late deformational intrusives

Four analyses from the granodiorite of Claraville (#1) show a considerable degree of discordance (Figure 43b,c). A concordia plot of the data (Figure 46) yields a chord that has an upper intercept of 1900 Ma, and a lower intercept of 90±2 Ma. The chord has a regression coefficient (r-factor) of 0.998. The data points all lie near the lower intercept, and show an orderly progression of increasing age with increasing size fraction away from the lower intercept. This pattern is interpreted to have resulted from those grains with an older core statistically experiencing a longer crystallization history, and not having to nucleate seed crystals. The array is interpreted as representing entrainment of zircon with a 1900 Ma isotopic signature in a magma that crystallized at about 90 Ma.

The tonalitic stock (#2) intrusive into the augen gneiss of Tweedy Creek and metamorphic framework rocks yielded three discordant analyses, but due to the lack of dispersion of the data points, it was not possible to construct intercept ages. Field relations that place the stock within the late deformational intrusive suite, and old $^{207}Pb^*/^{206}Pb^*$ ages and the likelihood of incorporation of zircon from the adjacent metamorphic septum rocks into the tonalite suggest an entrainment mechanism to produce the observed discordances similar to that operating in the granodiorite of Claraville. Thus, using the upper intercept of

Figure 46. Concordia diagram of the granodiorite of Claraville (Sample #1). All fractions (four) from the granodiorite are shown. The intercepts of the discordia chord with concordia are at 90±2 and 1900±210 Ma. The data points trend away from the lower intercept, leading to the interpretation of the array as incorporation of 1900 Ma zircon into a magma that crystallized at 90 Ma. The 1900 Ma age is the overall isotopic age of the contaminate zircon, and not its actual age.

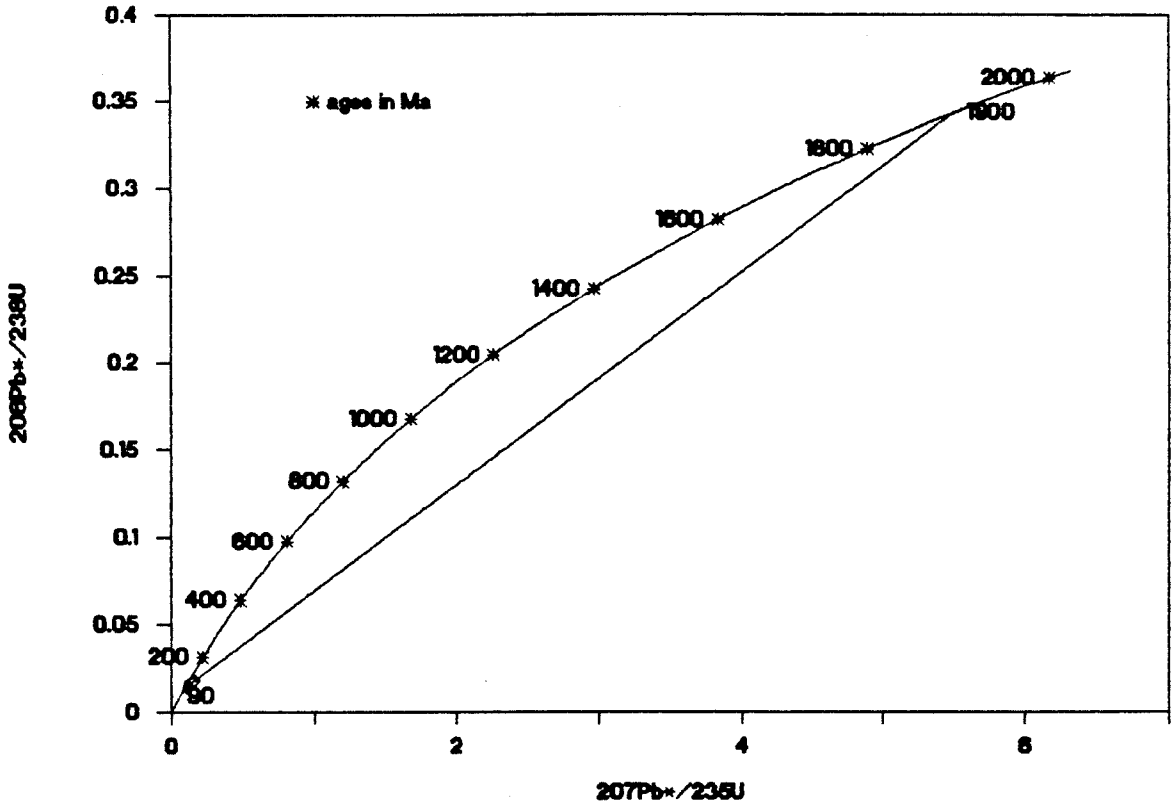
* ages in Ma
2000
1900
1800
1600
1400
1200
1000
800
600
400
200
90
206Pb*/238U
207Pb*/235U
0.4
0.35
0.3
0.25
0.2
0.15
0.1
0.05
0
0
2
4
6

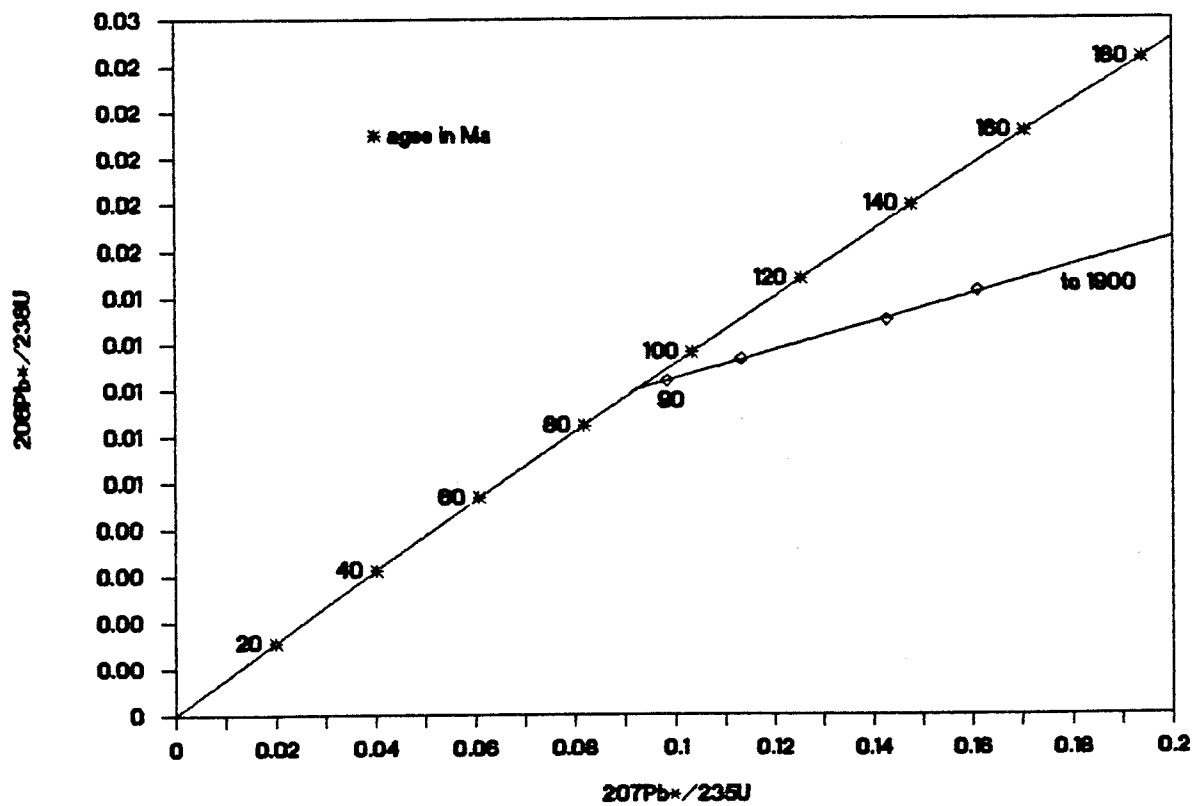
* ages in Ma
180
160
140
120
100
90
80
60
40
20
to 1900
206Pb*/238U
207Pb*/235U
0.03
0.02
0.02
0.02
0.02
0.02
0.02
0.01
0.01
0.01
0.01
0.01
0.00
0.00
0.00
0.00
0
0
0.02
0.04
0.06
0.08
0.1
0.12
0.14
0.16
0.18
0.2

1900 Ma from the Claraville sample, the tonalite stock would have a lower intercept of 93±3 Ma (Figure 43c), which is interpreted as the approximate igneous age of the sample.

Two additional samples from the late deformational suite were analyzed. One sample was from the pegmatite dike swarm (#3) in the Comanche Point area that cross-cuts foliation in the tonalite gneiss of Tejon Creek. This sample yielded an internally concordant age of 94±2 Ma that is believed to be an igneous age, based on field observations.

A second sample was a foliated, two-mica garnet granite dike (#4) that cross-cuts the main deformational fabric of the quartzo-feldspathic gneiss of Pastoria Creek. This dike shares a late stage deformational fabric with the gneiss. The garnet granite dike analyses are slightly discordant. On the basis of its heavy $\delta^{18}O$ and high initial $^{87}Sr/^{86}Sr$ ratios (Table 14), as well as its peraluminuous character, the dike is believed to contain a significant metasedimentary component. Therefore, the slight discordances may be related to a minor degree of inheritance. Using an upper intercept of either the paragneiss or quartzite, an igneous age assignment of 97±2 Ma is possible. This places a possible minimum constraint on the time of formation of the major deformational fabric within the gneiss complex. It also indicates continuing deformation coeval with the intrusion of the Bear Valley Springs suite. However, the strontium isotopic systematics of the granite dike suggest a petrogenetic affinity to the Pastoria Creek gneiss, with a considerably older inferred age (Chapter IV). Therefore, an age of 97 (+20/-2) is given for the dike, recognizing the possibility of open system lead loss behavior in the hot sub-solidus environment of the dike.

Gneiss complex of the Tehachapi Mountains

Within this section are discussed the thirteen samples from the gneiss complex of the Tehachapi Mountains (tonalite gneiss of Tejon Creek and quartzo-feldspathic gneiss of Pastoria Creek) and the two samples from the augen gneiss of Tweedy Creek. The Tweedy Creek samples are placed in this discussion because their zircon systematics are similar to those of the gneiss complex, and because of structural relations with younger intrusives.

The zircon systematics of this suite have U/Pb ages that cluster in the 110-120 Ma range, with considerable evidence of slight internal and/or external discordance. There is a clear distinction in the U/Pb zircon systematics between the samples in the Tehachapi suite, and those from the Bear Valley Springs suite. The slight discordances in the gneiss complex samples are exhibited by the dispersion of the error polygons along and slightly below concordia. The Pastoria Creek samples show more concordant behavior than the samples from the Tejon Creek unit, and will be discussed first.

The quartzo-feldspathic gneiss of Pastoria Creek, having such a wide range of lithotypes, was dated the most extensively of any unit in the gneiss complex (#22-29). All of the samples were concordant or very slightly discordant. Samples #22, 23, 25, 26, and 27 are all internally and externally concordant. They have an uncertainty of ±2 my derived from the overlap of their error polygons. The interpreted ages range from 111-115 Ma. Samples #24, 28, and 29 are all slightly externally discordant. Their assigned ages and associated errors (117±3, 113±4, 113±5) are dependent on the degree of overlap of their error polygons with one another, and with concordia. Note that the ages are all slighly above those of the concordant samples within the unit.

Samples #28 and 29 show a progression of younger U/Pb age with smaller grain size, with the $^{207}Pb^*/^{206}Pb^*$ ages of sample #28 inversely corellated to the U/Pb age. Sample #24 does not have a consistent pattern of age with respect to grain size. This pattern in the discordant samples and the relations of the error polygons with concordia are suggestive of igneous crystallization contemporaneous with that of the concordant samples, followed by migration down concordia due to limited open system lead loss behavior. The limited overlap pattern and near external discordant pattern of the error polygons for concordant samples #25 and 27 suggests the possibility of a similar, minor migration for these samples.

The ages in the quartzo-feldspathic gneiss of Pastoria Creek are interpreted as igneous ages followed by an extended residency at deep crustal levels in a high temperature environment, perhaps until the 100 Ma Bear Valley Springs thermal culmination (as discussed in the next chapter). The zircon populations under such conditions could have behaved to differing degrees as limited open systems. Therefore, the ages could represent either the igneous age (actual time of intrusion into the lower crust) or mildly disturbed igneous ages (end of the high temperature environment, and closure of the U/Pb system). The zircons show a range of uranium concentrations of 170-1900 ppm ^{238}U. There are no apparent differences between tonalitic and granitic members within the Pastoria Creek unit.

The augen gneiss of Tweedy Creek (#30) shows discordance at the level just beyond experimental error, while zircons from a mafic inclusion within the orthogneiss (#31) were strongly dominated by common lead. The discordance pattern of the orthogneiss is similar to that of the Pastoria Creek gneisses, therefore the interpreted age of the orthogneiss is given as 114±3 Ma. In the case of sample #30, sequential thermal events of 100 Ma (Bear Valley Springs), 93 Ma (tonalite stock) and 90 Ma (Claraville) may have affected the zircon systems in a manner

similar to that experienced in the extended high-temperature environment of the Pastoria Creek samples.

The tonalite gneiss of Tejon Creek was dated in five locations (#17-21). Samples #18 and 21 are internally and externally concordant, and have ages of 117 and 113 ±2 Ma. Samples #17, 19, and 20 show a moderate degree of discordance, but it was not possible to model them by standard concordia intercept theory due to a lack of dispersion between fractions. There is also an inconsistent pattern between age, fraction size, and uranium concentration within these samples. For samples #19 and 20, the coarse- and fine-grain sized fractions have the greater $^{206}Pb^*/^{238}U$ and $^{207}Pb^*/^{235}U$ ages, while the intermediate sized fractions have younger U/Pb ages. The $^{207}Pb^*/^{206}Pb^*$ ages ranged from 164-229 Ma (#19), and from 187-205 Ma (#20), and are not necessarily correlative to the U/Pb age. Replicate analyses of the coarsest-sized fraction from sample #17 were performed, and gave U/Pb ages that differed by 5-6 my. Again, the mid-sized fractions from #17 gave the younger U/Pb ages. Samples #19, 20, and 21 all have low ^{238}U concentrations. It would therefore take only a relatively small amount of inherited zircon to cause the discordance in these samples.

The discordances in samples #17, 19, and 20 in the tonalite gneiss of Tejon Creek may represent: 1) reworking or disturbance of lower Mesozoic to upper Paleozoic material; 2) incorporation of zircon from the paragneiss (they have intimate field relations that clearly show assimilation of paragneiss leucosomes by the tonalite gneiss), or similar sources; and/or 3) upper Cretaceous igneous crystallization and residency of the zircons under high temperature conditions over an extended period of time, with corresponding open system lead loss behavior.

The plot of the error polygons for these samples (Figure 44) is distinctly different than those from other gneiss complex samples. The error polygons all

plot below concordia and show minor dispersion along concordia. It is logical to assume that at least part of pattern can be related to dispersion resulting from limited open system behavior as discussed above for the Pastoria Creek gneisses. However, to produce the observed discordant patterns solely by this mechanism would require movement along and below concordia for a significant distance. This then would require downward migration from an early Mesozoic protolith or inheritance age. The Sierra Nevada batholith north of the study area contains Jurassic plutonics (Chen and Moore, 1982; Stern and others, 1981; Saleeby and Sharp, 1980; Evernden and Kistler, 1970). This could provide a source of Jurassic zircon for inheritance and/or disturbance by Cretaceous magmas. However, this is not the preferred model to explain the discordant zircon systematics. The coincidence of the data points in the narrow span of 115±5 Ma would be highly fortuitous; pre-Cretaceous rocks have not been found to intrude the Kings sequence framework rocks (Chen and Moore, 1982; Saleeby and others, 1978; Evernden and Kistler, 1970), and appear to be absent in the study area; and there is a lack of stronger, supporting evidence for such material in the zircon signatures from other samples.

The relations of the error polygons with concordia permit inheritance of Paleozoic zircon. To investigate this, a chord with a fixed 100 Ma (Bear Valley Springs) lower intercept was fit through the discordant analyses for samples #17, 19 and 20 (Figure 47). The 100 Ma lower intercept is assigned considering the gradational contact between the Tejon Creek unit and the tonalite of Bear Valley Springs, and the thermal maximum as represented by members of the voluminuous Bear Valley Springs intrusive suite. Upper intercept ages of 392, 730 and 526 Ma are then obtained. Thus, this model allows the Tejon Creek unit to have Bear Valley Springs igneous ages with discordances related to inheritance of heterogen-

Figure 47. Plots of error polygons and concordia diagrams for selected samples (#17, 19, 20) from the tonalite gneiss of Tejon Creek, showing alternative discordance mechanisms. The first mechanism involves incorporation of zircon with the indicated upper intercept ages (390, 730, 526 Ma) into magmas crystallizing at 100 Ma. The second model involves incorporation of upper- to mid-Proterozoic zircon (1400 to 1900 Ma) into magmas at about 117 Ma, followed by open system lead loss behavior.

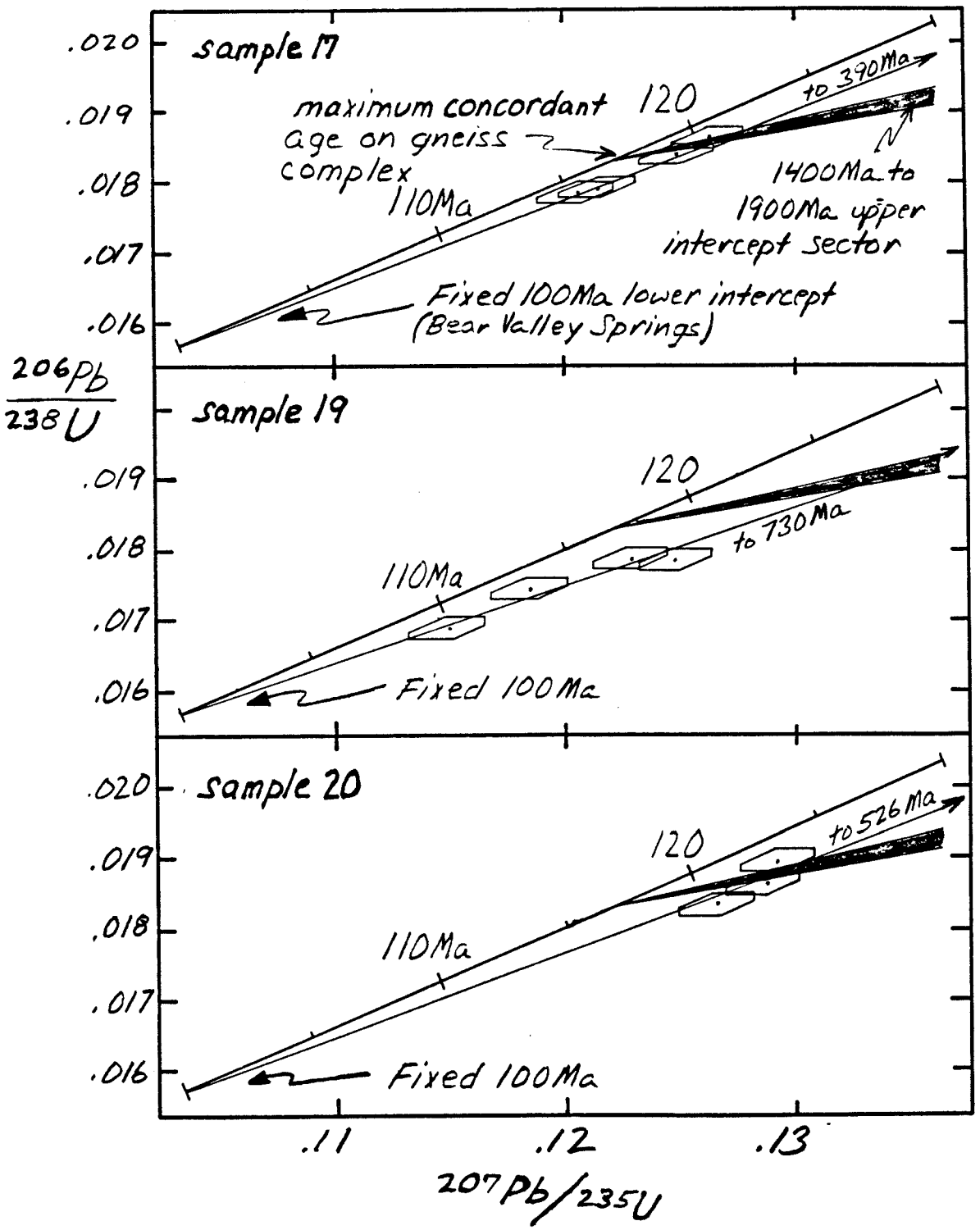
sample 17
maximum concordant age on gneiss complex
120
110Ma
to 390Ma
1400Ma to 1900Ma upper intercept sector
Fixed 100Ma lower intercept (Bear Valley Springs)
sample 19
120
110Ma
to 730Ma
Fixed 100Ma
sample 20
120
110Ma
to 526Ma
Fixed 100Ma
.020
.019
.018
.017
.016
.11
.12
.13
206Pb/238U
207Pb/235U

eous mixtures of contaminate zircon. There is no direct field evidence for such Paleozoic material within the field area, although Paleozoic ophiolitic material can be found to the north (Saleeby, 1982), and subsurface data suggests that similar material (plagioclase ± hornblende ± clinopyroxene diorite-gabbro) may underlie much of the southern end of the San Joaquin Valley (Ross, 1979), and may be related to oceanic and island arc assemblages of the western Sierra.

Alternatively, the discordances can be interpreted as the result of the entrainment of zircon from upper- to mid-Proterozoic metasedimentary framework material by a tonalitic melt. This is portrayed by the shaded sectors shown in Figure 47. The sectors have as their lower intercepts an age of 117 Ma, which is based on the maximum concordant age (sample #18) obtained from the gneiss complex. Extending from the 117 Ma lower intercept is a pair of lines that project to upper intercept ages of 1400 Ma and 1900 Ma. These are taken as likely end-members of Proterozoic inherited zircon populations based on data from samples #1, 2, 14, 32 and 33. The Proterozoic discordia sectors intercept the upper range of discordant data points. The dispersion of points to younger ages can be attributed to limited lead loss behavior in the samples. Thus, the data arrays of samples #17, 19, and 20 could be interpreted as incorporation of minor components of Proterozoic zircon during an ~117 Ma igneous event, followed by an extended history at hot subsolidus conditions. This could result in differential downward migration of the already slightly discordant data points, based on differing chemistry between the zircon populations. This Proterozoic material could be derived from the Kings sequence and Comanche Point metasedimentary framework rocks, as more clearly displayed in samples #1, 14, 32, and 33.

Thus, there are several possible methods to explain the observed discordances within the Tejon Creek unit. Incorporation of Proterozoic material is

highly likely, given the observed field relations. The interaction with pre-Cretaceous Mesozoic material is not favored due its apparent absence in the study and southern Sierran areas. Interaction with Paleozoic material is possible, given the fact that it is probably present in the basement adjacent to the study area. As discussed above relative to the Kings sequence rocks, and with regards the field relations and data on framework detrital zircon, such mixing is constrained to a structural level beneath the present level of exposure. A possible way of viewing such mixing is the deep-level inheritance of early Mesozoic to Paleozoic zircon and higher-level entrainment of Proterozoic zircon from Kings sequence and Comanche Point metasedimentary rocks. Likely limited open system lead loss behavior further complicates the zircon systematics.

In summary, the primary mechanism operating on the zircon populations in the samples from the gneiss complex of the Tehachapi Mountains is igneous crystallization from about 110-120 Ma. Secondary effects consist of the incorporation of Proterozoic zircon from metasedimentary material into the Cretaceous magmas, and lead loss until the 100 Ma Bear Valley Springs magmatic-thermal culmination. Tertiary, subtle effects could be attributed to incorporation of Phanerozoic zircon.

IV. U/PB ZIRCON GEOCHRONOLOGY AND THE PETROTECTONIC SIGNIFICANCE OF THE GNEISS COMPLEX OF THE TEHACHAPI MOUNTAINS

IV.1 Geochronology

Prephanerozoic sialic material is not known in the southernmost Sierra Nevada. Metasedimentary rocks (quartzite and paragneiss) and plutonic rocks contaminated by wallrock interaction show evidence of material with a zircon signature in the neighborhood of 1400 to 1900 Ma. This result is similar to discordant values seen in Tobisch and others (1985) and Chen and Tilton (1982) for the south-central Sierras, and is in keeping with the derivation of zircon from Precambrian source terranes in the craton (Silver and others, 1977). Many of the samples have zircon populations that are discordant just beyond the range of experimental error. These samples may well be showing evidence of 1) the high temperature conditions of the region which manifest themselves in a long period of open system behavior or zircon crystallization, and/or 2) inheritance or entrainment of early Mesozoic or older material. Of particular note is the general lack of consistent behavior between zircon grain size, uranium concentration, and discordancy in the gneiss complex of the Tehachapi Mountains. A typical observation of "normal" igneous zircon populations is an inverse correlation of uranium concentration with grain size. For samples displaying inheritance, a greater degree of discordance is correlated with increasing grain size and decreasing uranium concentration; while in disturbed samples there is a correlation between degree of disturbance and increasing uranium concentration and decreasing grain size (Saleeby and Sharp, 1980; Silver, 1962, 1964; this study, samples #1,33).

A prime example of such non-systematic behavior in the gneiss complex zircons can be seen in sample #17 (tonalite gneiss of Tejon Creek), where uranium concentration and discordancy are independent of grain size. To investigate this

phenomena, sample #17 was analyzed for intra-grain distribution and inter-grain inhomogeneity in uranium concentration. An internally and externally concordant sample from the tonalite of Bear Valley Springs (#8) was also analyzed for reference. The samples were irradiated by a neutron flux (1.3×10^{12} neutrons/cm^{2}sec) in a reactor to produce fission tracks in mica plates, and etched 14 minutes in concentrated hydrofluoric acid to expose the tracks (Burnett and Woolum, 1983). Photomicrographs of the mica plates are shown in Figure 48. The tonalite reference (Figure 48c,d) shows a fairly uniform density of fission tracks, with a rare hot spot (high uranium concentration) or core. In contrast, the tonalite gneiss grains (Figure 48a,b) show abundant evidence for inhomogeneity in the uranium concentration. Strongly zoned and cored zircons and hot spots are common, and three to four cycles of zonation can be observed. There are no systematic relationships between grain size and the zonation pattern with track density (and hence uranium concentration).

The zonation in uranium concentration in the tonalite gneiss of Tejon Creek can be explained by variations in the conditions of zircon crystallization, and/or by the population representing a polygenetic suite. In the first case the protolith for the tonalite gneiss could have existed at near-solidus conditions for an extended period of time at deep crustal levels. In such an environment one could expect multiple cycles of zircon nucleation, crystallization, and zonation, with influxes of varying uranium concentrations into the growing zircon crystal lattice. Variations in the uranium concentration could be the result of different liquid-solid partitioning relations due to influxes of differing composition magmas, or to the presence of magmatic and/or metamorphic fluids during the extended high temperature residency. Additional heterogeneities in the uranium concentration could be produced by the incorporation of pre-existing zircon into the tonalitic

Figure 48. Photomicrographs of zircons showing distribution of uranium. Dark specks are individual fission tracks from uranium-series decay events. The density of tracks is proportional to the uranium concentration. The zircons from the tonalite gneiss of Tejon Creek (#17) show a non-uniform distribution, with strong zonation and cores of zircons showing a higher concentration of uranium with respect to the rims. The zircons from the tonalite of Bear Valley Springs (#8) show a near-uniform concentration in uranium. Field of view is approximately 0.2 mm wide.


a
.05 mm

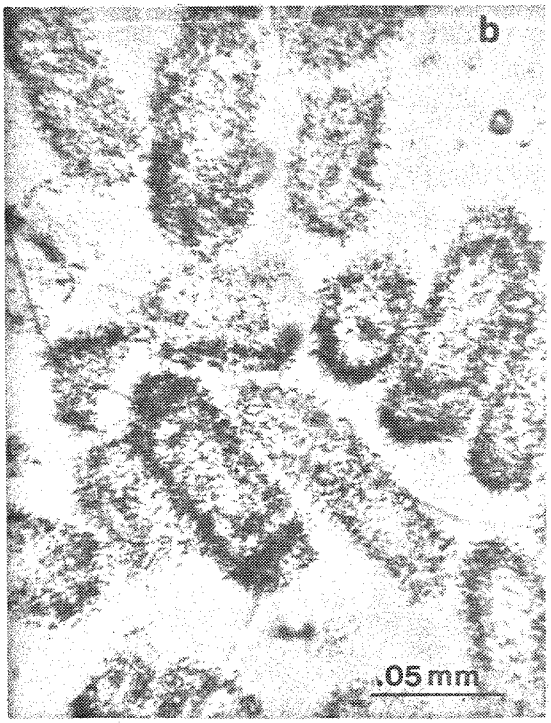
b
.05 mm

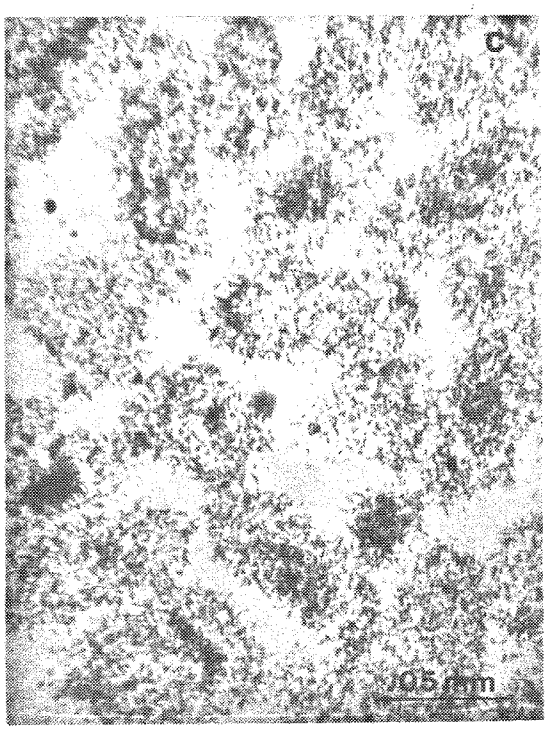
c
.05 mm

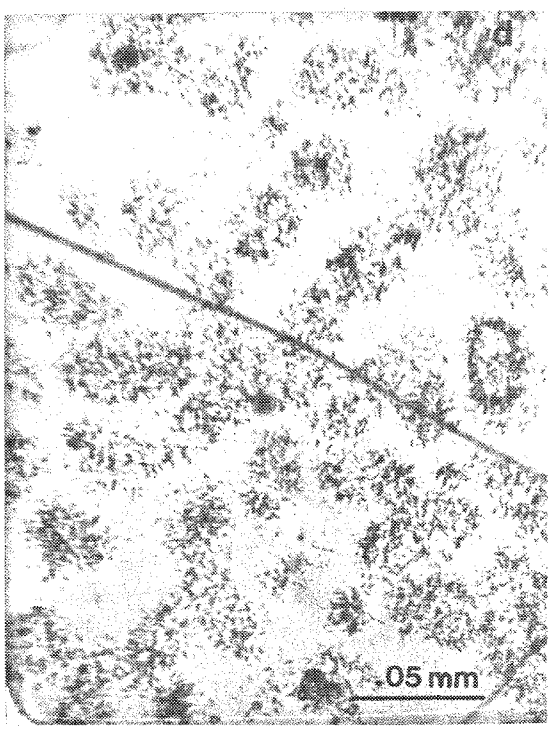
d
.05 mm

magma. The common occurrence of zonation in uranium concentration argues against extensive recrystallization of the zircon grains.

Detrital zircon populations in both the quartzite and paragneiss of Comanche Point are dominated by fine to very fine zircon grains (typically <45 μ). Such grains are possible candidates for the cores exhibited by the tonalite gneiss of Tejon Creek. In addition, the oldest and most discordant zircon fraction is often the finest fraction. It is possible that inheritance or entrainment of similar fine-grained detrital zircons may be responsible for the slight discordances noted in many of the samples in the gneiss complex.

Alternately and/or additionally, the variation in uranium concentration could be the result of the zircon population consisting of multiple members with differing ages and behavior of the constituent zircons. In this situation, there would not necessarily be a regular pattern of behavior of the zircon between different fractions and different samples.

Another possible explanation for the slight age discordances in the gneiss complex is the high temperature solidus to hot subsolidus environment that the complex experienced. The gneiss complex existed at upper amphibolite to granulite grade conditions from about 117 Ma (minimum upper bound) to about 100 Ma (Bear Valley Springs magmatic-thermal culmination). It is possible that the zircons were not completely closed systems at such high-grade conditions, and that various populations of zircons record differing closure times or different amounts of lead loss and/or uranium gain. This would result in the discordances between fractions of a single zircon sample, and between different samples from the same unit.

It is believed that much of the incorporated zircon was entrained from the Kings sequence and paragneiss framework rocks. Typically the finest-sized frac-

tions show the greater degree of discordance, while the zircons in the metasedimentary framework rocks are predominantly fine-grained. Secondly, the upper mantle magma source regimes probably do not contain much zircon for inheritance to be a factor. The entrained zircons could have been completely melted into the magmas, where there would not be any history of overgrowth on a previous zircon grain. The entrained zircons would not share their isotopic characteristics with the crystallizing zircon population, but would only add to the bulk rock composition.

The discordances within many of the units may be the result of incorporation of Paleozoic and/or Mesozoic material. There is no direct evidence for the existence of Paleozoic zircon in the area. There are, however, rocks forming part of the basement in the southern end of the San Joaquin Valley that resemble Paleozoic ophiolitic rocks to the north in the Kaweah River area (Ross, 1979; Saleeby, 1979). The trends of the rocks in the Kaweah River area project into the western part of the study area.

There are no known pre-Cretaceous Mesozoic igneous rocks in the southern Sierra Nevada south of Mineral King, some 100 km north of the study area. There are early Cretaceous to Triassic plutonic rocks to the east of the study area in the El Paso Mountains (Kistler and Peterman, 1978). The only known Mesozoic volcanics south of Lake Isabella are mid-Cretaceous in age (Saleeby, unpublished data; Sams and others, 1983). The only Mesozoic igneous material in the southern Sierra consists of Cretaceous plutons and volcanics. For this reason, interaction with pre-Cretaceous Mesozoic material is not the preferred model to explain the discordance seen in the southernmost Sierra.

Table 15 was constructed to analyze the potential contribution of zircons from metasedimentary framework rocks into various discordant fractions within

Table 15. Percentage of old zircon incorporated into intrusive rocks

Source material	R‡	^{238}U (ppm)	$^{206}Pb_m$ (ppm)	$^{206}Pb_{is}$ (ppm)	$^{206}Pb_l$ (ppm)	$^{206}Pb_u$ (ppm)
Quartzite (qte)						
#32 (100/1700)	0.244	512.2	37.95	6.93	31.02	127.32
Paragneiss (pg)	0.265	364.9	25.09	5.33	19.76	74.51
#33 (108/1450)	0.132	632.6	26.06	9.25	16.81	127.16
	0.121	684.4	27.00	10.01	16.99	140.50
	0.094	876.4	29.70	12.81	16.89	179.18
Tejon Creek gneiss (TJ)						
#17 (100/390)	0.062	1026	16.57	12.48	4.09	65.46
#20 (100/530)	0.045	216.6	3.55	2.64	0.92	20.57

Plutons	^{238}U (ppm)	$^{206}Pb_m$ (ppm)	$^{206}Pb_{is}$ (ppm)	$^{206}Pb_l$ (ppm)	$\%I_{min}$ (%)	$\%I_{max}$ (%)
Claraville	509.3	8.06	6.20	1.86	1.46	6.00qte
#1 (90/1900)	666.3	9.81	8.11	1.70	1.34	5.49qte
	787.6	10.45	9.58	0.87	0.68	2.80qte
	967.2	12.04	11.77	0.27	0.21	0.88qte
Bison Peak	318.3	4.44	4.39	0.05	0.04	0.16qte
#12 (101)					0.03	0.30pg
					0.08	0.30TJ17
					0.24	1.41TJ20
Tunis Creek	74.6	1.28	1.03	0.25	0.20	0.81qte
#14 (101)					0.14	1.49pg
Tejon Creek	1026	16.57	16.26	0.31	0.24	0.99qte
#17 (117)					0.17	1.84pg
#20 (117)	216.6	3.55	3.43	0.12	0.09	0.38qte
					0.07	0.71pg
Pastoria Creek	335.1	5.24	5.17	0.07	0.05	0.21qte
#27 (115)					0.04	0.39pg

R is the fraction of the distance along the discordia chord between the lower intercept and the data point divided by the distance from the lower intercept and the upper intercept: $R=(m-l)/(u-l)$. Pb_m is the measured radiogenic lead concentration (ppm). Pb_{is} is the amount of Pb produced by in situ decay: $Pb_{is}=(\exp(\lambda t)-1)\times U\times .8655$. Pb_l is the amount of Pb at time represented by lower intercept: $Pb_l=Pb_m-Pb_{is}$. Pb_u is the calculated original Pb at time represented by upper intercept: $Pb_u=Pb_l/R$. %I is the amount of zircon (in percent) incorporated by lead gain from the metasedimentary component: $\%I=100\times Pb_l(\text{pluton})/Pb_u(\text{ms})$. Max is the amount of zircon required using the fraction which has lost the greatest amount of Pb, min is the amount using the most Pb-rich fraction at the original Pb composition.

the plutonic rocks. A model involving simple mixing of lead in a one-stage process between the metasedimentary and intrusive components was used. The model allows estimations to be made on the order of magnitude of potential mixing, but it does not necessarily represent the actual mixing involved. In particular, the use of the U/Pb concentrations from the actual metasedimentary samples probably will not reflect the actual U/Pb systematics of the assimilated material. Thus, the model should only be used as a hypothetical situation.

The potential metasedimentary components used in the model are the quartzite (lower intercept of 100 Ma from the tonalite of Bear Valley Springs, upper intercept of 1700 Ma from projection through the data point from 100 Ma) and the paragneiss of Comanche Point (concordia intercepts of 108 and 1450). In addition, the Tejon Creek unit was used as a source component for the slightly externally discordant Bison Peak sample. The discordant intrusive samples investigated in Table 15 were samples #1 (granodiorite of Claraville), #12 (hypersthene tonalite of Bison Peak), #14 (metagabbro of Tunis Creek), and #17 and 20 (tonalite gneiss of Tejon Creek).

The first step in the model is to calculate the amount of radiogenic lead produced by in situ decay of uranium (denoted by Pb_{is}):

$$Pb_{is} = (\exp^{\lambda t}-1)\times U\times 0.8655 \qquad (1).$$

For this model, ^{206}Pb and ^{238}U are used, and $\lambda_{238}=1.5512\times10^{-10}$. The amount of in situ produced lead is subtracted from the measured lead (Pb_m) to give the amount of lead in the sample at the time represented by the lower intercept (Pb_l): $Pb_l=Pb_m-Pb_{is}$.

For the metasedimentary samples, the extent to which the daughter to parent ratio of the U/Pb system have been effected (R) was calculated (Faure,

1977). R is the distance along the discordia chord from the lower intercept with concordia (l) to the data point (m), divided by the distance along the discordia chord from the lower to the upper intercept with concordia (u). Therefore, R=(m-l)/(u-l). The upper intercept for the metasedimentary samples is interpreted as the overall isotopic "age" of its zircon population. Therefore, for this model, R measures the proportion of radiogenic lead remaining in the sample after lead loss at the time represented by the lower intercept (time of disturbance). To ascertain the amount of radiogenic lead in the sample before it experienced lead loss, the calculated radiogenic lead concentration (Pb_l) is divided by R, and is tabulated as Pb_u: $Pb_u=Pb_l/R$.

To ascertain the amount of zircon incorporated into the plutonic samples from the metasedimentary components (%I), Pb_l for the intrusive samples is divided by the radiogenic lead concentration of the metasedimentary component, and multiplied by 100 to yield the percent of metasedimentary zircon required to produced the observed discordances; $\%I=100\times Pb_l(\text{pluton})/Pb_u(\text{metasedimentary})$. Two different metasedimentary components for both the paragneiss and quartzite were investigated. In the first case, the lowermost fraction (fraction showing the greatest degree of lead loss, and therefore lowest Pb_l) was used. In the second case, the original calculated lead concentration (no lead loss, greatest Pb_u) was used. These two cases illustrate the range of possibilities, and place upper bounds on the possible amounts of incorporated metasedimentary zircon. They are tabulated in the rightmost columns on Table 15, along with the associated incorporated zircon source (quartzite, paragneiss, orthogneiss).

The results of the zircon mixing model are given in Table 15 as a weight percentage of zircon entrained from the metasedimentary component. In the case of the granodiorite of Claraville, the amounts range from 0.21 to 6.00%. The

quartzite is the assumed metasedimentary source, due to its closer field proximity, and the quartzite data point lying close to the Claraville discordia chord. There is an orderly progression of increasing proportion of entrained zircon with increasing grain size and increasing distance from the lower intercept.

The Bison Peak unit would require incorporation of ≤0.3% zircon from a metasedimentary source, and up to 1.4% from an orthogneiss (Tejon Creek) source. The fine-grained fraction from the metagabbro of Tunis Creek indicates 0.14% to 1.49% entrainment of metasedimentary zircon.

Two different samples from the tonalite gneiss of Tejon Creek were modeled, one that contains a high concentration of radiogenic lead (#17), and one that has a low concentration of radiogenic lead (#20). Both samples have similar $^{206}Pb^*/^{238}U$ and $^{207}Pb^*/^{235}U$ systematics. The sample with the high lead concentration would incorporate between 0.17 and 1.84% zircon (most likely from the paragneiss of Comanche Point, based on field relations) while the low lead concentration sample would require at most 0.18% from the same contaminate source.

A summary diagram of the zircon U/Pb ages for the southernmost Sierra Nevada is presented in Figure 49. In the figure the samples are grouped into three major suites based on field, structural, petrographic, and geochronological criteria. The suites are: 1) the Tehachapi suite (which includes the augen gneiss of Tweedy Creek), characterized by major deformational fabrics expressed by penetrative gneissic fabrics; 2) the Bear Valley Springs suite, which contains the tonalite of Bear Valley Springs, the hypersthene tonalite of Bison Peak, and the metagabbro of Tunis Creek, and has a late-stage deformational fabric; and 3) the late deformational intrusive suite, the constituents of which (the granodiorite of Claraville, pegmatite dikes, and the tonalite stock into the augen gneiss of Tweedy Creek) post-date and cross-cut the major deformational fabrics of the

Figure 49. Intrepretative composite concordia diagram (all fractions from Table 3) for the southernmost Sierra Nevada, with samples grouped into three suites (TGC, Tehachapi; BVS, Bear Valley Springs; LDI, late deformational intrusive). Inheritance trajectories were derived from using the upper intercepts of the granodiorite of Claraville and the paragneiss of Comanche Point, projected into the field of the Tehachapi samples. Lead loss trajectories were derived by the projection from the Tehachapi field towards the Bear Valley Springs intercept (100±2 Ma), which is believed to be the time of closure of the zircon U/Pb systems.

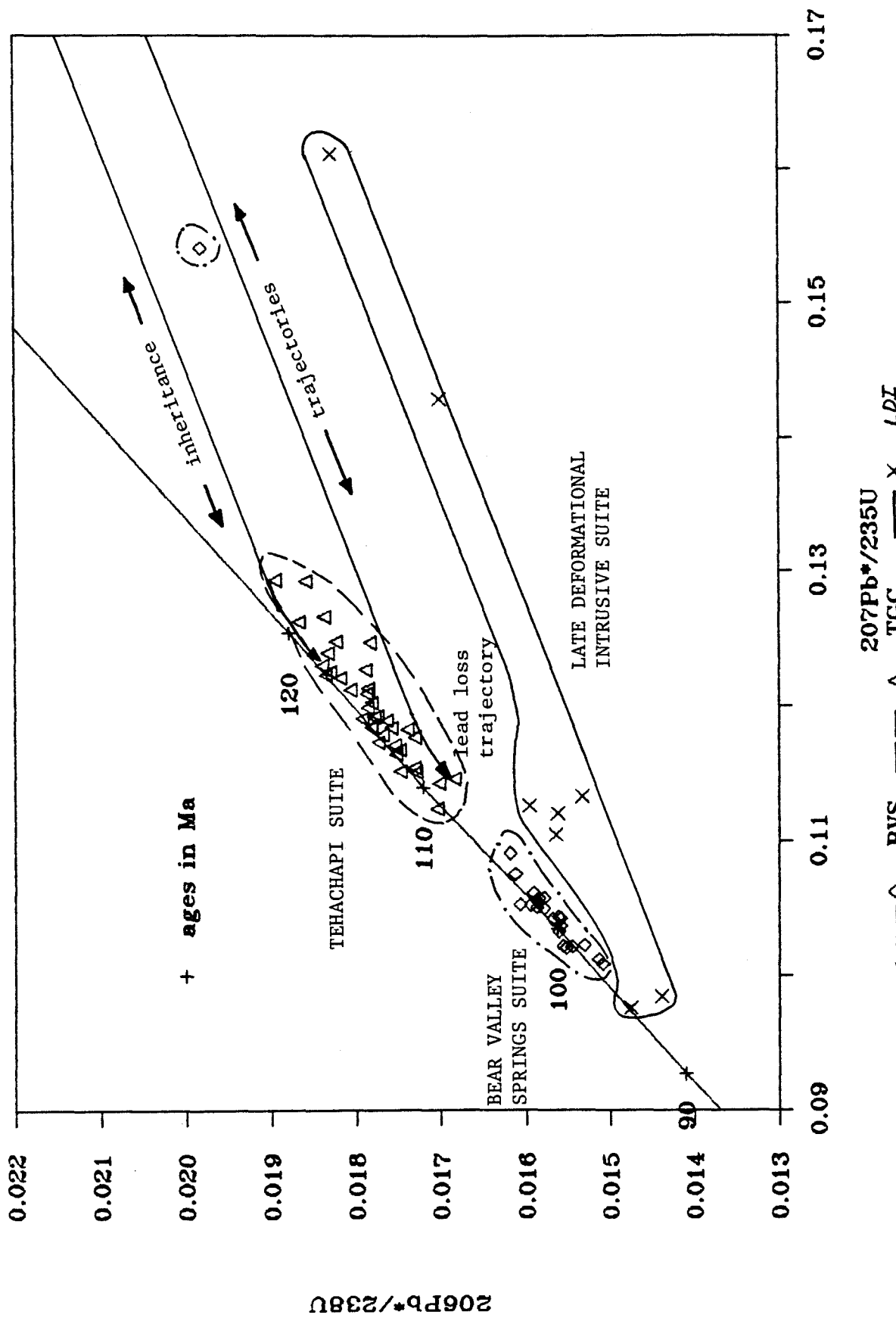
0.022
0.021
0.020
0.019
0.018
0.017
0.016
0.015
0.014
0.013
206Pb*/238U
0.09
0.11
0.13
0.15
0.17
207Pb*/235U
+ ages in Ma
inheritance
trajectories
120
110
100
90
lead loss
trajectory
TEHACHAPI SUITE
BEAR VALLEY
SPRINGS SUITE
LATE DEFORMATIONAL
INTRUSIVE SUITE
BVS
TGC
LDI

preceding suites. The Bear Valley Springs suite of samples is interpreted to represent a major intrusive event that was the culmination of high-temperature conditions within the southernmost Sierra Nevada. Such conditions may have existed in the deep crustal levels as represented by the gneiss complex of the Tehachapi Mountains from 115±5 Ma until the 100 Ma intrusion of the Bear Valley Springs suite.

Also shown on Figure 49 is a hypothetical lead evolution envelope which encloses the samples in the Tehachapi suite. The envelope is constrained by inheritance trajectories from Proterozoic ages to mid-Cretaceous, and superimposed open-system lead loss or uranium gain trajectories towards the 100 Ma Bear Valley Springs culmination. The limits of the inheritance trajectories are derived by projecting the upper intercepts from the granodiorite of Claraville, quartzite, paragneiss of Comanche Point, and metagabbro of Tunis Creek samples to concordia through the field of the Tehachapi suite data points. The upper intercepts (1900 Ma for the granodiorite of Claraville, 1700 Ma for the quartzite, 1450 Ma for the paragneiss of Comanche Point, and 1383 Ma for the metagabbro of Tunis Creek) reflect the overall isotopic character of the contaminate zircon. The zircon populations themselves may be multi-component systems. The downward dispersion of the ages from about 115 Ma is probably due to lead loss (or uranium gain) during the extended mid to lower crustal residency of the terrane, and the open-system behavior of the zircon U/Pb system.

It is suggested that the position of most or all of the points within the envelope reflects mainly igneous crystallization at 115±5 Ma, with discordances related to minor components of both inheritance and lead loss, and a resultant multistage history. Magmas that produced the gneiss complex orthogneisses inherited minor amounts of Proterozoic zircon from partial to complete melts derived from

metasedimentary framework rocks. Some of the magmas may have inherited small amounts of Phanerozoic zircon from deeper levels, as suggested by some of the zircon systematics displayed in the previous section. The overall zircon population was isotopically dominated by the growth of new mid-Cretaceous igneous zircon. Such igneous zircon may have crystallized over an extended period of time, and/or acted as partially open systems in the high temperature environment that lasted until the Bear Valley Springs intrusive event.

IV.2 Geochemistry - data and comments

Field, petrographic, and zircon data as discussed above suggest that the crystalline rocks of the southernmost Sierra Nevada were produced from a mixture of Cretaceous mantle-derived gabbroic to dioritic magmas and voluminuous Cretaceous tonalitic magmas of uncertain origin. Additional components were partial to complete melts derived from metasedimentary framework rocks.

The following sections will discuss the geochemical investigations that have been performed on samples from the study area. In particular, oxygen, strontium, and rubidium analyses have been done for many of the samples dated by U/Pb zircon techniques as reported in this paper. These investigations provide additional clues and constraints on the genesis of magmas and differentiation processes in the southern Sierra.

IV.2.1 Oxygen isotopic ratios

Oxygen is the most abundant element in most rock types, both in terms of percent by weight, and more importantly in terms of mole percent. It occurs in approximately equal amounts in the various silicate minerals. The small range of $\delta^{18}O$ values from all types of unaltered basaltic rocks ($+5.7 \pm 0.3°/_{oo}$ SMOW, Taylor, 1968) has been interpreted as indicative of a mantle with homogeneous oxygen isotopic characteristics. The mantle representative value of $+5.7°/_{oo}$ is

then taken as characteristic of primitive basaltic magmas derived from the upper mantle (Taylor, 1968, 1980). Petrologic processes within the mantle (partial melting, crystal fractionation, crystal-vapor equilibrium) or fractionation at lower magmatic temperatures within the crust appear to be able to change the oxygen isotopic ratio by at most +1.5°/$_{oo}$ (Taylor and Silver, 1978). Therefore, it appears that mantle-derived rocks have $\delta^{18}O$ values of less than about +7.5°/$_{oo}$. Ivan Barnes (personal communication, 1985) uses a range of $\delta^{18}O$ = +6.0 to +8.0°/$_{oo}$ as indicative of unaltered igneous rocks, while Taylor (1978) states that igneous rocks have $\delta^{18}O$ values of between +6.0 and +10.0°/$_{oo}$. This report will use the Taylor range for "igneous" $\delta^{18}O$ ratios.

High $^{18}O/^{16}O$ values can be found in the sedimentary environment (clays, shales, carbonates, cherts), where the rocks have undergone significant amounts of interaction with low-temperature surface waters. It therefore appears that processes that involve sedimentation, diagenesis, or low-temperature hydrothermal alteration are required to produce high $\delta^{18}O$ values (Taylor, 1980, 1968; Savin and Epstein, 1970). It then follows that $\delta^{18}O$ values greater than approximately +10°/$_{oo}$ require the incorporation of oxygen that has had a prior history at a near-surface, low-temperature environment, and/or interaction with low temperature surface waters.

Bulk rock $^{18}O/^{16}O$ determinations were done by Ivan Barnes at the U.S. Geological Survey in Menlo Park for most of the zircon samples that were investigated within this report (Table 14). The determinations have an absolute precision of ±0.02°/$_{oo}$, with an accuracy from replicate analyses of ±0.2°/$_{oo}$ (R.W. Kistler, personal communication, 1986). These data and data on additional samples are reported in Ross (1983a). The oxygen isotopic compositions reported in Table 14 are representative of the entire sample suite reported in Ross (1983a). A regional

synthesis of the data shows that plutons emplaced into Kings sequence framework rocks are enriched in ^{18}O relative to those emplaced to the west. This suggests contamination of the eastern and central plutonic rocks by metasedimentary material.

The $\delta^{18}O$ values reported in Table 14 are shown on a map of the southernmost Sierra Nevada in Figure 50. The map shows an increase in $\delta^{18}O$ along an west to east traverse across the tonalite of Bear Valley Springs - augen gneiss of Tweedy Creek - granodiorite of Claraville, and a possible weak increase southward in the tonalite of Bear Valley Springs. There is also a general increase in $\delta^{18}O$ values west within the gneiss complex of the Tehachapi Mountains. The $\delta^{18}O$ values are summarized in a histogram in Figure 51. For the non-metasedimentary rocks, the values range from +5.7 to +11.3°/$_{oo}$, while the metasediments have values of +17.4 and +18.3°/$_{oo}$. There is a very rough bimodal distribution to the data, with peaks at +9.5 and +10.5°/$_{oo}$, but with a continuum to the data.

In general, the rocks of the southernmost Sierra Nevada and Tehachapi Mountains show the result of wallrock contamination in the granodiorite of Claraville (#1), the tonalite stock at Tweedy Creek (#2), the augen gneiss of Tweedy Creek (#30), and the eastern border phase of the tonalite of Bear Valley Springs (#6). These samples are all emplaced into Kings sequence framework rocks. Samples from the late deformational suite (#1-4) have $\delta^{18}O$ values of between +10.0 and +11.3°/$_{oo}$, slightly above "normal" igneous values.

Within the Bear Valley Springs intrusive suite exclusive of the eastern phase of the batholith, isotopic values range from +5.7 to +9.6°/$_{oo}$, suggesting little to no metasedimentary component to the samples. Samples from the tonalite of Bear Valley Springs have $\delta^{18}O$ values that range from +8.6 to +9.6°/$_{oo}$ in its main phase, which may be classified as igneous or slightly contaminated values, to +9.1 to +10.1°/$_{oo}$ in samples of the eastern phase.

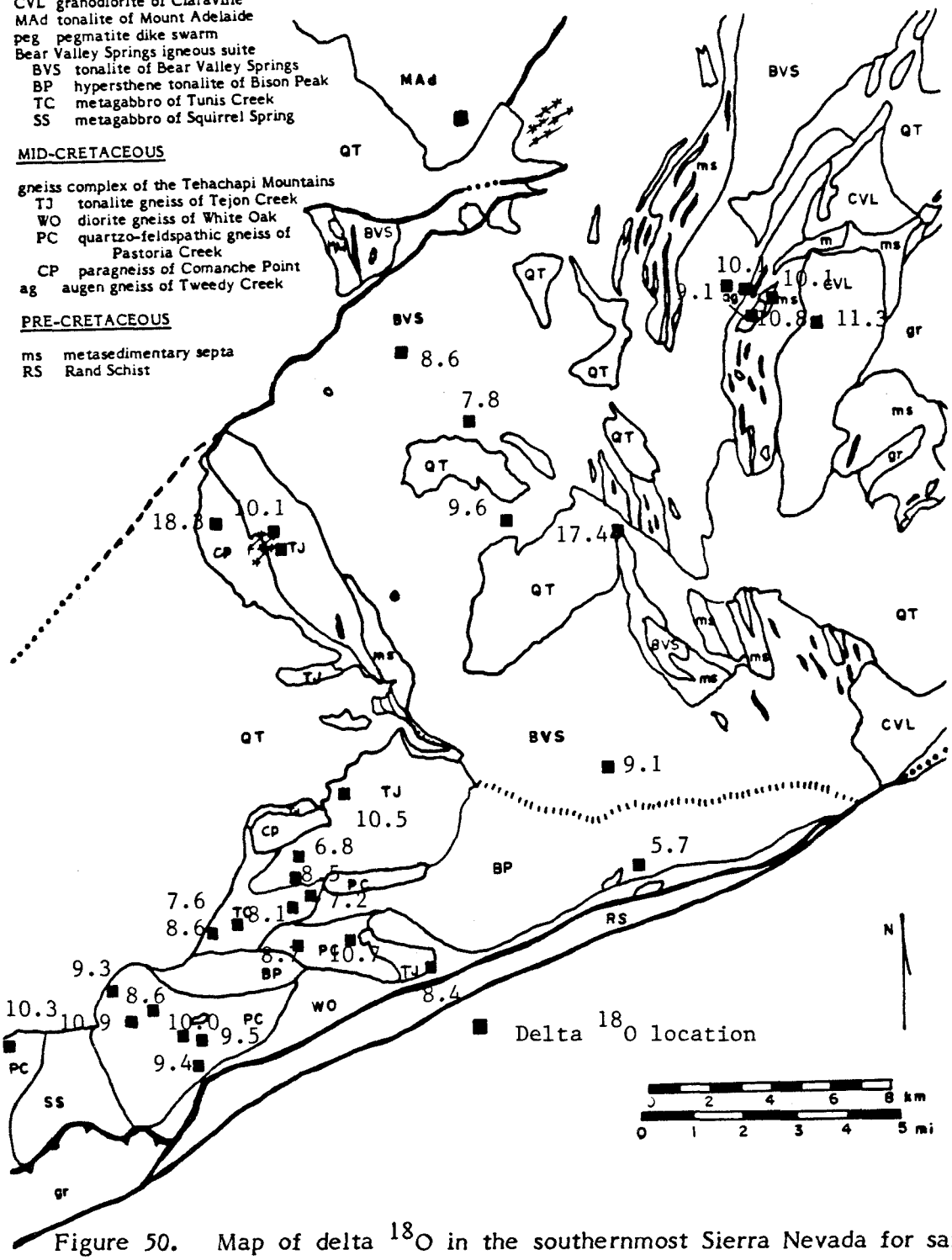

Figure 50. Map of delta ^{18}O in the southernmost Sierra Nevada for samples dated in this work (analyses by Ivan Barnes).

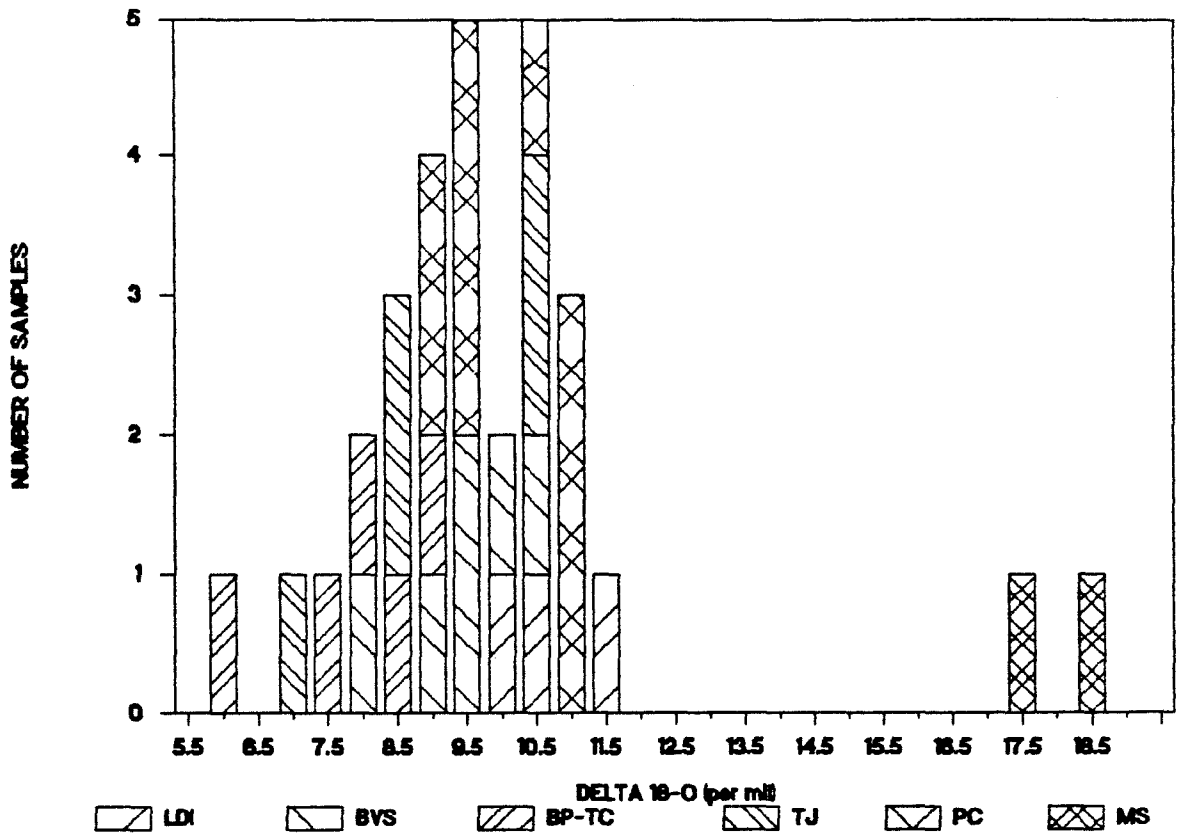

Figure 51. Histogram of delta ^{18}O, southernmost Sierra Nevada, for those samples plotted in Figure 50. With the exception of the metasedimentary samples, the data shows a narrow distribution of between +5.5 and +11.5 per mil. There is a possible bimodal distribution, with peaks at +9.5 and +10.5 per mil. LDI=late deformational intrusive rocks; BVS=tonalite of Bear Valley Springs; BP-TC=hypersthene tonalite of Bison Peak-metagabbro of Tunis Creek; TJ=tonalite gneiss of Tejon Creek; PC=quartzo-feldspathic gneiss of Pastoria Creek; ms=metasedimentary framework rocks.

A mafic inclusion near the center of the tonalite yielded a value of +7.8°/$_{oo}$. The inclusion has zircon systematics identical to those of the host tonalite, which suggests that the mafic inclusion experienced a similar geochemical history compared to the tonalite, or that it was geochemically equilibrated with the tonalite. The hypersthene tonalite of Bison Peak and the metagabbro of Tunis Creek have $\delta^{18}O$ values of +5.7 to +8.6°/$_{oo}$, well within the range of igneous rocks. Note that the Bison Peak unit has the lowest measured value of $\delta^{18}O$, and that it is also significantly lower than the values for the tonalite of Bear Valley Springs.

Within the gneiss complex of the Tehachapi Mountains, the tonalite gneiss of Tejon Creek has $\delta^{18}O$ values of +6.8 to +10.5°/$_{oo}$, suggesting at least some degree of contamination of an igneous protolith. The quartzo-feldspathic gneiss of Pastoria Creek has $\delta^{18}O$ rations of +8.4 to +10.9°/$_{oo}$. The values below +9.3°/$_{oo}$ correspond to the more mafic parts which show clearer signs of an igneous protolith, based on field and petrographic data. The higher values correspond to rocks with considerable K-feldspar components, and may represent a mixture of igneous and metasedimentary components.

A quartzite in the Kings sequence septum west of Tehachapi has a value of +17.4°/$_{oo}$. The paragneiss of Comanche Point has a +18.3°/$_{oo}$ value, consistent with a sedimentary protolith for the paragneiss. Incorporation of material derived from the paragneiss into the tonalite gneiss of Tejon Creek is therefore supported by the oxygen isotopic data.

A series of mixing models are presented in Table 16. The models assume simple two-component mixing in a linear fashion. The oxygen contents of the various samples and the sources were assumed to be approximately equal on an atom basis. The two end-members investigated consist of a primitive, upper mantle-derived component and a crustal metasedimentary component. Thus,

Table 16. Oxygen mixing models using variable end-member components

SAMPLE #	NAME	$\delta^{18}O$ °/$_{oo}$	PERCENT OXYGEN FROM METASEDIMENT Taylor 5.7/19.0	SSNa 5.7/18.3	F&C 8.5/19.0	SSNb 8.5/18.3
Late deformational intrusive suite						
1	TC27	11.3	42.1	44.4	26.7	28.6
2	TC40	10.1	33.1	34.9	15.2	16.3
4	PC35	10.0	32.3	34.1	14.3	15.3
Bear Valley Springs intrusive suite						
6	TC15	10.1	33.1	34.9	15.2	16.3
7	TC42	9.1	25.6	27.0	5.7	6.1
8	CM25	8.6	21.8	23.0	1.0	1.0
9	CM26	9.6	29.3	31.0	10.5	11.2
10	CM9	9.1	25.6	27.0	5.7	6.1
11	CM22b	7.8	15.8	16.7	-6.7	-7.1
12	TL197	5.7	0	0	-27	-29
13	WR84	7.2	11.3	11.9	-12	-13
14	WR86	8.1	18.0	19.0	-3.8	-4.1
15	WR190	7.6	14.3	15.1	-8.6	-9.2
16	PC227	8.6	21.8	23.0	1.0	1.0
Tehachapi suite						
17	CM630	10.1	33.1	34.9	15.2	16.3
18	WR643	10.5	36.1	38.1	19.0	20.4
19	WR171	6.8	8.3	8.7	-16	-17
20	WR30/2	8.5	21.1	22.2	0	0
21	WR39	8.4	20.3	21.4	-1.0	-1.0
22	PC31	9.3	27.1	28.6	7.6	8.2
23	PC32	10.9	39.1	41.3	22.9	24.5
24	PC34	8.6	21.8	23.0	1.0	1.0
25	PC36	9.5	28.6	30.2	9.5	10.2
26	PC37	9.4	27.8	29.4	8.6	9.2
27	PC129	10.3	34.6	36.5	17.1	18.4
28	WR91a	8.7	22.6	23.8	1.9	2.0
29	WR40	10.7	37.6	39.7	21.0	22.4
30	TC12a	10.8	38.3	40.5	21.9	23.5

Percentages are simple mixing of an upper mantle component with a metasedimentary component, on an equal atom basis. The mantle component has $\delta^{18}O$ = +5.7 per mil (Taylor, 1968, 1980; hypersthene tonalite of Bison Peak, this study; models #1,2) or $\delta^{18}O$ = +8.5 per mil for the mantle component, based on the maximum possible enrichment due to mantle magmatic processes (Fleck and Criss, 1985; models #3,4). The metasediments have $\delta^{18}O$ = +19.0 per mil (Taylor, 1968, 1980; models #1,3) or +18.3 per mil (paragneiss of Comanche Point, this study; models #2,4). Samples analyzed by Ivan Barnes, U.S.G.S., Menlo Park, California on most of the samples investigated by U/Pb zircon dating techniques in this study. Precision is ±0.2 per mil.

$$\% \text{ metasediment} = \frac{\delta^{18}O_{\text{sample}} - \delta^{18}O_{\text{upper mantle}}}{\delta^{18}O_{\text{metasediment}} - \delta^{18}O_{\text{upper mantle}}} \times 100 \qquad (2).$$

Two different models consisting of two different sets of components each were investigated. For the first model a pristine upper mantle component was assumed, while the second model used an altered mantle component. Each model used endpoint values for the mantle and metasedimentary components from other workers, and/or from the range of values found in this study. Table 16 presents the data showing the percentage of metasedimentary oxygen contributed to low $\delta^{18}O$ magmas to produce the observed isotopic compositions.

For the first model, a value of $\delta^{18}O = +5.7°/_{oo}$ was used for the mantle component (Taylor, 1980). Metasedimentary component values of $+19.0°/_{oo}$ (Taylor "set") from Taylor (1968, 1980) and $+18.3°/_{oo}$ (SSNa) from the paragneiss of Comanche Point (#33) were used. The following summarizes the results of this model. The late deformational intrusives would incorporate 32-44% of a metasedimentary component; the tonalite of Bear Valley Springs, 16-35%; the hypersthene tonalite of Bison Peak, no metasedimentary oxygen; the metagabbro of Tunis Creek, 11-23%; the tonalite gneiss of Tejon Creek, 8-38%; the augen gneiss of Tweedy Creek, 38-40%; and the quartzo-feldspathic gneiss of Pastoria Creek, 22-41%. There is very little difference in the use of the different metasedimentary endpoints. It appears by this model that up to one-third of the oxygen isotopic ratio of the rocks of the southern Sierras can be attributed to incorporation of metasedimentary material, with the more mafic samples, and samples from the Bear Valley Springs intrusive suite having greater igneous components relative to the other samples.

The second model used an upper mantle end-member value of $+8.5°/_{oo}$. This would be the approximate limit to values for alteration of a "pristine" value of

+5.7°/$_{oo}$ by mantle magmatic processes and/or hydrothermal alteration of oceanic crust (Fleck and Criss, 1985; Taylor and Silver, 1978). The same metasedimentary endpoint values of +19.0°/$_{oo}$ (F&C set) and +18.3°/$_{oo}$ (SSNb) were used as described for the first model. For the second model, there is a significant difference (a halving in most cases) in the amount of metasedimentary material incorporated into the magmas. For the metagabbro of Tunis Creek and hypersthene tonalite of Bison Peak, very little (or negative amounts) metasedimentary material was incorporated, while the tonalite of Bear Valley Springs would require up to 16%. The quartzo-feldspathic gneiss of Pastoria Creek would incorporate between 1% and 24% of a crustal component. The late deformational intrusives are the units most heavily enriched in a metasedimentary component, some 14 to 29%.

The value of $\delta^{18}O$ for the hypersthene tonalite of Bison Peak indicates that at least some magmatic material was intruded into the crust at the current level of exposure with their original mantle compositions intact. Also, the negative values for many of the samples in the second model presented in Table 16 (large number of samples with $\delta^{18}O < +8.5°/_{oo}$) suggests that this is not an isolated occurrence. Several samples show contamination of their zircon populations with Proterozoic zircon (Tunis Creek, Claraville, tonalite stock), indicating some degree of metasedimentary contamination for these samples. In addition, the first model indicates up to a 44% metasedimentary contamination, inconsistent with bulk chemistry. It therefore appears that the mantle-derived magmas had variable initial ratios of between +5.7 and +8.5°/$_{oo}$.

IV.2.2 Rubidium and strontium isotopic ratios

Samples representative of primitive basaltic magmas believed to be derived from the upper mantle have low initial $^{87}Sr/^{86}Sr$ ratios (denoted by Sr_o). Representative mantle values of Sr_o are taken as equal to 0.703 ± 0.001 (Taylor, 1968;

Hart, 1971) or 0.7035 (Fleck and Criss, 1985). The value of Sr_o = 0.7035 is taken in this report as a mantle representative point (Taylor, 1980). High $^{87}Sr/^{86}Sr$ ratios are produced from the decay of ^{87}Rb to ^{87}Sr. Reservoirs of high $^{87}Sr/^{86}Sr$ are generally believed to be old continental rocks or sediments derived from such.

A variation distribution in the Sr_o of Mesozoic plutons was noted by Kistler and Peterman (1973, 1978) whereby a set of isopleths could be drawn along the trend of the Sierra Nevada batholith. They also noted that those plutons east of the Sr_o=0.706 isopleth had field, petrographic, and geochemical characteristics suggestive of interaction with Proterozoic sialic material. Conversely, they noted that those plutons west of the Sr_o=0.706 isopleth appeared to have had little or no interaction with such material. Kistler and Peterman (1973, 1978) therefore defined the line where Mesozoic plutonic samples have $Sr_o > 0.706$ as approximating the western boundary of the Paleozoic continental margin.

Reconnaissance neodymium and strontium analyses on Mesozoic plutonic rocks of the south-central Sierra Nevada were performed by DePaolo (1981b). He considered samples from plutons east of the Sr_o=0.706 isopleth to have been derived from approximately equal mixtures of Cretaceous mantle-derived igneous material with Proterozoic sial-derived material. He further believed such mixtures were obtained within the crust prior to intrusion of the plutons. DePaolo (1981b), Saleeby and others (1978), and Chen and Tilton (1978) considered samples of plutonic rocks that have $Sr_o \leq 0.7060$ to be of an oceanic affinity, and to have had an upper mantle source.

In previous work on the southernmost Sierra Nevada, Ross (1983d) reports $^{87}Sr/^{86}Sr$ ratios of two rock samples in the gneiss complex of the Tehachapi Mountains in Grapevine Canyon of 0.7036 and 0.7045. Sharry (1981b) determined $^{87}Sr/^{86}Sr$ values for a number of units in the gneiss complex: the hypersthene

tonalite of Bison Peak had values of 0.7053 to 0.7060; the metagabbro of Tunis Creek 0.7044 to 0.7058; and the diorite gneiss of White Oak 0.7054 to 0.7064. Using the decay constant for $\lambda^{87}_{Rb}=1.42\times10^{-11}$ (Steiger and Jaeger, 1977), and the zircon U/Pb ages contained herein, initial $^{87}Sr/^{86}Sr$ ratios have been recalculated for Sharry's (1981b) samples. The results: the hypersthene tonalite of Bison Peak was found to have an $Sr_o=0.7049$, the metagabbro of Tunis Creek $Sr_o=0.7050$, and the diorite gneiss of White Oak $Sr_o=0.7054$.

Initial Sr ratios of 0.7050 and 0.7055 were determined by Kistler and Peterman (1978) for the tonalite of Bear Valley Springs. These last two values were determined using an Rb/Sr age of 80 Ma (Rb/Sr bulk rock age). Using a U/Pb age of 100 Ma, the recalculated Sr_o would be 0.7049 and 0.7054, respectively. All of the preceding samples fall on the "primitive" or "oceanic-affinity" side of the 0.7060 model line, with some samples (metagabbro of Tunis Creek and Grapevine area samples) approaching the value for the mantle reference point.

Rubidium and strontium analyses were performed by R.W. Kistler of the U.S. Geological Survey, Menlo Park, for many of the samples dated in this study. These results are presented in Table 17. The uncertainty in the $^{87}Sr/^{86}Sr$ analyses are ±0.008% of the value reported. Replicate analyses allow an absolute precision of ±0.0001 to be reported (R.W. Kistler, personal communication, 1986). Using the zircon U/Pb ages reported herein, initial $^{87}Sr/^{86}Sr$ ratios have been calculated for these samples to account for in situ decay of ^{87}Rb (Table 17).

The values of Sr_o are shown on the southern Sierra base map in Figure 52, and summarized in a histogram in Figure 53. The map pattern resembles that for the $\delta^{18}O$ data, with increasing Sr_o eastward from the tonalite of Bear Valley Springs to the granodiorite of Claraville, and southwards within the tonalite. The samples within the tonalite create a smear in the $Sr_o=0.706$ isopleth as originally

Table 17. Rubidium and Strontium results

SAMPLE #	NAME	Rb ppm	Sr ppm	1/Sr x1000	Rb/Sr	$^{87}Rb/^{86}Sr$	$^{87}Sr/^{86}Sr$ measured	$^{87}Sr/^{86}Sr$ initial
Late deformational intrusive suite								
1	TC27	71.2	562	1.779	0.127	0.367	O.70777	0.70731
2	TC40	48.1	578	1.730	0.083	0.241	0.70735	0.70703
4	PC35	149	50	20.202	3.010	8.720	0.71965	0.70776
Bear Valley Springs intrusive suite								
6	TC15	18.5	360	2.778	0.051	0.148	0.70603	0.70583
7	TC42	30.8	341	2.933	0.090	0.261	0.70606	0.70570
8	CM25	55.9	399	2.506	0.140	0.405	0.70648	0.70591
9	CM26	69.2	392	2.551	0.177	0.512	0.70708	0.70637
10	CM9	104	388	2.577	0.268	0.775	0.70785	0.70677
11	CM22b	16.0	265	3.774	0.060	0.173	0.70629	0.70605
12	TL197	36.6	330	3.030	0.111	0.321	0.70542	0.70496
13	WR84	3.7	583	1.715	0.006	0.018	0.70502	0.70499
14	WR86	2.2	504	1.984	0.004	0.013	0.70506	0.70504
15	WR190	5.7	500	2.000	0.011	0.033	0.70504	0.70499
16	PC227	4.2	709	1.410	0.006	0.017	0.70495	0.70493
Tehachapi suite								
17	CM630	36.1	257	3.891	0.140	0.405	0.70534	0.70472
18	WR643	21.0	367	2.725	0.057	0.165	0.70545	0.70518
19	WR171	35.8	308	3.247	0.116	0.336	0.70518	0.70467
20	WR30/2	1.9	447	2.237	0.004	0.012	0.70480	0.70478
21	WR39	2.4	696	1.437	0.003	0.010	0.70501	0.70499
22	PC31	52.1	215	4.651	0.242	0.700	0.70627	0.70519
23	PC32	145	79	12.642	1.833	5.300	0.71336	0.70510
24	PC34	33.3	352	2.841	0.095	0.273	0.70511	0.70469
25	PC36	11.2	324	3.086	0.035	0.100	0.70515	0.70500
26	PC37	69.7	222	4.505	0.314	0.908	0.70613	0.70469
27	PC129	40.6	332	3.012	0.122	0.352	0.70650	0.70594
28	WR91a	18.7	353	2.833	0.053	0.153	0.70560	0.70536
29	WR40	56.7	138	7.246	0.411	1.180	0.70670	0.70480
30	TC12a	66.7	216	4.630	0.309	0.890	0.70818	0.70682
Metamorphic framework rocks								
32	CM640	32.3	90.3	11.074	0.358	1.037	0.72581	0.72434
33	CM110	110	165	6.061	0.667	1.931	0.71442	0.71146

Initial $^{87}Sr/^{86}Sr$ ratios were corrected for in situ ^{87}Rb decay by using U/Pb age determined for the sample, except for samples #15,16, where the age of the unit (101 Ma) determined on samples #13,14 was used. For the metasedimentary units, the lower intercept was used for the paragneiss of Comanche Point (108 Ma) and the tonalite of Bear Valley Springs age (100 Ma) was used for the quartzite. Samples analyzed by R.W. Kistler. Uncertainties are ±0.00010.

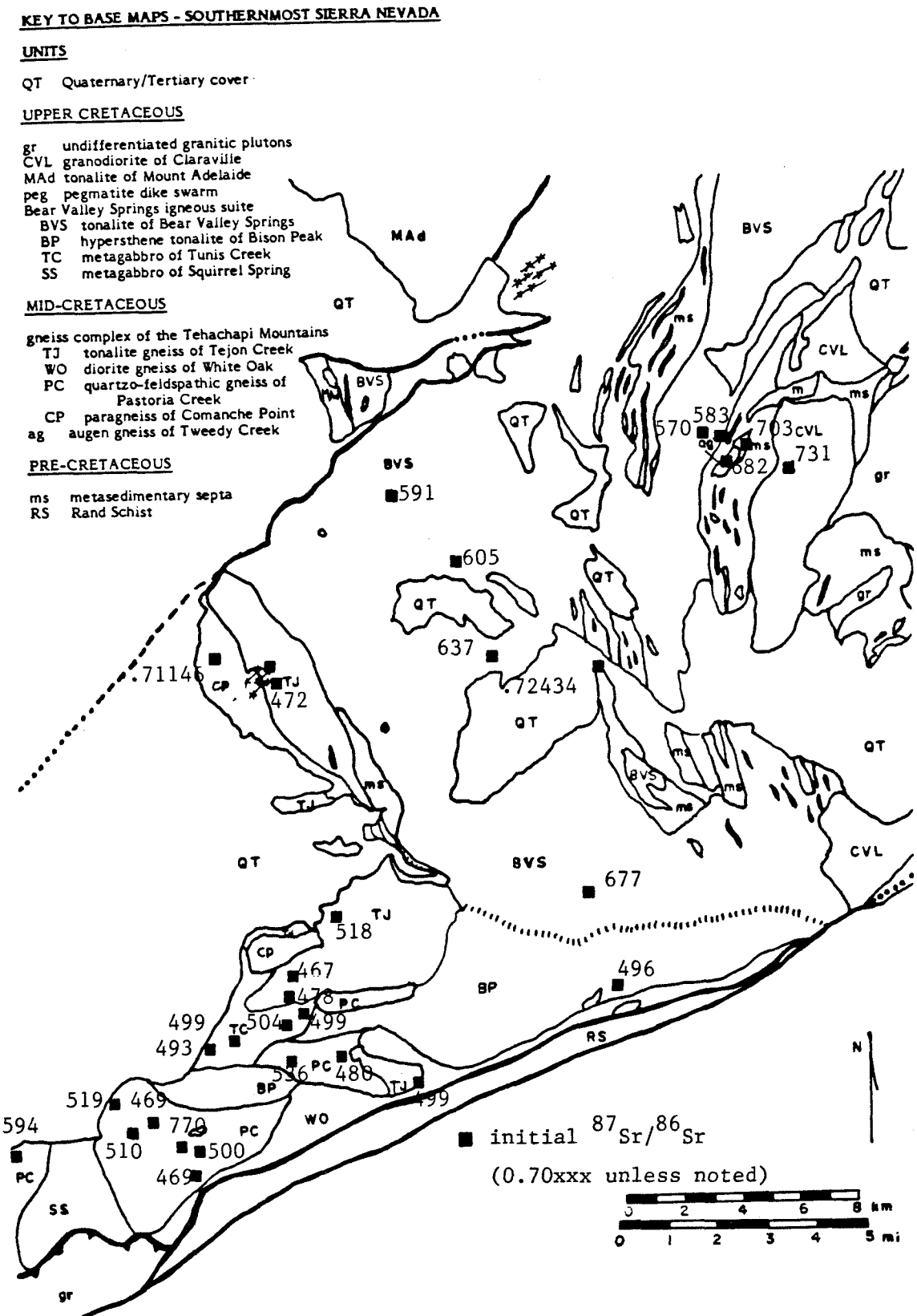

Figure 52. Map of initial $^{87}Sr/^{86}Sr$ in the southernmost Sierra Nevada for those samples dated in this study (analyses by R.W. Kistler).

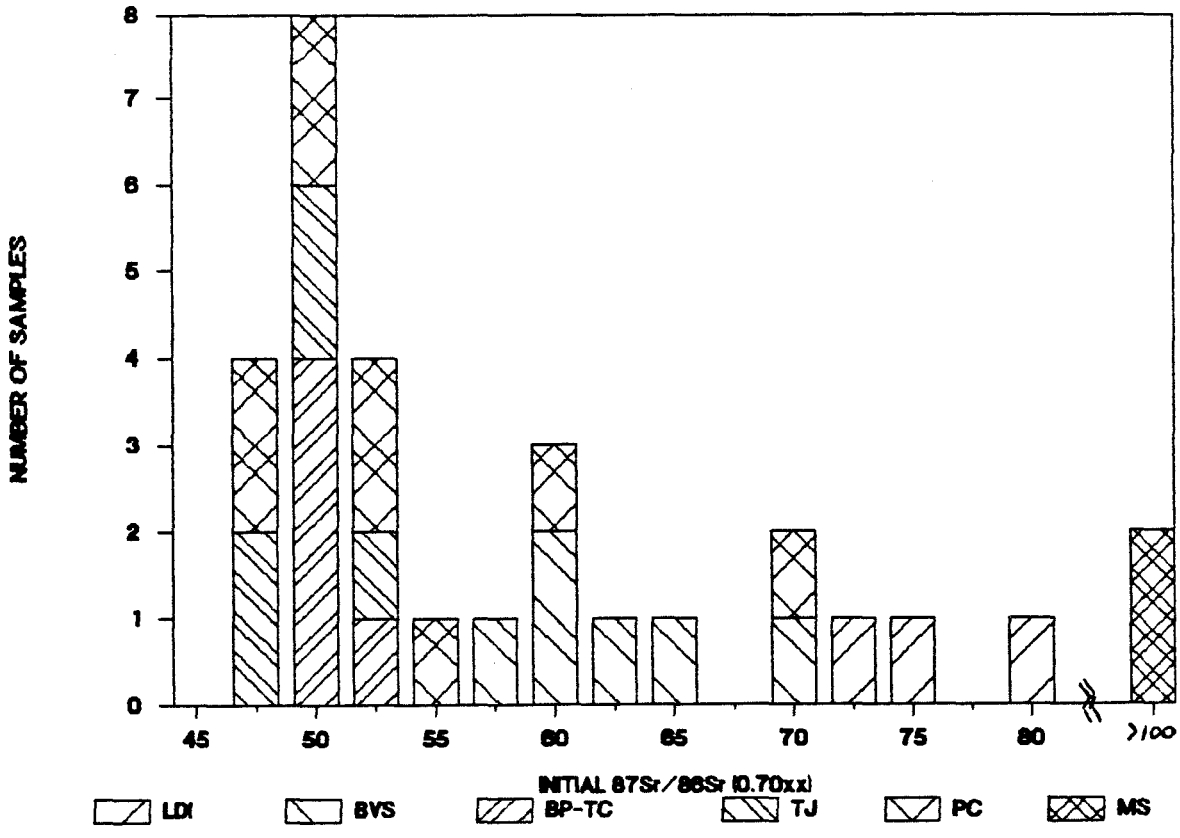

Figure 53. Histogram of initial $^{87}Sr/^{86}Sr$ in the southernmost Sierra Nevada for the data given in Figure 52. The data has a weak bimodal distribution (peaks at Sr_o=0.7050 and 0.7070). The tonalite of Bear Valley Springs samples create a smear in the Sr_o=0.7060 isopleth. LDI=late deformational intrusive rocks; BVS=tonalite of Bear Valley Springs; BP-TC=hypersthene tonalite of Bison Peak-metagabbro of Tunis Creek; TJ=tonalite gneiss of Tejon Creek; PC=quartzo-feldspathic gneiss of Pastoria Creek; ms=metasedimentary framework rocks.

defined by Kistler and Peterman (1973, 1978). There is also a weak increase west from Tejon Creek to the Grapevine in the gneiss complex of the Tehachapi Mountains. Note the prominent drop in Sr_o along the southern and southwestern margins of the tonalite of Bear Valley Springs. This isotopic "jump" may represent a change in the isotopic reservoir or basement, and coincides with the boundary between the Kings sequence and paragneiss of Comanche Point metasedimentary framework rocks. There is one anomalous value of 0.7078 in the quartzo-feldspathic gneiss of Pastoria Creek, the 97 Ma garnet granite dike intrusive into the gneiss. This sample is discussed in detail later in this section. The histogram (Figure 53) shows a strong peak at 0.7050, with a spread of values from 0.7047 to 0.7078.

With regards to the abundances of strontium and rubidium, Figure 54, a map of Sr content in ppm, exhibits a generally random geographic pattern, with the more mafic units (especially the metagabbro of Tunis Creek) having the higher Sr contents. Figure 55, a histogram of the Sr content data, has a large peak and broad distribution of analyses centered at 400 ppm Sr. Figure 56, a map distribution of the Rb content, shows very roughly the same pattern of increasing Rb content as Figure 50 does for $\delta^{18}O$, and Figure 52 does for initial $^{87}Sr/^{86}Sr$ (west to east increase from the tonalite of Bear Valley Springs to the granodiorite of Claraville, and a general north to south increase within the gneiss complex of the Tehachapi Mountains). Note the low values corresponding to the metagabbro of Tunis Creek and the tonalite gneiss of Tejon Creek. A histogram of the data, Figure 57, shows a broad, almost uniform distribution from 0 to 70 ppm Rb, with two samples from the quartzo-feldspathic gneiss of Pastoria Creek (one being the 97 Ma dike) anomalously rich in Rb (150 ppm).

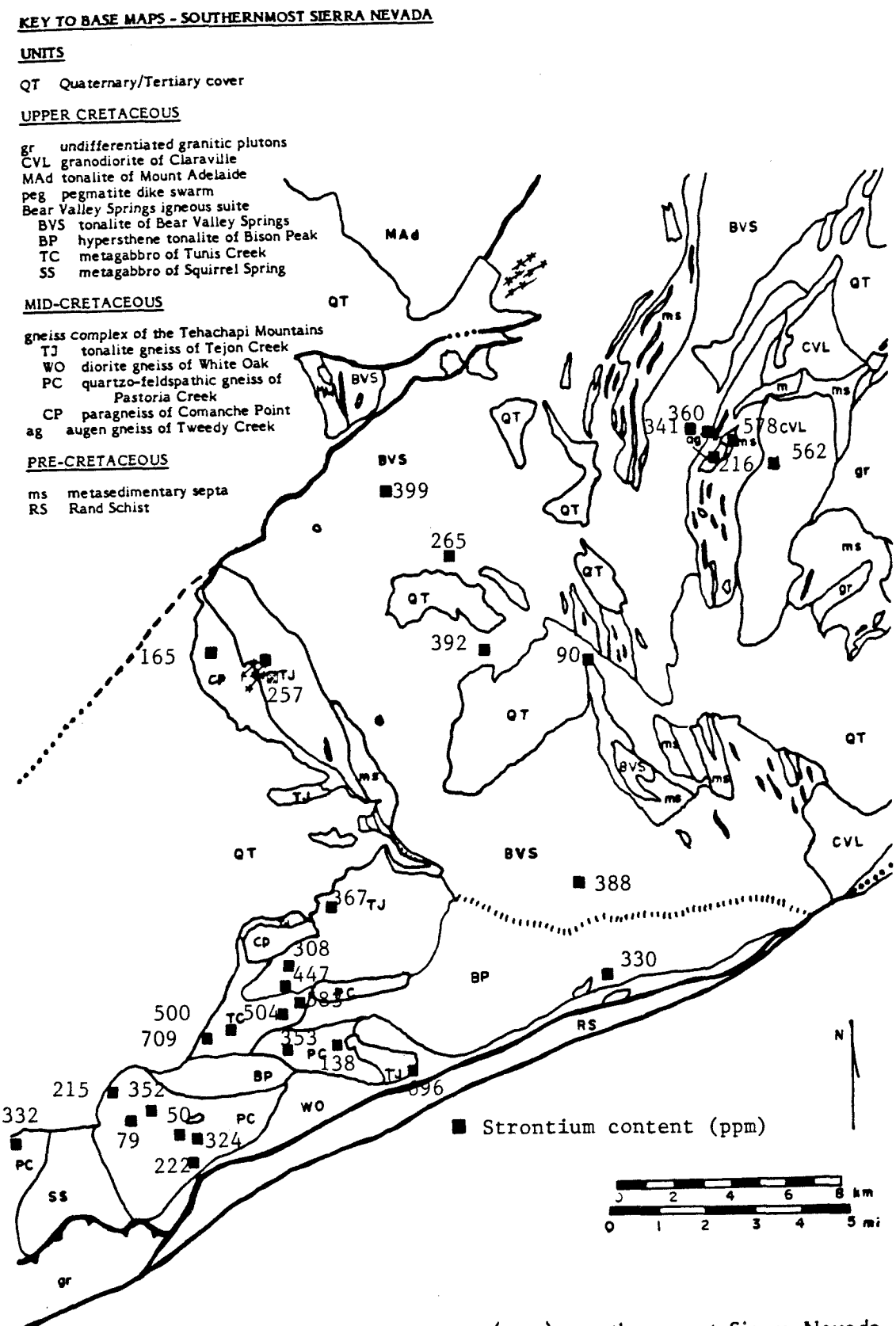

Figure 54. Map of strontium content (ppm), southernmost Sierra Nevada, for those samples dated in this study (analyses by R.W. Kistler).

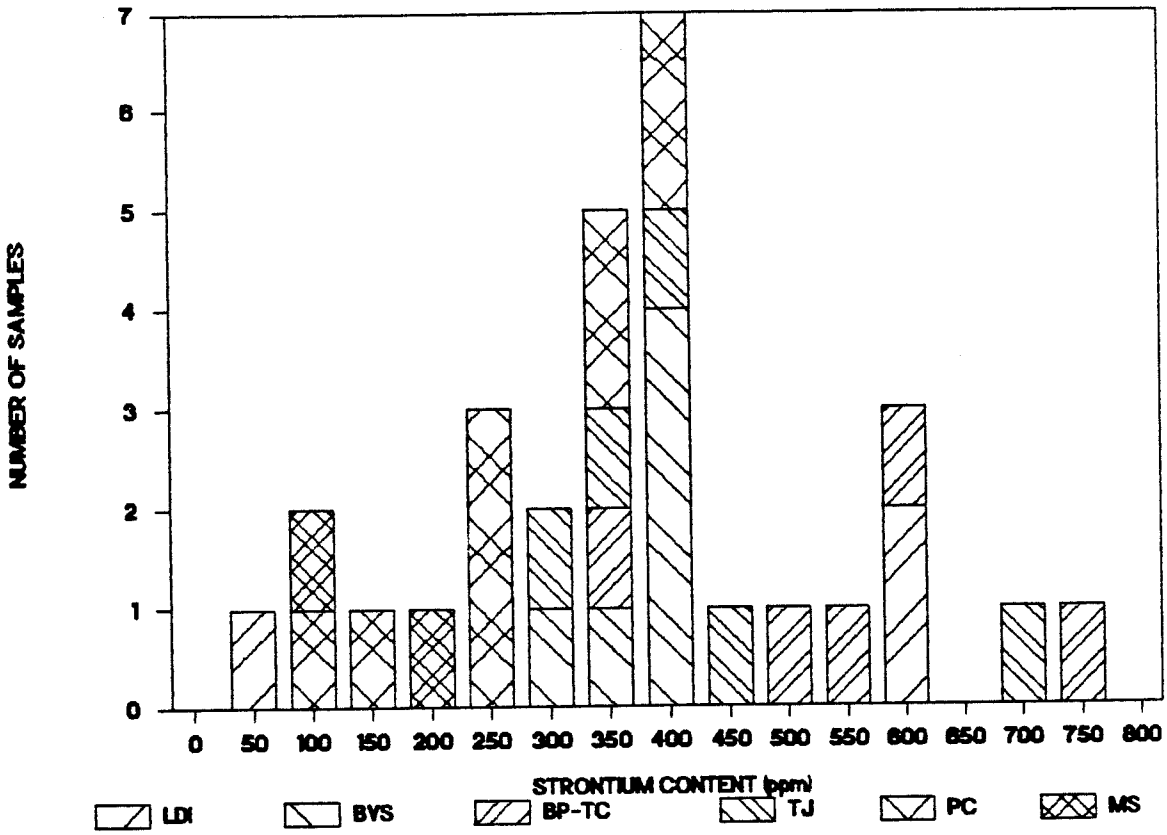

Figure 55. Histogram of strontium content (ppm), southernmost Sierra Nevada, for the data given in Figure 54. The data shows a broad distribution around 400 ppm strontium. LDI=late deformational intrusive rocks; BVS=tonalite of Bear Valley Springs; BP-TC=hypersthene tonalite of Bison Peak-metagabbro of Tunis Creek; TJ=tonalite gneiss of Tejon Creek; PC=quartzo-feldspathic gneiss of Pastoria Creek; ms=meta-sedimentary framework rocks.

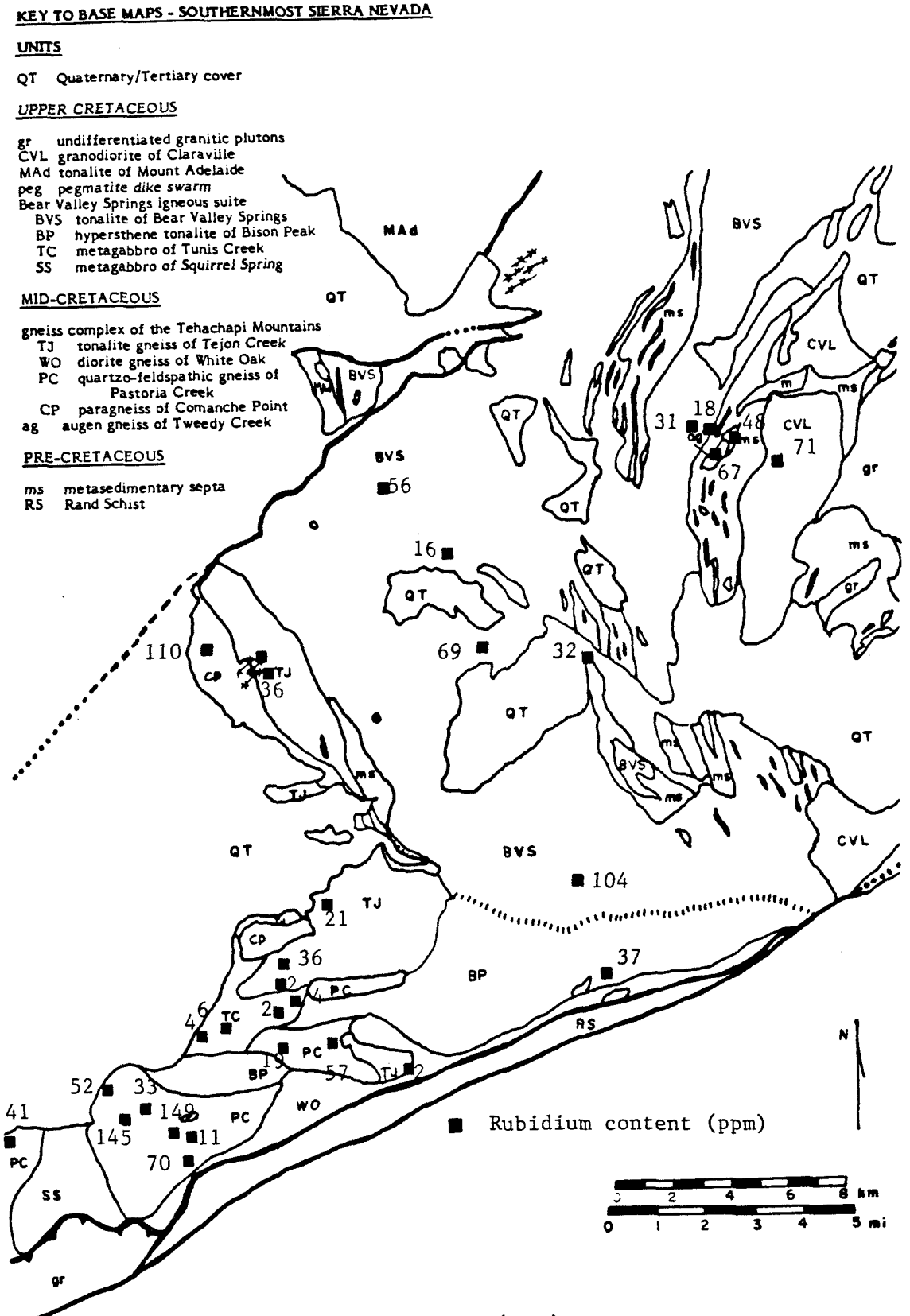

Figure 56. Map of rubidium content (ppm), southernmost Sierra Nevada, for samples investigated in this study (analyses by R.W. Kistler).

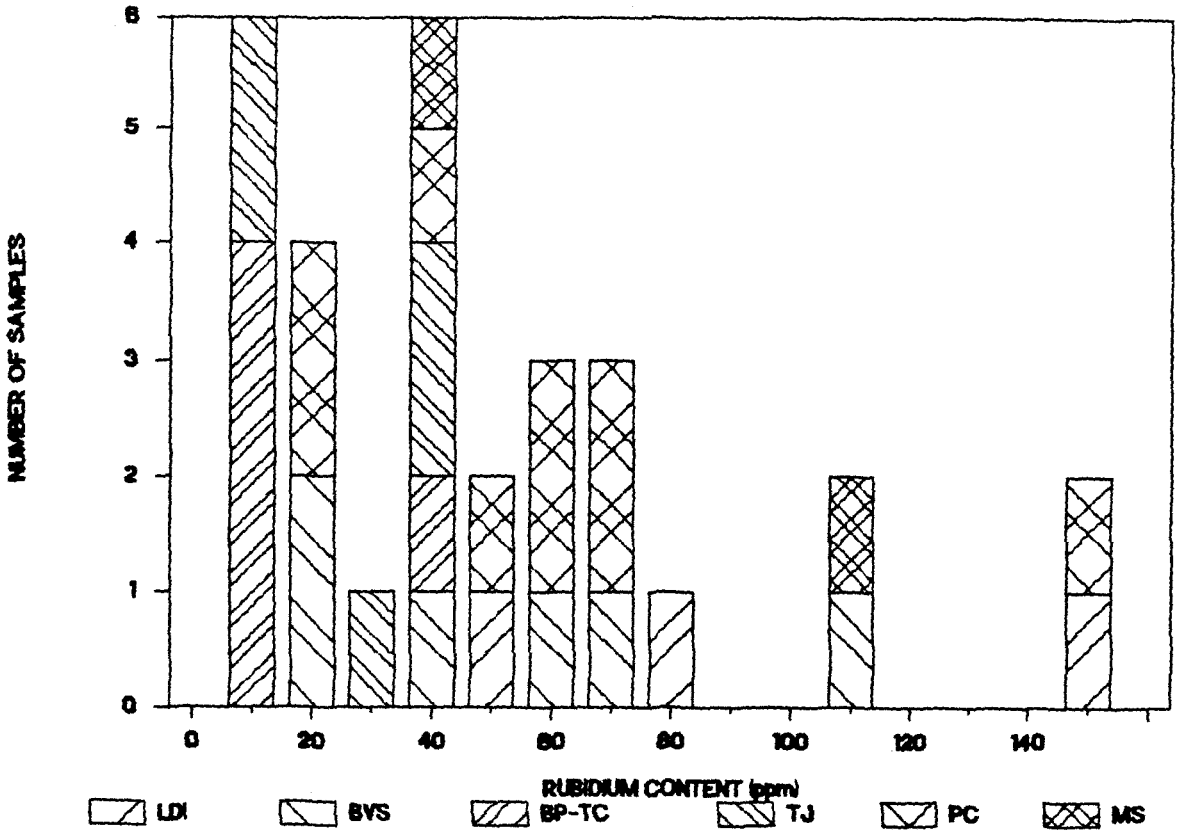

Figure 57. Histogram of rubidium content (ppm) in the southernmost Sierra Nevada for those samples given in Figure 56. The samples all have a generally low concentration in rubidium, with a broad distribution with peaks at 10 and 40 ppm Rb. LDI=late deformational intrusive rocks; BVS=tonalite of Bear Valley Springs; BP-TC=hypersthene tonalite of Bison Peak-metagabbro of Tunis Creek; TJ=tonalite gneiss of Tejon Creek; PC=quartzo-feldspathic gneiss of Pastoria Creek; ms=metasedimentary framework rocks.

The following discusses the strontium and rubidium data for each of the units in a sequential manner. For rocks in the late deformational intrusive suite (#1-4), and for the augen gneiss of Tweedy Creek (#30), $Sr_o \geq 0.7068$, i.e., on the continental side of the 0.7060 isopleth. This includes the garnet granite dike at Pastoria Creek, and accounts for all samples with $Sr_o > 0.7068$. The high Sr_o is indicative of interaction with metasedimentary material. The garnet granite dike itself has an Rb/Sr ratio of 3, indicating a highly differentiated granitoid melt product (Faure, 1977). Its isotopic characteristics are considerably different from other samples from the gneiss complex of the Tehachapi Mountains, and are believed to have been produced by partial melting of Pastoria Creek gneiss material during the Bear Valley Springs thermal episode.

Samples from the tonalite of Bear Valley Springs have Sr_o that straddle the 0.7060 isopleth (0.7057 to 0.7068). These results are somewhat higher than the data reported by Kistler and Peterman (1973, 1978), and could indicate broadening of the isopleth into a diffuse zone at this level of exposure. The variation in Sr_o for the tonalite may be due to inhomogeneity in the source, or a reflection of the higher level mixing that the tonalite experienced. The mafic inclusion within the tonalite (#11) has Rb/Sr characteristics within the range of the tonalitic samples. This data, along with $\delta^{18}O$ and zircon age data, is supportive of a cogenetic origin for the mafic inclusions, and indicates that the inclusions were either geochemically equilibrated with the tonalite source material or with the tonalite itself during magma mixing and crystallization.

The hypersthene tonalite of Bison Peak and metagabbro of Tunis Creek each have initial $^{87}Sr/^{86}Sr$ ratios ≤ 0.7050. The metagabbro has Rb contents of less than 6 ppm, with a Rb/Sr ratio ≤ 0.01. These results are similar to those of Sharry (1981b), and are indicative of a primitive upper mantle source and/or the effect of crystal accumulation processes (Faure, 1977).

Samples from the gneiss complex of the Tehachapi Mountains show a bimodal distribution with regards Sr_o and Rb/Sr ratios. The tonalite gneiss of Tejon Creek has an Sr_o of between 0.7047 and 0.7052, with an Rb/Sr ratio less than 0.12. The quartzo-feldspathic gneiss of Pastoria Creek has an Sr_o of between 0.7047 and 0.7059. Tonalites in the Pastoria Creek gneiss have Rb/Sr ratios ≤ 0.1, while granites have a range of Rb/Sr ratios of 0.2 to 1.8. The general interpretation of the data is for an upper mantle source for the orthogneisses, with the tonalite gneiss of Tejon Creek and the tonalites in the Pastoria Creek gneiss representing relatively primitive magmas, and the granites in the Pastoria Creek gneiss representing moderately differentiated and more contaminated magmas (Faure, 1977). Based on field, Rb/Sr, and oxygen isotopic data, metasedimentary material was mixed into these units, probably at the level of emplacement.

Metasedimentary framework rocks have rubidium and strontium systematics distinct from the remainder of the samples. The paragneiss of Comanche Point (#33) has an $^{87}Sr/^{86}Sr$ ratio at 108 Ma (lower intercept disturbance age) of 0.7115, while the quartzite (#32) at 100 Ma (tonalite of Bear Valley Springs age) has a ratio of 0.7243. The distinction in the $^{87}Sr/^{86}Sr$ ratios and detrital zircon systematics, in addition to their geographic distribution, suggests different source terranes for the two metasedimentary representatives, although they could have been derived from the same stratigraphic sequence.

The inverse correlation of high Sr content and low Sr_o with low Sr content and high Sr_o has been taken as representing simple mixing of primary orogenic magmas with continental crustal material in the plutonic rocks of the Idaho batholith (Fleck and Criss, 1985). Their data showed two distinct trends. For the first trend (Sr_o correlated with 1/Sr content), they constructed a simple mixing model, with the two end-members represented by the extremes in the plutonic and wall-

rock samples. They envisioned a situation where intrusion of orogenic magmas initiated anatexis and mixing of wallrock material in varying proportions to the original magmas. These magmas initially had low Sr_0 and high Sr that were altered by assimilation of the high Sr_0, low Sr containing crustal material (Fleck and Criss, 1985). The second trend is flat-lying, with little variation in the Sr regardless of initial $^{87}Sr/^{86}Sr$. The explanation for this trend was that of magmatic processes operating on oceanic igneous rock suites, and to produce the two trends with no intervening fan-shaped distribution of data points required juxtaposition of two crustal types and petrogenetic regimes (Fleck and Criss, 1985).

A similar graph has been constructed for the data from the southernmost Sierra Nevada (Figure 58). Analogous to the situation in Fleck and Criss (1985), two general trends can be distinguished, a poor correlation between Sr_0 and Sr content, and a flat trend with little variation in Sr content with Sr_0. The first trend has as its end-members the most primitive samples (low Sr_0, high Sr: hypersthene tonalite of Bison Peak and metagabbro of Tunis Creek) and the metasedimentary samples, while the flat-lying trend contains the granitic members of the gneiss complex, and extends into the same general low Sr_0, high Sr field. There is a smaller range in initial $^{87}Sr/^{86}Sr$ compared to that from the Idaho batholith. The data may actually represent a set of lines with subtlely different end-members, especially in the metasedimentary component. However, a fan-shaped distribution to the data cannot be ruled out.

A simple two-component mixing model based on strontium isotopic compositions is presented in Table 18, where

$$\% \text{ metasediment} = \frac{C_{\text{sample}} - C_{\text{upper mantle}}}{C_{\text{metasediment}} - C_{\text{upper mantle}}} \times 100 \qquad (3),$$

$$C = Sr_0 \times Sr \text{ (ppm)} \qquad (4).$$

Figure 58. Plot of initial $^{87}Sr/^{86}Sr$ vs. 1/Sr content, southernmost Sierra Nevada, for those samples studied by U/Pb zircon methods in this paper. The data is concentrated at low values of initial $^{87}Sr/^{86}Sr$ and high strontium content. In particular, the metagabbro of Tunis Creek and tonalite gneiss of Tejon Creek lie in this region. There are two trends evident in the data. The first is an inverse correlation of Sr_o with Sr content. The metasedimentary samples form the upper end of the trend. The second is a flat-lying trend with little or no change in Sr_o with decreasing Sr content. The quartzo-feldspathic gneiss of Pastoria Creek samples define this trend. LDI=late deformational intrusive rocks; BVS=tonalite of Bear Valley Springs; BP-TC=hypersthene tonalite of Bison Peak-metagabbro of Tunis Creek; TJ=tonalite gneiss of Tejon Creek; PC=quartzo-feldspathic gneiss of Pastoria Creek; ms=metasedimentary framework rocks.

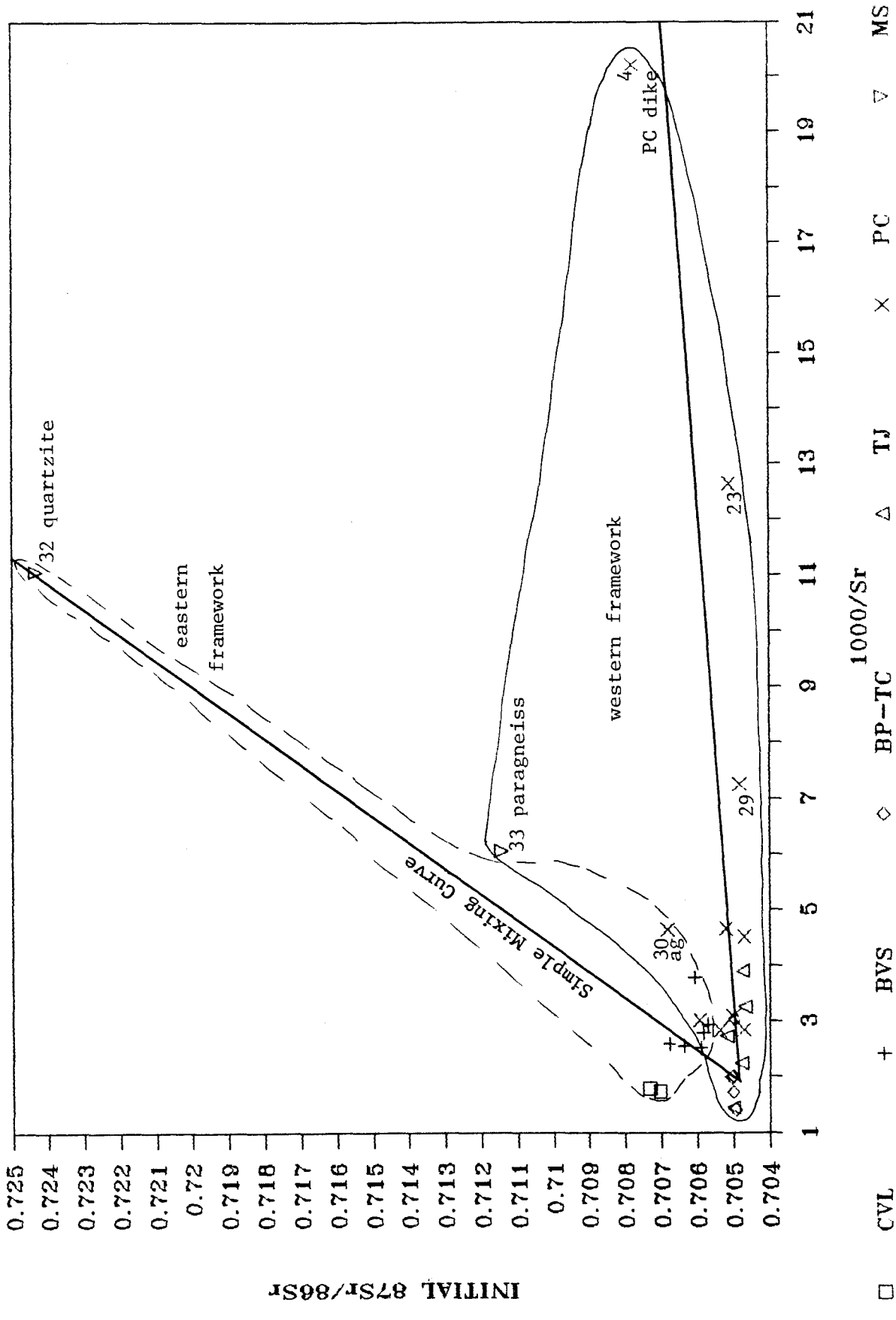
INITIAL 87Sr/86Sr
0.725
0.724
0.723
0.722
0.721
0.72
0.719
0.718
0.717
0.716
0.715
0.714
0.713
0.712
0.711
0.71
0.709
0.708
0.707
0.706
0.705
0.704
1
3
5
7
9
11
13
15
17
19
21
1000/Sr
□ CVL
+ BVS
◇ BP-TC
△ TJ
× PC
▽ MS
32 quartzite
eastern framework
Simple Mixing Curve
33 paragneiss
western framework
4×
PC dike
23×
29×
30×
ag

Table 18. Rubidium and strontium mixing models

SAMPLE #	NAME	$^{87}Sr/^{86}Sr$ initial	Atom percent incorporated metasediment SSN-qa 0.7035 0.7243	SSN-qb 0.7047 0.7243	SSN-pa 0.7035 0.7115	SSN-pb 0.7047 0.7115
Late deformational intrusive suite						
1	TC27	0.70731	18.3	13.4	47.9	38.9
2	TC40	0.70703	16.9	12.0	44.3	34.8
4	PC35	0.70776	20.4	15.7	53.5	45.5
Bear Valley Springs intrusive suite						
6	TC15	0.70583	11.2	5.9	29.3	17.1
7	TC42	0.70570	10.6	5.2	27.6	15.2
8	CM25	0.70591	11.6	6.3	30.3	18.3
9	CM26	0.70637	13.8	8.6	36.1	25.0
10	CM9	0.70677	15.7	10.7	41.1	30.9
11	CM22b	0.70605	12.2	7.0	32.0	20.3
12	TL197	0.70496	7.0	1.5	18.0	4.3
13	WR84	0.70499	7.1	1.6	18.7	4.7
14	WR86	0.70504	7.4	1.9	19.3	5.4
15	WR190	0.70499	7.1	1.6	18.7	4.7
16	PC227	0.70493	6.9	1.3	18.0	3.8
Tehachapi suite						
17	CM630	0.70472	5.9	0.3	15.3	0.7
18	WR643	0.70518	8.1	2.6	21.1	7.5
19	WR171	0.70467	5.6	0.0	14.7	0.0
20	WR30/2	0.70478	6.1	0.6	16.1	1.6
21	WR39	0.70499	7.1	1.6	18.7	4.7
22	PC31	0.70519	8.1	2.6	21.2	7.7
23	PC32	0.70510	7.7	2.2	20.1	6.3
24	PC34	0.70469	5.7	0.1	14.9	0.3
25	PC36	0.70500	7.2	1.7	18.8	4.9
26	PC37	0.70469	5.7	0.1	14.9	0.3
27	PC129	0.70594	11.7	6.5	30.7	18.7
28	WR91a	0.70536	8.9	3.5	23.4	10.2
29	WR40	0.70480	6.2	0.7	16.3	1.9
30	TC12a	0.70682	15.9	10.9	41.7	31.7

The amount of metasedimentary component is tabulated as: q=quartzite, p=paragneiss. Upper mantle component initial $^{87}Sr/^{86}Sr$=0.7035 (SSN-qa,SSN-pa), from Fleck and Criss (1985) and Taylor (1980), or 0.7047 (SSN-qb,SSN-pb), from southern Sierran data. Metasedimentary initial $^{87}Sr/^{86}Sr$=0.7243 (SSN-q), or 0.7115 (SSN-p) from the southern Sierran data. Sr_o values were calculated for the metasedimentary components at 100 Ma (quartzite, tonalite of Bear Valley Springs age, Sr_o=0.7258) or 108 Ma (paragneiss of Comanche Point lower intercept, Sr_o=.7144).

Four sets of calculations were performed. The first (SSN-qa) and third (SSN-pa) sets used a pristine, non-contaminated upper mantle Sr_o of 0.7035, based on the Idaho batholith end-member of Fleck and Criss (1985), an analysis from a gabbro in the study area (D.A. Pickett, unpublished data, 1986), and from gabbros in the western Cretaceous part of the Sierra Nevada (Saleeby and Chen, 1978), and the respective metasedimentary Sr_o values from the quartzite (0.7243) and paragneiss (0.7115). The second (SSN-qb) and fourth (SSN-pb) sets used the contaminated extreme low Sr_o value from the southern Sierran data (0.7047) as a lower end-member, with the appropriate metasedimentary upper end-member. Based partly on the zircon discordance patterns, the "contaminated" Sr_o=0.7047 may represent the Sr isotopic signature from a potential third component in the mixing system that was introduced into the magmas at lower crustal levels below the level of emplacement. This material may be part of the lower crust beneath the Kings sequence framework rocks, or altered oceanic crustal materials introduced into the magma genesis zone by subduction.

A general result of the initial Sr mixing model indicates 2.5 to 3 times as much paragneiss would be required as a metasedimentary component compared to the quartzite, and samples with an uncontaminated upper mantle source would require more metasedimentary material than a source that carries a higher Sr_o into the mixing area. Granitic rocks, and rocks east of the Sr_o=0.706 isopleth require a larger metasedimentary component. With the exception of the samples east of the Sr_o=0.706 isopleth, an uncontaminated mantle source indicates 6-16% quartzite and 15-36% paragneiss, while a contaminated source indicates 0-11% quartzite and 0-25% paragneiss. These results are comparable to or slightly lower than those derived from simple mixing using the $\delta^{18}O$ isotopic ratios (Table 17). Overall, the amount of metasedimentary material incorporated into the rocks of

the southern Sierra Nevada is considerably less than the amount calculated for the Idaho batholith (up to 75%, Fleck and Criss, 1985).

Fleck and Criss (1985) tested the simple mixing model by comparing initial $^{87}Sr/^{86}Sr$ with Rb content. Their data showed a very rough concave upward curve that grossly fit the data. Figure 59 shows the same plot (Sr_o vs Rb) for the southern Sierra. There appears to be little correlation of Sr_o with Rb in Figure 59. This may represent difficulties with the mixing model, or a reflection of the lower degree of mixing involved (as per the above discussion). In addition, the quartzite end-member does not have a high Rb content compared to the paragneiss of Comanche Point, possibly the result of bulk composition.

The Rb/Sr results from this study are summarized on a series of strontium evolution diagrams (Figure 60). A pair of pseudoisochrons can be constructed for the gneiss complex samples. The first pseudoisochron can be drawn through the Pastoria Creek samples, and extrapolates just below the field of the Tunis Creek samples (Figure 60a,c). The pseudoisochron has an "age" of 120 Ma, with a Sr_o=0.7047, which is the same as the minimum value obtained from the southernmost Sierra. The samples which plot along this trend belong to parts of the Tejon Creek and Pastoria Creek units, including all granitic samples from the gneiss complex. The pseudoisochron can be interpreted as the mixing of a two component system represented by a low $^{87}Sr/^{86}Sr$-low $^{87}Rb/^{86}Sr$ end-member and a Pastoria Creek granitic end-member. Thus, the Tejon Creek samples have Rb/Sr characteristics suggestive of mixing of the previously mentioned two end-members. An alternate interpretation could be that the line is a true isochron, perhaps indicating anatexis and melt production in the mid-Cretaceous. Nonetheless, the granitic rocks show Rb/Sr enrichment relative to tonalitic and gabbroic samples. A second pseudoisochron can be drawn through the remainder of the

Figure 59. Plot of initial $^{87}Sr/^{86}Sr$ versus rubidium content. There are no strong correlations evident in the data. The values for Sr_o show little variation with rubidium content, with the exception of the quartzite (high initial $^{87}Sr/^{86}Sr$, low Rb content). LDI=late deformational intrusive rocks; BVS=tonalite of Bear Valley Springs; BP-TC=hypersthene tonalite of Bison Peak-metagabbro of Tunis Creek; TJ=tonalite gneiss of Tejon Creek; PC=quartzo-feldspathic gneiss of Pastoria Creek; ms=metasedimentary framework rocks.

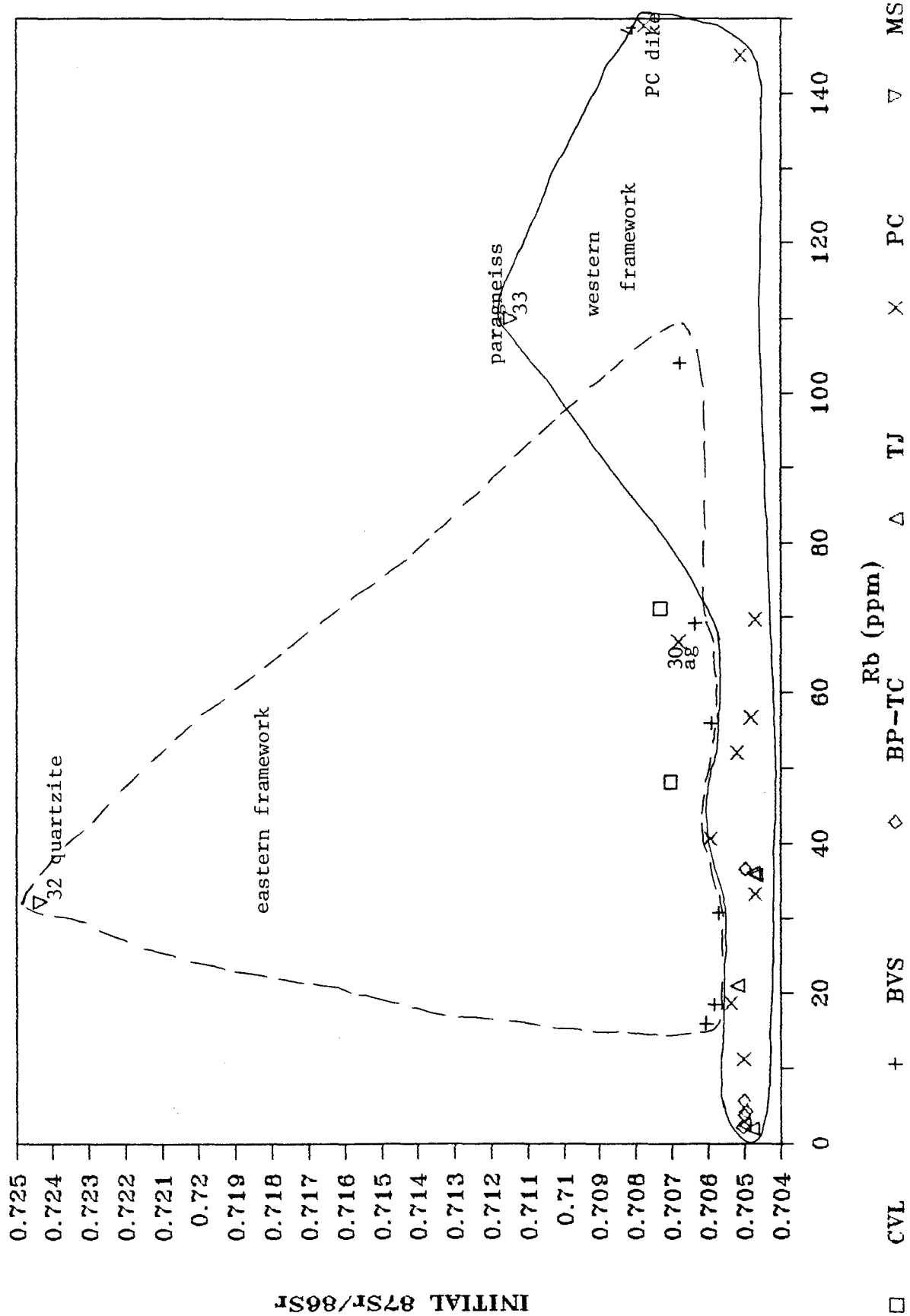
INITIAL 87Sr/86Sr
0.725
0.724
0.723
0.722
0.721
0.72
0.719
0.718
0.717
0.716
0.715
0.714
0.713
0.712
0.711
0.71
0.709
0.708
0.707
0.708
0.705
0.704
0
20
40
60
80
100
120
140
Rb (ppm)
CVL
BVS
BP-TC
TJ
PC
MS
quartzite
32
eastern framework
paragneiss
33
western framework
PC dike
30
ag

Figure 60. Strontium evolution diagrams for the southernmost Sierra Nevada, a plot of $^{87}Rb/^{86}Sr$ against $^{87}Sr/^{86}Sr$. There is a grouping of the data at low values for $^{87}Sr/^{86}Sr$ and $^{87}Rb/^{86}Sr$. (a) shows all samples from the study area, including the metasedimentary samples, along with the 120 Ma and 250 Ma pseudoisochrons; (b) is an enlargement of the area of low $^{87}Sr/^{86}Sr$ and low $^{87}Rb/^{86}Sr$; (c) includes all samples from the gneiss complex of the Tehachapi Mountains, with the 120 Ma isochron and 335 Ma pseudoisochron; (d) includes samples from the Bear Valley Springs intrusive suite, with the 95 Ma isochron and the 250, 565 Ma pseudoisochrons; (e) shows the family of isochrons and pseudoisochrons constructed in the earlier plots (a-d), along with samples enriched in $^{87}Sr/^{86}Sr$ and $^{87}Rb/^{86}Sr$. LDI=late deformational intrusive rocks; BVS=tonalite of Bear Valley Springs; BP-TC=hypersthene tonalite of Bison Peak-metagabbro of Tunis Creek; TJ=tonalite gneiss of Tejon Creek; PC=quartzo-feldspathic gneiss of Pastoria Creek (t=tonalite, g=granite); ms=metasedimentary framework rocks.

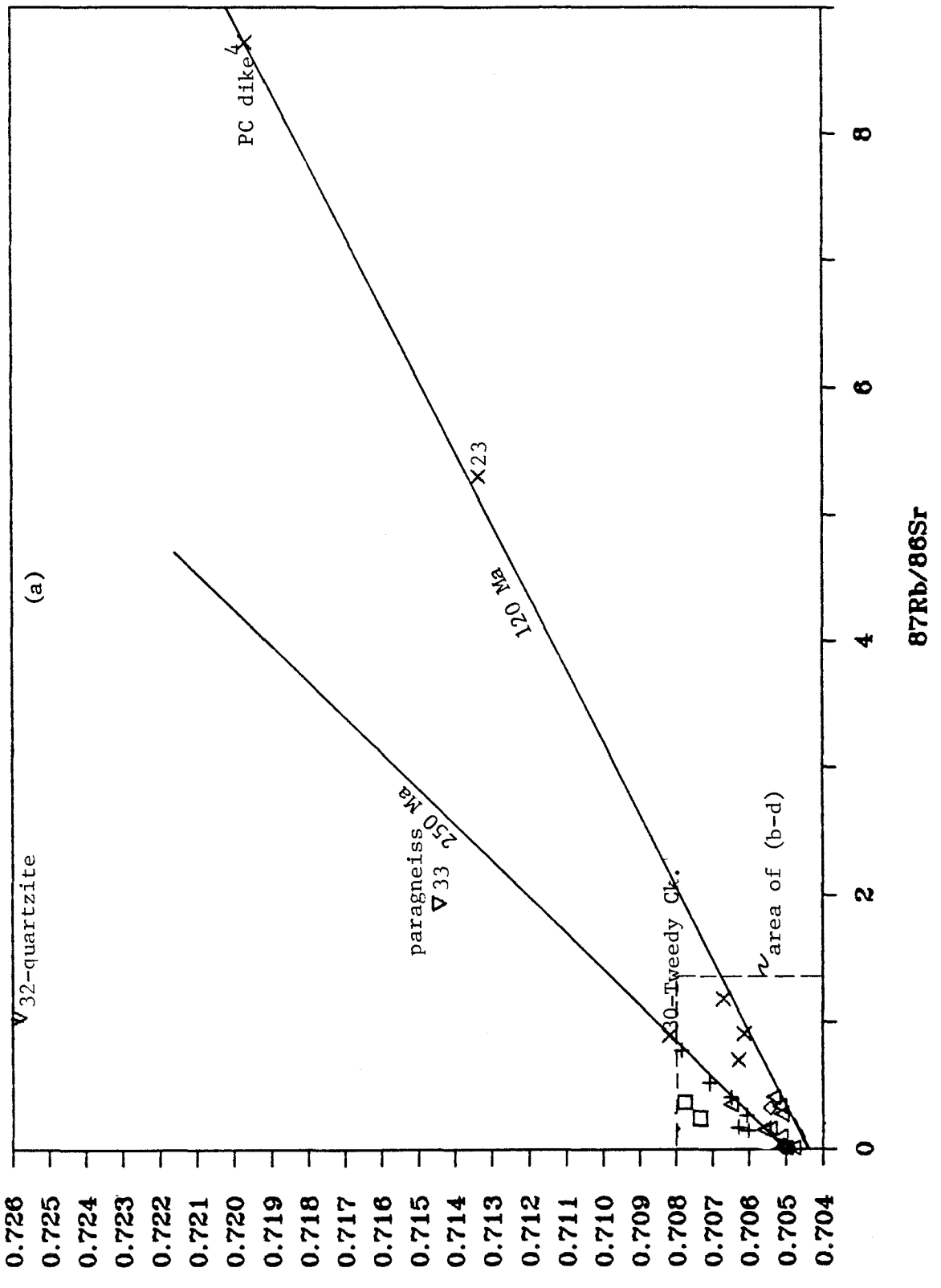
(a)
32-quartzite
PC dike
X23
120 Ma
paragneiss
33
250 Ma
30-Tweedy Ck.
area of (b-d)
0.726
0.725
0.724
0.723
0.722
0.721
0.720
0.719
0.718
0.717
0.716
0.715
0.714
0.713
0.712
0.711
0.710
0.709
0.708
0.707
0.706
0.705
0.704
0
2
4
6
8
87Sr/86Sr
87Rb/86Sr

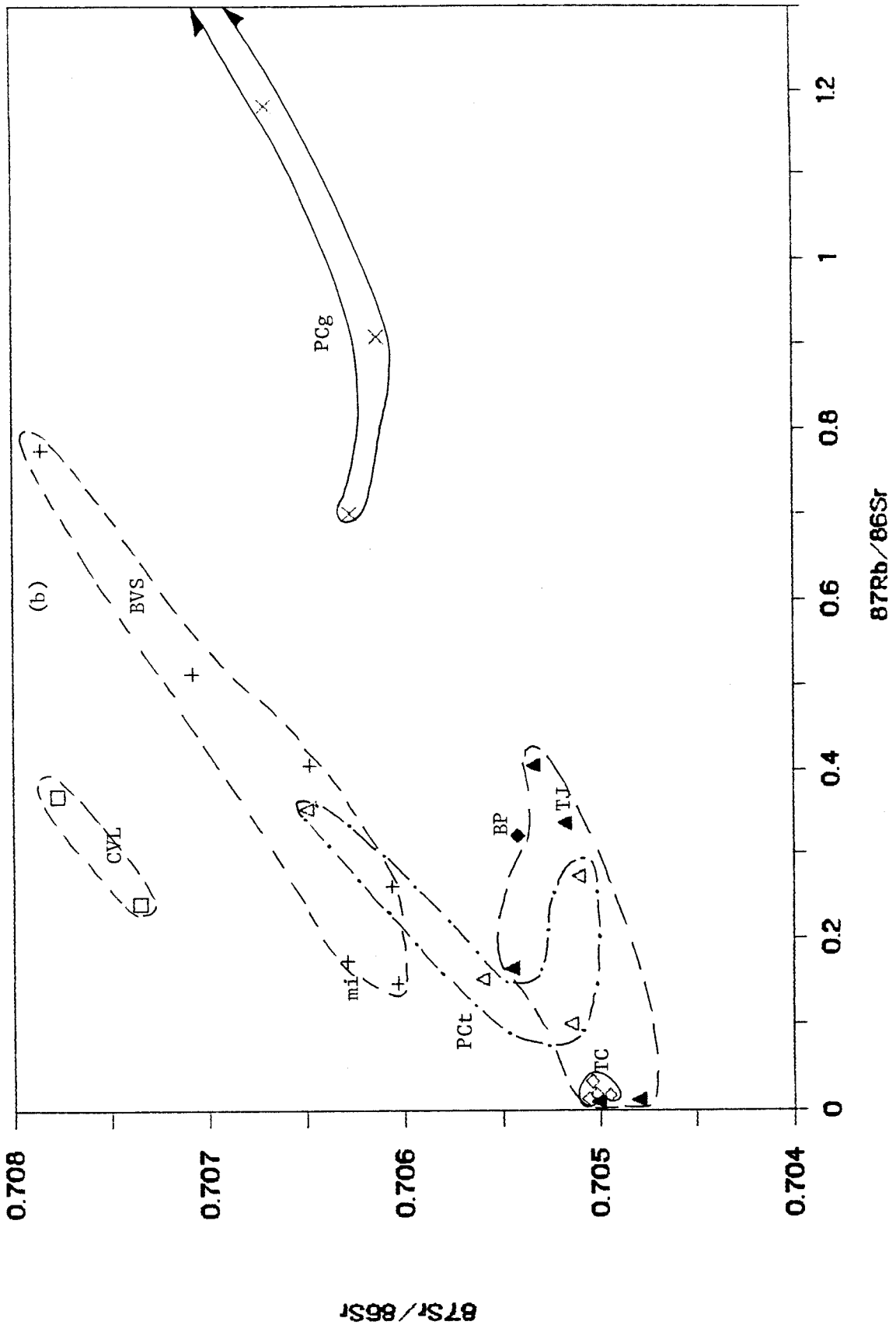
(b)
PCg
BVS
CWL
mi
PCt
BP
TJ
TC
0.708
0.707
0.706
0.705
0.704
0
0.2
0.4
0.6
0.8
1
1.2
87Sr/86Sr
87Rb/86Sr

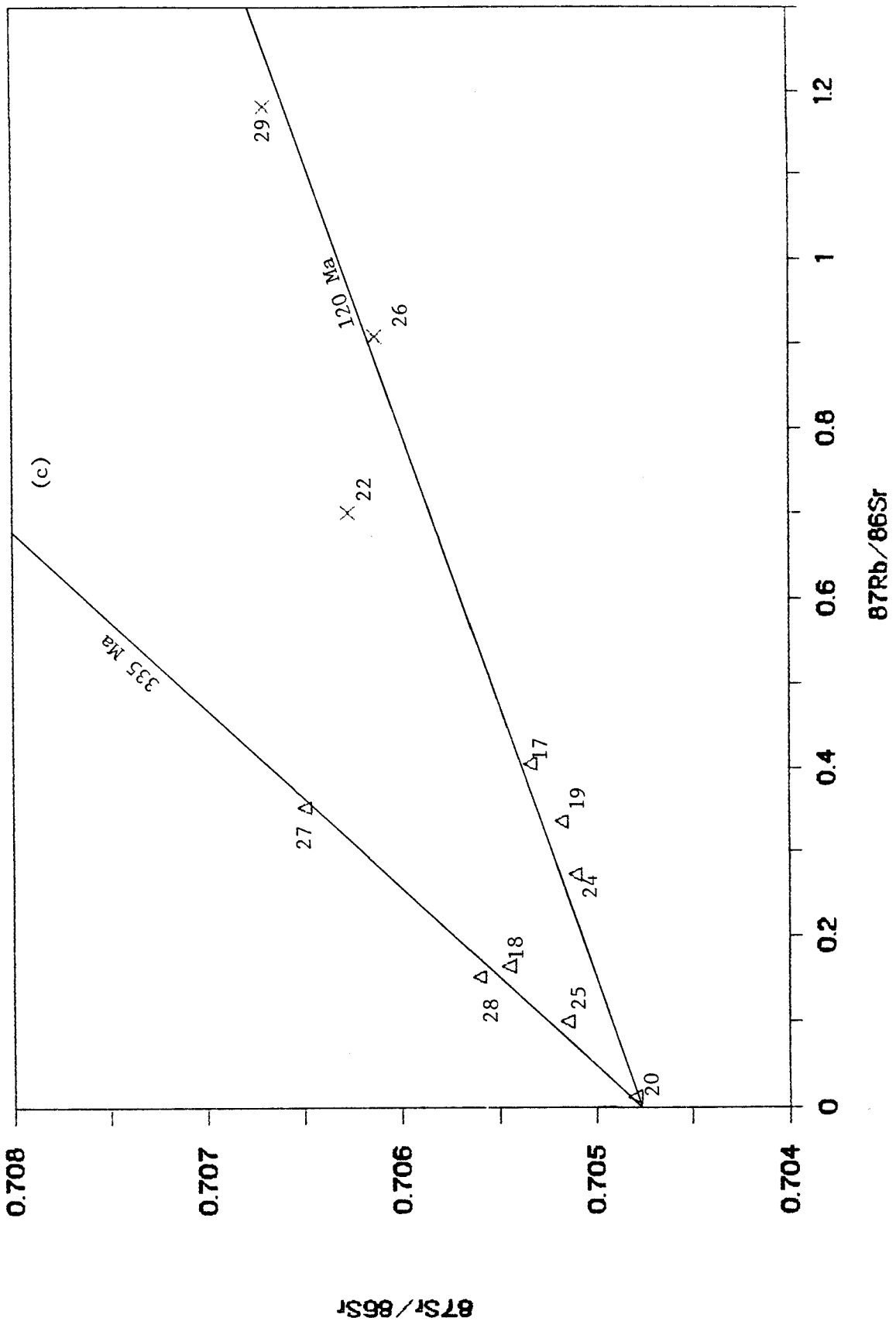
(c)
335 Ma
120 Ma
27
28
18
25
20
17
19
24
22
26
29
0.708
0.707
0.706
0.705
0.704
87Sr/86Sr
0
0.2
0.4
0.6
0.8
1
1.2
87Rb/86Sr

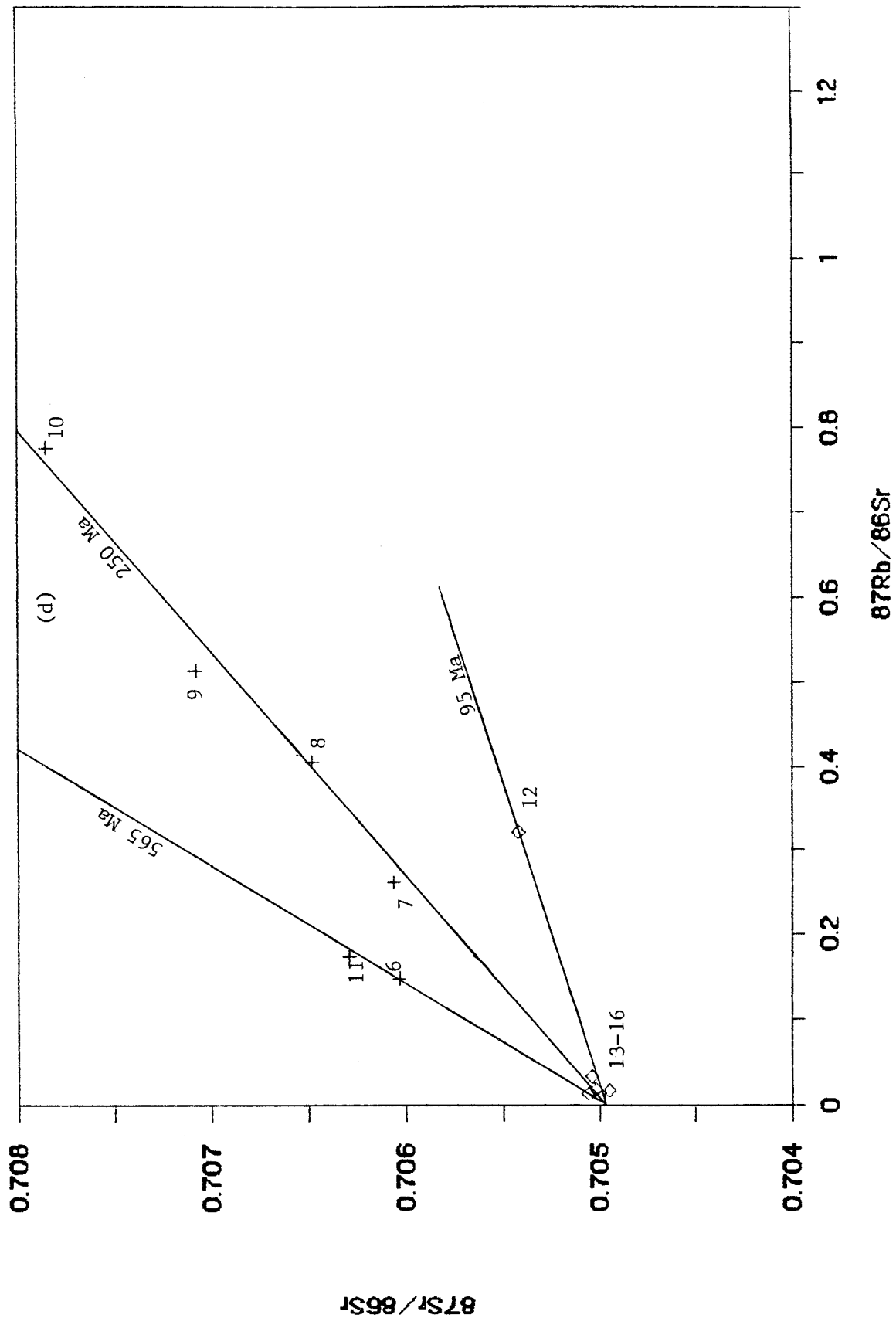
(d)
565 Ma
250 Ma
95 Ma
10
9
8
7
6
11
12
13-16
0.708
0.707
0.706
0.705
0.704
0
0.2
0.4
0.6
0.8
1
1.2
87Sr/86Sr
87Rb/86Sr

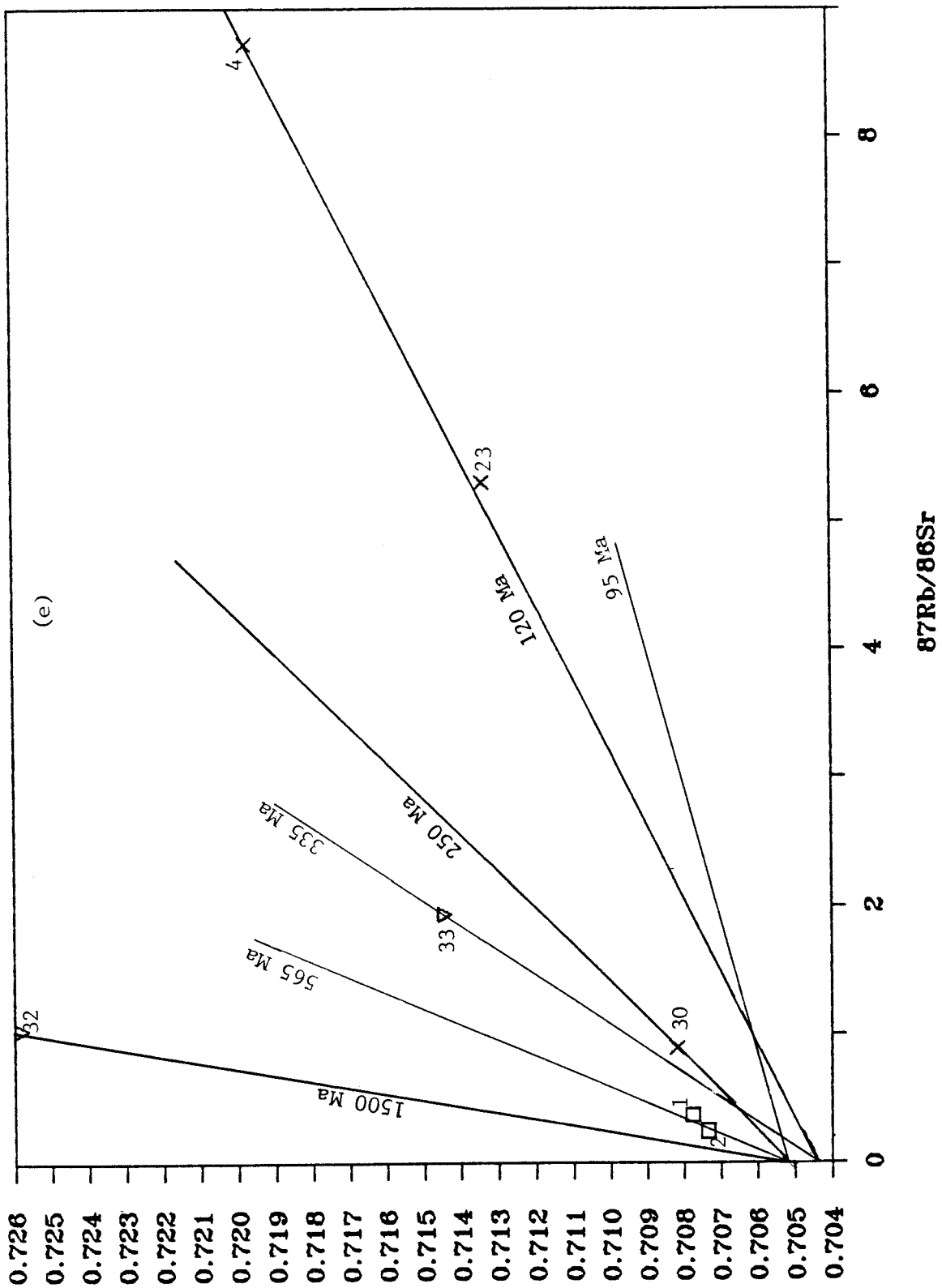
87Sr/86Sr
87Rb/86Sr
(e)
1500 Ma
565 Ma
335 Ma
250 Ma
120 Ma
95 Ma
1
2
30
33
23
4
32
0.726
0.725
0.724
0.723
0.722
0.721
0.720
0.719
0.718
0.717
0.716
0.715
0.714
0.713
0.712
0.711
0.710
0.709
0.708
0.707
0.706
0.705
0.704
0
2
4
6
8

gneiss complex samples (Figure 60c). It has an "age" of 335 Ma, and the same Sr_o as the previous pseudoisochron. The samples which plot along this line are tonalites from both the Tejon Creek and Pastoria Creek units.

A second set of pseudoisochrons can be constructed through the field of the Bear Valley Springs suite of samples. They have "ages" of 95, 250, and 565 Ma, with Sr_o=0.7050, within the Tunis Creek field. The 95 Ma line (Figure 60d) contains the Bison Peak sample, with an age that approximates the zircon age for the sample. The 250 Ma line (Figure 60a,d) contains analyses from the main and eastern phases of the tonalite of Bear Valley Springs furthest removed from metamorphic framework rocks. The third line (Figure 60d) contains the eastern phase sample near the margin of the pluton, and a mafic inclusion within the pluton. A possible explanation for the latter two relations (R.W. Kistler, personal communication, 1985) could be mixing of 100 Ma (concordant zircon age) and older magmatic products derived from older crustal materials. The older material may represent Paleozoic to upper Mesozoic oceanic crust or upper mantle (Saleeby, 1982; Saleeby and Sharp, 1980), and/or a lower continental crustal (Hill, 1984) end-member. The Paleozoic ages can also be found as the potential "upper intercepts" of some of the discordant U/Pb ages. However, these ages are not associated with the tonalite of Bear Valley Springs, which has seven concordant analyses. In addition, there is no direct evidence for such material in the southern Sierra. The only evidence for its existence is this data, basement core data from beneath the southern end of the San Joaquin Valley (Ross, 1979), and extrapolation of regional trends of appropriate aged material in the Kaweah River area (Saleeby, 1979) southeastward 100 km into the study area. Thus, the Paleozoic "ages" may well be artificial.

Figure 60e shows the four pseudoisochrons derived from the plutonic and orthogneiss samples, and those samples with high $^{87}Sr/^{86}Sr$ and $^{87}Rb/^{86}Sr$ ratios. Several coincidences between pseudoisochrons and data points can be seen. The 120 Ma line, the Pastoria Creek sample (#32), and garnet granite dike (#4) coincide. This pattern suggests that the 120 Ma line is a true isochron with an age approximately equal to the oldest age determined from the gneiss complex (117 Ma). The 335 Ma line and the paragneiss (#33) coincide. Intimate field relations clearly show mixing of the paragneiss and Tejon Creek units. The 250 Ma line coincides with the Tweedy Creek sample (#30), while the 565 Ma line coincides with the Claraville (#1) and tonalite stock (#2) samples. For each of the latter two cases the geographic settings are the same, and thus the 250, 335, and 565 Ma pseudoisochrons could represent mixing relations as discussed above.

The Pastoria Creek dike (#4) is a two mica, garnet granite dike that has a peraluminuous character and is highly enriched in $^{87}Rb/^{86}Sr$. It falls on an extreme extrapolation of the 120 Ma isochron, which is not likely due to mere coincidence. The zircon age of the sample has an age of 97 Ma, with evidence for a minor amount of inheritance. Field relations suggest an origin as a partial melt product derived from the Pastoria Creek gneisses. Therefore, its Rb/Sr systematics are believed to represent a magmatic event at approximately 120 Ma that produced the Pastoria Creek orthogneisses, with the 97 Ma zircon age representing the time of partial melting and production of the dike related to the Bear Valley Springs thermal event.

A plot of $^{87}Rb/^{86}Sr$ vs. initial $^{87}Sr/^{86}Sr$ is shown in Figure 61. It has a large cluster of points at low Sr_o, low $^{87}Rb/^{86}Sr$, similar to Figure 58. Two trends can be seen in Figure 61, which is analogous to what Fleck and Criss (1985) found, and almost identical to the result in Figure 58 (Sr_o vs 1/Sr). The first trend

Figure 61. Plot of $^{87}Rb/^{86}Sr$ versus initial $^{87}Sr/^{86}Sr$. The data is concentrated at low values of Sr_o and low $^{87}Rb/^{86}Sr$. Two weak trends can be constructed through the data. The first is a flat-lying trend (little to no change in Sr_o with respect to $^{87}Rb/^{86}Sr$), while the second is a positive correlation between $^{87}Sr/^{86}Sr$ and $^{87}Rb/^{86}Sr$. This line trends towards values for the metasedimentary samples. LDI=late deformational intrusive rocks; BVS=tonalite of Bear Valley Springs; BP-TC=hypersthene tonalite of Bison Peak-metagabbro of Tunis Creek; TJ=tonalite gneiss of Tejon Creek; PC=quartzo-feldspathic gneiss of Pastoria Creek; ms=metasedimentary framework rocks.

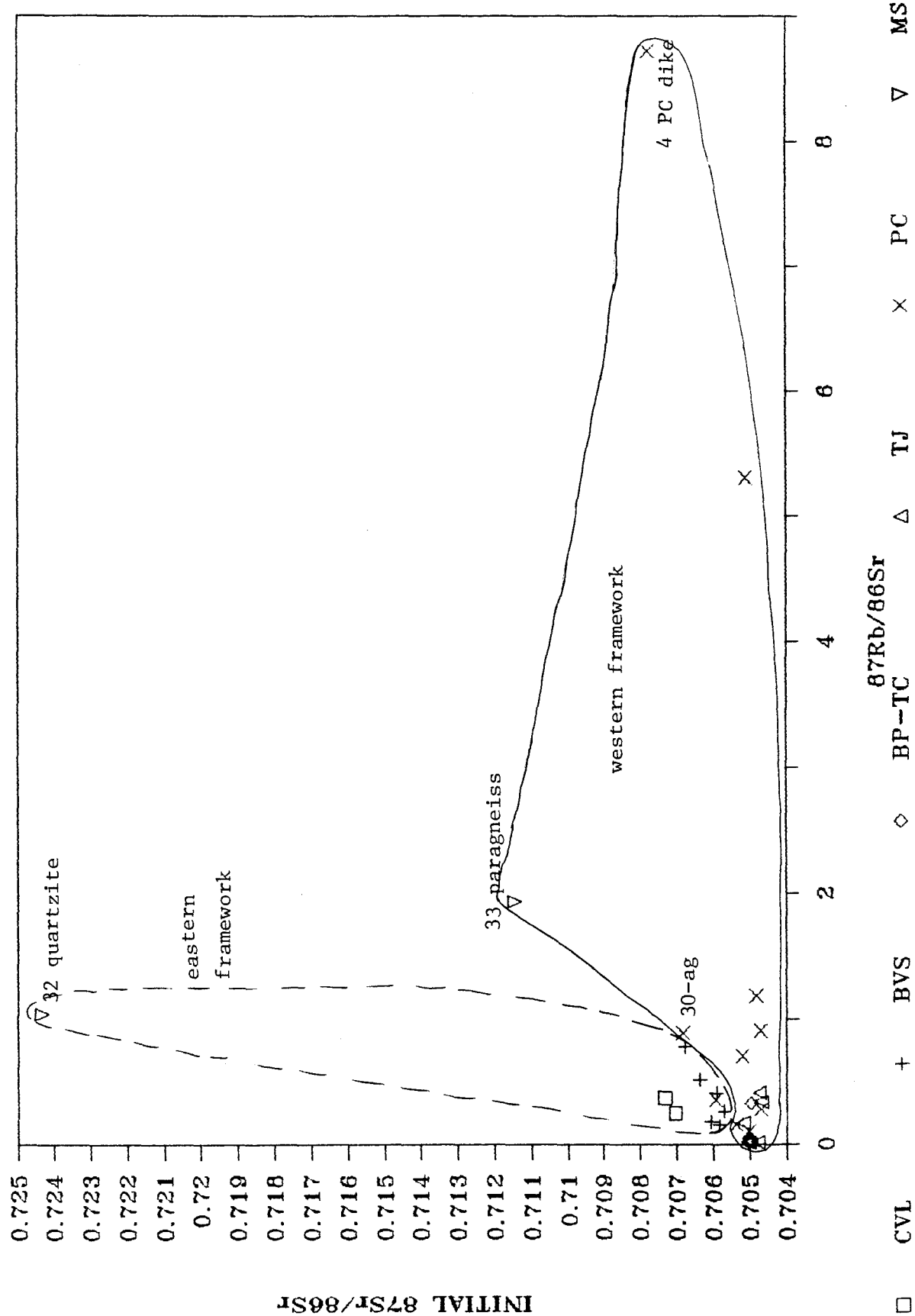
INITIAL 87Sr/86Sr
0.725
0.724
0.723
0.722
0.721
0.72
0.719
0.718
0.717
0.716
0.715
0.714
0.713
0.712
0.711
0.71
0.709
0.708
0.707
0.706
0.705
0.704
0
2
4
6
8
87Rb/86Sr
32 quartzite
eastern framework
33 paragneiss
western framework
4 PC dike
30-ag
CVL
BVS
BP-TC
TJ
PC
MS

is flat-lying, with little variation in Sr_0 relative to Rb/Sr. This is believed to represent crystal fractionation. The second trend is a weak general increase of Sr_0 with Rb/Sr towards the metasedimentary samples. Fleck and Criss (1985) have interpreted a correlation of Sr_0 with $^{87}Rb/^{86}Sr$ as representing mixing of upper mantle and metasedimentary components, and the existance of two trends as requiring two different magmatic and mixing processes.

IV.2.3 Summary and discussion of the geochemistry

This section will discuss the oxygen, rubidium, and strontium isotopic variations relative to one another, and relative to the zircon U/Pb data. Following that will be a discussion of the data as it relates to each unit in a sequential fashion, and a summary of the zircon, oxygen, and strontium mixing models.

Using the values given in Table 14 and Table 17, U/Pb age data, $\delta^{18}O$, Rb, Sr, and initial $^{87}Sr/^{86}Sr$ values have been plotted against one another (Figures 62a-d, 63). Figures 62a-d (U/Pb age vs. $\delta^{18}O$, Rb, Sr, and initial $^{87}Sr/^{86}Sr$) show an overlap of the Pastoria Creek and Tejon Creek fields (most strongly when related to $\delta^{18}O$ and initial $^{87}Sr/^{86}Sr$), with a clear distinction between those samples and samples from the Bear Valley Springs and late deformational intrusive suites. On Figure 63 ($\delta^{18}O$ vs. initial $^{87}Sr/^{86}Sr$ for plutonic rocks), the field of the Peninsular Ranges batholith (Taylor and Silver, 1978) and the field of the San Jacinto block samples are shown. With the exception of the tonalite of Bear Valley Springs, samples from the southernmost Sierra Nevada plot within the Peninsular Ranges field, and show evidence of two-component (upper mantle and metasedimentary) mixing. The tonalite of Bear Valley Springs samples trend toward the San Jacinto field. Hill (1984) interprets the San Jacinto samples as representing a third component, namely lower crustal material. The tonalite of Bear Valley Springs may have had a similar source region. Support for this can be found in the strontium pseudoisochrons that have ages of 250 and 565 Ma.

Figure 62. Plots of U/Pb zircon age against various geochemical parameters for the crystalline rocks of the southernmost Sierra Nevada. (a)=$\delta^{18}O$, (b)=initial $^{87}Sr/^{86}Sr$, (c)=strontium content, (d)=rubidium content. These plots show a distinct age gap between 102 and 110 Ma. Each unit plots in a distinct field, with the exception of the the quartzo-feldspathic gneiss of Pastoria Creek and tonalite gneiss of Tejon Creek units, which overlap. LDI=late deformational intrusive rocks; BVS=tonalite of Bear Valley Springs; BP-TC=hypersthene tonalite of Bison Peak-metagabbro of Tunis Creek; TJ=tonalite gneiss of Tejon Creek; PC=quartzo-feldspathic gneiss of Pastoria Creek; ms=meta-sedimentary framework rocks.

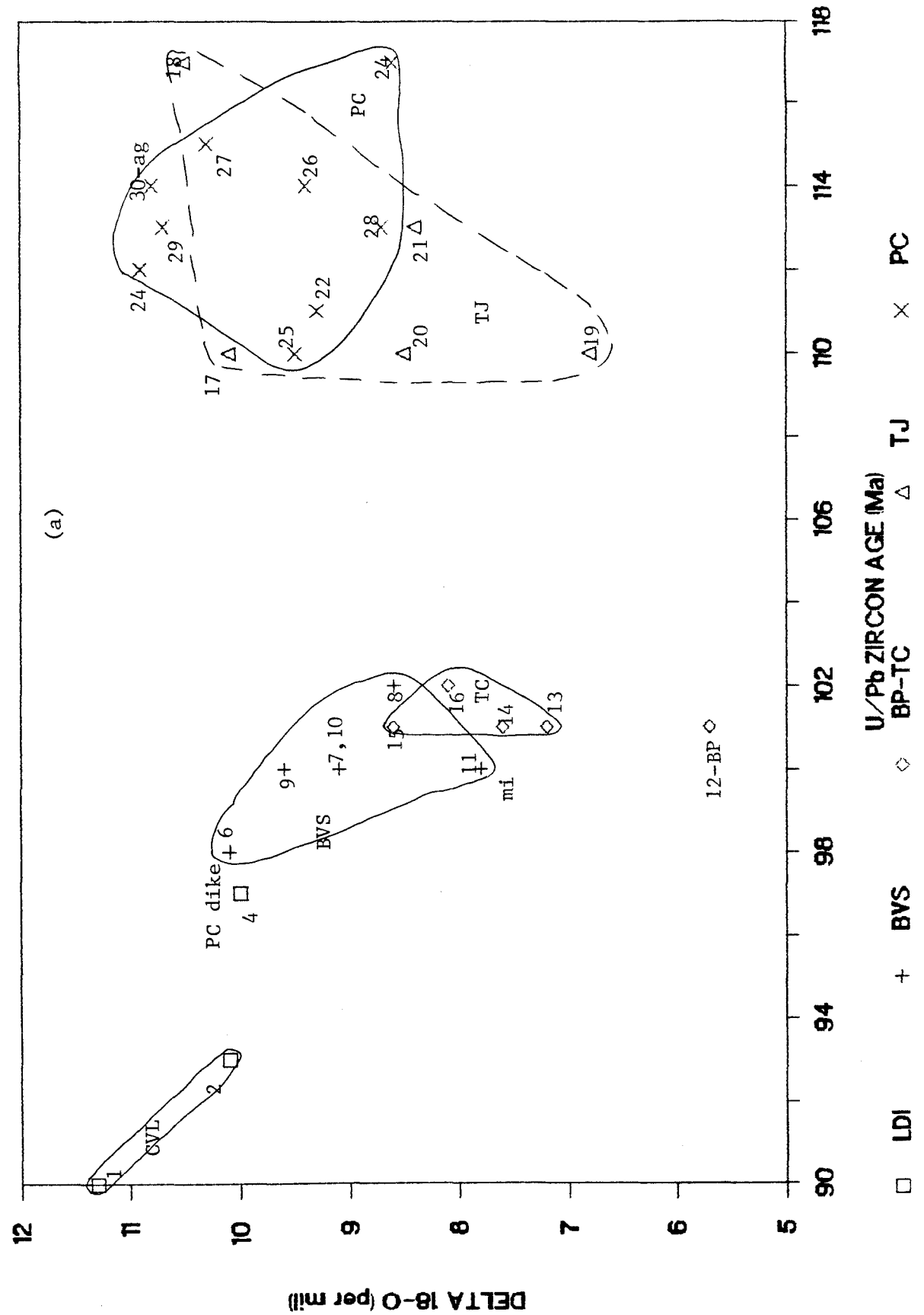
DELTA 18-O (per mil)
12
11
10
9
8
7
6
5
90
94
98
102
106
110
114
118
U/Pb ZIRCON AGE (Ma)
□ LDI
+ BVS
◇ BP-TC
△ TJ
× PC
(a)
PC dike
4
+6
9+
+7,10
BVS
15
8+
16
TC
14
13
11
+
mi
12-BP
17
Δ
25
×22
24
29
30-ag
27
×26
28
21
Δ
PC
24
18
Δ20
TJ
Δ19

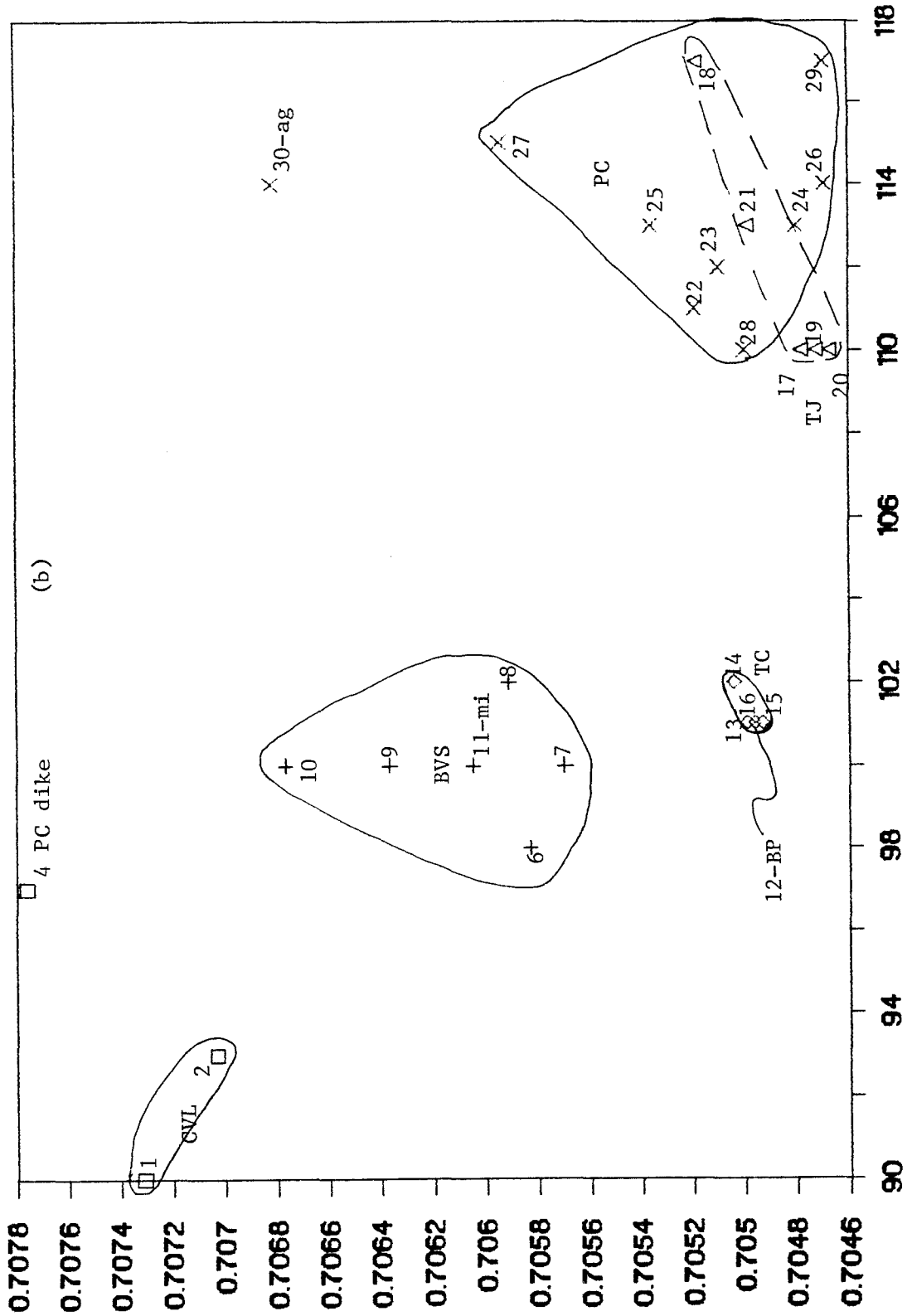
INITIAL 87Sr/86Sr
0.7078
0.7076
0.7074
0.7072
0.707
0.7068
0.7066
0.7064
0.7062
0.706
0.7058
0.7056
0.7054
0.7052
0.705
0.7048
0.7046
90
94
98
102
106
110
114
118
U/Pb ZIRCON AGE (Ma)
(b)
4 PC dike
30-ag
CVL
BVS
PC
TJ
TC
12-BP
LDI
BVS
BP-TC
TJ
PC

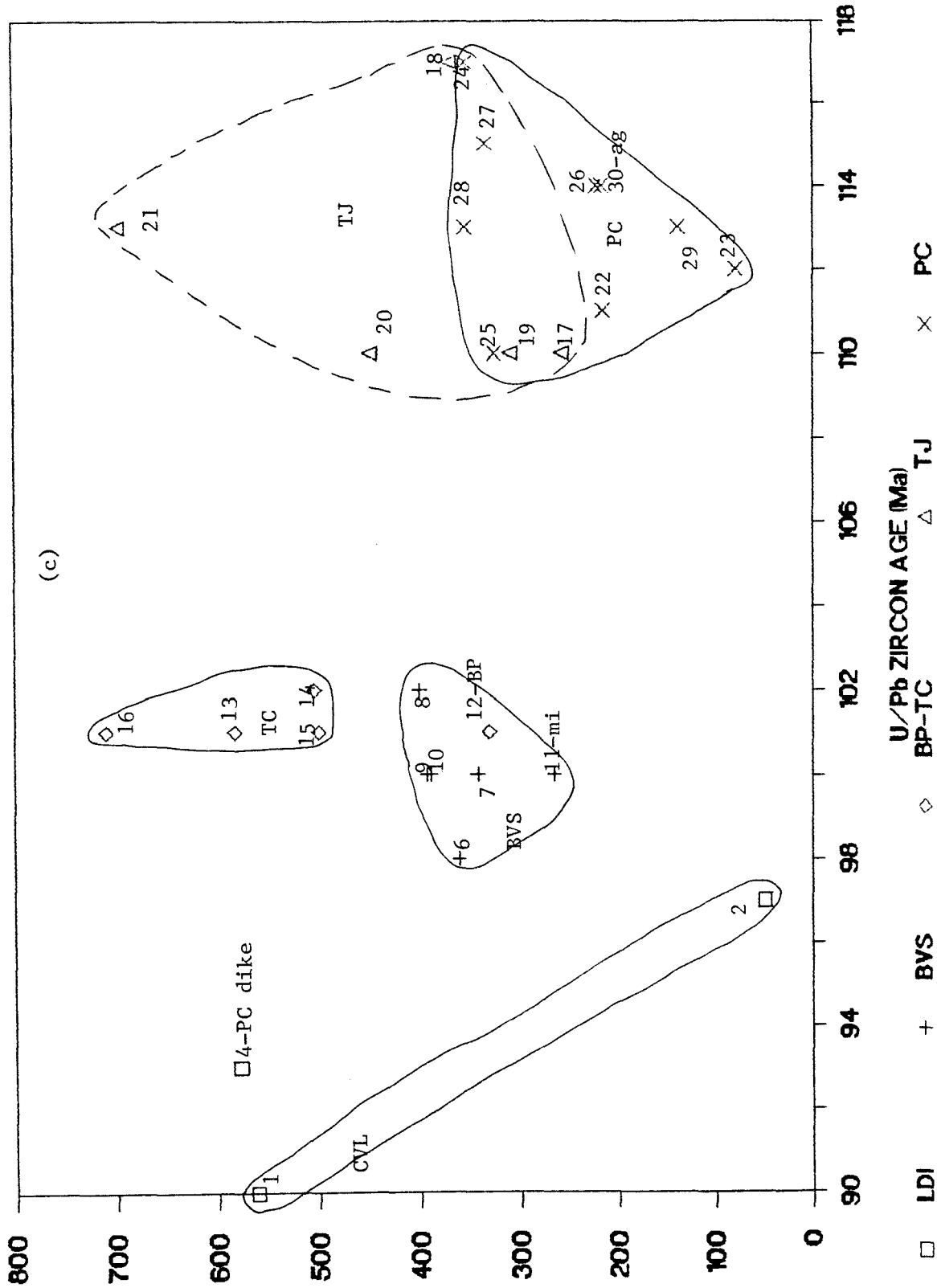
STRONTIUM CONTENT (ppm)
800
700
600
500
400
300
200
100
0
90
94
98
102
106
110
114
118
U/Pb ZIRCON AGE (Ma)
LDI
BVS
BP-TC
TJ
PC
(c)
4-PC dike
CVL
TC
TJ
PC
BVS
11-mi
12-BP

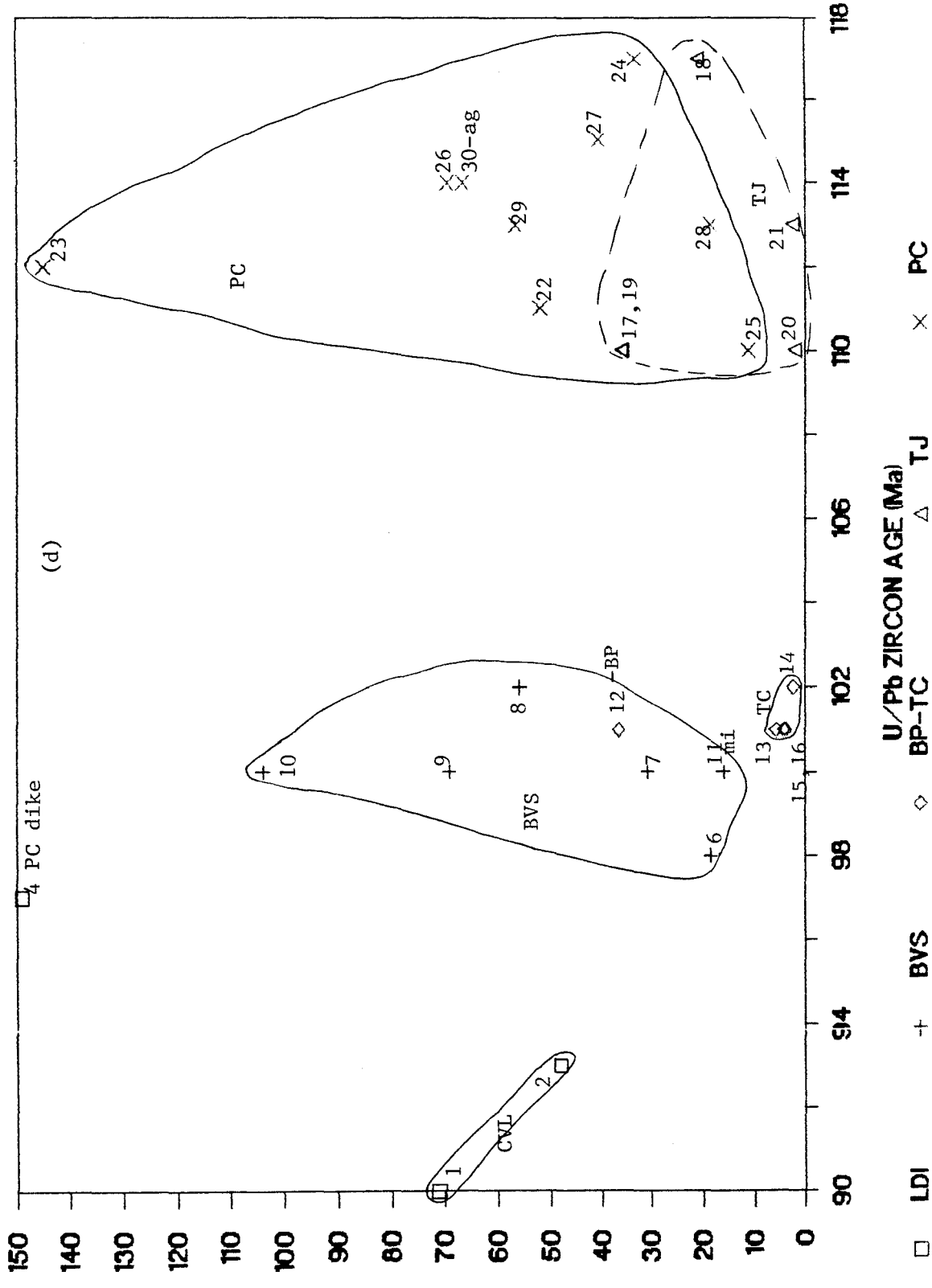
RUBIDIUM CONTENT (ppm)
150
140
130
120
110
100
90
80
70
60
50
40
30
20
10
0
90
94
98
102
106
110
114
118
U/Pb ZIRCON AGE (Ma)
(d)
4 PC dike
PC
BVS
CWL
BP
TC
TJ
mi
1
2
6
7
8
9
10
11
12
13
14
15
16
17,19
18
20
21
22
23
24
25
26
27
28
29
30-ag
□ LDI
+ BVS
◇ BP-TC
△ TJ
× PC

Figure 63. Plot of $\delta^{18}O$ against initial $^{87}Sr/^{86}Sr$ for plutonic rocks of the southernmost Sierra Nevada. Most of the samples plot within the field of the Peninsular Ranges batholith as defined by Taylor and Silver (1978). The majority of samples have low initial $^{87}Sr/^{86}Sr$ and low $\delta^{18}O$, while the samples from the granodiorite of Claraville and the augen gneiss of Tweedy Creek plot at moderate values of Sr_o and $\delta^{18}O$. These samples trend towards the field for the metasedimentary rocks (high Sr_o, high $\delta^{18}O$). Samples from the tonalite of Bear Valley Springs trend away from the Peninsular Ranges batholith field, toward and partly within the San Jacinto block field (Taylor and Silver, 1978). LDI=late deformational intrusive rocks; BVS=tonalite of Bear Valley Springs; BP-TC=hypersthene tonalite of Bison Peak-metagabbro of Tunis Creek; TJ=tonalite gneiss of Tejon Creek; PC=quartzo-feldspathic gneiss of Pastoria Creek; ms=metasedimentary framework rocks.

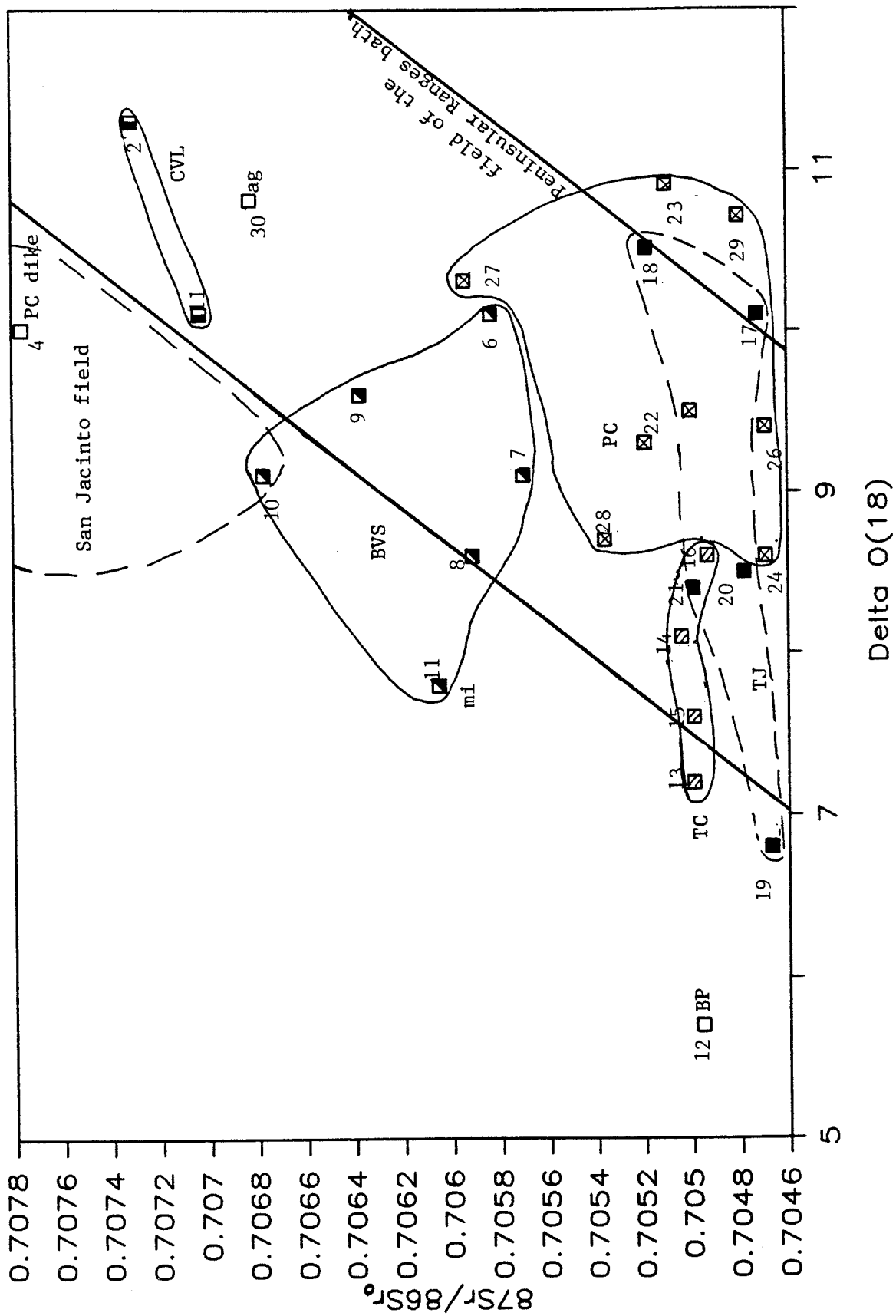
Field of the Peninsular Ranges batholith
San Jacinto field
PC dike
CVL
ag
BVS
PC
TC
TJ
BP
mi
0.7078
0.7076
0.7074
0.7072
0.707
0.7068
0.7066
0.7064
0.7062
0.706
0.7058
0.7056
0.7054
0.7052
0.705
0.7048
0.7046
87Sr/86Sr
5
7
9
11
Delta O(18)

Figure 63 is enlarged in Figure 64 ($\delta^{18}O$ vs. initial $^{87}Sr/^{86}Sr$) to cover all samples in the southernmost Sierras. The quartzite and paragneiss of Comanche Point at 100 and 108 Ma are also shown as potential metasedimentary end-members. The data have been grouped into two sectors based on their geographic distribution. The eastern sector samples are those that lie along and east of the Sr_o=0.706 isopleth (tonalite of Bear Valley Springs, granodiorite of Claraville, tonalite stock and augen gneiss of Tweedy Creek), and have the quartzite as representative of their metamorphic framework. The western sector samples are those with Sr_o<0.706 (metagabbro of Tunis Creek, hypersthene tonalite of Bison Peak, gneiss complex of the Tehachapi Mountains), and have the paragneiss as their representative metamorphic framework rock.

A positive correlation between $\delta^{18}O$ and initial $^{87}Sr/^{86}Sr$ can be shown that roughly fits a pair of hyperbolic curves or trajectories that project toward their respective metasedimentary end-members. The two sectors are distinctly separated on the plot with little overlap, except for the anomalous Pastoria Creek dike. This suggests that the rocks east and north of Tejon Creek were contaminated preferentially by Kings sequence rocks, while those to the south and west interacted with the paragneiss. This sort of dual metasedimentary nature is consistent with the zircon, oxygen, and strontium isotopic data. The inherited zircons in the eastern sector have zircons with 1700-1900 Ma upper intercepts {(granodiorite of Claraville (#1), tonalite stock (#2), quartzite (#32)}, while the western sector zircons have 1385-1450 Ma upper intercepts {(paragneiss of Comanche Point (#33), metagabbro of Tunis Creek (#13,14)}.

A hyperbolic curve generally fits the data from the Idaho batholith (Fleck and Criss, 1985), where the curve represents a two-component mixing trajectory between an upper mantle component (low $\delta^{18}O$, low initial $^{87}Sr/^{86}Sr$) and a

Figure 64. Plot of $\delta^{18}O$ versus initial $^{87}Sr/^{86}Sr$ for all rocks (plutonic and metasedimentary) of the southernmost Sierra Nevada. This is an enlargement of Figure 63 encompassing data from all samples investigated within this study. The data exhibit a general positive correlation of Sr_o with $\delta^{18}O$. A pair of hyperbolic, two-component simple mixing curves are shown that would involve upper mantle and metasedimentary end-members. The data has been grouped into two sectors based on their geographic distribution relative to the Sr_o=0.706 isopleth. The eastern sector trends towards the quartzite as its metasedimentary end-member, while the western sector trends towards the paragneiss of Comanche Point as its metasedimentary end-member. These metasedimentary rocks form the metamorphic framework into which the respective sectors were emplaced. LDI=late deformational intrusive rocks; BVS=tonalite of Bear Valley Springs; BP-TC=hypersthene tonalite of Bison Peak-metagabbro of Tunis Creek; TJ=tonalite gneiss of Tejon Creek; PC=quartzo-feldspathic gneiss of Pastoria Creek; ms=metasedimentary framework rocks.

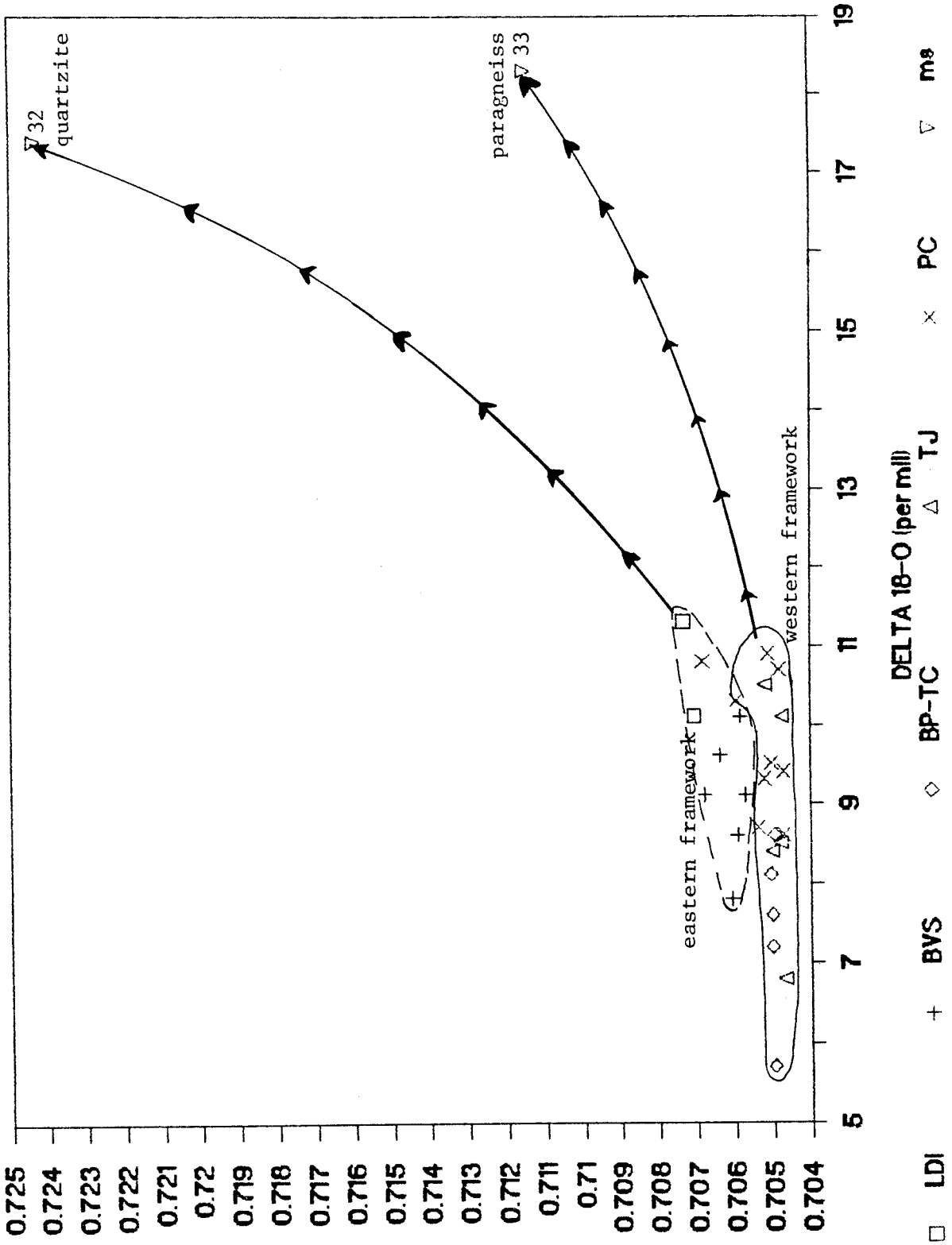
quartzite
32
paragneiss
33
eastern framework
western framework
INITIAL 87Sr/86Sr
0.725
0.724
0.723
0.722
0.721
0.72
0.719
0.718
0.717
0.716
0.715
0.714
0.713
0.712
0.711
0.71
0.709
0.708
0.707
0.706
0.705
0.704
5
7
9
11
13
15
17
19
DELTA 18-O (per mil)
LDI
BVS
BP-TC
TJ
PC
ms

crustal, metasedimentary component (high $\delta^{18}O$, high Sr_o). Fleck and Criss interpret the elemental covariations in ^{87}Sr and ^{18}O as requiring two different mechanisms, that when coupled (as in the case of Figure 64) require contamination of the orogenic magmas with crustal rocks prior to intrusion of the magmas, rather than simply assimilation of or interaction with wallrock material (Fleck and Criss, 1985). This is due to the fact that post-crystallization changes in the oxygen isotopic characteristics are independent of the concentration and isotopic ratios of strontium. Taylor (1980) stated that closed-system fractional crystallization or partial melting would not create appreciable changes in the $\delta^{18}O$ or initial $^{87}Sr/^{86}Sr$ values, and that the covariation then would be related to incorporation of high Sr_o, high $\delta^{18}O$ material directly into the magmas.

The various mixing models (zircon, Table 15; $\delta^{18}O$, Table 16; initial $^{87}Sr/^{86}Sr$, Table 18) are summarized in Table 19. In the Table, the rocks from the eastern sector are limited to the quartzite strontium signature, while those from the western sector are limited to the paragneiss. The oxygen variation between units is considered insignificant. For the oxygen mixing models, a metasedimentary component value of $+18.3°/_{oo}$ was used (southern Sierran data). Two values for the upper mantle component were used, the first a primitive value of $+5.7°/_{oo}$ (Taylor, 1980) and the second a value of $+8.5°/_{oo}$, indicative of alteration by oceanic crustal and/or mantle processes (Fleck and Criss, 1985). For the strontium mixing models, the appropriate southern Sierran metasedimentary value was used (quartzite, 0.7243; paragneiss, 0.7115). Again, two values were used for the upper mantle component. The first was a primitive value of 0.7035 (Fleck and Criss, 1985; Taylor, 1980), and the second an enriched value of 0.7047 (lowest value from the sample set). The column labelled "overlap" shows the amount of overlap values that exist between the oxygen and strontium models.

Table 19. Mixing models based on strontium and oxygen isotopic compositions

SAMPLE	$\delta^{18}O‰$ (SMOW)	% METASED‡ 5.7	% METASED‡ 8.5	INITIAL $^{87}/^{86}Sr$	% METASED‡‡ 0.7035	% METASED‡‡ 0.7047	% M.S.§ Overlap
late deformational intrusives - quartzite metasedimentary framework							
1 gr	11.3	44.4	28.6	0.70731	18.3	13.4	18-29?
2 tn	10.1	34.9	16.3	0.70703	16.9	12.0	16-17
4 gr	10.0	34.1	15.3	0.70776	53.5	45.5	34-46?
tonalite of Bear Valley Springs - quartzite metasedimentary framework							
6 tn	10.1	34.9	16.3	0.70583	11.2	5.9	10-16?
7 tn	9.1	27.0	6.1	0.70570	10.6	5.2	6-11
8 tn	8.6	23.0	1.0	0.70591	11.6	6.3	6-12
9 tn	9.6	31.0	11.2	0.70637	13.8	8.6	11-14
10 tn	9.1	27.0	6.1	0.70677	15.7	10.7	11-16
11 dr	7.8	16.7	-7.1	0.70605	12.2	7.0	7-12
hypersthene tonalite of Bison Peak - paragneiss metasedimentary framework							
12 tn	5.7	0.0	-28.6	0.70496	18.3	4.3	0?
gabbroid of Tunis Creek - paragneiss metasedimentary framework							
13 gb	7.2	11.9	-13.3	0.70499	18.7	4.7	5-12
14 gb	8.1	19.0	-4.1	0.70504	19.3	5.4	5-19
15 gb	7.6	15.1	-9.2	0.70499	18.7	4.7	5-15
16 gb	8.6	23.0	1.0	0.70493	18.0	3.8	4-18
tonalite gneiss of Tejon Creek - paragneiss metasedimentary framework							
17 tn	10.1	34.9	16.3	0.70472	15.3	0.7	15-16
18 tn	10.5	38.1	20.4	0.70518	21.1	7.5	20-21
19 tn	6.8	8.7	-17.3	0.70467	14.7	0.0	0- 8
20 dr	8.5	22.2	0.0	0.70478	16.1	1.6	2-16
21 tn	8.4	21.4	-1.0	0.70499	18.7	4.7	5-19
quartzo-feldspathic gneiss of Pastoria Creek - paragneiss framework							
22 gr	9.3	28.6	8.2	0.70519	21.2	7.7	8-21
23 gr	10.9	41.3	24.5	0.70510	20.1	6.3	20-25
24 tn	8.6	23.0	1.0	0.70469	14.9	0.3	1-15
25 tn	9.5	30.2	10.2	0.70500	18.8	4.9	10-19
26 gr	9.4	29.4	9.2	0.70469	14.9	0.3	9-15
27 tn	10.3	36.5	18.4	0.70594	30.7	18.7	19-31
28 tn	8.7	23.8	2.0	0.70536	23.4	10.2	10-23
29 gr	10.7	39.7	22.4	0.70480	16.3	1.9	16-22
augen gneiss of Tweedy Creek - quartzite metasedimentary framework							
30 gr	10.8	40.5	23.5	0.70682	15.9	10.9	16-24?
quartzite, Kings sequence							
31	17.4			0.72434 at 100 Ma			
paragneiss of Comanche Point							
32	18.3			0.71146 at 108 Ma			

‡ Lower end-member value of +5.7°/$_{oo}$ from Taylor (1980) and extreme in southernmost Sierra Nevada data set, +8.5°/$_{oo}$ from Fleck and Criss (1985); upper end-member taken as +18.3°/$_{oo}$ from southernmost Sierran data set.

‡‡ Lower end-member value of 0.7035 from Taylor (1980), or 0.7047 from southernmost Sierra data set. Upper end-member value taken as 0.7243 (quartzite) and 0.7115 (paragneiss), depending on geographic setting of sample.

§ Overlap derived from least common range in percent between strontium and oxygen models. Question mark denotes no overlap in different constraints, overlap then is taken as range between greatest lower and least upper bounds.

The values obtained by observing the overlap between the two models indicates a range in incorporation of metasedimentary material of between 0-46%. Rocks of the late deformational intrusive suite exclusive of the Pastoria Creek dike have a range of 16-29%, with a preferred range of 17-18%. "Preferred" ranges are taken here as that range in which all samples from the unit overlap. In other words, it is a least common denominator range for the unit. Samples from within the units frequently do not show an overlap between all analyses. In this case the least upper and greatest lower ranges bound the "preferred" range. The tonalite of Bear Valley Springs has a range of 6-16%, and a preferred value of 11%. The hypersthene tonalite of Bison Peak indicates no appreciable metasedimentary component. The metagabbro of Tunis Creek has a range of 4-19%, and a preferred range of 5-12% incorporated metasedimentary material. The tonalite gneiss of Tejon Creek has a range of 0-21%, with a preferred range of 9-15%. The quartzo-feldspathic gneiss of Pastoria Creek has a range of 1-31%, and a preferred range of 15-20%. Tonalitic samples from the Pastoria Creek unit generally indicate a lower percentage of a metasedimentary component, but they have an overall range slightly greater than that for the granitic samples. This suggests some degree of separation of the mechanism that resulted in the assimilation of metamorphic framework material between the tonalitic and granitic gneisses.

There is a general agreement between the strontium and oxygen mixing models. Many samples appear to have entered the area of mixing with the metamorphic framework rocks with $\delta^{18}O$ and initial $^{87}Sr/^{86}Sr$ values elevated above primitive or pristine mantle values. This suggests that these samples experienced mantle processes that altered their original isotopic concentrations, and/or that there is a third component in the system at a level beneath the current depth of exposure. The values for assimilation of metasedimentary material are generally

lower than the 33% value obtained by DePaolo (1981b) using oxygen isotopes and slightly lower than or comparable to the 20-30% value obtained using neodymium isotopes (next section). His work, however, was on rocks east of the Sr_o=0.706 isopleth. Samples from that region generally indicate a higher proportion of metasedimentary component relative to those to the west, but they are still in the range of 16-29%.

Comparing the results from Table 19 with the hypothetical zircon mixing model presented in Table 15, one can see that all samples modelled for incorporation of older zircon (except for the Bison Peak unit) show significantly lower amounts of metasedimentary zircon than bulk rock metasedimentary oxygen and strontium. There is a general consistency in the degree of incorporation of metasedimentary material between samples in comparing the zircon and geochemical models. One explanation for the lower amounts of zircon is that the zircon inheritance model does not accurately reflect the amount of bulk rock material actually incorporated into the magmas. The detrital zircons would not necessarily all be retained by the magma (most could be completely melted and their contribution to the zircon population lost), while the bulk rock chemistry would be retained. A further explanation is that the actual inherited zircons experienced a greater degree of disturbance relative to those from the sampled source metasedimentary framework rocks. The actual inherited zircon grains were at and above solidus for a considerable period of time in order for them to be incorporated into the melt, whereas the measured framework rock zircon samples were clearly not at solidus temperatures. In addition, those rocks whose field relations show evidence for assimilation of partial melts from the metasedimentary rocks do not display much evidence of zircon discordance. This implies a resetting or dissolution of the contaminate zircon grains. If this is true, then the actual inherited zircon would

have a lower lead concentration, and more zircon would then be required to produce the observed data. Thus, the model presented in Table 15 is only a crude approximation of the actual zircon inheritence.

The apparent lack of a metasedimentary oxygen and strontium signature for the Bison Peak unit appears to require inheritance of zircon from the adjacent tonalite gneiss (Tejon Creek orthogneiss), or from the source region of the hypersthene tonalite to explain the minor discordant zircon patterns observed within the Bison Peak unit.

The bulk of the geochemical data on the crystalline rocks of the southernmost Sierra Nevada (zircon U/Pb discordances; covariation of initial $^{87}Sr/^{86}Sr$ with $\delta^{18}O$, Sr content, $^{87}Rb/^{86}Sr$; and the mixing models) points to mixing of upper mantle orogenic magmas with crustal metasedimentary material. A third component can be used to explain the generation of the isotopic arrays in the tonalite of Bear Valley Springs and perhaps the discordant zircon arrays in the tonalite gneiss of Tejon Creek. The imperfect fit of the data to the models indicates that simple one-stage mixing of mantle isotopic systems with systems represented by the metasedimentary samples is an oversimplification to the actual process. The simple mixing models do not account for complications in the isotopic systems, such as heterogeneous source regions, contributions from other isotopic reservoirs, or possible multi-stage history. Such a multi-stage history could have involved the production of oceanic crustal material and its tectonic accretion into the lower crust beneath the observed basement framework rocks preceeding melting and incorporation into the observed magmatic products. A different multi-stage history could involve reworking and assimilation of lower continental crustal sialic material into the sampled magmatic systems.

Tectonically accreted oceanic crustal and island arc assemblages comprise a significant part of the basement framework in the western part of the Sierra Nevada metamorphic belt. Episodes of magmatism in such assemblages have been observed in the central and northern part of the range through zircon studies, and have yielded ages of 200-300 Ma (Ando and others, 1983; Saleeby, 1982; Saleeby and Sharp, 1980), ~400 Ma (Saleeby and others, 1986c), and ~570 Ma (Saleeby and others, 1986c; Wallin, 1986; d'Allura and others, 1977).

The pseudoisochrons in Figure 60 (250, 335, 565 Ma) could correspond to similar episodes of oceanic crustal and/or island arc growth in the southern Sierra, and mixing of such material could account for the strontium isotopic characteristics observed in the tonalite of Bear Valley Springs, granodiorite of Claraville, and parts of the tonalite gneiss of Tejon Creek. Also, zircons inherited from these episodes could perhaps account for the slight discordances observed in the tonalite gneiss of Tejon Creek (potential contaminate population ages of 370, 535, and 720 Ma, Figure 47).

Remnants of such rocks have not been found in the study area. Extrapolation from the closest known location of oceanic crustal material (100 km north in the Kaweah River area, Saleeby, 1979) along regional trends would indicate their presence in the western part of the study area, perhaps as substrate beneath the exposed metasedimentary framework rocks. Possible analoguous rocks are found in basement cores from the southern end of the San Joaquin Valley, where plagioclase ± clinopyroxene ± hornblende gabbro-diorite has been described (Ross, 1979). Thus, the potential contribution from such rocks should not be ignored.

In summary, the mixing of mantle magmas having compositions similar to those observed in the metagabbro of Tunis Creek and the hypersthene tonalite of Bison Peak with metasedimentary framework rocks such as those observed in the

area can account for the gross patterns observed in the various isotopic and zircon data arrays and mixing models, and is the favored mechanism to produce such. Postulated third (and additional) components would present second-order effects that would presumably alter the initial pre-intrusion mantle magmatic compositions from the modelled mantle end-member strontium and oxygen values.

IV.2.3 Other geochemical data

A reconnaissance study of the Nd/Sm isotopic ratios of batholithic and metasedimentary rocks from the central Sierra Nevada and Peninsular Ranges batholiths east of the Sr_0=0.706 isopleth was performed by DePaolo (1981b). His results showed an inverse correlation of ε_{Nd} to both initial $^{87}Sr/^{86}Sr$ and $\delta^{18}O$. He derived a model Nd/Sm age for the metasedimentary rocks of between 1.5 and 1.9 Ga. His model for the generation of the batholithic rocks involves a mixture of mantle-derived island-arc type magmas and metasedimentary or craton-derived components. The approximate percentages are: modelled by Nd systematics, 70 to 80% upper mantle, 20 to 30% crustal; using $\delta^{18}O$, two-thirds mantle to one-third crustal (DePaolo, 1981b). Chen and Tilton (1978) constructed Pb evolution diagrams from feldspar data on plutonic rocks of the south-central Sierra Nevada, and obtained a similar 1.8 Ga model age for the source region for the batholithic magmas. They believed that the source region for the batholith was in part Proterozoic, non-oceanic material. Kistler and Peterman (1978), based on initial $^{87}Sr/^{86}Sr$ ratios, constructed a limiting isochron of 1.7 Ga (Sr_0 = 0.7020, slope equivalent to 1.6 Ga at 100 Ma) for intrusive rocks of the south-central Sierras. They believed that magmas formed by melting at depths that ranged from upper mantle (west of the Sr_0 = 0.706 isopleth) to the lower crust (east of the 0.706 isopleth), and that the source reservoirs formed at 1.7 Ga. Based on neodymium-sumarium and rubidium-strontium studies of mid- to lower-crustal xenoliths in the

central Sierra, Domenick and others (1983) suggest that the covariation in Sr_o with $^{87}Rb/^{86}Sr$ and $\delta^{18}O$ is not due to simple mixing of a two end-member system, and that the source region for Sierran magmas was heterogeneous. Domineck and others believed that the generation of magmas was a result of partial melting of crustal rocks (sediments from the crustal margin), lower crustal-upper mantle rocks, and/or oceanic crustal rocks and sediments, and that the melting zone was in the lower crust or upper mantle, and that these partial melt products were further mixed with old continental crust (1.6 Ga) and/or depleted mantle components.

The data presented in this chapter generally support the model for the source for the magmas that formed the southernmost Sierra Nevada batholith as requiring "primitive", upper mantle derived magmas that incorporated varying amounts of cratonal derived metasedimentary material prior to crystallization. The metagabbro of Tunis Creek represents one end-member, the upper mantle component. The quartzite within the Kings sequence metasedimentary septa and the paragneiss of Comanche Point represents the second end-member. A third cryptic crustal component(s) appears to be required to explain the isotopic variation in the tonalite of Bear Valley Springs and the tonalite gneiss of Tejon Creek beyond that allowed from the two component system. Such a third component could be Paleozoic and early Mesozoic orogenic rocks of oceanic and/or continental affinity.

IV.3. Discussion of other investigations

IV.3.1 Paleomagnetic studies

Most paleomagnetic work on the Sierra Nevada (for example, Gromme and others, 1965, 1967) indicate the existence of the central Sierran block at stable North American paleolatitudes at mid-Cretaceous times, with no rotation or

translation relative to the craton. Frei and others (1984) reported paleomagnetic results from the central Sierra Nevada constraining movement since about 90 Ma to 5±8° of poleward translation, and 7±11° of clockwise rotation. Frei and others (1982) studied plutonic rocks in the Yosemite area, and reported results of 5±4° of poleward translation and 5±7° of clockwise rotation of the central Sierras with respect to stable North America since 83 Ma.

In the southernmost Sierra Nevada, Kanter and McWilliams (1980, 1982) performed paleomagnetic studies on the tonalite of Bear Valley Springs northwest of Tehachapi and 16 Ma Miocene volcanic rocks northeast of Tehachapi. They used K/Ar and Rb/Sr dates (80 to 86 Ma) for the age of the pluton, rather than the U/Pb age of 100 Ma reported here. The existence of widespread 80 to 90 Ma Rb/Sr and K/Ar ages are indicative of a regional cooling event. The use of the younger date is probably acceptable because of two points, the "blocking" temperature of the magnetism, and polarity constraints. The Rb/Sr ages would approximate the time of cooling of the pluton through the Curie point, and the setting of the paleomagnetic indicators at above 450 to 500°C (Kanter and McWilliams, 1982). The polarity at the time used (about 80 Ma) was reversed, corresponding to a reversed interval from 84 to 79 Ma (Harland and others, 1982), in contrast to a period of normal polarity from 110 to 85 Ma (Harland and others, 1982). Kanter and McWilliams (1980, 1982) reported 45±15° of clockwise rotation and no resolvable translation of the tonalite of Bear Valley Springs with respect to stable North America between 80 and 16 Ma. Further, they found no discernable deviation from the expected pole position since 16 Ma.

Further paleomagnetic work in the southern Sierra was done by McWilliams and Li (1983, 1985) and Plescia and Calderone (1986). Both sets of workers reported that the tonalites of Bear Valley Springs and Mount Adelaide to the west of

the White Wolf-Breckenridge-Kern Canyon fault system (~25 km to the northwest of the area of Kanter and McWilliams) show no rotation or translation with respect to the craton since the late Cretaceous. McWilliams and Li (1983, 1985) reported that rocks from the gneiss complex in the vicinity of the Edmonston pumping station near the mouth of Pastoria Creek had been rotated clockwise 59±16°, while Plescia and Calderone working in the same area reported a clockwise rotation of 40±10° since about 25 Ma (K/Ar age on volcanic strata overlapping the crystalline basement). McWilliams and Li (1983) reported that the granodiorite of Lebec (south of the Garlock fault) has 90°+ of clockwise rotation. Plescia and Calderone (1986) suggest the "tail" of the Sierras underwent 20° of clockwise rotation between 80 and 25 Ma, and 40° clockwise rotation between 25 and 16 Ma. The southern end of the Sierra Nevada therefore appears to have been rotated between about 80 and 16 Ma by up to 90° with respect to the central part of the batholith, with an increasing amount of rotation southwards.

IV.3.2 Geobarometry and geothermometry

Geobarometry and geothermometry on rocks in the gneiss complex was performed by Sharry (1981b). On the hypersthene tonalite of Bison Peak, he used the two-pyroxene geothermometer of Wood and Banno (1973), modified by Wells (1980). This involves the exchange of $Mg_2Si_2O_6$ between clinopyroxene and orthopyroxene. This assumes ideal site solutions, and assumptions on the effects of other cation species. Pressure dependence is assumed to be negligible. Results should be accurate to ±70°C. Sharry's results averaged 850°C (range of 837 to 934°C) for the Wood and Banno calibration, and 925°C (range of 867 to 965°C) for the Wells calibration. Sharry also compared clinopyroxene and orthopyroxene compositional data with experimental two-pyroxene solvus data (Lindsley and others, 1974). This involves the assumption of a negligible pressure dependence,

and a negligible effect from minor cation components. Sharry's data points fall at compositions on the solvus indicating equilibration at a temperature below 810°C. Sharry interpreted these temperatures as erroneously high. However, as discussed below, the pyroxenes are interpreted herein as magmatic, not metamorphic, products, and the pyroxene analyses are within the range of values from two-pyroxene intrusive rocks of the western Sierra Nevada and Klamath Mountains (Snoke and others, 1981; Saleeby, unpublished data). Thus, the two-pyroxene data is taken to represent the approximate crystallization and chemical isolation temperature of the pyroxenes from a magma.

On rocks from the quartzo-feldspathic gneiss of Pastoria Creek, Sharry applied the garnet-biotite geothermometer of Ferry and Spear (1978), and the garnet-biotite-plagioclase-muscovite geobarometer of Ghent and Stout (1981). The pressure effect on temperature is small (4°C/kb). Sharry's results gave a temperature of 739°C (range of 640 to 784°) and a pressure of 8.3 kb (range of 8.1 to 8.5 kb).

All the thermo-barometric work involves the assumption of negligible effects of minor cations, temperature or pressure dependency of the applied system, and equilibration of the minerals. The effect of vapor pressure is an unknown factor, but was assumed to be very small in under the assumed dehydrating conditions. A small to negligible vapor pressure effect is questionable because hydrous minerals (amphiboles and biotite) constitute 25 to 50 volume percent of the rocks investigated. The two-pyroxene geothermometers have been shown to record temperatures from 50 to 150°C too high for rocks in the Adirondacks, and to show an inconsistent pattern with respect to metamorphic zonation (Bohlen and Essene, 1979). Their result is consistent with the results of the hypersthene tonalite of Bison Peak compared to the quartzo-feldspathic gneiss, and

suggests a maximum metamorphic temperature of around 740°C, consistent with the pyroxene solvus data. This may indicate an approximate crystallization temperature for the involved phases. This temperature would only be a rough approximation due to the retrograde mineral growth sequence, and lack of equilibrium in the tonalite. The geobarometer is dependent on the presence of muscovite. The muscovite in the gneiss complex is retrograde (Sharry, 1981b), and will thus yield answers in excess of the true metamorphic pressures (Elan, 1985), due to the lack of equilibrium between the muscovite and other minerals.

Perhaps the most important factor regarding the use of metamorphic P-T work on much of the gneiss complex of the Tehachapi Mountains is the interpretation in this report of the granulites as igneous rocks. This interpretation is more fully discussed in a later section, but may be briefly summarized as follows: many igneous textures are preserved in the rocks of the hypersthene tonalite of Bison Peak and the metagabbro of Tunis Creek. These textures include typical hypidiomorphic granular textures, zoned plagioclase, cumulate features, and abundant retrograde reactions involving olivine → pyroxene → amphibole. Evidence for prograde reactions is rare in the gneiss complex. $\delta^{18}O$ values for these units are all within the range for normal igneous rocks. Therefore, the rocks are believed to be igneous rocks that crystallized under upper amphibolite to lower granulite facies conditions as defined by the P-T relations and the predominance of hydrous mafic phases.

As discussed in the field and petrographic section, garnets are seen to be growing statically at the expense of hornblende in a disequilibrium setting in veins developed across earlier igneous layering and flow features (Figure 23). These features are common in the gabbros and tonalites, and are especially visible in the metagabbro of Tunis Creek. Experimental phase diagrams for dry to wet (~5%

water) basaltic and andesitic magmatic systems from Green (1982) are shown in Figure 65. Isobaric cooling of the gabbroic to tonalitic melts through and below the solidus would cross a garnet-in phase boundary at pressures between 6 and 8 kb as shown by the dashed line. The widespread and scattered occurrence of the nonequilibrium garnet porphyroblasts throughout the southernmost part of the study area is thought to be indicative of the descending temperature trajectories from a magma under high pressure conditions. Such hot sub-solidus conditions probably persisted for a considerable period of time to produce the large (up to 5 cm diameter) garnets. The garnets represent a retrograde P-T path from magmatic crystallization, not a prograde metamorphic path. Supporting evidence for this conclusion is the young age of the Tunis Creek unit relative to the gneiss complex, the non- to weakly deformed state of the metagabbro, and the dominance of retrograde and paucity of prograde reactions.

Additional evidence for a high pressure origin for rocks of the gneiss complex of the Tehachapi Mountains has been discussed in relation to the epidote-bearing tonalites in the quartzo-feldspathic gneiss of Pastoria Creek. This magmatic epidote suggests crystallization depths of 6-8 kb for the gneiss complex, based on the sparse experimental data presented by Zen (1985) and Zen and Hammarstrom (1984). Therefore, several lines of evidence all suggest a depth of crystallization for the southernmost Sierra Nevada at depths of about 25 km.

The only other geobarometric and geothermometric study in the southern Sierras was by Elan and Thomas (1984) and Elan (1985). They performed geobarometric studies at Lake Isabella in which they report a result of about 3.0 kb and 600 to 700°C for the metamorphism of the country rocks. Textural evidence from the augen gneiss of Tweedy Creek (brittlely deformed feldspar and ductilely deformed quartz) leads to a P-T estimate for the formation of the gneissic fabric

Figure 65. Phase diagrams for wet (5% vapor) andesite and tholeiite (Green, 1982). Isobaric cooling of a system from the solidus at between six and eight kilobars would cross a garnet-in reaction. The petrographic setting of garnet as a late-stage nonequilibrium phase in the gabbroic to tonalitic rocks of the southernmost Sierra Nevada suggests such pressures existed in the study area during and after crystallization.

wet tholeiite

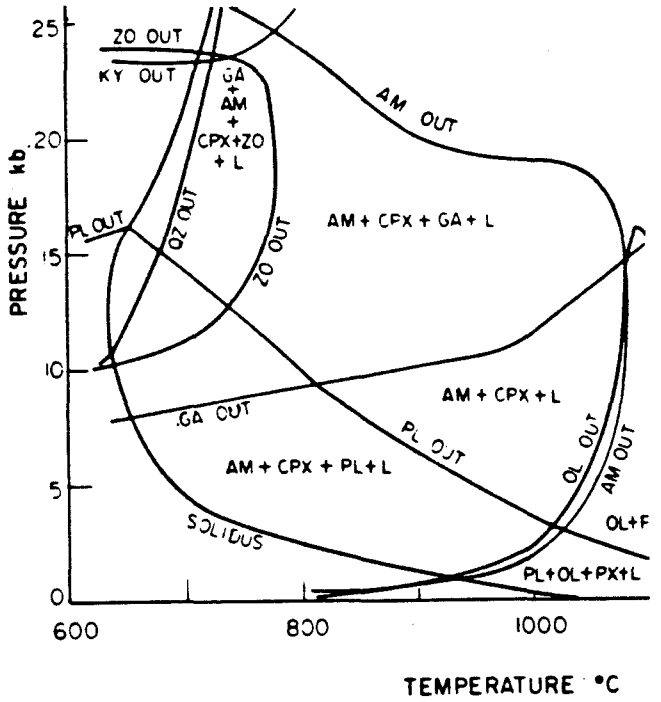

wet andesite

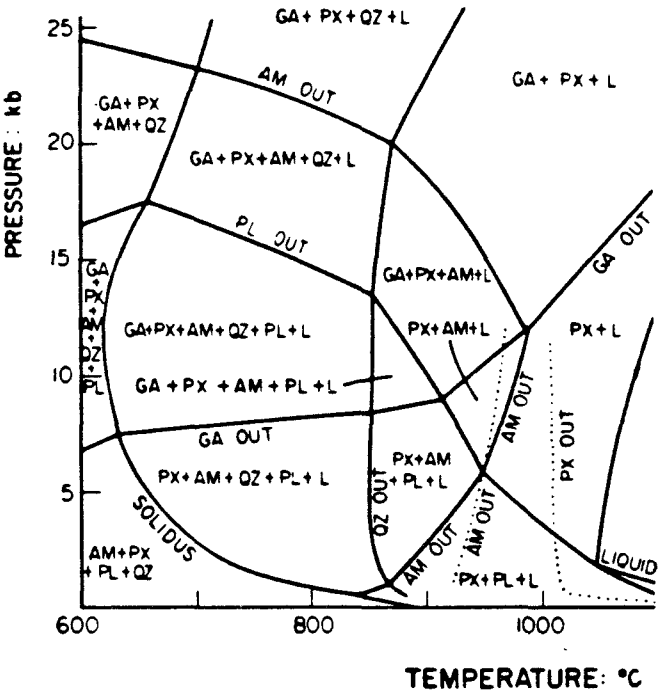

Green, 1982

in the orthogneiss as occurring at 2-5 kb and 400-500°C, and between 115 and 100 Ma. Combined with Sharry's 8 kb and 700°C for the metamorphic rocks in the gneiss complex of the Tehachapi Mountains, there is a progressive increase in pressure in the Sierras south from Lake Isabella (Saleeby and others, 1986a). The southernmost Sierras appear to represent a cross-sectional view of the lowermost portion of the Sierra Nevada batholith.

IV.4. Structure and geologic history

IV.4.1 Structural and petrologic configuration of the gneiss complex of the Tehachapi Mountains, and its relation to the tonalite of Bear Valley Springs

The contact between the Bear Valley Springs batholith and the gneiss complex is important in understanding the processes deep within batholithic terranes, and the structural relations between the southern Sierra Nevada and the Tehachapi Mountains. Both the tonalite of Bear Valley Springs and the hypersthene tonalite of Bison Peak with which it is in contact have zircon ages of 100±2 Ma. The two tonalites have a similar overall mineralogy, and are difficult to distinguish in the field. Along upper Tejon Creek, the batholith becomes increasingly deformed as it approaches the Bison Peak unit. The deformation appears to have occurred under solidus to immediate hot sub-solidus conditions, as evidenced by ductilely deformed quartz, by recrystallized, blastomylonitic textures seen in the tonalite, and by the preferred orientation of the mafic inclusions and mafic minerals within the tonalite. The high aspect ratios and alignment of the mafic inclusions is believed to have resulted from plastic deformation and preferential orientation of the mafic inclusions accompanying emplacement and magmatic flow of the tonalite (Bateman and others, 1963). There is, however, no single area in which to say that a contact between the two units exists; the contact is a gradational one.

Along lower Tejon Creek and trending northwesterly toward the White Wolf fault is a more complex contact zone, with the tonalite of Bear Valley Springs showing increasing deformation towards the gneiss complex of the Tehachapi Mountains. The tonalite grades into the tonalite gneiss of Tejon Creek, which has a complex gradation with other units in the gneiss complex (in this case, the migmatitic paragneiss of Comanche Point). The tonalite gneiss of Tejon Creek frequently has sharp intrusive contacts into the paragneiss; in other locations migmatitic rocks are intergradational with the gneiss. In addition, the tonalite gneiss of Tejon Creek contains mafic layers of material that may represent either material related to the metagabbro of Tunis Creek, or an intrusive basaltic component into the gneiss. Alternatively, the mafic lenses may be restite material. However, a $\delta^{18}O$ value of $+8.4^{o}/_{oo}$ from a mafic layer within the tonalite gneiss suggests a basaltic, magmatic origin to the mafic layers.

Along Comanche Point Road, there exists an intimate mixture of layers of the tonalite gneiss of Tejon Creek and paragneiss of Comanche Point for about two kilometers (apparent lit-par-lit injection zone). Regions exist which show migmatitic stringers and leucosomes derived from the paragneiss grading into the tonalite. The tonalite gneiss appears to have been derived from a mixing of tonalitic magmas with tonalitic to granodioritic melts derived from the paragneiss of Comanche Point. This is in part suggested by the discordant zircon data, Rb/Sr data, and intermediate $\delta^{18}O$ values (Table 14) from the tonalite gneiss of Tejon Creek, in addition to the field observations.

The metagabbro of Tunis Creek also shows gradational contacts with the tonalite gneiss of Tejon Creek and the paragneiss of Comanche Point. These contacts appear to be similar to those of the tonalite of Bear Valley Springs, but are not as well exposed. The contacts are for the most part gradational, with a

change in composition from gabbro to tonalite, along with an increase in degree of foliation. The contact zone is a region of increasing assimilation of paragneiss material by the gabbroid magma. The metagabbro has rare intrusive relations into the tonalite gneiss of Tejon Creek.

The hypersthene tonalite of Bison Peak is interpreted to represent the marginal or floor phase of the tonalite of Bear Valley Springs, and may occupy the conduit to the tonalite together with the metagabbro. The moderate deformation of the Bison Peak unit may be the result of differential motion between the ascending and spreading batholithic mass and the return flow of the country rocks.

Figure 66 combines poles to foliation for many of the units in the southern Sierra Nevada into two equal-area stereoplots. Figure 66a, the Tehachapi suite of samples, shows a random orientation to the data, interpreted as the result of a static, lower crustal ultrametamorphic environment. In contrast is the Bear Valley Springs suite (Figure 66b), which shows a strong preferred orientation, suggesting a nonisotropic stress field. This implies a spatial change in the stress regime coincident or perhaps due to the intrusion of the Bear Valley Springs suite.

A structural cross-section for the southernmost Sierra Nevada at 100 Ma has been constructed as follows. Figure 67a is the geologic map of the southern Sierra from Lake Isabella to Grapevine Canyon in the Tehachapi Mountains that is used as a basis for construction of the cross-section. Depth constraints on the cross-section were assigned by using geobarometric work that indicates a depth of emplacement at 100 Ma of about 3 kb (Elan, 1985; Elan and Thomas, 1984) at Lake Isabella, and about 8 kb in the Pastoria Creek area (Sharry, 1981b). On Figure 67b, the southernmost end of the study area has had 45-60° of clockwise rotation restored, with a greater degree of rotation restored to the south (restoration of the paleomagnetic results of Kanter and McWilliams, 1982, 1984;

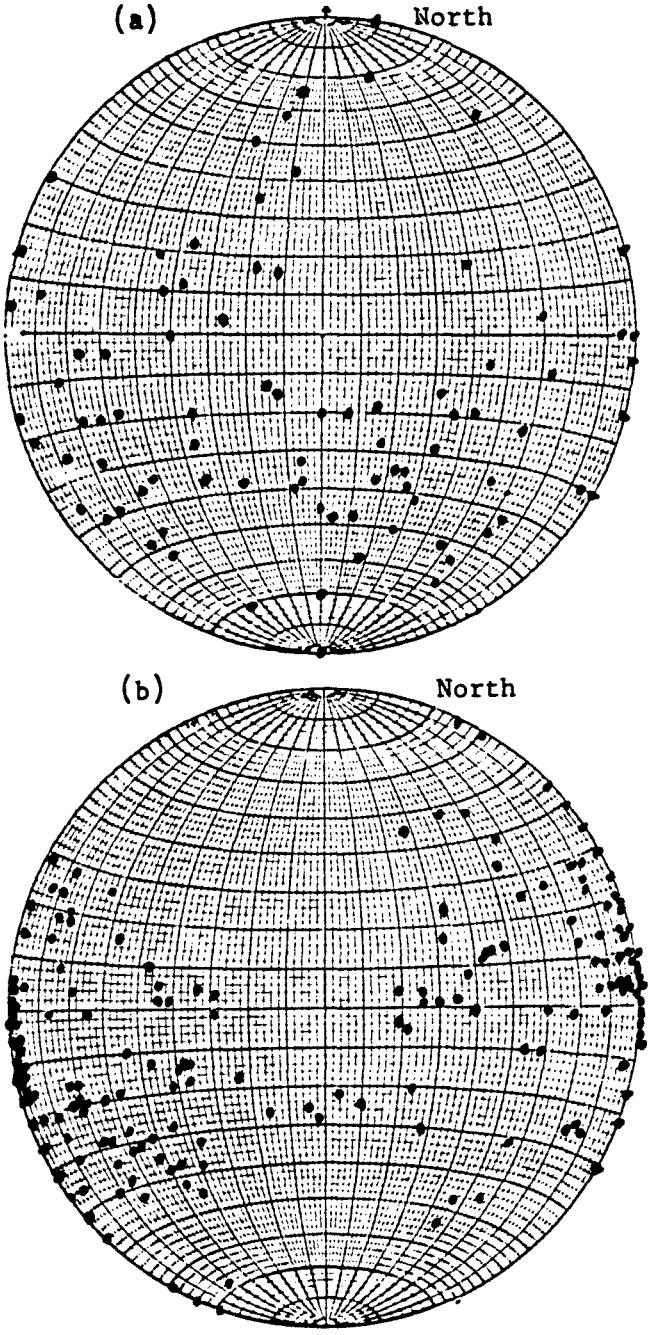

Figure 66. Diagram of the lower hemisphere projections, equal area stereoplot of poles to foliation for the Tehachapi and Bear Valley Springs suites. The data from the Tehachapi suite (a) shows a random orientation, while the Bear Valley Springs suite (b) shows a strong preferential direction to the data.

Figure 67. Structural cross-sections of the southern Sierra Nevada. (a) is a generalized geologic map of the southern Sierra from Lake Isabella in the north to Grapevine Canyon in the south. (b) shows the southern Sierra with 45-60° of clockwise rotation restored, with structural projection line for (c) given as A-A'. (c) shows the rotation-restored block projected from A-A' to a cross-section of the crust from 3 kb pressure at Lake Isabella, to 8 kb at Pastoria Creek. (d) is the structural cross-section, showing the southern Sierra at emplacement depths of between 10 and 30 km at 100 Ma.

(a)

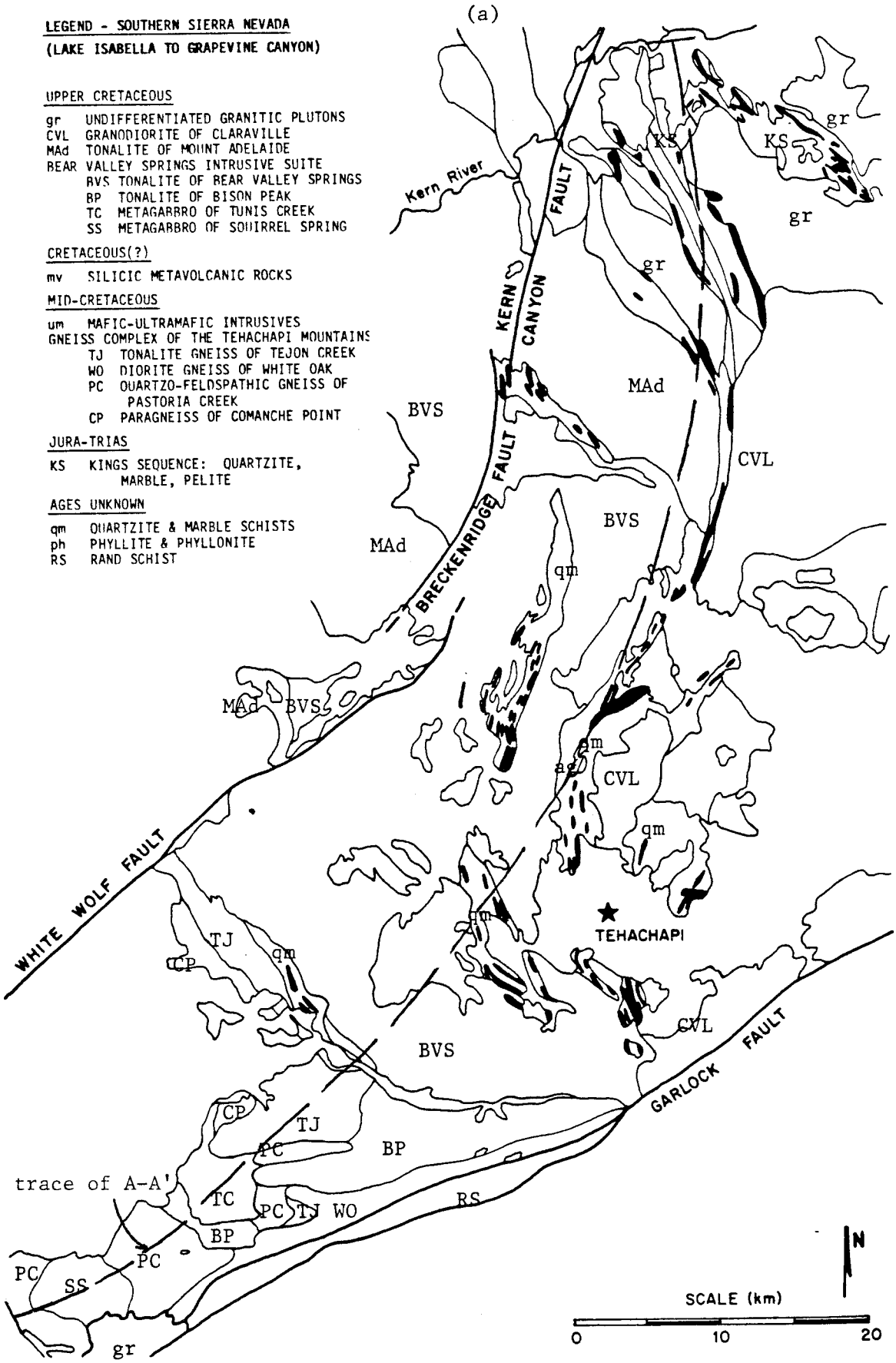
LEGEND - SOUTHERN SIERRA NEVADA
(LAKE ISABELLA TO GRAPEVINE CANYON)
UPPER CRETACEOUS
gr UNDIFFERENTIATED GRANITIC PLUTONS
CVL GRANODIORITE OF CLARAVILLE
MAd TONALITE OF MOUNT ADELAIDE
BEAR VALLEY SPRINGS INTRUSIVE SUITE
BVS TONALITE OF BEAR VALLEY SPRINGS
BP TONALITE OF BISON PEAK
TC METAGABBRO OF TUNIS CREEK
SS METAGABBRO OF SQUIRREL SPRING
CRETACEOUS(?)
mv SILICIC METAVOLCANIC ROCKS
MID-CRETACEOUS
um MAFIC-ULTRAMAFIC INTRUSIVES
GNEISS COMPLEX OF THE TEHACHAPI MOUNTAINS
TJ TONALITE GNEISS OF TEJON CREEK
WO DIORITE GNEISS OF WHITE OAK
PC QUARTZO-FELDSPATHIC GNEISS OF PASTORIA CREEK
CP PARAGNEISS OF COMANCHE POINT
JURA-TRIAS
KS KINGS SEQUENCE: QUARTZITE, MARBLE, PELITE
AGES UNKNOWN
qm QUARTZITE & MARBLE SCHISTS
ph PHYLLITE & PHYLLONITE
RS RAND SCHIST
Kern River
KERN CANYON FAULT
BRECKENRIDGE FAULT
WHITE WOLF FAULT
GARLOCK FAULT
TEHACHAPI
trace of A-A'
SCALE (km)
0
10
20
N

(b)

(c)

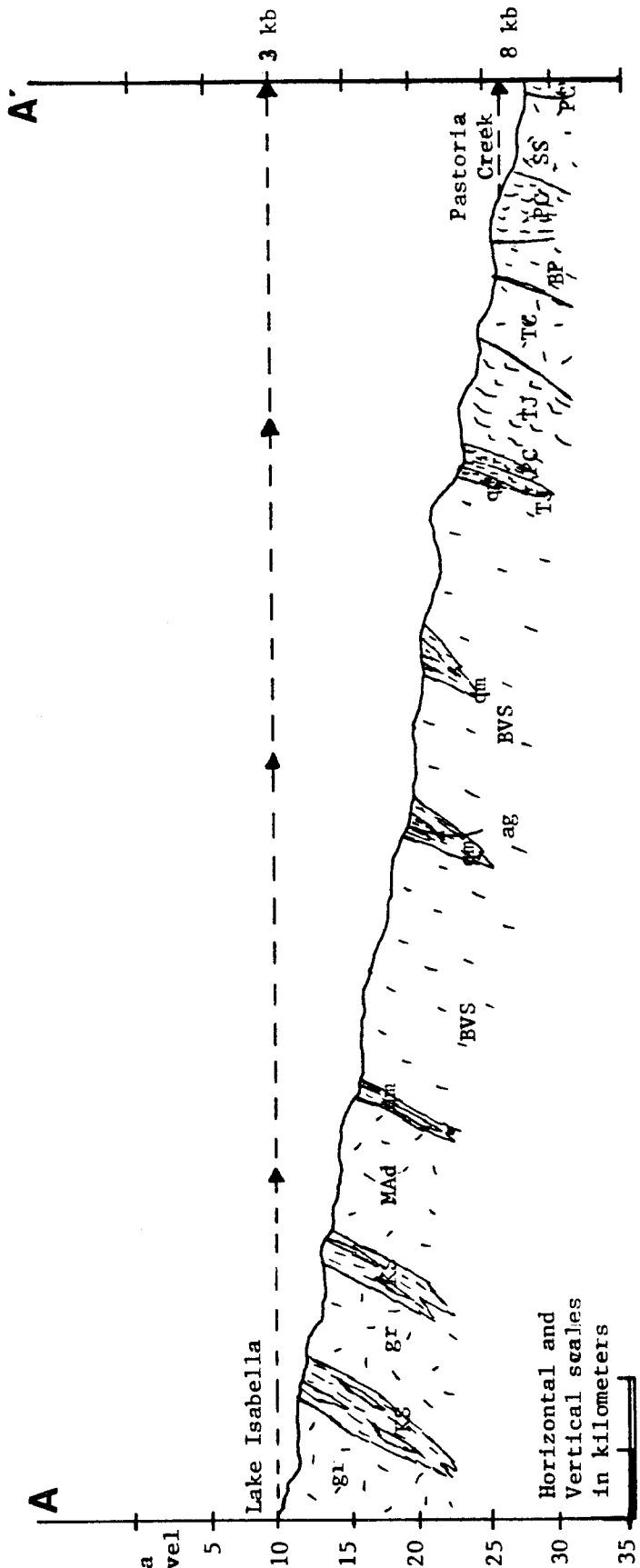
A
A'
Sea Level
5
10
15
20
25
30
35
Lake Isabella
3 kb
8 kb
Pastoria Creek
gr
KS
MAd
BVS
ag
dm
TC
TJ
SS
BP
PC
Horizontal and Vertical scales in kilometers
0
5
10

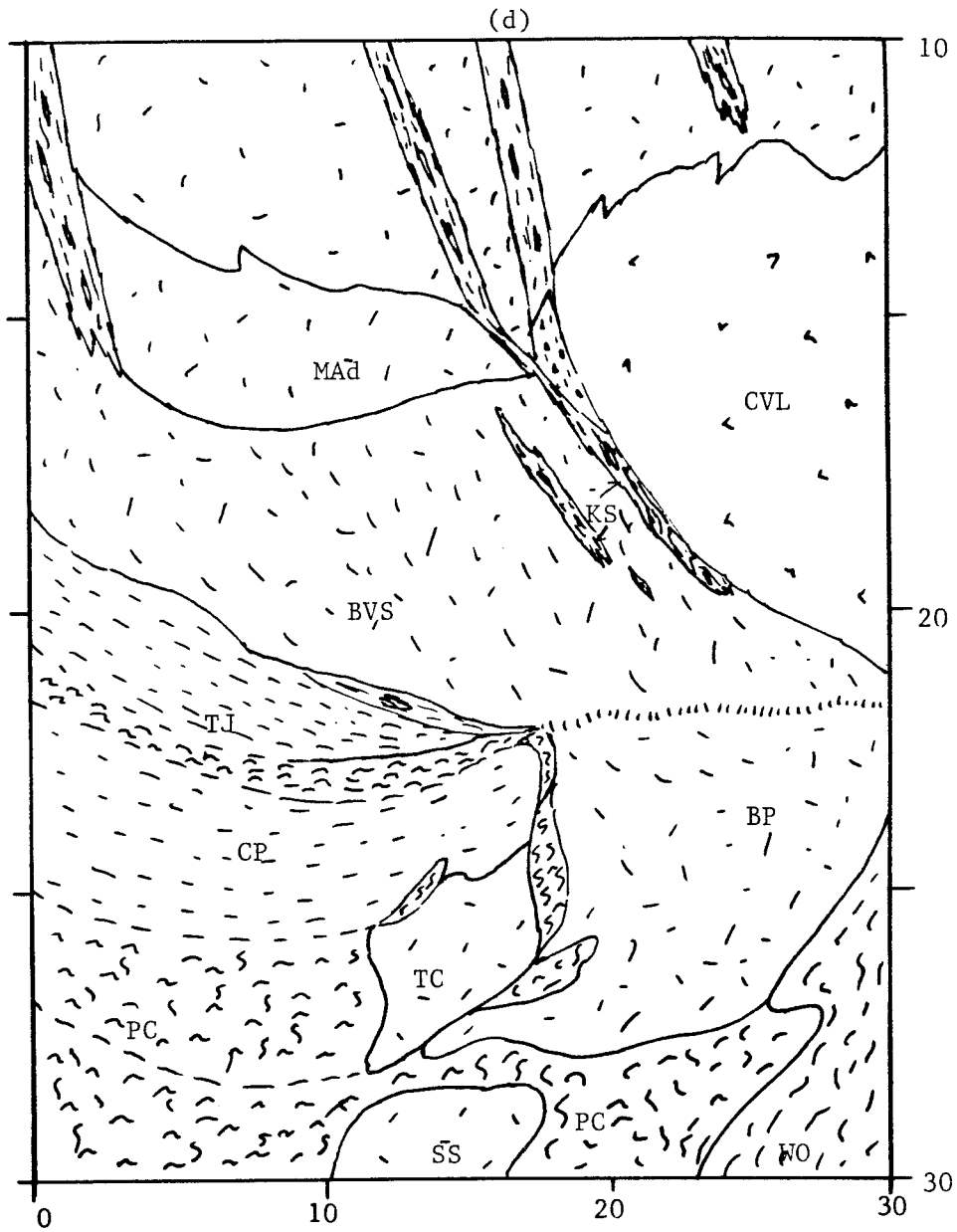

Horizontal and Vertical Scales in kilometers

McWilliams and Li, 1983, 1985; Plescia and Calderone, 1986). The line A-A' is then used as the basis for the projection of the surface geology from Figure 67b onto the cross-section, as shown in Figure 67c. The result is shown in Figure 67d. If regional tilting of 60-90° is restored (Eocene strata overlapping the tonalite and gneiss complex have dips of greater than 60° to the north), then the construct given in Figure 67d is similar to a map pattern of the area. In other words, the map pattern closely resembles an elongated and distorted cross-sectional view.

The structural cross-section shows major batholiths extending from catazonal to mesozonal levels in the southern Sierra. In particular, the tonalite of Bear Valley Springs extends from depths of about 12-20 km. Metamorphic framework rocks form screens and septa down to depths of about 20 km. Below about 20 km, the rocks become dominantly gneissic. The intrusive rocks of the Bear Valley Springs suite continue to depths in the order of 25 km, forming what appears to be the walls of what may have been the conduit through which the tonalite of Bear Valley Springs was intruded into the middle crust. The floor of the tonalite of Bear Valley Springs is seen grading into the hypersthene tonalite of Bison Peak which occupies part of the conduit to the batholith. Also shown in the conduit are the metagabbros of Tunis Creek and Squirrel Springs.

The tonalite gneiss of Tejon Creek and the diorite gneiss of White Oak are shown as the margins and substrate of much of the batholith, and along the walls of its conduit. The epidote-bearing tonalites are shown as discrete intrusive bodies in the quartzo-feldspathic gneiss of Pastoria Creek, which is taken as country rock to the Bear Valley Springs intrusive suite, and exists as a number of small, tonalitic, dioritic, and granitic intrusive bodies.

Two additional cross-sections have been constructed in the southernmost Sierra Nevada (Figure 68). Their surface traces run in lines northeast-southwest

Figure 68. Cross-sections of the southernmost Sierra Nevada. (a) is the generalized surface geology map, with cross-section lines given as B-B' and C-C'. (b) is the section B-B', southwest from Tehachapi to Grapevine Canyon. (c) is the section C-C', southeast across the Tehachapi Mountains.

KEY TO BASE MAPS - SOUTHERNMOST SIERRA NEVADA

(a)

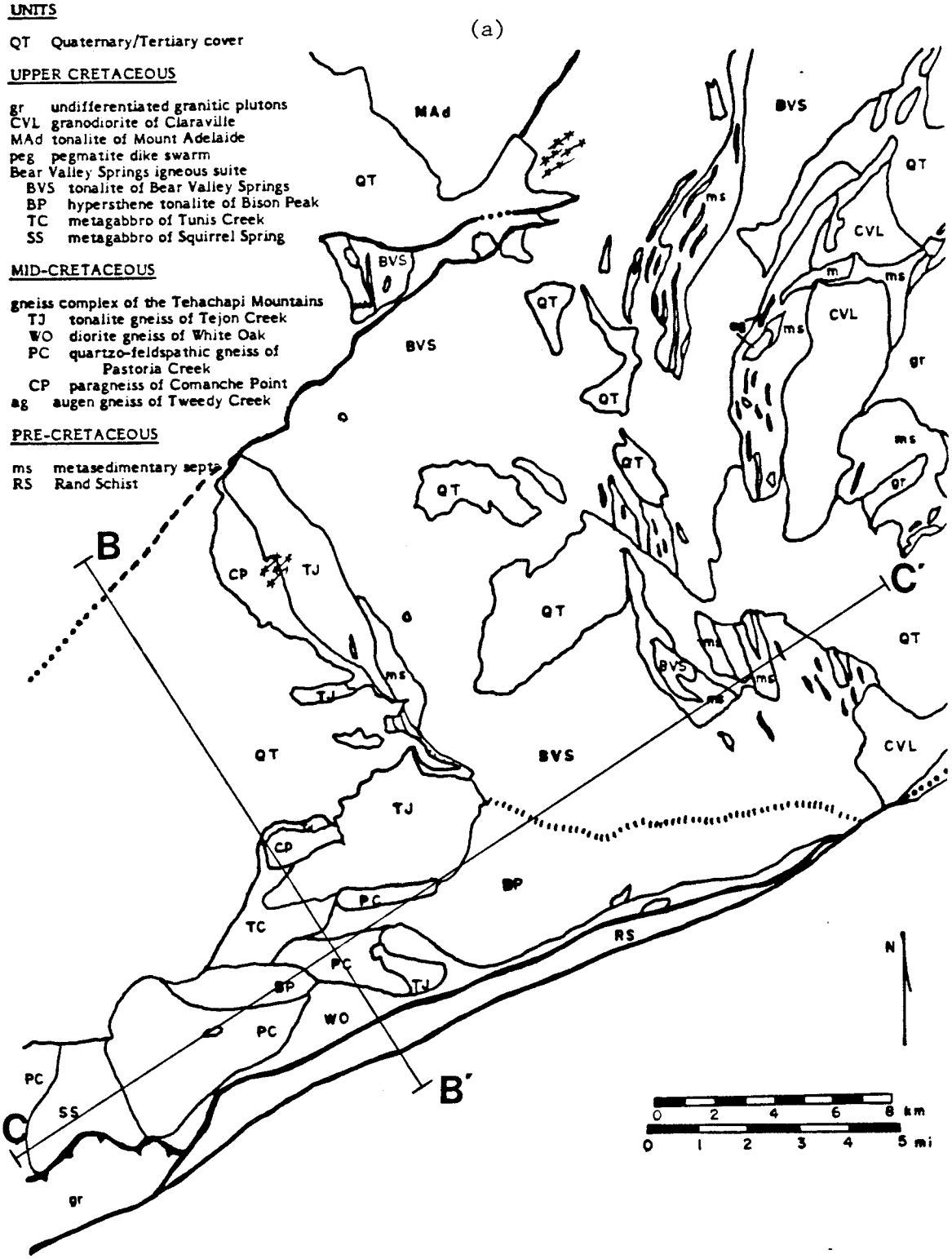

(b)

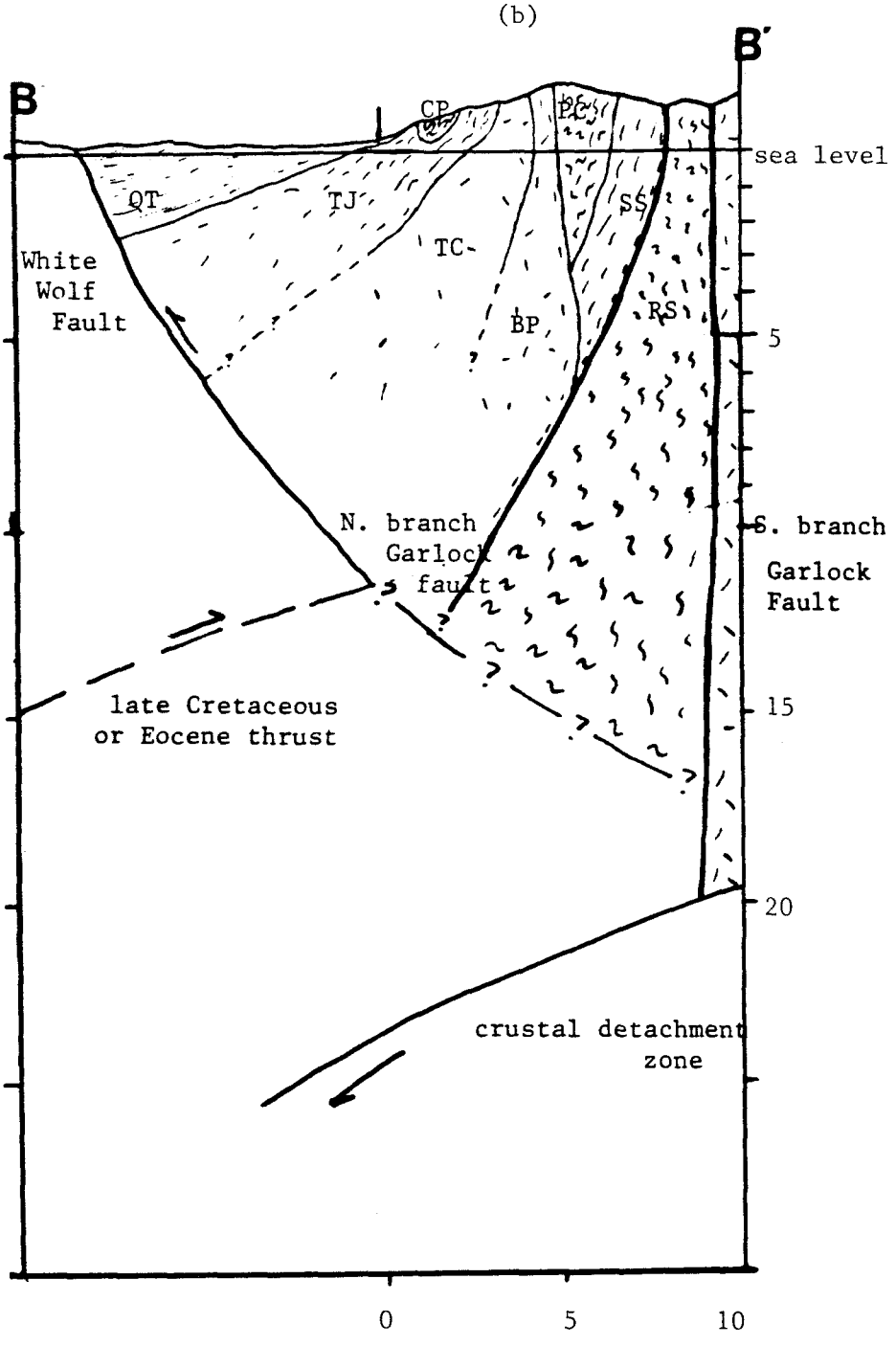

Vertical and Horizontal scales in km.

(c)

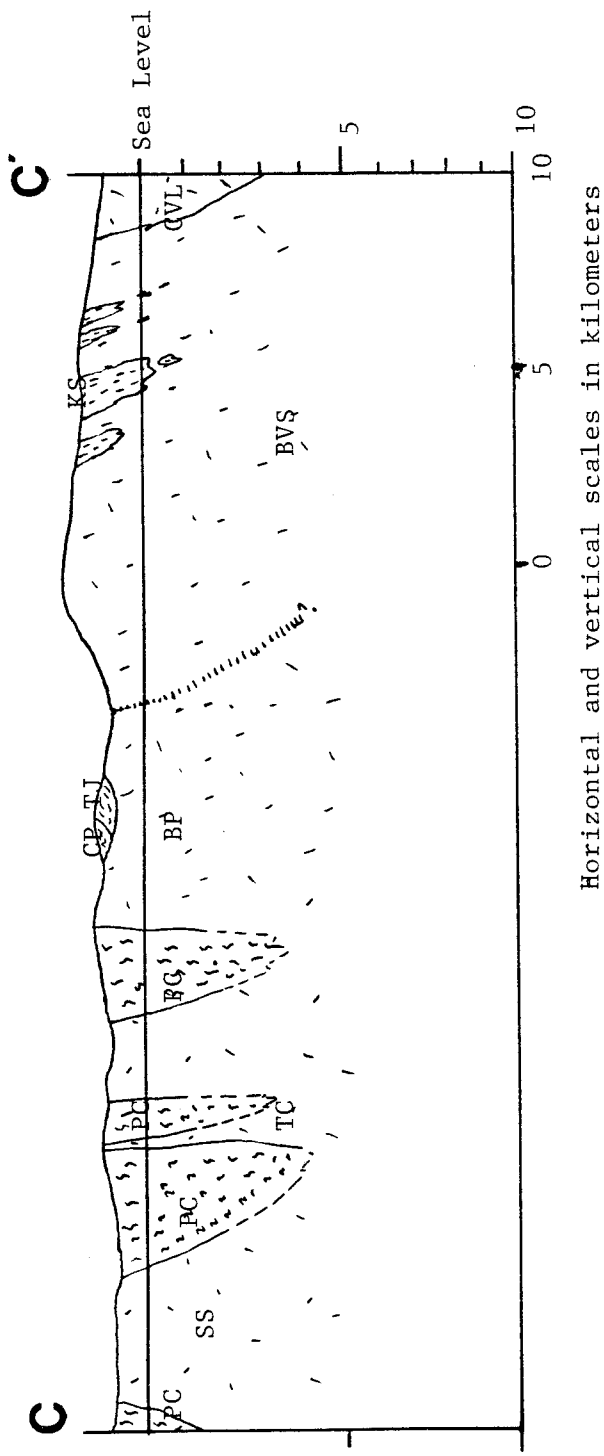

Horizontal and vertical scales in kilometers

from Tehachapi to Grapevine Canyon, and northwest-southeast across the heart of the Tehachapi Mountains, as shown on Figure 68a. The rocks of the gneiss complex of the Tehachapi Mountains occur as discrete bodies alongside and beneath the batholith. On section C-C' (Figure 68c), several deep structures are shown. The White Wolf fault dips south beneath the gneiss complex, forming its northern border, while the north branch of the Garlock fault dips north beneath the complex (Sharry, 1981b; Crowell, 1954). A shallow level structure is seen truncating this steeper structure, and is believed to be part of a late-Cretaceous or Eocene detachment surface. This surface is perhaps responsible for the rapid uplift of the gneiss terrane, and the southern California thrusting event of Silver (1983, 1982). An even deeper-level, flat-lying surface is shown as the detachment of Bird and Rosenstock (1984) and Humphreys and others (1984), where there is down-welling of the lower crust (?) and mantle beneath the Tehachapi Mountains.

IV.4.2 Granulite occurrence and roots of the Sierra Nevada batholith

The interpretation of granulites and granulite affinity rocks in the gneiss complex of the Tehachapi Mountains is based primarily on the presence of pyroxenes in the rocks. The rocks in question commonly appear to have a borderline igneous-metamorphic texture, with a wide range of textures. This is perhaps due to conditions where the distinction between the two regimes (igneous and metamorphic) breaks down into a continuum of processes. Sharry (1981b) referred to the gneiss complex as a granulite terrane, with the metagabbro of Tunis Creek and the hypersthene tonalite of Bison Peak as his primary granulite units. Ross (1985, 1986) mentions a number of petrographic indicators that suggest upper amphibolite and/or lower granulite facies conditions for the gneiss complex, and cites the Tunis hot spot as an area from which metamorphic grade descends from granulite facies. Alternately, Sams and others (1983) describe many of the rocks within the

gneiss complex as meta-igneous, with granulite facies conditions present as local hot spots in a crystallizing and deforming batholith. The similarity of zircon ages between the gneiss complex and plutonic rocks gradational into the complex suggests a common history at and closely following igneous crystallization.

Many of the rocks are herein believed to have an igneous protolith, and to be related to gabbroic to tonalitic rocks of the western Cretaceous belt of the Sierra Nevada batholith, based on field, petrographic, and age considerations. Within the western Cretaceous belt, various assemblages contain 1) hornblende-rich gabbro, with olivine, olivine ± hypersthene, or hypersthene ± clinopyroxene ± cummingtonite; 2) two-pyroxene gabbro-diorite ± hornblende ± red biotite; and 3) hypersthene hornblende biotite quartz diorite to tonalite ± cummingtonite ± clinopyroxene (Best, 1963; Ehrreich, 1965; Mack and others, 1979; Saleeby and Williams, 1979; Saleeby and Sharp, 1980). Ultramafic rocks are locally found along with those assemblages. Brown hornblende and calcic plagioclase are the dominant mineral phases. They occur in interlocked adcumulate textures that resemble annealed metamorphic textures, and as okiocrysts of hornblende poikilitically enclosing plagioclase. Olivine and hypersthene can be found poikilitically enclosed within hornblende with reaction rims of pyroxene (olivine) and cummingtonite (hypersthene).

All of these mafic assemblages, as well as local lenses and pods of ultramafic rock, and the above described textures can be found in the southernmost Sierra Nevada, especially within the metagabbro of Tunis Creek and the hypersthene tonalite of Bison Peak. Hornblende ± olivine gabbros with hornblende poikilitically enclosing calcic plagioclase (Figure 21), two-pyroxene quartz diorite to tonalite with hornblende poikilitically enclosing pyroxene in equilibrium settings (Figure 19), and cumulate textures (Figure 24, 25) can all be found in the

study area. Olivine is seen as relict or ghost grains in the metagabbro of Tunis Creek. Plagioclase is frequently well twinned and weakly zoned, suggesting a melt phase was present.

There are, however, important differences between the mafic rocks of the western Cretaceous Sierra Nevada belt and rocks of the southernmost Sierra. Epidote-bearing tonalites which are interpreted as deep-seated igneous rocks are present in the study area. Second, porphyroblastic garnet occurs as a post-crystallization sub-solidus product (Figure 23). This local late-stage garnet growth is believed to represent an extended period of hot sub-solidus conditions where the garnets were able to grow without appreciable pressure changes. These differences in mineralogy are the result of a deeper level of intrusion within the study area relative to the western part of the Cretaceous Sierran batholith to the north.

Other rocks in the gneiss complex of the Tehachapi Mountains have an obvious metasedimentary origin. They are marbles, calc-silicates, semi-pure quartzites, and paragneisses. The presence of microcline and myrmekitic structures, seen in a number of locations, can be ascribed to either plutonic or high-grade metamorphic conditions. The presence of sillimanite in metamorphic septa rocks, most notably found near the gneiss complex, indicates pressures and temperatures in excess of 3.5 kb and 500°C (Holdaway, 1971). The lack of sillimanite in the varied lithologies within the gneiss complex is due to the near absence of pelitic rocks. These obvious metasedimentary rocks are the only rocks with observed prograde metamorphic reactions. The metasedimentary rocks typically lack assemblages that would yield prograde minerals (being primarily quartzite and marble), as the psammitic and quartzo-feldspathic members were almost completely melted and assimilated by the voluminuous batholith. However, local

lenses of granulite facies paragneiss and granofels can be found adjacent to the more mafic intrusive rocks. The relative paucity of prograde mineral reactions and metasedimentary material is believed to be the result of the gneiss complex of the Tehachapi Mountains being dominated by igneous rock assemblages, and having experienced magmatic conditions at peak metamorphic pressures and temperatures.

Migmatitic structures as seen in the paragneiss of Comanche Point are suggestive of depths of 12 to 25 km (Hamilton, 1981). Hamilton suggests that such structures occur in rocks ranging in grade from upper amphibolite to lower granulite facies, where garnet and brown hornblende are characteristic. Ghent and others (1977) describe migmatitic amphibolitic rocks from British Columbia which appear to be similar to rocks from the southern Sierra as representing depths of up to 25 km. Domenick and others (1983) have studied xenoliths contained in late Tertiary volcanic rocks of the central Sierras. Some of the xenoliths resemble many of the rocks found in the gneiss complex. They describe a garnet granulite (clinopyroxene, garnet, plagioclase, and orthopyroxene, with minor quartz, biotite, and hornblende) as representing a residue of a source which partially melted to produce granodiorite. They describe this upper granulite facies xenolith as having an origin at greater than 30 km. This mineral association appears to be of a higher grade than rocks in the gneiss complex of the Tehachapi Mountains, since the association garnet + two pyroxenes is not found in the gneiss complex. Other xenoliths described include diorite amphibolites and a sillimanite gneiss. The amphibolites contain hornblende and plagioclase, with lesser amounts of quartz, orthopyroxene, and biotite. These xenoliths, similar to the majority of the gneiss complex, are thought to have come from about 15-20 km. The sillimanite gneiss xenolith contains plagioclase, biotite, garnet, and minor sillimanite and horn-

blende. This mineralogy is similar to that of the southernmost Sierran metasedimentary septa rocks, and the xenolith was thought by Domenick and others (1983) to originate at about 10-15 km.

Overall, the rocks in the gneiss complex of the Tehachapi Mountains appear to belong to upper amphibolite rather than lower granulite facies, and to have an origin of 15 to 25 km depth. Most likely, the gneiss complex has seen a large variation of metamorphic zones that are highly dependent on local vapor pressure and proximity to igneous phases. The occurrence of granulite grade assemblages is most likely due to the dehydration effect of the removal of water from the system due to the presence of granitoid melts.

The tonalite of Bear Valley Springs has characteristics that indicate an emplacement depth greater than other Sierran plutons. In the classification of Buddington (1959), it would be considered a catazonal (deep or lower crustal level) pluton that has concordant contacts with country rocks. It contains frequent, widespread, ovoid to stretched-out mafic inclusions that are amphibolitic or hypersthene-bearing. These inclusions are generally mineralogically and geochemically equilibrated with their host. Dark gneissic patches and streaks, schlieren, and mylonite zones are present. Hypersthene, fresh in appearance and in equilibrium with the rest of the rock, is locally present in the tonalite. Hornblende and biotite occur as anhedral grains and clumps. The mafic minerals together with the mafic inclusions give the rock a crude gneissic fabric. The tonalite appears to grade into the gneiss complex, which consists of igneous, sedimentary, and unknown protoliths. The tonalite therefore appears to be a plutonic unit that has undergone considerable deformation, and has assimilated material from the gneiss complex, with which it has an intimate history.

Possible mechanisms for the origin of the crystalline rocks of the southernmost Sierra Nevada are ultrametamorphism and anatexis, local batholithic melt production due to the intrusion of a major heat source(s), or intrusion of a batholithic melt into a pre-existing high-grade terrane. The possible mechanisms are detailed below.

White and Chappell (1977) describe high-grade (granulitic) terranes of andesitic to basaltic composition as consisting of a two pyroxene + quartz + feldspar granulite. Ultrametamorphism of the terrane will yield a melt + residuum (restite). The residue of ultrametamorphism (granitoid melt production through metamorphism and anatexis) is a granulite. Removal of a granitoid melt containing water would be a mechanism to raise amphibolite facies rocks to granulite facies conditions through dehydration (White and Chappell, 1977; O'Hara and Yarwood, 1978). There would be no need for an increase in either pressure or temperature. The restite or residue after removal of the granitoid melt would be mafic- and hornblende-rich, with pyroxene. Both the melt and residuum can move together during diapiric ascent, with the mafic inclusions in the granitoid representing residuum material.

With respect to the southernmost Sierras, Weise (1950) suggested ultrametamorphism as a mechanism for the production of his gabbro unit (most of the metagabbro of Tunis Creek). Some of the more mafic portions of the gneiss complex could well represent restite material from which a melt has been removed; the melt itself could be represented by the tonalite of Bear Valley Springs. In this case, much of the dark amphibolitic material found in the tonalite as inclusions would be material from the probable source region (residuum), and similar to the rocks of the gneiss complex as suggested by Ross (1983c, 1985, 1986).

The above interpretation is discounted due to the similar zircon ages, and oxygen, strontium, and rubidium systematics between the granitoid melt (tonalite of Bear Valley Springs) and the "restite" (metagabbro of Tunis Creek), the gradational contacts between the units, the poorly preserved dike-form structures of the mafic inclusions, and the lack of migmatitic structures and local melts between the restite and the melt. Similarly, no evidence is available to support a model for the creation of the tonalite of Bear Valley Springs by melting of the country rocks through the addition of a major heat source.

As an example of the third mechanism, Obata (1980) describes the origin of the Ronda peridotite, southern Spain, as a partially crystalline mass cooling and crystallizing during ascent to produce a range of P-T paths for various parts of the mass. In particular, the central portion shows a lower crystallization pressure than the margins. The margins show pronounced shearing, which is related to movement between the peridotite and the surrounding rocks. The central, "insulated" portion remains unsheared. In addition, the central portion has slightly younger ages, due to its later-stage crystallization. A similar history is envisioned for the southernmost Sierra Nevada.

The margins of the tonalite of Bear Valley Springs, in particular the southern and southwestern margins, show pronounced shearing and a complex zone of apparent mixing with rocks of the gneiss complex. The preferred interpretation for the origin of the tonalite of Bear Valley Springs (shown schematically in Figure 69), and for much of the gneiss complex, is that of a large batholithic body ascending through deep crustal levels and spreading out, crystallizing and becoming blastomylonitic along its lower margins and floor due to extensive interaction and differential movement between magma and country rocks. The batholith ascends as a diapir to the Conrad discontinuity where, due to a lower-density

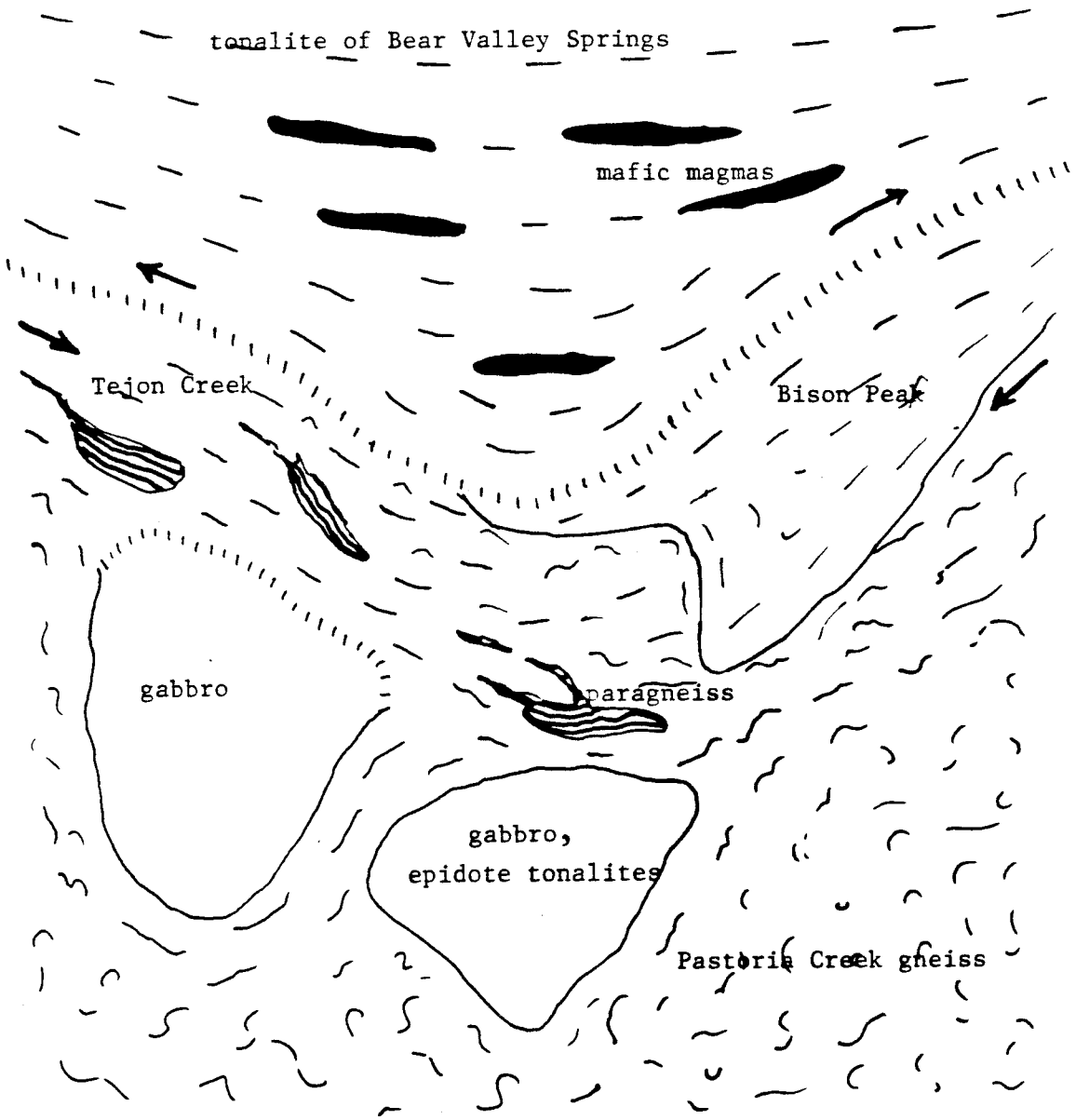

Figure 69. Schematic cross-section of the structural relations between the Bear Valley Springs intrusive suite and the gneiss complex of the Tehachapi Mountains.

environment, it spreads out laterally and slows or stops its ascent. The location of the discontinuity would be at about 25-30 km depth (Saleeby and others, 1986c), where granulitic rocks are thought to exist beneath the Sierra Nevada batholith (Saleeby and others, 1986c; Christensen and Fountain, 1975).

The mafic inclusions and metagabbros are interpreted as mafic co-magmatic material that was intruded along with the tonalite. As such, they may represent the vestiges of mafic mantle-derived material that provided the heat required to initiate melt production that resulted in the tonalite. Synplutonic masses that may be related to the mafic inclusions in the tonalite are the metagabbros of the Tunis Creek and Squirrel Spring areas, and perhaps the mafic (basaltic?) lenses within the tonalite gneiss of Tejon Creek. As the tonalite ascended through and spread out at deep crustal levels, its lower margins and floor reacted with the surrounding country rock locally producing melts, becoming plastically deformed, cooling, and crystallizing while the remainder of the pluton was ascending. The floor may be represented by the hypersthene tonalite of Bison Peak.

The tonalite of Bear Valley Springs crystallized during ascent and spreading-out through the lower crust. The earlier crystallizing regions were the border or floor phases along the southern and southwestern margins of the pluton, as well as coeval gabbros. They have an age that, although analytically identical, could be interpreted as older than that of the main interior portion of the tonalite. These marginal regions were deformed at or near the solidus, contain local hypersthene, and have weakly zoned plagioclase. The foliation was probably originally close to flat-lying. The resulting foliation development was in part due to the spreading out of the batholith over its gneissic substrate, while linear shape fabrics in the mafic inclusions may be the result of development of constrictional strain related to batholithic magma transport and corresponding return flow of the surrounding rock.

The pluton continued to crystallize from the margins inward as it continued to rise and spread. The less deformed interior part of the pluton around and north of Tehachapi where plagioclase is more strongly zoned, and the possibly younger age of the tonalite of Mount Adelaide and main phase of the tonalite of Bear Valley Springs support this. The tonalite probably completed crystallization at more "typical" Sierran mesozonal depths, where deformation is generally absent and plagioclase is normally zoned. Thus, the tonalite exhibits a progressively greater depth of emplacement and possible earlier crystallization history southward in the batholith.

The Bear Valley Springs plutonic suite is herein defined to include the tonalite of Bear Valley Springs, the hypersthene tonalite of Bison Peak, and the metagabbros of Tunis Creek and Squirrel Spring. These rocks are igneous rocks that effectively crystallized under regional upper amphibolite to lower granulite facies conditions, perhaps with an upper limit defined by the P-T relations in the quartzo-feldspathic gneiss of Pastoria Creek. The granulite facies conditions were experienced by the Bear Valley Springs suite in the descent through the solidus defined by retrograde reactions, as seen in the southernmost part of the pluton, the hypersthene tonalite of Bison Peak, and the metagabbro of Tunis Creek. The suite is the result of mixing of mantle-derived magmas and crustal anatectic melts during batholith generation. As such it generally supports DePaolo's model (1981b) for the generation of the Sierra Nevada batholith.

The tonalite of Bear Valley Springs could represent part of a large intrusive complex that provided heat to the gneiss complex rocks, and initiated melt production from it. The more siliceous parts of the gneiss complex - the quartzofeldspathic gneisses and metasedimentary gneisses - are country rocks through which the tonalite ascended. This is one possible origin for the southernmost

Sierra Nevada, but is not the preferred one, due to the lack of evidence for additional large heat sources. Shearing in the tonalite becomes weaker inwards from the margins, and northwards in the mass. Thus, if the intrusion of the Bear Valley Springs suite is modelled similar to the Ronda peridotite in its ascent through the crust, the southernmost Sierras would represent a cross-sectional slice or down-dip view through the deeper portions of a batholith - from mesozonal regions in the vicinity of Lake Isabella, to lower crustal areas of possible melt production in the Tehachapi Mountains.

Granitoid magmas are produced by complex, deep-seated, multi-stage processes involving partial melting, contamination and assimilation, and differentiation (Hamilton and Meyers, 1967; Green, 1980; Hamilton, 1981) with potential sources for the magmas being mantle peridotite, continental crust, subducted oceanic crust, or a mixture thereof (Atherton and Tarnet, 1979; DePaolo, 1981b). The observed granitoids are not primary magmas from the mantle or deep crustal regions (Wyllie, 1983b). Dehydration of subducted oceanic crust releases aqueous fluids that can cause partial melting of the subducted oceanic crust, overlying peridotite mantle, or deep continental crust. Mantle derived magmas cause partial melting of the heterogeneous crustal rocks, and exchange with, hybridize with, and mobilize the crustal rocks (Atherton and Tarnet, 1979). The deep crust is dominated by gabbro-tonalite and their metamorphic equivalents ± metamorphosed shale and greywacke, and anatexis of such at high grade conditions will yield granitic to granodioritic melts, or yield melts of tonalitic composition possible at temperatures above 1100°C (Wyllie, 1983a). Also, tonalites can be generated by recrystallization of residual rock from which a granitic liquid has been extracted (Wyllie, 1983a). Thus, tonalitic batholiths are likely generated by the infusion of heat and material into crustal materials by less siliceous deeper-level magmas.

The geochemical and zircon age data on rocks of the southernmost Sierra Nevada points to upper mantle mafic magmas as the primary source for the observed magmatic products, and the generation of the voluminuous tonalitic batholith as a result of significant interaction with crustal material. A third component, probably subducted oceanic crustal material, is likely present in the zone of magma genesis or was mixed with the mantle magmas during ascent into the middle crust.

The mid-crustal levels are believed to be comprised of migmatitic material under lower granulite to upper amphibolite facies conditions (Hamilton, 1981) with mafic to intermediate compositions, where considerable anatexis, multiple deformations, polymetamorphism, and reworking of older crustal material occurs (Fountain and Salisbury, 1981). Thus, field and isotopic evidence from this study indicates the southernmost Sierra Nevada is a deep-seated batholithic terrane derived from mixing of mantle-derived material and crustal metasedimentary assemblages, ± various admixtures of Phanerozoic ensimatic material, and that the middle crust has been tectonically and magmatically reworked into a new sialic crustal section.

IV.4.3 Possible origins and protoliths

The protoliths for the crystalline rocks for the southernmost Sierra Nevada are varied. Evidence for igneous and meta-igneous rocks is seen in the relict igneous textures and mineralogy (olivine and pyroxene cores), oxygen isotopic ratios in the igneous range (+5.7 to +8.6°/$_{oo}$), and zircon ages virtually the same as those of the tonalite of Bear Valley Springs.

Textural features consist of remnant olivine grains, and the retrograde reactions involving the replacement of olivine with orthopyroxene and pyroxenes with amphiboles. Hypidiomorphic granular and cumulate textures are infrequent,

but present. Normally zoned plagioclase, in particular where it is not in contact with minerals to alter the anorthite content, is indicative of igneous conditions. Magmatic epidote is present. Intrusive relations are not common, but some diking is present involving the Bison Peak and Tunis Creek units with other units. Much of the terrane consists of rocks that seem to have an igneous mineralogy and bulk composition, and suggestions of igneous textures. Units that are interpreted to be igneous or meta-igneous are members of the Bear Valley Springs intrusive sequence (hypersthene tonalite of Bison Peak, metagabbros of Tunis Creek and Squirrel Spring) and the tonalite gneiss of Tejon Creek. In addition, much of the rock within the quartzo-feldspathic gneiss of Pastoria Creek is thought to be meta-igneous. These rocks are primarily diorites-tonalites and differentiated granites that have low initial $^{87}Sr/^{86}Sr$ and $\delta^{18}O$.

Obvious metasediments (marbles, quartzites, calc-silicates, and paragneiss) are present in minor amounts. They are frequently found as lenses or enclaves within surrounding units, and as the mappable paragneiss of Comanche Point. They have $\delta^{18}O$ values that range from +10 to +18°/$_{oo}$. The remainder of the gneiss complex consists of rocks that do not have indications of a protolith. Generally, these gneisses are of a granitic to granodioritic composition, and are relatively strongly deformed, obscuring evidence of a protolith.

IV.4.4 Geologic history

The basement of the southern part of the Sierra Nevada is of an unknown character. Based on Ross (1980, 1985, 1986), DePaolo (1981b), Saleeby and others (1980), Kistler and Peterman (1973, 1978), and Chen and Tilton (1978), it consists of oceanic-affinity rocks to the west of the quartz diorite and initial $^{87}Sr/^{86}Sr$= 0.7060 lines (which are approximately the same), and sialic, continental material to the east of the line. This line runs approximately through the tonalite of Bear Valley Springs.

Sedimentary material derived at least in part from the craton (containing zircon with a 1400-1900 Ma age signature, Silver and others, 1977) was deposited across sialic and perhaps ophiolitic basement. The metasediments are now represented by the Kings sequence septa and the paragneiss of Comanche Point. Between 120 and 110 Ma, small pulses of igneous material were injected into the sedimentary pile, possibly along shear zones (augen gneiss of Tweedy Creek and much of the gneiss complex). Injection was concurrent with regional deformation in a high grade environment. The tonalite gneiss of Tejon Creek and much of the quartzo-feldspathic gneiss of Pastoria Creek represent similar small intrusive bodies of the 110-120 Ma age range. Much of the country rock was displaced by or assimilated into these intrusives, with small remnants appearing as paragneiss enclaves, and patches of quartzite, calc-silicate material, marble, and quartzo-feldspathic gneiss.

At about 100 Ma, the region was engulfed in a major pulse of batholithic activity, culminating in the intrusion of the Bear Valley Springs plutonic suite. Deformation of the region continued synplutonic with and/or because of the intrusion of the suite. Deformation waned and essentially ceased with the end of the Bear Valley Springs episode. The deformation at and prior to 100 Ma could be related to a deformation observed in the Peninsular Ranges batholith, and to the cause of the age and isotopic step between the western and eastern portions of that batholith (Silver and others, 1979; Todd and Shaw, 1979). At that time, subduction is thought to have changed from a moderately steep-angled, stable subduction zone with a static arc, to a shallower-angled, east-progressing, transgressive arc. Continued batholithic activity over about 10 my resulted in the intrusion of the remainder of the southern Sierran plutons (the granodiorite of Claraville) in a situation analogous to that in the eastern part of the Peninsular Ranges batholith.

The rocks of the gneiss complex of the Tehachapi Mountains and the tonalite of Bear Valley Springs show evidence of a major mid-Cretaceous deformation. Eastern wallrocks of the tonalite of Bear Valley Springs contain a concordantly emplaced sheet of granitic orthogneiss. The gneiss (augen gneiss of Tweedy Creek) has an igneous crystallization age of 114 Ma. Similar 114 to 117 Ma augen gneisses occur interlayered in the gneiss complex of the Tehachapi Mountains with blastomylonitic and protoclastic gneisses. At Tweedy Creek, the augen gneiss has in turn been intruded by a stock of tonalite which has an igneous crystallization age of about 93 Ma and is blastomylonitically deformed. The tonalite of Bear Valley Springs shows moderate degrees of blastomylonitic deformation in the vicinity of metamorphic septa, and is relatively nondeformed at locations far removed from wallrock interaction. The deformation along the margins of the pluton could be related to the interaction between a crystallizing magmatic body and its wallrocks, or it could be the result of a Cretaceous shear zone. The intrusion of the isolated body into the septa at Tweedy Creek suggests a weakening of the crust along such a zone. Within the gneiss complex of the Tehachapi Mountains, high-grade recrystallization was the prominant early deformational feature under solidus to hot sub-solidus conditions. Later deformational fabrics consist of ductile deformation under lower grade, post-peak metamorphic conditions perhaps after the Bear Valley Springs culmination. The granitic rocks exhibit a greater degree of deformation relative to the tonalite gneisses, perhaps as the result of bulk rock physical properties that concentrated the deformation in the more easily deformed quartz.

At about 85 Ma, the region was uplifted, resulting in a broad-scale cooling event and closure of the K/Ar and Rb/Sr isotopic age systems. Work by Sharry (1981b, 1982) has postulated an origin at about 25-30 km for parts of the gneiss

complex of the Tehachapi Mountains. Work by Elan and Thomas (1984) at Lake Isabella suggests metamorphism at about 3 kb and 700°C. Rb/Sr and K/Ar ages of between 80 and 90 Ma on the gneiss complex of the Tehachapi Mountains and tonalite of Bear Valley Springs indicate a major cooling event at about 85 Ma. Mid- to late-Eocene marine sediments unconformably above the tonalite of Bear Valley Springs and the gneiss complex of the Tehachapi Mountains (Nilsen and Clarke, 1975; Harris, 1954) indicate that the crystalline terrane was exposed by that time. The above evidence points to a rapid uplift of the deep-seated southern end of the Sierra Nevada following a major deformational event expressed by the profound ductile deformation of the southern Sierra Nevada batholith and its wallrocks. Such an event seems to correspond in time with the cessation of major Sierran batholithic activity. This could be the related to the southern California thrusting event(s) that removed a thick layer from the southernmost Sierras (Silver, 1982, 1983), and/or of underthrusting of the Rand schist beneath the southern Sierras. The thrusting event produced greenschist facies retrograde metamorphism in the region, developed primarily in the White Oak unit, and local cataclastic and mylonitic zones. At some time between 80 and 16 Ma, the southern portion of the batholith was rotated 45-60° in a clockwise direction, possibly as the result of the aforementioned thrusting event. The structural consequences of the thrusting, uplift, and rotation on the southernmost Sierra Nevada is the exposure of deep- and sub-batholithic levels.

IV.4.6 Tehachapi Mountains as the southward continuation of the Sierra Nevada crystalline basement terrane

There are several lines of evidence showing that rocks of the Tehachapi Mountains are the southward continuation of the Sierran crystalline terrane. First is the continuation of metamorphic framework rocks into the vicinity of Tejon

Creek. Second is the continuation of the sequence of paragneiss-tonalite gneiss along the southwestern and western margins of the crystalline rock exposures. Third is the intimate gradational contact between rocks in the gneiss complex and the tonalite of Bear Valley Springs. Fourth is the similarity in history of deformation. Fifth is the similarities in age data, and the common existence of two sets of age ranges. All these features argue for a common geologic history for the two regions, with the Tehachapi crystalline rocks representing a deeper level of exposure.

IV.4.7 Regional comparisons

IV.4.7.1 Northern and central Sierra Nevada

A number of Jurassic plutons in the western Sierra Nevada and Klamath Mountains were investigated by Snoke and others (1982). They noted that the plutons typically contain a sequence of lithologies that range in composition from an ultramafic rock that is clinopyroxene-rich, through a region of biotite, two-pyroxene diorite to gabbro, to hypersthene tonalite.

Several workers have noted the existence of pyroxene in plutonic rocks in the western Cretaceous batholithic belt of the central and northern Sierra Nevada. Saleeby and Sharp (1980) describe 125 to 115 Ma plutonic rocks of the west margin of the south-central Sierran batholith as consisting in part of olivine-hornblende±clinopyroxene gabbros, hypersthene-hornblende-clinopyroxene gabbros to diorites, and hypersthene-hornblende-biotite tonalites. Hypersthene occurs as a rim around olivine, and clinopyroxene is intergradational with hornblende. They describe the existence of these rocks as a magmatic evolution of andesitic lavas from mantle-derived basalts.

The Academy pluton in the central Sierras has been described by Mack and others (1979) as a zoned pluton from a center of hornblende quartz norite, through

a region of hypersthene quartz diorite, to a margin of biotite-hornblende tonalite. The contacts in all cases were gradational. Most of the pluton had an age of 120 Ma, while the marginal tonalite was dated at 114 Ma. The quartz norite contained augite and cummingtonite and/or biotite coronas surrounding hypersthene. The quartz diorite also contained cummingtonite coronas. The progression from center to margins involved a lower calcic content in plagioclase, a greater content of quartz and biotite, less hypersthene, and a lower color index. The majority of the pluton was believed to represent one intrusive body, while the marginal phases were believed to be a separate intrusive from a more evolved, fractionated, similar type parent magma.

The western foothills of the Sierra Nevada in the vicinity of Fresno were investigated by Ehrreich (1965), who described mid-Cretaceous cummingtonite- and pyroxene-bearing hornblende gabbros and quartz diorites. He also noted the presence of migmatites related to the intrusion of those units.

The works summarized above indicate that pyrogenic pyroxene is widespread in Mesozoic plutonic rocks of the western part of the Sierra Nevada, which is consistent with the hypothesis that the hypersthene-bearing tonalite of Bear Valley Springs and the hypersthene tonalite of Bison Peak, as well as the metagabbros of Tunis Creek and Squirrel Springs (the Bear Valley Springs plutonic cycle) may be considered part of the western Cretaceous batholith belt in the Sierra Nevada. The occurence of pyroxene in granitoids is not an isolated instance, and certainly not demanding the interpretation of a metamorphic origin.

IV.4.7.2 Salinian block

The Salinian block has been suggested as the displaced continuation of the southern Sierra Nevada (Page, 1981, 1982; Silver, 1982, 1983; Ross, 1984). This is due to the truncation of the Sierran crystalline terrane at the Garlock fault, and

the search for its continuation elsewhere. The correlation is attractive for tectonic reasons, and is based in part on the overall similarity of the crystalline rocks of the two areas, and on palinspastic reconstructions of San Andreas fault zone movement.

Hypersthene-bearing granitic and metamorphic rocks (charnockites) are common in the western Santa Lucia Range in the Salinian block (Compton, 1960, 1966; Ross, 1976a,b,c). Zircons from two samples of hypersthene-bearing tonalite yield U/Pb ages of 97 and 100 Ma (Mattinson, 1978). Hamilton (1981) notes granulitic metamorphic rocks from the same area yield a U/Pb zircon age (analyses by L.T. Silver) of around 100 Ma. Similar rocks in the southern Sierras yield zircon ages in the same range (100 Ma for the tonalite of Bear Valley Springs, which locally contains hypersthene; 102 Ma for hypersthene tonalite and metagabbro in the gneiss complex). However, the southern Sierras contain a suite of 110 to 120 Ma rocks not seen within the Salinian province. Thus, the geologic environments were similar for the two regions at roughly the same time.

Hypersthene-bearing tonalite in the Santa Lucia Range has a lower quartz content than does the tonalite of Bear Valley Springs, contains hornblende in marked excess of biotite (rather than subequal or in excess), and contains only trace amounts of potassium feldspar (similar). Thus, the tonalites from the two areas have notable petrographic differences.

Other similarities and differences between the regions have been noted by Ross (1986). Granofels and quartzites are similar in both regions. These rocks have a granoblastic texture, and contain red-brown biotite, graphite, brown hornblende, and red garnet, while lacking sillimanite. In addition, the Santa Lucia rocks are rich in marbles relative to the rest of the metamorphic rocks, the opposite of the pattern seen in the Tehachapis.

Mattinson (1978) noted that the emplacement of the plutons in the Santa Lucia Range occurred at considerable depths. Wiebe (1970a,b) suggested that the granulitic metamorphic rocks and hypersthene-bearing tonalites (charnockites) in the Salinian block were indicative of depths of 15 to 20 km and temperatures of 650 to 700°C. These are within the realm of P-T for the southernmost Sierran rocks.

The Santa Lucia Range and southern Sierran rocks contain similar hypersthene "granulites", hypersthene-bearing tonalites, and distinctive hornfels. Both regions developed at roughly the same crustal depths at the same geologic time. Both areas have sillimanite-bearing, upper-amphibolite-grade metamorphic septa, with a decreasing metamorphic grade northward and eastward. However, there are no unique ties, and lithologic and age differences exist between these two areas.

Recent paleomagnetic work by Champion and others (1984, 1980) and Kanter (1982) suggests the northward translation of the Salinian block by over 1500 km relative to stable North America between the late Cretaceous and early Eocene, with post-Eocene slip on the San Andreas of less than about 500 km. If these studies prove to be conclusive, then the similarities between the Salinian and Sierran regions are based on their genesis in petrotectonic settings, rather than on their being physically correlative. It is highly likely that the two terranes represent the same tectonic setting, as the mid-Cretaceous saw peak batholithic magmatism for greater than 1000 km along the Sierra Nevada and Peninsular Ranges batholiths (Evernden and Kistler, 1970; Silver and others, 1979; Saleeby and Sharp, 1980; Stern and others, 1981; Chen and Moore, 1982).

IV.4.7.3 Peninsular Ranges batholith

The area of the southernmost Sierra Nevada west of the initial $^{87}Sr/^{86}Sr$= 0.7060 line and the quartz diorite line (the tonalite of Bear Valley Springs and the gneiss complex of the Tehachapi Mountains) share many similarities with the western portion of the Peninsular Ranges batholith. Both batholithic belts are characterized by low initial $^{87}Sr/^{86}Sr$ ratios, $\delta^{18}O$ values of between +5.5 and +8.5°/$_{oo}$, U/Pb ages of between 120 and 100 Ma, and a more mafic mineralogy as compared to batholithic rocks to the east (for the southernmost Sierra Nevada: this study; Sams and others, 1983; Saleeby, 1980; Ross, 1986; for the Peninsular Ranges batholith: Silver and others, 1979, 1975; Taylor and Silver, 1978). They also appear to share a similar mid-Cretaceous deformational episode expressed by intense ductile strain fabrics (this study; Sams and others, 1983; Silver and others, 1979; Todd and Shaw, 1979). Thus, the southern Sierra Nevada and the Peninsular Ranges batholiths appear to represent the same petrotectonic setting within the Cordilleran Cretaceous batholith.

VI. APPENDIX - GEOCHRONOLOGY

VI.1. Introduction and previous work

The southernmost Sierra Nevada has received reconnaissance geochronological investigations that were widely scattered and without precise definition. One of the main goals of this study was to characterize the igneous, metamorphic, and deformational events of the area, and to determine zircon U/Pb ages for regional correlation of units.

A summary of geochronological data on rocks in the southernmost Sierras (Ross 1983a, 1985b) is included here as Figure A1 and Table A1. The data consist of K/Ar and Rb/Sr determinations, and were performed by Evernden and Kistler (1970), Kistler and Peterman (1973, 1978), and Sharry (1981b).

As shown in Table A1, the tonalite of Bear Valley Springs was dated in three locations. The ages obtained were 1) near Keene (about thirteen km west of Tehachapi), in inclusion-rich tonalite near the central Kings sequence metamorphic septum, an Rb/Sr whole rock age of 81 Ma (Kistler and Peterman, 1978), and a K/Ar biotite age of 81 Ma (Evernden and Kistler, 1970); 2) along Water Canyon (about five km south of Tehachapi), in gneissic tonalite near the eastern septa, an Rb/Sr bulk rock age of 80 Ma (Kistler and Peterman, 1978); and 3) on the north slope of Cummings Mountain (about fifteen km southwest of Tehachapi), in somewhat deformed but near "normal" tonalite, K/Ar ages of 88.1±2.6 Ma on hornblende and 85.9±2.6 Ma on biotite (Ross, 1985b, 1983a). This latter sample is within a few kilometers of my sample CM9.

The gneiss complex of the Tehachapi Mountains, dated in the vicinity of the Grapevine along Interstate Route 5, yielded K/Ar ages of 77 Ma on hornblende and 86 Ma on biotite (Evernden and Kistler, 1970), and 87 Ma on biotite (Ross, 1985b, 1983a). Sharry (1981a,b) reports an Rb/Sr bulk rock age of 86±14 Ma for the

KEY TO BASE MAPS - SOUTHERNMOST SIERRA NEVADA

UNITS

QT Quaternary/Tertiary cover

UPPER CRETACEOUS

gr undifferentiated granitic plutons
CVL granodiorite of Claraville
MAd tonalite of Mount Adelaide
peg pegmatite dike swarm
Bear Valley Springs igneous suite
BVS tonalite of Bear Valley Springs
BP hypersthene tonalite of Bison Peak
TC metagabbro of Tunis Creek
SS metagabbro of Squirrel Spring

MID-CRETACEOUS

gneiss complex of the Tehachapi Mountains
TJ tonalite gneiss of Tejon Creek
WO diorite gneiss of White Oak
PC quartzo-feldspathic gneiss of Pastoria Creek
CP paragneiss of Comanche Point
ag augen gneiss of Tweedy Creek

PRE-CRETACEOUS

ms metasedimentary septa
RS Rand Schist

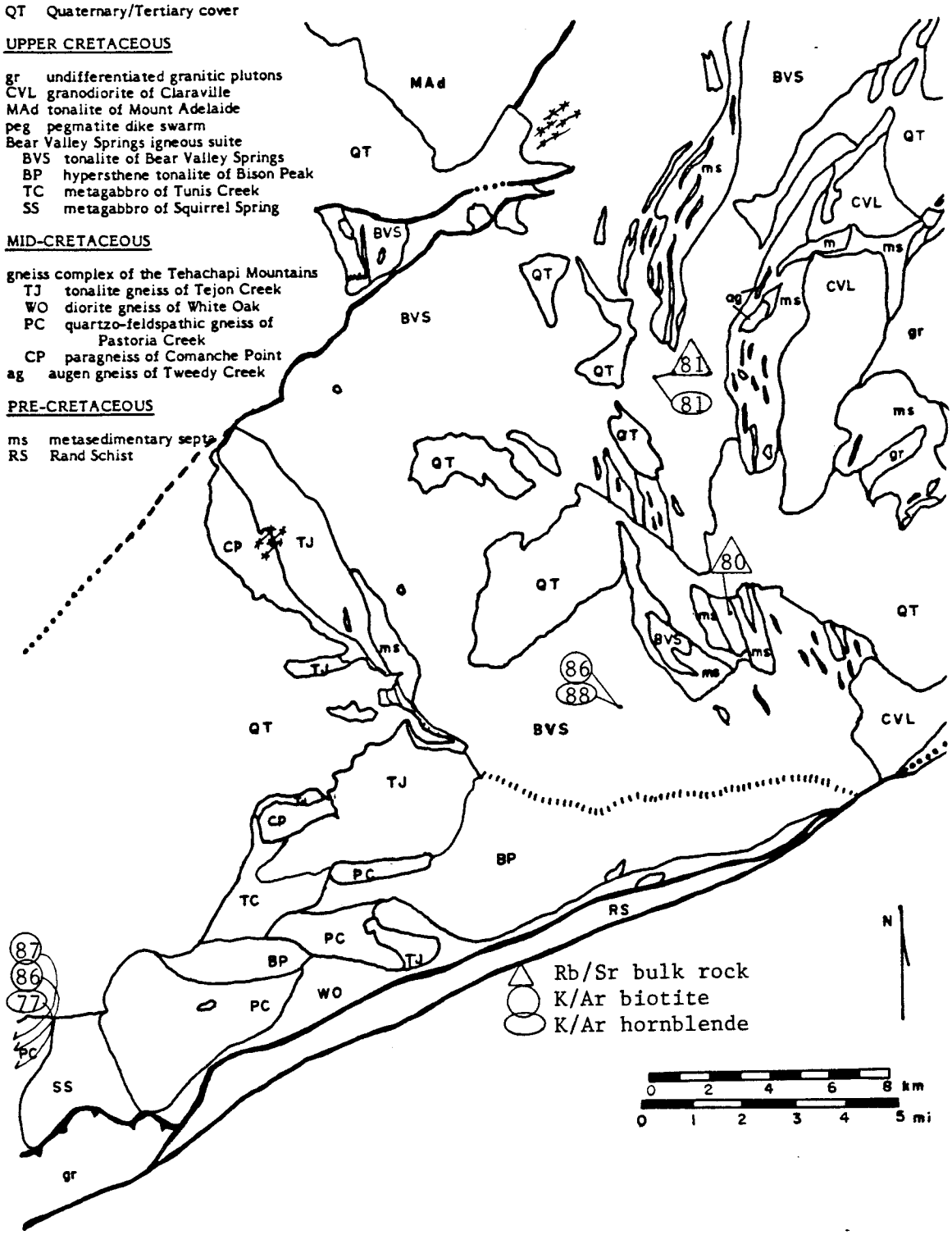

Figure A1. Map of Rb/Sr and K/Ar ages in the southernmost Sierra Nevada.

Table A1. K/Ar and Rb/Sr ages in the southern Sierra Nevada

SAMPLE#	LOCATION	SYSTEM	AGE‡	REFERENCE
Tonalite of Bear Valley Springs				
SR-14-73	Tehachapi Mountain Park, 5 km south of Tehachapi	Rb/Sr	80w	Kistler and Peterman 1978
SR-15-73	Keene area, 13 km west of Tehachapi	Rb/Sr	81w	ditto
140-1621	ditto	K/Ar	81b	Evernden and Kistler, 1970
3596	N. slope Cummings Mtn., 15 km west of Tehachapi	K/Ar K/Ar	86b 88h	Ross, 1983
Gneiss Complex of the Tehachapi Mountains, Grapevine Canyon				
153-1682	elevation 3150'	K/Ar	77h	Evernden and
142	elevation 2600'	K/Ar	86b	Kistler, 1970
no number	near the bottom	K/Ar	87b	Ross, 1985b

‡ h = hornblende, b = biotite, w = bulk rock

hypersthene tonalite of Bison Peak. Although this sample shows great scatter which may be the result of nonhomogeneity in the sample, the age falls within the range for the rest of the Rb/Sr age determinations.

There are no recognizable patterns with regards to isotopic system in the data (Figure A1). With regards to location, and excepting the 77 Ma age in the gneiss complex, the older ages (86 to 88 Ma) are south of the younger ages (80 to 81 Ma).

VI.2. Analytical methods of this study

Thirty-three samples of crystalline rocks from the southernmost Sierra Nevada and Tehachapi Mountains were collected for zircon U/Pb age determinations. These consisted of both the metamorphic framework and granitoid rocks of the Sierra Nevada batholith, along with an array of samples from the gneiss complex of the Tehachapi Mountains. Samples were selected to represent each of the major rock types in the region. Samples were also selected to place age constraints on deformational fabrics. Seven samples of the tonalite of Bear Valley Springs were selected to observe possible differences in the batholith from the margins towards the center. The freshest rock available for each sample was chosen for collection. Each sample was from a single outcrop. These were typically in road cuts and along stream channels.

Sample descriptions and localities are given in Table 12 and shown on Plate 1. Table 12 includes outcrop relations, geographic locations, petrographic descriptions, and zircon yield data. The samples ranged from 10 to 74 kg of homogeneous rock that was collected at a single outcrop. The samples were crushed in a jaw crusher to gravel-size, and disk pulverized with a 0.015 inch gap. The sample was concentrated on a Wilfley table, and acetylene tetrabromide (specific gravity of 2.96) and methylene iodide (s.g. 3.32) were used to remove the

various heavy minerals. Grains larger than 165 microns were removed by sieving. A Frantz isodynamic magnetic separator was used to separate the zircon using a current of 1.7 amps and collecting the non-magnetic fraction. The zircons were sieved into four size fractions: 165 to 120 microns (coarse, -100+150 mesh), 120 to 80 microns (medium, -150+200 mesh), 80 to 45 microns (fine, -200+325 mesh), and less than 45 microns (very fine, -325 mesh). Yields ranged from zero to 160 mg zircon per kg of sample. Zircon fraction characteristics are given in Table A2.

The zircon was washed in hot 16M nitric acid for about an hour to remove surface impurities. Zircon fractions of up to 46 mg were hand-picked to >99% purity on the basis of clarity, lack of inclusions, and euhedral igneous appearance. The zircon grains were colorless to pale red in color. The sample was washed briefly a second time in ultraclean warm 16M nitric acid in a TFE dissolution capsule. Dissolution was accomplished in the sealed capsule with ultraclean concentrated hydroflouric acid at 220°C for a week (Krogh, 1973). The HF was evaporated off and the sample redissolved overnight in ultraclean 6N HCl at 220°C in the pressurized capsule. At this point the sample was split into two aliquots, one aliquot of approximately 40% of the total sample receiving a mixed ^{208}Pb-^{235}U spike, the other aliquot receiving no spike. Lead and uranium were chemically extracted using an ion exchange column, Pb using a 3N HCl wash and 6N HCl extraction, U extracted using either a 2N HCl - 1N HF or a 1N HBr solution (Saleeby and Sharp, 1980). The product was evaporated with one drop of 0.25M H_3PO_4, washed with a drop of hot 16M nitric acid, and re-evaporated. Reagents were purified by a first distillation using a quartz still, followed by a sub-boiling distillation using a two-bottle teflon still in multiple cycles (Mattinson, 1972.) All sample processing beyond the heavy liquids separation was done in a clean air filtered laboratory. All chemistry was performed in laminar flow hoods.

Table A2. Zircon sample fraction characteristics

SAMPLE #	UNIT‡		FRACTION PROPERTIES‡‡		
1	TC27	Claraville granodiorite	nm	10/20	c-y,e-s,z,f
2	TC40	tonalite stock	nm	4/20	c-r,e-s,i,m
3	CM620	pegmatite x-cuts TJ	nm	1/20	c,e,m
4	PC35	granite dike xcuts PC	nm	2/20	c-y,e-s,i,m
5	BM684	tonalite (BVS-A)	nm	2/20	c,e,m
6	TC15	tonalite (BVS-e)	nm	2/20	c-r,e-s,i,m
7	TC42	tonalite (BVS-e)	nm	2/20	c-y,e-s,i,m
8	CM25	tonalite (BVS-m)	nm	1/20	c-y,e-s,i,m
9	CM26	tonalite (BVS-m)	nm	2/20	c-r,e,m
10	CM9	tonalite (BVS-m)	nm	1/20	c-y,e,f
11	CM22b	mafic inclusion (BVS-m)	nm	1/20	c-r,e,m
12	TL197	tonalite gneiss (BP)	nm	0/20	c-r,e,l
13	WR84	metagabbro (TC)	nm	1/20	c,e,m
14	WR86	metagabbro (TC)	nm	2/20	c-r,e,m
17	CM630	tonalite gneiss (TJ)	nm	1/20	c-y,e,f
18	WR643	tonalite gneiss (TJ)	nm	1/20	c-y,e,l
19	WR171	tonalite gneiss (TJ)	nm	1/20	c-y,e-s,m
20	WR30/2	quartz diorite (TJ)	nm	1/20	c-y,e,m
21	WR39	tonalite gneiss (TJ)	nm	-1/20	c-y,e-s,i,l
22	PC31	granite gneiss (PC)	nm	2/20	c-y,e-s,i,m
23	PC32	granite gneiss (PC)	nm	2/20	c-y,e-s,i,f
24	PC34	tonalite gneiss (PC)	nm	1/20	c-y,e-s,i,l
25	PC36	tonalite gneiss (PC)	nm	1/20	c-y,e-s,i,m
26	PC37	granite gneiss (PC)	nm	1/20	c-y,e-s,i,z
27	PC129	tonalite (PC)	nm	0/20	c-y,e-s,i,m
28	WR91a	tonalite gneiss (PC)	nm	-1/20	c-r,e-s,i,m
29	WR40	granite gneiss (PC)	nm	1/20	c-y,e-s,i,f
30	TC12a	Tweedy Creek augen gneiss	nm	10/20	c,e,f
31	TC12b	mafic inclusion in above	nm	10/20	c,e,f
32	CM640	quartzite, mmic septa	pm	-1/20	c-r,s-d,f
33	CM110	paragneiss (TGC)	pm	0/20	c-r,s-d,f

‡ BVS = tonalite of Bear Valley Springs (A = Mount Adelaide, e = eastern, m = main); BP = hypersthene tonalite of Bison Peak; TC = metagabbro of Tunis Creek; TGC = gneiss complex of the Tehachapi Mountains: PC = quartzo-feldspathic gneiss of Pastoria Creek; TJ = tonalite gneiss of Tejon Creek

‡‡ all samples separated on a Frantz isodynamic separator with a 1.7 amp current. nm denotes non-magnetic fraction, pm the para-magnetic fraction. 1/20 represents the side and front slopes respectively of the instrument. The properties of the fractions: c = clear, y = pale yellow to yellow-red, r = pale red; e = euhedral, s = subhedral, with slightly rounded corners, d = detrital-rounded; i = inclusion-rich, z = zoned or cored; f = fine, m = medium, l = coarse (as general grain sizes) Most fractions have the cleanest, most euhedral zircons as the finest grain size, and the zircons become less euhedral, more colored, and more inclusion-rich with size.

Isotopic compositions were measured on a solid source mass spectrometer using degassed Rhenium filaments. The mass spectrometer is a Neir-type, 30 cm radius of curvature, 60°-sector with an accelerating voltage of 10KV. The instrument is equipped with magnetic peak switching and on-line data processing. The silica gel - phosphoric acid technique was used for lead analyses, and the graphite - phosphoric acid technique was used for uranium. All isotopes except for ^{204}Pb were measured using a Faraday cup, while $^{206}Pb/^{204}Pb$ or $^{207}Pb/^{204}Pb$ ratios were measured using a secondary electron multiplier detector. An operating current of 2.2 amps was used for Pb, producing an operating temperature of about 1175°C with a signal current that averaged 10^{-11} amps of ^{206}Pb (10^{11} ohm resistor). The lead runs lasted three to four hours during which some signal decay occurred. Uranium runs of about two hours were done at a filament current of 4.2 amps and 1800°C, with a signal strength of about 10^{-11} amps of ^{238}U (10^{11} ohm resistor). Isotopic data were corrected for instrumental mass fractionation of 0.09% ± 0.04% per mass unit for lead, and 0.12% ± 0.04% per mass unit for uranium based on replicate analyses of U.S. National Bureau of Standards Pb and U standards (Tables A3 and A4). Pb blank determinations were made (Table A5), and are similar to long-term laboratory reproducibility. A total of 86 fractions (10 repeats of poor or unusable runs) from 31 samples were analyzed.

VI.3. Data and error analysis

For each set of analyses, the $^{207}Pb/^{206}Pb$ ratio of the spiked aliquot has been adjusted for the amount of ^{207}Pb and ^{206}Pb added due to the spike. Initial lead determinations were not made. Common lead corrections used were: $^{206}Pb/^{204}Pb = 18.8$, $^{207}Pb/^{204}Pb = 15.6$, and $^{208}Pb/^{204}Pb = 37.7$, based on common lead determinations from mid-Mesozoic batholithic rocks of the south-central Sierra Nevada (Chen and Moore, 1982), and from laboratory blank lead composition measurements.

Table A3. Lead isotopic standard data

STANDARD	$^{206}Pb/^{207}Pb$	$^{206}Pb/^{208}Pb$	$^{206}Pb/^{204}Pb$
NBS SRM983‡	14.0447(79)	73.43(13)	2695(140)
this work:			
cumulative	14.047(12)	73.306(97)	2694(70)
early	14.047(15)	73.357(90)	2762(41)
middle	14.049(20)	73.30(12)	2645(69)
late	14.0468(61)	73.292(85)	2704(47)

Amount of lead measured per analysis is about 50 ng. Numbers in parentheses are 2 sigma errors of the least significant figures. Standards for this work consisted of three completely different runs (spikes), consisting of 5 sets of data (early), 13 sets (middle), and 20 sets (late), for a total of 38 sets.

‡ from Catanzaro and others (1968).

Table A4. Uranium isotopic standard data

STANDARD	$^{235}U/^{238}U$	
NBS U500‡	0.9997(9)	
this work	0.9988(22)	cumulative - 11 sets
	0.9974(18)	Faraday Cup - 5 sets
	0.9999(18)	Multiplier - 6 sets

Amount of uranium measured per analysis is about 500 ng. Numbers in parentheses are 2 sigma errors of the least significant figures.

‡ from Catanzaro and others (1968).

Table A5. Laboratory blank determination data

ISOTOPE	ng. LEAD	
^{204}Pb	0.0014	
^{206}Pb	0.0253	
^{207}Pb	0.0213	
^{208}Pb	0.0516	
total blank	0.0982	(≈ 100 pg)

From analysis of ^{205}Pb spike of 0.026 gm, and determination of $^{205}Pb/^{208}Pb$ and $^{205}Pb/^{206}Pb$ ratios. ^{207}Pb from common lead ratios of ^{204}Pb:^{206}Pb:^{207}Pb:^{208}Pb = 1:18.8:15.6:37.7.

To assess the possible effect of initial lead ratios being different than the assigned ratios, possible alternative ratios were investigated (Table A6). For sample #1 ($^{206}Pb/^{204}Pb$ = 2800), an error in the $^{206}Pb/^{204}Pb$ or $^{208}Pb/^{204}Pb$ ratio of 0.1 (0.5 and 0.3% error, respectively) did not change the calculated ages. A change in the $^{207}Pb/^{204}Pb$ ratio of 0.1 (0.6% error) would have an error in the $^{207}Pb^*/^{235}U$ and $^{207}Pb^*/^{206}Pb^*$ ages of 0.1%. Thus, for the majority of samples ($^{206}Pb/^{204}Pb$ ratios >2000), the potential error from incorrect initial lead ratios is of a lower magnitude than the instrumental error (see below for a discussion of instrumental error).

For measured $^{206}Pb/^{204}Pb$ ratios in the order of 1000 (sample #4), a 0.1 error in the $^{206}Pb/^{204}Pb$ or the $^{208}Pb/^{204}Pb$ initial ratios would not change the calculated ages. A 0.1 error in the $^{207}Pb/^{204}Pb$ ratio would have a 0.2 and a 3.4% error in the $^{207}Pb^*/^{235}U$ and the $^{207}Pb^*/^{206}Pb^*$ ages. These errors are comparable to instrumental error.

The isotopic composition of the unspiked aliquot was corrected for 0.1 ng blank lead with a composition of $^{206}Pb/^{204}Pb$ = 18.8, $^{207}Pb/^{204}Pb$ = 15.6, and $^{208}Pb/^{204}Pb$ = 37.7 (Table A5). The amount of blank lead was determined by isotope dilution analysis involving dissolution, chemical separation, and filament loading procedures. The isotopic composition of the spiked aliquot has been adjusted for blank lead by balancing of the $^{207}Pb/^{206}Pb$ and $^{206}Pb/^{204}Pb$ ratios between the spiked and unspiked aliquots. Blank lead accounts for at most 50% of the common lead in a sample. Common lead remaining after correction for blank lead is assumed to be initial lead, and was assigned a blank lead composition. Initial lead most probably comes from inclusions and surface impurities.

The decay constants and isotopic abundances used in this study are: $\lambda^{238}U = 1.5513 \times 10^{-10}$, $\lambda^{235}U = 9.8485 \times 10^{-10}$ (Jaffey and others, 1971); $^{238}U/^{235}U$ (atom) = 137.88 (Chen and Wasserburg, 1981).

Table A6. Possible errors associated with the use of incorrect initial Pb ratios

"initial ratio	% error	$^{206}Pb^*/^{238}U$ age	error	$^{207}Pb^*/^{235}U$ age	error	$^{207}Pb^*/^{206}Pb^*$ age	error
Sample #1		$^{206}Pb/^{204}Pb$ = 2800					
actual	none	116.1	none	150.6	none	735	none
18.9[1]	0.5	116.1	0	150.6	0	735	0
19.8[1]	5.4	116.1	0	150.6	0	736	0.1
15.7[2]	0.6	116.1	0	150.5	0.1	734	0.1
16.6[2]	6.4	116.1	0	149.8	0.5	723	1.7
37.8[3]	0.3	116.1	0	150.6	0	735	0
38.8[3]	2.6	116.1	0	150.6	0	735	0
Sample #6		$^{206}Pb/^{204}Pb$ = 1100					
actual	none	94.0	none	95.1	none	123	none
18.9[1]	0.5	94.0	0	95.1	0	123	0
19.8[1]	5.4	93.9	0.1	95.1	0	125	1.6
15.7[2]	0.6	94.0	0	94.9	0.2	119	3.4
16.6[2]	6.4	94.0	0	93.4	1.8	79	56
37.8[3]	0.3	94.0	0	95.1	0	123	0
38.8[3]	2.6	94.0	0	95.1	0	123	0

Analysis was performed by calculating the $^{206}Pb^*/^{238}U$, $^{207}Pb^*/^{235}U$, and $^{207}Pb^*/^{206}Pb^*$ ages for a sample using different values for the initial lead composition, and comparing the results to "actual" values (values corresponding to the given initial ratios) to obtain a potential error for using an incorrect initial lead ratio.

Actual initial ratios given as $^{204}Pb:^{206}Pb:^{207}Pb:^{208}Pb$ = 18.8:15.6:37.7 were used in this report. Listed value is "changed" initial ratio: [1] = change in $^{206}Pb/^{204}Pb$; [2] = change in $^{207}Pb/^{204}Pb$; and [3] = change in $^{208}Pb/^{204}Pb$.

Based on Chen and Moore (1982), the analytical error (σ) in the calculated U/Pb age, given by

$$T = \frac{1}{\lambda} \ln(1 + \frac{x}{y}) \qquad (A1),$$

is estimated from

$$\sigma_T^2 = (\frac{T}{\lambda})^2 \sigma_\lambda^2 + [((\frac{\sigma_x}{y})^2 + (\frac{x\sigma_y}{y^2})^2) / \lambda^2 (1+\frac{x}{y})^2] \qquad (A2),$$

where:

$T = {}^{206}Pb^*/{}^{238}U$ age;

$\lambda = {}^{238}U$ decay constant;

$y = {}^{238}U$;

$x = {}^{206}Pb^*$ (radiogenic);

with analaguous equations for the ${}^{207}Pb^*/{}^{235}U$ system. The errors, σ_λ/λ, for ${}^{238}U$ and ${}^{235}U$ are 0.054 and 0.068%, respectively (Jaffey and others, 1971). The value for radiogenic lead is given by

$$x = u(1-vw), \qquad (A3),$$

where:

u = total ${}^{206}Pb$;

v = ${}^{204}Pb/{}^{206}Pb$ measured;

w = ${}^{206}Pb/{}^{204}Pb$ initial ratio.

The errors in (A3) are given by

$$\sigma_x^2 = (1-vw)^2\sigma_u^2 + (uw)^2\sigma_v^2 + (uv)^2\sigma_w^2 \qquad (A4).$$

Calculating σ_T for sample #1 ($^{206}Pb/^{204}Pb$ ratio of 2800), the errors in the $^{206}Pb^*/^{238}U$, $^{207}Pb^*/^{235}U$, and the $^{207}Pb^*/^{206}Pb^*$ ages (Table A7) ranged from 0.5 to 1.8, 0.6 to 2.1, and 10 to 36 Ma, respectively. For sample #6 ($^{206}Pb/^{204}Pb$ ratio of 1100), the errors were comparable: 0.5 to 0.7, 0.6 to 0.9, and 10 to 14 Ma.

In terms of reproducibility of results, five samples of the tonalite of Bear Valley Springs are compared. The overall results of the analyses gave the following ages: $^{206}Pb^*/^{238}U = 99.5 \pm 1.5$; $^{207}Pb^*/^{235}U = 99.8 \pm 1.5$; and $^{207}Pb^*/^{206}Pb^* = 109 \pm 13$ Ma. The magnitude of the deviation between samples is comparable to the magnitudes of the previously mentioned errors associated with a single analysis.

In a U/Pb analysis, most of the errors are in the determination of the spike concentration and composition, and in the working characteristics of the mass spectrometer. The most precisely determined age is the $^{206}Pb^*/^{238}U$ age, and this is what is referred to as the "age" of a concordant sample. The uncertainty in the age is based on the uncertainties in the ^{206}Pb and ^{238}U concentration determinations and in the reproducibility of ages. The $^{207}Pb^*/^{235}U$ age has a greater degree of uncertainty due to the difficulty in measuring the ^{207}Pb concentration. Based on the preceeding discussion, the uncertainty in the $^{206}Pb^*/^{238}U$ age is given as ±1.0 to 1.5% of the quoted age, while the uncertainty in the $^{207}Pb^*/^{235}U$ age is given as ±1.5 to 2.0% of the quoted age.

The uncertainty in the $^{207}Pb^*/^{206}Pb^*$ age is based on the long term reproducibility of NBS standards (NBS SRM983, see Table A3), common and initial lead compositional uncertainties, and agreement between the ages determined for both the spiked and unspiked aliquots. The uncertainty is dependent on the amount of common lead; samples with a larger measured $^{206}Pb/^{204}Pb$ ratio have a smaller error. These uncertainties typically exceed those calculated from mass spectrom-

Table A7. Analytical errors in calculated U/Pb ages

Sample Number	errors (Ma) $^{206}Pb^*/^{238}U$	$^{207}Pb^*/^{235}U$	$^{207}Pb^*/^{206}Pb^*$
#1	0.5	0.6	10
$^{206}Pb/^{204}Pb$	0.6	0.7	12
= 2800	1.8	2.1	36
	0.5	0.6	10
#6	0.7	0.9	14
$^{206}Pb/^{204}Pb$	0.5	0.6	10
= 1100			

Errors in the calculated U/Pb ages are dependent on errors in the uranium decay constants, and the measured U and Pb ratios. The tabulated errors are systematic errors, and are a function primarily of the working characteristics of the mass spectrometer, as well as the experimental procedure. The equations relating the errors are given in the text, and are from Chen and Moore (1982).

eter data sets. A histogram showing the difference between the $^{207}Pb^*/^{206}Pb^*$ ages of the unspiked and spiked aliquots is shown in Figure A2. There is considerable disagreement in $^{207}Pb^*/^{206}Pb^*$ ages between the two aliquots, most likely due to the operating characteristics of the mass spectrometer. Based on all of the preceeding factors, the uncertainties in the $^{207}Pb^*/^{206}Pb^*$ ages are given as ±15 Ma.

VI.4. Concordia

The following discussion is based on Wetherill (1956) and Faure (1977). A concordant system is a system that consists of minerals that are closed to uranium, lead, and intermediate daughter product loss or gain throughout its history. A discordant system is one that does not satisfy the above conditions. A U/Pb analysis is considered to be concordant if the ages, within analytical uncertainty, agree and lie on concordia. Concordant ages are usually assumed to represent igneous crystallization ages.

In well-behaved discordant zircon populations, the normal sequence of ages is $^{206}Pb^*/^{238}U < ^{207}Pb^*/^{235}U < ^{207}Pb^*/^{206}Pb^*$. The dispersion of ages within and between fractions is most likely due to the loss or gain of radiogenic lead or uranium. One process by which this occurs is a primary magmatic zircon incorporating pre-existing zircon from a magmatic source rock (inheritance), or entrainment of country material. Such zircon commonly shows older cores with overgrowth by new zircon. A second process is a post crystallization disturbance which results in lead loss and/or uranium gain in the dated zircon.

Concordia is defined (Faure, 1977) as the curve that is the locus of all points corresponding to concordant pairs of $^{206}Pb^*/^{238}U$ (ordinate) and $^{207}Pb^*/^{235}U$ (abscissa) ages for U/Pb systems (Figure A3). It is based on the modern cosmic value of $^{235}U/^{238}U$. The shape of concordia changes through geologic time. The

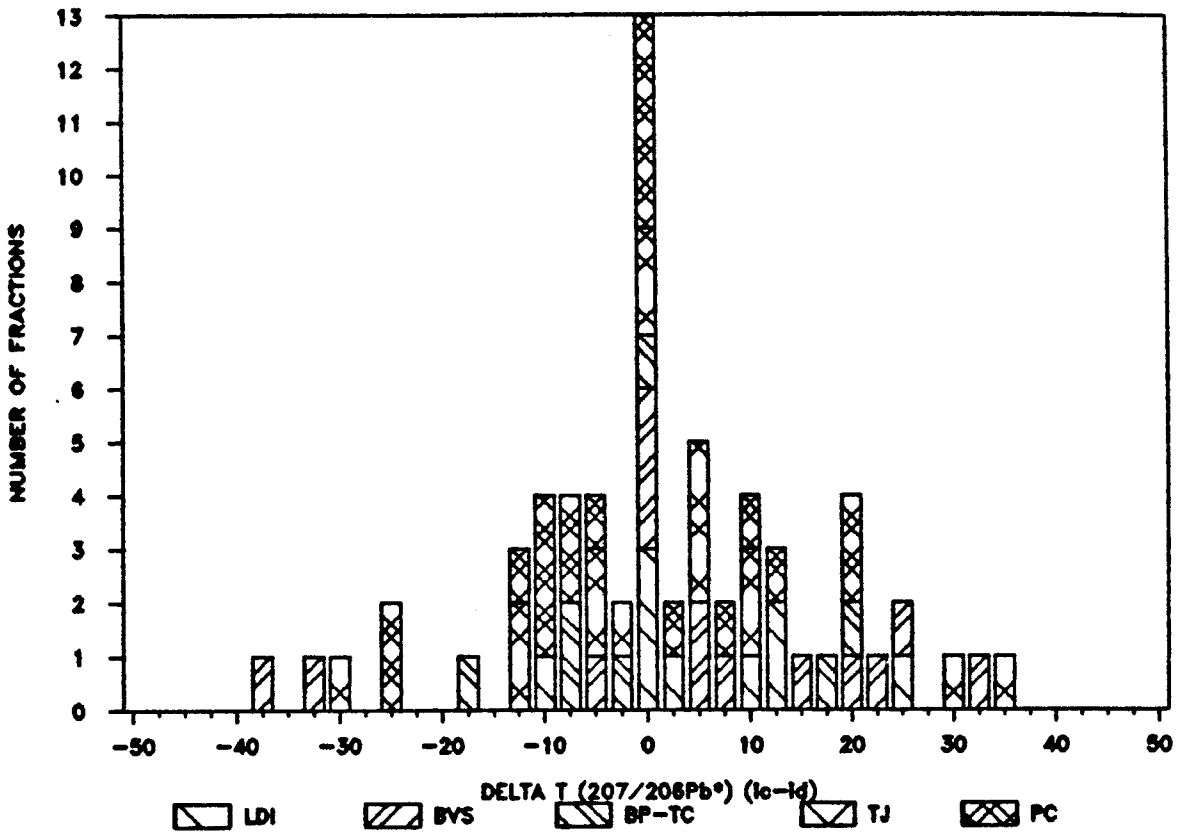

Figure A2. Histogram of the difference in $^{207}Pb^*/^{206}Pb^*$ ages between unspiked (ic) and spiked (id) aliquots.

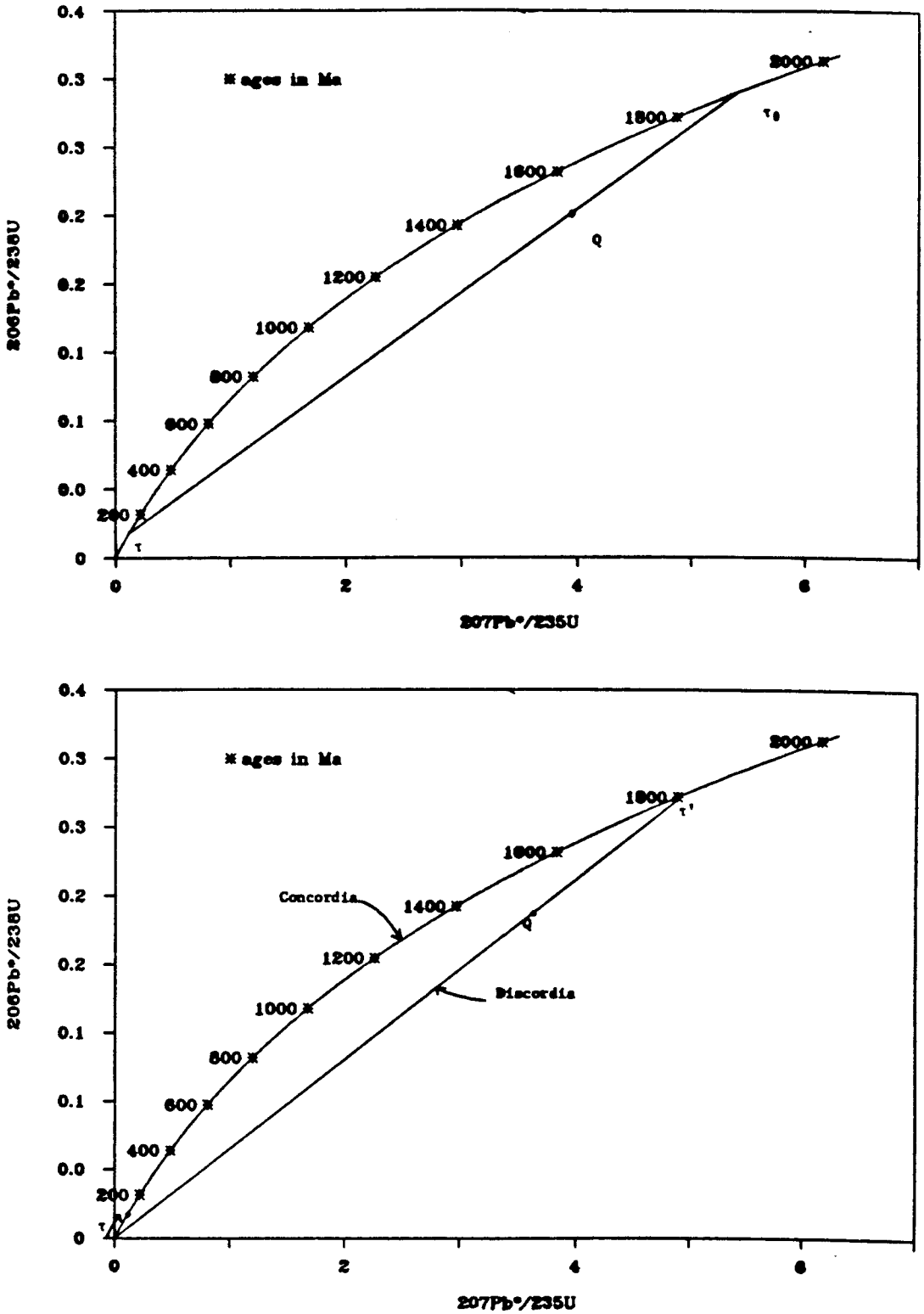

Figure A3. Concordia diagram illustrating discordia and intercepts.

curve as currently plotted is relative to modern time = 0. It is a projection from modern time back, with a specific modern $^{235}U/^{238}U$ ratio.

At the time of crystallization, a mineral system (typically zircon) contains no radiogenic lead, and plots at the origin. As long as the system remains closed, its U/Pb ages plot on concordia, are concordant, and indicate the crystallization age of the system (the time since closure is indicated by the position of the point along concordia).

Now suppose a U/Pb system on concordia at time τ' experiences an episode of lead loss (or uranium gain), typically through thermal metamorphism. The loss of radiogenic lead moves the point along a chord (called discordia) connecting τ' with the origin at the time of lead loss. Partial lead loss is represented by the point Q, and yields discordant U/Pb ages (Figure A3a). The position of Q on discordia depends on the proportion of radiogenic lead that is lost. A system that loses all of its radiogenic lead will return to the origin, and will subsequently move along concordia once the system becomes closed. After time τ it will lie on concordia at τ, with concordant U/Pb ages equal to the time elapsed since closure.

Zircon typically loses only a fraction of its radiogenic lead (Silver, 1964), and different crystals in a sample lose varying amounts even though all crystals experienced the same set of conditions. Lead loss appears to be a function of size and uranium concentration, where smaller grain size and higher uranium concentrations result in a greater degree of lead loss (Silver, 1964). It is often possible to obtain several zircon fractions from a single sample that plot as a series of points along discordia. One can then determine the position of discordia by fitting a straight line to the set of points representing zircons that have lost varying proportions of their radiogenic lead. By extrapolating discordia, one can obtain two intersections with concordia (Figure A3b). The points are τ_o and τ, where τ_o

is the time elapsed since the original crystallization of minerals, and τ is the time elapsed since closure of the system after lead loss (or uranium gain).

In the case of inheritance or entrainment of pre-existing zircon, the data points most commonly fall on discordia trending away from the lower intercept with concordia. The upper intercept with concordia reflects the overall isotopic character of the contaminate zircon, which may be a multi-component system. The lower intercept may represent the igneous crystallization age (Tobisch and others, 1985). In the case of a post-crystallization disturbance, the data points most commonly fall on discordia trending away from the upper intercept. The lower intersection with concordia represents the time of lead loss (uranium gain), with the upper intercept representing a possible igneous crystallization age (Faure, 1977).

The above discussion assumes episodic lead loss. Discordance may also be interpreted to result from continuous diffusion (Tilton, 1960), radiation damage allowing lead to be lost (Goldich and Mudrey, 1972), or the result of chemical weathering (Stern and others, 1966).

A difficulty arises in trying to interpret discordance in Mesozoic samples. This is due to the near linearity of concordia between the origin and 300 Ma which may allow the disturbance of a zircon isotopic system to be expressed by the downward migration of the data points without resolvable deviation from concordia. In addition, the dispersion of Mesozoic zircon populations is often insufficient to adequately determine upper and lower intercepts with concordia (Saleeby, 1982).

A U/Pb zircon analysis is considered to be "internally concordant" if the $^{206}Pb^*/^{238}U$ and $^{207}Pb^*/^{235}U$ ages agree within analytical uncertainty (about 2% of the ages), and "externally concordant" if the $^{206}Pb^*/^{238}U$ age from two or

more fractions from one sample or multiple samples from the same unit agree within analytical uncertainty (about 2% of the ages) (Chen and Moore, 1982; Saleeby, 1982). In order to address this problem, multiple splits of a zircon population into different physical groups (fractions) are required. Multiple fraction analyses were performed on all samples that yielded sufficient zircon for such an analysis. The fractions were physically separated in this study on the basis of size, color, magnetic susceptibility, and shape. This yielded fractions with differing uranium concentrations. Externally concordant zircon ages usually are assumed to represent igneous crystallization ages.

Within the southern and south-central Sierra Nevada a number of workers have obtained results with considerable discordance: Chen and Moore (1982) 40% internally discordant, and 50% externally discordant; Stern and others (1981) 69% internally discordant; and Busby-Spera (1982) 50% discordant. The results reported here are 77% internally concordant, 53% externally concordant, and 23% discordant, and are summarized in Table A8. The final age assignments are shown on a map of the southernmost Sierra Nevada in Figure 41.

Table A8. Summary of preferred U/Pb zircon ages and age types

	SAMPLE #	UNIT‡	PREFERRED AGE	AGE TYPE‡‡
1	TC27	Claraville granodiorite	90/1900	d
2	TC40	tonalite cupola	96	d
3	CM620	pegmatite x-cuts BVS,TJ	94	ic
4	PC35	granite gneiss (PC)	98	ic
5	BM684	tonalite (BVS)	100	ic,ec
6	TC15	tonalite (BVS)	98	ic,ec
7	TC42	tonalite (BVS)	100	ic,ec
8	CM25	tonalite (BVS)	102	ic,ec
9	CM26	tonalite (BVS)	100	ic,ec
10	CM9	tonalite (BVS)	100	ic,ec
11	CM22b	mafic inclusion in BVS	100	ic,ec
12	TL197	tonalite gneiss (BP)	102	ic
13	WR84	metagabbro (TC)	102	ic,ec
14	WR86	metagabbro (TC)	102	ic,ec
17	CM630	tonalite gneiss (TJ)	110	d
18	WR643	tonalite gneiss (TJ)	117	ic,ec
19	WR171	tonalite gneiss (TJ)	110	d
20	WR30/2	quartz diorite (TJ)	110	d
21	WR39	tonalite gneiss (TJ)	113	ic,ec
22	PC31	granite gneiss (PC)	111	ic,ec
23	PC32	granite gneiss (PC)	112	ic,ec
24	PC34	tonalite gneiss (PC)	110	ic
25	PC36	tonalite gneiss (PC)	110	ic,ec
26	PC37	granite gneiss (PC)	114	ic,ec
27	PC129	tonalite (PC)	114	ic,ec
28	WR91a	tonalite gneiss (PC)	110	ic
29	WR40	granite gneiss (PC)	116	ic
30	TC12a	Tweedy Creek augen gneiss	110	ic
32	CM640	quartzite, mmic septa	100/1700§	d
33	CM110	paragneiss (TGC)	108/1450	d

‡ BVS = tonalite of Bear Valley Springs
BP = hypersthene tonalite of Bison Peak
TC = metagabbros of Tunis Creek
TGC = gneiss complex of the Tehachapi Mountains
PC = quartzo-feldspathic gneiss of Pastoria Creek
TJ = tonalite gneiss of Tejon Creek

‡‡ ic = internally concordant, ec = externally concordant,
d = discordant

§ The quartzite does not form a discordia chord.

COMBINED REFERENCES

Ando, C.J., Irwin, W.P., Jones, D.L., and Saleeby, J.B., 1983, The ophiolitic North Fork terrane in the Salmon River region, central Klamath Mountains, California: Geological Society of America Bulletin, v. 94, p. 236-252.

Atherton, M.P., and Tarnet, J., 1979, Origin of granite batholiths; geochemical evidence: Liverpool, United Kingdom: Shiva Publications.

Bartow, J.A., and Dibblee, T.W., Jr., 1981, Geology of the Tejon Hills area - Arvin and Tejon Hills quadrangles, Kern County, California: United States Geological Survey Open-File Report, v. 81-297.

Bateman, P.C., Clark, L.D., Huber, N.K., Moore, J.G., and Rinehart, C.D., 1963, The Sierra Nevada batholith, a synthesis of recent work across the central part: United States Geological Survey Professional Paper, v. 414-D, 46 pp.

Bates, R.L., and Jackson, J.A., eds., 1980, Glossary of Geology, second edition: Falls Church, Virginia: American Geological Institute.

Best, M.G., 1963, Petrology and structural analysis of metamorphic rocks in the southwestern Sierra Nevada foothills, California: University of California Publications in Geological Sciences, v. 42, p. 111-159.

Best, M.G., 1982, Igneous and Metamorphic Petrology: San Francisco, California: W.H. Freeman, Inc.

Best, M.G., and Weiss, L.E., 1964, Mineralogical relations in some pelitic hornfelses from the southern Sierra Nevada: American Mineralogist, v. 49, p. 1240-1266.

Bird, P., and Rosenstock, R.W., 1984, Kinematics of present crust and mantle flow in southern California: Geological Society of America Bulletin, v. 95, p. 946-957.

Bohlen, S.R., and Essene, E.J., 1979, A critical evaluation of two-pyroxene thermometers in Adirondack granulites: Lithos, v. 12, p. 335-345.

Buddington, A.F., 1959, Granite emplacement with special reference to North America: Geological Society of America Bulletin, v. 70, p. 671-747.

Burnett, D.S., and Woolum, D.S., 1983, In situ trace element microanalysis: Annual Review of Earth and Planetary Science, v. 11, p. 329-358.

Busby-Spera, C.J., 1982, Paleogeographic reconstruction of a submarine volcanic center: geochronology, volcanology, and sedimentology of the Mineral King roof pendant, Sierra Nevada, California: Princeton, New Jersey: Ph.D. thesis, Princeton University, 291 pp.

Busby-Spera, C.J., Saleeby, J.B., and Kistler, R.W., 1986, Pb/U zircon and Rb/Sr geochronology of the Mineral King roof pendant, southern Sierra Nevada, California: Geological Society of America Bulletin, in press.

Buwalda, J.P., and St. Amand, P., 1955, Geological effects of the Arvin-Tehachapi earthquake: California Division of Mines and Geology Bulletin, v. 171, p. 41-56.

Catanzaro, E.J., Murphy, W.R., Shields, W.R., and Garner, E.L., 1968, Absolute isotopic ratios of common equal-atom and radiogenic lead isotopic standards: Journal of Research of the National Bureau of Standards, v. 72A, p. 261-267.

Champion, D., Gromme, S., and Howell, D.G., 1980, Paleomagnetism of the Cretaceous Pigeon Point formation and the inferred northward displacement of 2500 km for the Salinian block: EOS (Transactions of the American Geophysical Union), v. 61, p. 948.

Champion, D.E., Howell, D.G., and Gromme, C.S., 1984, Paleomagnetic and geologic data indicating 2500 km of northward displacement for the Salinian and related terranes, California: Journal of Geophysical Research, v. 89, p. 7736-7752.

Chen, J.H., and Moore, J.G., 1982, Uranium-lead isotopic ages from the Sierra Nevada batholith: Journal of Geophysical Research, v. 87, p. 4761-4784.

Chen, J.H., and Tilton, G.T., 1978, Lead and strontium isotopic studies of the southern Sierra Nevada batholith, California: Geological Society of America Abstracts with Programs, v. 10, p. 99-100.

Chen, J.H., and Wasserburg, G.J., 1981, Isotopic determinations of uranium in picomole and subpicomole quantities: Analytical Chemistry, v. 53, p. 2060-2067.

Christensen, N.I., and Fountain, D.M., 1975, Constitution of the lower continental crust based on experimental studies of seismic velocities in granulite: Geological Society of America Bulletin, v. 86, p. 227-236.

Compton, R.R., 1960, Charnockitic rocks of Santa Lucia Range, California: American Journal of Science, v. 258, p. 609-636.

Compton, R.R., 1966, Granitic and metamorphic rocks of the Salinian block, California Coast Ranges: California Division of Mines and Geology Bulletin, v. 190, p. 277-287.

Crowell, J.C., 1952, Geology of the Lebec Quadrangle, California: California Division of Mines and Geology Special Report 24, 23 pp.

d'Allura, J.A., and others, 1977, Paleozoic rocks of the northern Sierra Nevada: their structural and paleogeographic implications: Pacific Section, Society of Economic Paleontologists and Mineralogists, Pacific Coast Paleogeography Symposium, v. 1, p. 395-408.

Davis, G.A., and Burchfiel, B.C., 1973, Garlock fault: an intracontinental transform structure, southern California: Geological Society of America Bulletin, v. 84, p. 1407-1422.

DePaolo, D.J., 1981a, Trace element and isotopic effects of combined wallrock assimilation and fractional crystallization: Earth and Planetary Science Letters, v. 53, p. 189-202.

DePaolo, D.J., 1981b, A neodymium and strontium isotopic study of the Mesozoic calc-alkaline granitic batholiths of the Sierra Nevada and Peninsular Ranges, California: Journal of Geophysical Research, v. 86, p. 10470-10488.

Dibblee, T.W., Jr., and Chesterman, C.W., 1953, Geology of the Breckenridge Mountain quadrangle, California: California Division of Mines and Geology Bulletin, v. 168, 56 pp.

Dibblee, T.W., Jr., and Louke, G.P., 1970, Geologic map of the Tehachapi quadrangle, Kern County, California.: United States Geological Survey Miscellaneous Geological Investigations Map I-607, with text, scale 1:62,500.

Dibblee, T.W., Jr., and Warne, A.H., 1970, Geologic map of the Cummings Mountain quadrangle, Kern County, California: United States Geological Survey Miscellaneous Geological Investigations Map I-611, with text, scale 1:62,500.

Domenick, M.A., Kistler, R.W., Dodge, F.C.W., and Tatsumoto, M., 1983, Nd and Sr isotopic study of crustal and mantle inclusions from the Sierra Nevada and implications for batholith petrogenesis: Geological Society of America Bulletin, v. 94, p. 713-719.

Ehlig, P.L., 1968, Causes of distribution of Pelona, Rand, and Orocopia schists along the San Andreas and Garlock faults: Stanford University Publications on Geological Science, v. 11, p. 294-306.

Ehlig, P.L., 1981, Origin and tectonic history of the basement terrane of the San Gabriel Mountains, central Transverse Ranges, in Ernst, W.G., ed., The Geotectonic Development of California, Englewood Cliffs, New Jersey: Prentice Hall, p. 253-283.

Ehrreich, A.L., 1965, Metamorphism, migmatization, and intrusion in the foothills of the Sierra Nevada, Madera, Mariposa, and Merced counties: Los Angeles, California: Ph.D. thesis, University of California, Los Angeles, 320 pp.

Elan, R., 1985, High grade contact metamorphism at the Lake Isabella north shore roof pendant, southern Sierra Nevada, California: Los Angeles, California: Ph.D. thesis, University of Southern California, 202 pp.

Elan, R., and Thomas, W.M., 1984, High grade, moderate pressure contact metamorphism in the southern Sierra Nevada, and its tectonic implication for Sierran uplift: Geological Society of America Abstracts with Programs, v. 16, p. 500.

Evernden, J.F., and Kistler, R.W., 1970, Chronology of emplacement of Mesozoic batholithic complexes in California and western Nevada: United States Geological Survey Professional Paper 623, 42 pp.

Faure, G., 1977, Principles of isotope geology: New York, New York: John Wiley and Sons, Inc.

Ferry, J.M., and Spear, F.S., 1978, Experimental calibration of the partitioning of Fe and Mg between biotite and garnet: Contributions to Mineralogy and Petrology, v. 66, p. 113-117.

Fleck, R.J., and Criss, R.E., 1985, Strontium and oxygen isotopic variations in Mesozoic and Tertiary plutons in central Idaho: Contributions to Mineralogy and Petrology, v. 90, p. 291-308.

Fountain, D.M., and Salisbury, M.H., 1981, Exposed cross-sections through the continental crust: implications for crustal structure, petrology, and evolution: Earth and Planetary Science Letters, v. 56, p. 263-277.

Frei, L.S., Magill, J.R., and Cox, A.V., 1982, Paleomagnetic results from the central Sierra Nevada: constraints on reconstructions of the western US: EOS (Transactions of the American Geophysical Union), v. 63, p. 916.

Frei, L.S., Magill, J.R., and Cox, A.V., 1984, Paleomagnetic results from the central Sierra Nevada: constraints on reconstructions of the western US: Tectonics, v. 3, p. 157-177.

Ghent, E.D., Nichols, J., Stout, M.Z., and Tottenfusser, B., 1977, Clinopyroxene amphibolite boudins from the Three Valley Gap, British Columbia: Canadian Mineralogist, v. 15, p. 269-282.

Ghent, E.D., Robbins D.B., and Stout, M.Z., 1979, Geothermometry, geobarometry and fluid compositions of metamorphosed calc-silicates and pelites, Mica Creek, British Columbia: Contributions to Mineralogy and Petrology, v. 64, p. 855-874.

Ghent, E.D., and Stout, M.Z., 1981, Geobarometry and geothermometry of plagioclase-biotite-garnet-muscovite assemblages: Contributions to Mineralogy and Petrology, v. 76, p. 92-97.

Goldich, S.S., and Mudrey, M.G., Jr., 1972, Dilatancy model for discordant U-Pb zircon ages: in Tugarinov, A.I., ed., Contributions to Recent Geochemistry and Analytical Chemistry, p. 415-418.

Green, T.H., 1982, Anatexis of mafic crust and high pressure crystallization of andesite, in Thorpe, R.S., ed., Andesites, New York, New York: John Wiley and Sons.

Gromme, C.S., Merrill, R.T., and Verhoogen, J., 1967, Paleomagnetism of Jurassic and Cretaceous plutonic rocks in the Sierra Nevada, California, and its significance for polar wandering and continental drift: Journal of Geophysical Research, v. 72, p. 5661-5684.

Gromme, C.S., and Merrill, R.T., 1965, Paleomagnetism of Late Cretaceous granitic plutons in the Sierra Nevada, California - further results: Journal of Geophysical Research, v. 70, p. 3407-3420.

Hall, N.T., 1984, Recurrence interval and late Quaternary history of the eastern Pleito thrust fault, northern Transverse Ranges, California: Final Technical Report, June 1984, U.S. Geol. Survey Earthquake Hazards Reduction Program, 89 pp.

Hamilton, W., 1969, Mesozoic California and the underflow of the Pacific mantle: Geological Society of America Bulletin, v. 80, p. 2409-2430.

Hamilton, W., 1981, Crustal evolution by arc magmatism: Philosophical Transactions of the Royal Society of London, Serial A, v. 301, p. 279-291.

Hamilton, W., and Myers, W.B., 1967, The nature of batholiths: Unites States Geological Survey Professional Paper, v. 554-C.

Harland, W.B., Cox, A.V., Llewellyn, P.G., Pickton, C.A.G., Smith, A.G., and Walters, R., 1982, A geologic time scale: Cambridge, Great Britain: Cambridge University Press.

Harris, P.B., 1954, Geology of the Tunis Creek-Pastoria Creek area, Kern County: California Division of Mines and Geology Bulletin, v. 170, Map Sheet 2.

Hart, S.R., 1971, K, Rb, Cs, Sr, and Ba contents and Sr isotopic ratios of ocean floor basalts: Philosophical Transactions of the Royal Society of London, Serial A, v. 268, p. 573-587.

Haxel, G.B., and Dillon, J., 1978, The Pelona-Orocopia schist and Vincent-Chocolate Mountain thrust system, southern California: Pacific Section, Society of Economic Paleontologists and Mineralogists, Pacific Coast Paleogeography Symposium, v. 2, p. 453-469.

Hill, R.I., 1984, Petrology and petrogenesis of batholithic rocks, San Jacinto Mountains, southern California: Pasadena, California: Ph.D. thesis, California Institute of Technology, 684 pp.

Holdaway, M.J., 1971, Stability of andalusite and the aluminum silicate phase diagram: American Journal of Science, v. 271, p. 97-131.

Humphreys, E., Clayton, R.W., and Hager, B.H., 1984, A tomographic image of mantle structure beneath southern California: Geophysical Research Letters, v. 11, p. 625-627.

Jaffey, A.H., Flynn, K.F., Glendenin, L.E., Bentley, W.C., and Essling, A.M., 1971, Precision measurement of half-lives and specific activities of ^{235}U and ^{238}U: Physics Reviews, v. C4, p. 1889-1906.

James, O., 1971, Origin and emplacement of the ultramafic rocks of the Emigrant Gap area, California: Journal of Petrology, v. 12, p. 523-560.

Kanter, L.R., 1982, Preliminary paleomagnetic results from the Gualala block, northern California: Geological Society of America Abstracts with Programs, v. 14, p. 177.

Kanter, L.R., and McWilliams, M.O., 1980, Tectonic rotation of the southernmost Sierra Nevada, California: EOS (Transactions of the American Geophysical Union), v. 61, p. 948.

Kanter, L.R., and McWilliams, M.O., 1982, Rotation of the southernmost Sierra Nevada, California: Journal of Geophysical Research, v. 87, p. 3819-3830.

Kistler, R.W., and Peterman, Z.E., 1973, Variations in Sr, Rb, K, Na and initial $^{87}Rb/^{87}Sr$ in Mesozoic granitic rocks and intruded wall rocks in central California: Geological Society of America Bulletin, v. 84, p. 3489-3512.

Kistler, R.W., and Peterman, Z.E., 1978, Reconstruction of crustal blocks of California on the basis of initial strontium isotopic compositions of Mesozoic granitic rocks: United States Geological Survey Professional Paper, v. 1071, 17 pp.

Krogh, T.E., 1973, A low-contamination method for hydrothermal decomposition of zircon and extraction of U and Pb for isotopic age determinations: Geochimica Cosmochimica Acta, v. 37, p. 485-494.

Lindsley, D.H., King, H.E., Jr., and Turnock, A.C., 1974, Composition of synthetic augite and hypersthene coexisting at 810°C: application to pyroxenes from lunar highlands rocks: Geophysical Research Letters, v. 1, p. 134-136.

Mack, S., Saleeby, J.B., and Ferrell, J.F., 1979, Origin and emplacement of the Academy pluton, Fresno County, California: Geological Society of America Bulletin, v. 90, Part I: p. 321-323; Part II: p. 633-694.

Marshall, L.A., and Sparks, R.S.J., 1984, Origins of some mixed-magma and net-veined ring intrusions: Journal of the Geological Society of London, v. 141, p. 171-182.

Mattinson, J.M., 1972, Preparation of hydrofluoric, hydrochloric and nitric acids at ultralow lead levels: Analytical Chemistry, v. 44, p. 1715-1716.

Mattinson, J.M., 1978, Age, origin, and thermal histories of some plutonic rocks from the Salinian block of California: Contributions to Mineralogy and Petrology, v. 67, p. 233-245.

McWilliams, M., and Li, Y., 1983, A paleomagnetic test of the Sierran orocline hypothesis: EOS (Transactions of the American Geophysical Union), v. 64, p. 686.

McWilliams, M., and Li, Y., 1985, Oroclinal bending of the southern Sierra Nevada batholith: Science, v. 230, p. 172-175.

Michel-Levy, 1877, De l'emploi du microscope polisant a lumiere parallele: Annuales Mineralogies, v. 12, p. 392-471.

Nilsen, T.H., and Clarke, S.H., Jr., 1975, Sedimentation and tectonics in the early Tertiary continental borderland of central California: United States Geological Survey Professional Paper, v. 925, 64 pp.

Nokleberg, W.J., and Kistler, R.W., 1980, Paleozoic and Mesozoic deformations in the central Sierra Nevada, California: United States Geological Survey Professional Paper, v. 1145, 24 pp.

Nourse, J.A., and Silver, L.T., 1986, Structural and kinematic evolution of sheared rocks in the Rand "thrust" complex, northwest Mojave Desert, California: Geological Society of America Abstracts with Programs, v. 18, p 165.

O'Hara, M.J., and Yarwood, G., 1978, High pressure-temperature point on an Archaen geotherm, implied magma genesis by crustal anatexis, and consequences for garnet-pyroxene thermometry and barometry: Philosophical Transactions of the Royal Society of London, Serial A, v. 288, p. 441-456.

Obata, M., 1980, The Ronda peridotite: garnet-, spinel-, and plagioclase-lherzolite facies and the P-T trajectories of a high-temperature mantle intrusion: Journal of Petrology, v. 21, p. 533-572.

Page, B.M., 1981, The southern Coast Ranges: in Ernst, W.G., ed., The Geotectonic Development of California: Englewood Cliffs, New Jersey: Prentice-Hall, Inc., p. 329-417.

Page, B.M., 1982, Migration of Salinian composite block, California, and disappearance of fragments: American Journal of Science, v. 282, p. 1694-1734.

Plescia, J.B., and Calderone, G.J., 1986, Paleomagnetic constraints on the timing and extent of rotation of the Tehachapi Mountains, California: Geological Society of America Abstracts with Programs, v. 18, p. 171.

Ross, D.C., 1976a, Reconnaissance geologic map of the pre-Cenozoic basement rocks, northern Santa Lucia Range, Monterey County, California: United States Geological Survey Miscellaneous Field Investigations, Map MF-750, Scale 1:125,000.

Ross, D.C., 1976b, Modal data and notes on mineral assemblages for metamorphic rocks of the Santa Lucia Range, Salinian block, California: National Technical Information Service Report, v. PB-262-505, 38 pp.

Ross, D.C., 1976c, Maps showing distribution of metamorphic rocks and occurrences of garnet, coarse graphite, sillimanite, orthopyroxene, clinopyroxene, and plagioclase amphibolite, Santa Lucia Range, Salinian block, California: United States Geological Survey Miscellaneous Field Studies Map MF-791.

Ross, D.C., 1979, Summary of petrographic data of basement rock samples from oil wells in the southeast San Joaquin Valley, California: United States Geological Survey Open-File Report, v. 79-400, 11pp.

Ross, D.C., 1980, Reconnaissance geologic map of the southernmost Sierra Nevada (north to 35° 30' N.): United States Geological Survey Open-File Report, v. 80-307, 22 pp.

Ross, D.C., 1983a, Generalized geologic map of the southern Sierra Nevada, California, showing the location for which K-Ar radiometric age data and Rb/Sr data have been determined: United States Geological Survey Open-File Report, v. 83-231, scale 1:250,000.

Ross, D.C., 1983b, Hornblende-rich high-grade metamorphic terranes in the southernmost Sierra Nevada, California, and implications for crustal depths and batholith roots: United States Geological Survey Open-File Report, v. 83-465, 51 pp.

Ross, D.C., 1983c, Petrographic (thin section) notes on selected samples from hornblende-rich metamorphic terranes in the southernmost Sierra Nevada, California: United States Geological Survey Open-File Report, v. 83-587, 36 pp.

Ross, D.C., 1983d, Generalized geologic map of the southern Sierra Nevada, California, showing the location of basement samples for which whole rock ^{18}O has been determined: United States Geological Survey Open-File Report, v. 83-904, scale 1:250,000.

Ross, D.C., 1984, Possible correlations of basement rocks across the San Andreas, San Gregorio-Hosgri, and Rinconada-Reliz-King City faults, California: United States Geological Survey Professional Paper, v. 1317, 37 pp.

Ross, D.C., 1985, Mafic gneissic complex (batholithic root?) in the southernmost Sierra Nevada, California: Geology, v. 13, p. 288-291.

Ross, D.C., 1986, The metamorphic and plutonic rocks of the southernmost Sierra Nevada, California, and their tectonic framework: United States Geological Survey Professional Paper, in press.

Saleeby, J.B., 1979, Kaweah serpentine melange, southwest Sierra Nevada Foothills, California: Geological Society of America Bulletin, v. 90, p. 29-46.

Saleeby, J.B., 1981, Ocean floor accretion and volcano-plutonic arc evolution of the Mesozoic Sierra Nevada: in Ernst, W.G. ed., The Geotectonic Development of California: Englewood Cliffs, New Jersey: Prentice-Hall, Inc., p. 132-181.

Saleeby, J.B., 1982, Polygenetic ophiolite belt of the California Sierra Nevada - geochronological and tectonostratigraphic development: Journal of Geophysical Research, v. 87, p. 1803-1824.

Saleeby, J.B., 1983, Accretionary tectonics of the North American Cordillera: Annual Reviews in the Earth and Planetary Sciences, v. 15, p. 45-73.

Saleeby, J.B., and Busby-Spera, C., 1986, Fieldtrip guide to the metamorphic framework rocks of the Lake Isabella area, southern Sierra Nevada, California: in Dunne, G.C., ed., Mesozoic and Cenozoic structural evolution of selected areas, east-central California: Guidebook for the Cordilleran Section, Geological Society of America, p. 81-94.

Saleeby, J.B., and Chen, J.H., 1978, Preliminary report on initial lead and strontium isotopes from ophiolitic and batholithic rocks, southwestern foothills Sierra Nevada, California: United States Geological Survey Open-File Report, v. 78-701, p. 375-376.

Saleeby, J.B., Goodin, S.E., Sharp, W.D., and Busby, C.J., 1978, Early Mesozoic paleotectonic-paleogeographic reconstruction of the southern Sierra Nevada region: Pacific Section, Society of Economic Paleontologists and Mineralogists, Pacific Coast Paleogeography Symposium, v. 2, p. 311-336.

Saleeby, J.B., Sams, D.B., and Tobisch, O.T., 1986a, A down-plunge view of the Sierra Nevada batholith: from resurgent caldera to ultrametamorphic levels: Geological Society of America Abstracts with Programs, v. 18, p. 179.

Saleeby, J.B., Shaw, H.F., Chen, J.H., and Wasserburg, G.J., 1986c, Nd-Sr-Pb systematics and age of the Kings River ophiolite: Contributions to Mineralogy and Petrology, in preparation.

Saleeby, J.B., and Sharp, W.D., 1980, Chronology of the structural and petrologic development of the southwest Sierra Nevada Foothills, California: Geological Society of America Bulletin, v. 91, Part I: p. 317-320; Part II: p. 1416-1535.

Saleeby, J.B., and Williams, H., 1978, Possible origin of California Great Valley gravity-magnetic anomalies: EOS (Transactions of the American Geophysical Union), v. 59, p. 1189.

Saleeby, J.B., and 12 others, 1986b, Ocean-continent transect, corridor C2, Monterey Bay offshore to the Colorado Plateau: Geological Society of America Map and Chart Series, 2 sheets, with text, scale 1:50,000, in press.

Sams, D.B., and Saleeby, J.B., 1986, U/Pb zircon ages, and implications on the structural and petrologic development of the southernmost Sierra Nevada: Geological Society of America Abstracts with Programs, v. 18, p. 180.

Sams, D.B., Saleeby, J.B., and Kistler, R.W., 1986, Geochronological and petrotectonic significance of the crystalline rocks of the southernmost Sierra Nevada, in preparation.

Sams, D.B., Saleeby, J.B., Ross, D.C., and Kistler, R.W., 1983, Cretaceous igneous, metamorphic and deformational events of the southernmost Sierra Nevada, California: Geological Society of America Abstracts with Programs, v. 15, p. 294.

Savin, S.M., and Epstein, S.E., 1970, The oxygen and hydrogen isotope geochemistry of ocean sediments and shales: Geochemica Cosmochemica Acta, v. 34, p. 43-63.

Schweickert, R.A., and Cowan, D.S., 1975, Early Mesozoic tectonic evolution of the western Sierra Nevada, California: Geological Society of America Bulletin, v. 86, p. 1329-1336.

Sharry, J., 1981a, Tectonic implications of granulite facies rocks from the western Tehachapi Mountains, California: EOS (Transactions of the American Geophysical Union), v. 62, p. 1048.

Sharry, J., 1981b, The geology of the western Tehachapi Mountains, California: Boston, Massachusetts: Ph.D. thesis, Massachusetts Institute of Technology, 215 pp.

Sharry, J., 1982, Minimum age and westward continuation of the Garlock fault zone, Tehachapi Mountains, California: Geological Society of America Abstracts with Programs, v. 14, p. 233.

Silver, L.T., 1964, The relationship between radioactivity and discordance in zircons: in Nuclear Geophysics, Publication 1075, Nuclear Sciences Serial Report, v. 38, p. 34-39.

Silver, L.T., 1982, Evidence and a model for west-directed early to mid-Cretaceous basement overthrusting in southern California: Geological Society of America Abstracts with Programs, v. 14, p. 617.

Silver, L.T., 1983, Paleogene overthrusting in the tectonic evolution of the Transverse Ranges, Mojave and Salinian regions, California: Geological Society of America Abstracts with Programs, v. 15, p. 438.

Silver, L.T., Anderson, C.A., Crittenden, M., and Robertson, J.M., 1977, Chronostratigraphic elements of the Precambrian rocks of the southwestern and far western United States: Geological Society of America Abstracts with Programs, v. 9, p. 1176.

Silver, L.T., Early, T.O., and Anderson, T.H., 1975, Petrological, geochemical and geochronological asymmetries of the Peninsular Ranges batholith: Geological Society of America Abstracts with Programs, v. 7, p. 375-376.

Silver, L.T., and Nourse, J.A., 1986, The Rand "thrust" complex in comparison with the Vincent thrust-Pelona schist relationship, southern California: Geological Society of America Abstracts with Programs, v. 18, p. 185.

Silver, L.T., Sams, D.B., Bursik, M.I., Graymer, R.W., Nourse, J.A., Richards, M.A., and Salyards, S.L., 1984, Some observations on the tectonic history of the Rand Mountains, Mojave Desert, California: Geological Society of America Abstracts with Programs, v. 16, p. 333.

Silver, L.T., Taylor, H.P., Jr., and Chappell, B., 1979, Some petrological, geochemical, and geochronological observations of the Peninsular Ranges batholith near the international border of the U.S.A. and Mexico: in Abbott, P.L., and Todd, V.R., eds., Mesozoic crystalline rocks: Peninsular Ranges batholith and pegmatites, Point Sal ophiolite, p. 83-110.

Snoke, A.W., Quick, J.E., and Bowman, H.R., 1981, Bear Mountain Igneous complex, Klamath Mountains, California: an ultrabasic to silicic calc-alkaline suite: Journal of Petrology, v. 22, p. 501-552.

Snoke, A.W., Sharp, W.D., Wright, J.E., and Saleeby, J.B., 1982, Petrotectonic significance of mid-Mesozoic peridotitic to dioritic intrusive complexes, Klamath Mountains, California: Geology, v. 10, p. 160-166.

Stern, T.W., Bateman, P.C., Morgan, B.A., Newell, M.F., and Peck, D.L., 1981, Isotopic U-Pb ages of zircon from granitoids of the central Sierra Nevada, California: United States Geological Survey Professional Paper, v. 1185, 17 pp.

Stern, T.W., Goldich, S.S., and Newell, M.F., 1966, Effects of weathering on the U-Pb ages of zircon from the Morton Gneiss: Earth and Planetary Science Letters, v. 1, p. 369-371.

Stieger, R.H., and Jaeger, E., 1977, Subcommission on geochronology: Convention on the use of decay constants in geo- and cosmochronology: Earth and Planetary Science Letters, v. 36, p. 359-362.

Streckeisen, A.L., 1973, Plutonic rock - classification and nomenclature recommended by the IUGS Subcommission on the systematics of igneous rocks: Geotimes, v. 18, no. 10, p. 26-30.

Streckeisen, A.L., 1976, To each plutonic rock its proper name: Earth Science Reviews, v. 12, p. 1-33.

Taylor, H.P., Jr., 1968, The oxygen isotope geochemistry of igneous rocks: Contributions to Mineralogy and Petrology, v. 19, p. 1-71.

Taylor, H.P., Jr., 1978, Oxygen and hydrogen isotopic studies of plutonic granitic rocks: in Allegre, C.J., and Hart, S.R., eds., Trace Elements in Igneous Petrology (Gast Volume), Earth and Planetary Science Letters, v. 38, p. 177-210.

Taylor, H.P., Jr., 1980, The effects of assimilation of country rocks by magmas on $^{18}O/^{16}O$ and $^{87}Sr/^{86}Sr$ systematics in igneous rocks: Earth and Planetary Science Letters, v. 47, p. 243-254.

Taylor, H.P., Jr., and Silver, L.T., 1978, Oxygen isotope relationships in plutonic igneous rocks of the Peninsular Ranges batholith, southern and Baja California: in Zartman, R.E., ed., Short Papers of the Fourth International Conference on Geochronology, Cosmochronology, and Isotope Geology: United States Geological Survey Open-File Report, v. 78-701, p. 423-426.

Tilton, G.R., 1960, Volume diffusion as a mechanism for discordant lead ages: Journal of Geophysical Research, v. 65, p. 2933-2945.

Tobisch, O.T., and Fiske, R.S., 1982, Repeated parallel deformation in part of the eastern Sierra Nevada, California, and its implications in the dating of structural events: Journal of Structural Geology, v. 4, p. 177-195.

Tobisch, O.T., Saleeby, J.B., and Fiske, R.S., 1985, Structural history of continental volcanic arc rocks, eastern Sierra Nevada, California: a case for extensional tectonics: Tectonics, v. 5, p. 65-94.

Todd, V.R., and Shaw, S.E., 1979, Structural, metamorphic and intrusive framework of the Peninsular Ranges batholith in southern San Diego county, California: in Abbott, P.L., and Todd, V.R., eds., Mesozoic crystalline rocks: Peninsular Ranges batholith and pegmatites, Point Sal ophiolite, p. 177-231.

Tullis, J., and Yund, R.A., 1977, Deformational behavior of quartz and feldspar in experimentally deformed granite: EOS (Transactions of the American Geophysical Union), v. 58, p. 513.

Wallin, E.J., 1986, Eocambrian-early Cambrian plutonic rocks in the eastern Klamath Mountain province, northern California: Geological Society of America Abstracts with Programs, v. 18, p. 195.

Wells, R.A., 1980, Thermal models for the magmatic accretions and subsequent metamorphism of continental crust: Earth and Planetary Science Letters, v. 46, p. 253-265.

Wetherill, G.W., 1956, Discordant uranium-lead ages, I: EOS (Transactions of the American Geophysical Union), v. 37, p. 320-326.

White, A.J.R., and Chappell, B.W., 1977, Ultrametamorphism and granitoid genesis: Tectonophysics, v. 43, p. 7-22.

Wiebe, R.A., 1970a, Relations of granitic and gabbroic rocks, northern Santa Lucia Range, California: Geological Society of America Bulletin, v. 81, p. 105-116.

Wiebe, R.A., 1970b, Pre-Cenozoic tectonic history of the Salinian block, western California: Geological Society of America Bulletin, v. 81, p. 1837-1842.

Wiese, J.H., 1950, Geology and mineral deposits of the Neenach quadrangle, California: California Division of Mines and Geology Bulletin, v. 153, 53 pp.

Williams, H., Turner, F.J., and Gilbert, C.M., 1982, Petrography (an introduction to the study of rocks in thin section): San Francisco, California: W.H. Freeman, Inc.

Wise, D.U., Dunn, D.E., Engelder, J.T., Geiser, P.A., Hatcher, R.D., Kish, S.A., Odom, A.L., and Schamel, S., 1984, Fault-related rocks: suggestions for terminology: Geology, v. 12, p. 391-394.

Wood, B.J., and Banno, S., 1973, Garnet-orthopyroxene and orthopyroxene-clinopyroxene relationships in simple and complex systems: Contributions to Mineralogy and Petrology, v. 42, p. 109-124.

Wyllie, P.J., 1983a, Experimental studies on biotite- and muscovite-granites and some crustal magmatic sources: in Migmatites, Melting, and Metamorphism, Atherton, M.P., and Gribble, C.D., eds., Nantwich, England: Shiva Publications, p. 12-26.

Wyllie, P.J., 1983b, Experimental and thermal constraints on the deep-seated parentage of some granitoid magmas in subduction zones: in Migmatites, Melting, and Metamorphism, Atherton, M.P., and Gribble, C.D., eds., Nantwich, England: Shiva Publications, p. 37-51.

Yeats, R.S., 1981, Quaternary flake tectonics of the California Transverse Ranges: Geology, v. 9, p. 16-20.

Zen, E-an, 1985, Implications of magmatic epidote-bearing plutons on crustal evolution in the accreted terranes of northwestern North America: Geology, v. 13, p. 266-269.

Zen, E-an, and Hammarstrom, J.N., 1984, Magmatic epidote and its petrologic significance: Geology, v. 12, p. 515-518.

KEY TO COMPILATION MAP AND TOPOGRAPHIC MAPS

SOUTHERNMOST SIERRA NEVADA AND TEHACHAPI MOUNTAINS

UNITS

- QT Quaternary/Tertiary cover
- Tv Tertiary hypabyssal volcanics
- Tp Pliocene strata
- Tm Miocene strata
- Td Oligocene strata
- Te Eocene strata

UPPER CRETACEOUS

- gr undifferentiated granitic plutons
- CVL granodiorite of Claraville
- peg pegmatite dike swarm
- Bear Valley Springs igneous suite
  - MAd tonalite of Mount Adelaide
  - BVS tonalite of Bear Valley Springs
    internal contacts; m=main, e=eastern, x=mixed phases
  - BP hypersthene tonalite of Bison Peak
  - TC metagabbro of Tunis Creek
  - SS metagabbro of Squirrel Spring

MID-CRETACEOUS

- um mafic-ultramafic intrusives
- gneiss complex of the Tehachapi Mountains
  - TJ tonalite gneiss of Tejon Creek
  - WO diorite gneiss of White Oak
  - PC quartzo-feldspathic gneiss of Pastoria Creek
    t=tonalite, g=granite gneisses
  - CP paragneiss of Comanche Point
- ag augen gneiss of Tweedy Creek

PRE-CRETACEOUS

- ms Kings sequence metasedimentary septa
- metasedimentary lenses
  - qfg quartzo-feldspathic gneiss
  - m marble
  - q quartzite
  - u granulite
  - dg diorite gneiss

AGES UNKNOWN

- RS Rand Schist

KEY TO COMPILATION MAP AND TOPOGRAPHIC MAPS

SOUTHERNMOST SIERRA NEVADA AND TEHACHAPI MOUNTAINS

UNITS

- QT Quaternary/Tertiary cover
- Tv Tertiary hypabyssal volcanics
- Tp Pliocene strata
- Tm Miocene strata
- Td Oligocene strata
- Te Eocene strata

UPPER CRETACEOUS

- gr undifferentiated granitic plutons
- CVL granodiorite of Claraville
- peg pegmatite dike swarm

Bear Valley Springs igneous suite

- MAd tonalite of Mount Adelaide
- BVS tonalite of Bear Valley Springs
  m=main; e=eastern; x=mixed phases —·— internal contacts
- BP hypersthene tonalite of Bison Peak
- TC metagabbro of Tunis Creek
- SS metagabbro of Squirrel Spring

MID-CRETACEOUS

- um mafic-ultramafic intrusives

gneiss complex of the Tehachapi Mountains

- TJ tonalite gneiss of Tejon Creek
- WO diorite gneiss of White Oak
- PC quartzo-feldspathic gneiss of Pastoria Creek
  t=tonalite; g=granite gneisses
- CP paragneiss of Comanche Point
- ag augen gneiss of Tweedy Creek

PRE-CRETACEOUS

- ms Kings sequence metasedimentary septa
- qfg quartzo-feldspathic gneiss
- m marble
- q quartzite } metasedimentary lenses
- u granulite
- dg diorite gneiss

AGES UNKNOWN

- RS Rand Schist

SYMBOLS

- notebook station
- hand sample/thin section
- photograph
- strike/dip of foliation
- strike/dip bedding
- trend/plunge of lineation
- contact, well exposed, approximate, covered, gradational
- fault, well exposed, approximate, covered
- pegmatite dike swarm
- geochronology/geochemistry location

special symbol:
lithology
texture

LITHOLOGY

- G granite
- Z quartz monzonite
- R granodiorite
- T tonalite
- D gabbro/diorite/quartz diorite
- U ultramafic
- B marble
- Q quartzite
- F quartzo-feldspathic
- S schist

MINERALOGY

- u microcline
- K myrmekite
- P zoned plagioclase

TEXTURE

- A annealed
- X recrystallized
- I igneous
- M mylonitic/protomylonitic augen gneiss/flasered
- C cataclastic
- L cumulate
- N granoblastic/gneissic